F 1503/2

BULETINUL INSTITUTULUI POLITEHNIC DIN IAȘI

Tomul XXXVI (XL)

Fasc. 1–2

Secția II

CHIMIE ȘI INGINERIE CHIMICĂ

1990

BULETINUL INSTITUTULUI POLITEHNIC DIN IAŞI

BIBLIOTECA CENTRALĂ UNIVERSITATEA TEHNICĂ „GHEORGHE ASACHI" DIN IAŞI

Tomul XXXVI (XL)

Fasc. 1–2

Secţia II

CHIMIE ŞI INGINERIE CHIMICĂ

1990

EDITORIAL STAFF

Prof dr. ing. **VITALIE BELOUSOV** (President)

Prof. dr. doc. **D. I. MANGERON** (Honorary President)

Conf. dr. ing. **MIRCEA MANOLOVICI** (Secretary)

Conf. dr. ing. **MATEI MACOVEANU**

Prof. dr. doc. **ALFRED BRAIER** (Editor)

Prof. dr. ing. **HUGO ROSMAN** (Editor)

Prof. dr. ing. **MIHAIL VOICU** (Head of the Exchange Service)

Prof. dr. **AUREL BEJANCU**

Prof. dr. ing. **VICTOR BULACOVSCHI**

Prof. dr. ing. **MIHAI LUCANU**

Prof. dr. ing. **SPIRIDON CREȚU**

Prof. dr. ing. **ADRIAN RADU**

Prof. dr. ing. **AURELIA GRIGORIU**

BULETINUL INSTITUTULUI POLITEHNIC DIN IAŞI
BULLETIN OF THE POLYTECHNIC INSTITUTE OF JASSY
ИЗВЕСТИЯ ЯССКОГО ПОЛИТЕХНИЧЕСКОГО ИНСТИТУТА
Tomul XXXVI (XL), Fasc. 1–2 1990

Secţia II

CHIMIE ŞI INGINERIE CHIMICĂ

SUMAR

Pag

I. ROŞCA, E. ŞTEFANCU, N. FOCA şi M. PALMARU, Sinteza şi studiul polifosfinaţilor de Nb (IV) (rusă, rez. rom.) 1
I. BERDAN, AL. CAŞCAVAL şi G. BUNDUC, Complecşi polinucleari ai Cr (III) (franc., rez. rom.) 9
S. D. MIRON, AL. CECAL şi T. BARAN, Efectul radioprotector al rutin-cisteinei determinat cu ajutorul rezonanţei electronice de spin (engl., rez. rom.) 17
D. HRIŢCU, L. ODOCHIAN şi GH. IONESCU, Aspecte cinetice şi termodinamice privind descompunerea apei oxigenate prin cataliza omogenă (engl., rez. rom.) 21
S. PETRESCU, C. CALISTRU şi C. PETRESCU, Studiul echilibrului cristalizării sulfatului de potasiu în sistemul K^+, NH_4^+ // Cl^-, SO_4^{2-} — H_2O (engl., rez. rom.) 27
I. SIMINICEANU şi C. PETRILĂ, Reformarea gazului natural la un raport scăzut abur/carbon (engl., rez. rom.) 33
C. HAGIU şi G. YAHIA, Cercetarea comportării deşeului de oase calcinate în procesul obţinerii îngrăşămintelor complexe (franc., rez. rom.) 41
R. Z. TUDOSE şi F. MUSTAŢĂ, Distribuţia temperaturii la curgerea în filme subţiri de lichide nenewtoniene care respectă modelul Ellis (engl., rez. rom.) 47
GH. CRISTIAN, R. STAICU şi I. VEREŞ, Studii de cinetica uscării copolimerului stiren-divinilbenzen (I). (engl., rez. rom.) 51
F. IACOMI, G. I. RUSU, E. POPOVICI, M. RUSU, FL. IOAN, ŞT. CURCĂNEANU şi I. D. BURSUC, Creşterea calităţii maselor plastice prin încorporare de zeoliţi (rusă, rez. rom.) 59
E. POPOVICI, F. IACOMI, EL. TRIF, I. MÎNDRECI, AL. NICULA, Dehidrogenarea metanolului la zeoliţi naturali şi la formele lor modificate (rusă, rez. rom.) 63
S. IFRIM, Prepararea unor coloranţi azoici folosind lignina drept componentă de cuplare (franc., rez. rom.) 67
M. CAPROŞU, ŞT. CILIANU, R. BOZGA, I. CIOCOIU, M. PETROVANU şi E. BICU, Sinteza unor noi derivaţi piridazinici cu eventuală activitate fiziologică (franc., rez. rom) 71
C. LEONTE, E. CARP, S. DUMITRESCU, ŞT. CILIANU şi R. BOZGA, Structuri amidice cu acţiune asupra sistemului nervos central) (III) (franc. rez. rom.) 75

H. SELIGER, E. HAPP (R. F. Germană) şi Al. CAŞCAVAL, Noi derivaţi ai 4-cromanonei ca fotostabilizatori pentru polimeri (engl., rez. rom.) · 81
C. VASILE, GH. ADAMESCU, L. ODOCHIAN, I. POINESCU, L. CHICU şi M. BADEA, Reţele semiinterpătrunse ale PVC şi esterilor metacrilici (I) (engl., rez. rom.) · · · · · · 87
N. OIŢĂ, M. NICU, V. NICU şi E. TĂTARU, Contribuţii la studiul reacţiei de acilare a poliolilor în prezenţa clorurii de zinc (engl., rez. rom.)+ · · · · · · 91
M. RUSU, S. PETROVAN şi C. IBĂNESCU, Filme din copolimerii etilenă-acetat de vinil (engl., rez. rom.) · · · · · · 97
RECENZII · · · · · · 99

BULETINUL INSTITUTULUI POLITEHNIC DIN IAŞI
BULLETIN OF THE POLYTECHNIC INSTITUTE OF JASSY
ИЗВЕСТИЯ ЯССКОГО ПОЛИТЕХНИЧЕСКОГО ИНСТИТУТА
Tome XXXVI (XL), Fasc. 1—2 1990

Section II

CHEMISTRY AND CHEMICAL ENGINEERING

CONTENTS

I. ROŞCA, E. ŞTEFANCU, N. FOCA and M. PALAMARU, The Synthesis and Study of Nb(IV) Polyphosphinate (Russian., Romanian summary) 1
I. BERDAN, AL. CAŞCAVAL et G. BUNDUC, Complexes polynucleaires du Cr (III) (French, Romanian summary) 9
S. D. MIRON, Al. CECAL and T. BARAN, Radioprotection Effect of Rutin-Cysteine Determined by Electronic Paramagnetic Resonance (E.P.R.) (English, Romanian summary) 17
D. HRIŢCU, L. ODOCHIAN and GH. IONESCU, Kinetical and Thermodynamical Aspects on the Decomposition of Hydrogen Peroxide in Homogeneous Catalysis (English, Romanian summary) 21
ST. PETRESCU, C. CALISTRU and C. PETRESCU, The Study of the Crystallization Equilibrium of Potassium Sulphate in the $K^+, NH_4^+ \| Cl^-, SO_4^{2-} - H_2O$ System (English, Romanian summary) 27
I. SIMINICEAHU and C. PETRILĂ, Natural Gaz Reforming at Low Steam/Carbon Ratios (English, Romanian summary) 33
C. HAGIU et G. YAHIA, Recherches sur le comportement des déchets d'os calcinés dans le processus d'obtention des engrais complexes (French, Romanian summary) 41
R. Z. TUDOSE and F. MUSTAŢĂ, Temperature Distribution in Flow of Thin Films of Non-Newtonian Fluids which Respect Ellis Model (English, Romanian summary) 47
GH. CRISTIAN, R. STAICU and I. VEREŞ, Studies on Drying Kinetics of Styrene Divinylbenzene Copolymer (I) (English, Romanian summary) 53
F. IACOMI, G. I. RUSU, E. POPOVICI, M. RUSU, FL. IOAN, ŞT. CURCĂNEANU and I. D. BURSUC, The Increase of the Quality of Plastics by Zeolite Incorporation (Russian, Romanian summary) 59
S. IFRIM, Préparation de quelques colorants azoïques utilisant la lignine comme
E. POPOVICI, F. IACOMI, EL. TRIF, I. MÎNDRECI and AL. NICULA, Metanol Dehydrogenation on Natural Zeolite and on their Modified Forms (Russian, Romanian summary) 63
composant de copulation (French, Romanian summary) 67
M. CAPROŞU, ŞT. CILIANU, R. BOZGA, I. CIOCOIU, M. PETROVANU et E. BÎCU, Synthèse de quelques nouveaux dérivés pyrudaziniques doués d'activite physiologique (French, Romanian summary) 71
C. LEONTE, E. CARP, S. DUMITRESCU, ŞT. CILIANU et R. BOZGA, Structures amidiques avec action sur le système nerveux central (III) (French, Romanian summary) 75

H. S. SELIGER, E. HAPP (West Germany) and AL. CAŞCAVAL, New 4-Chromanone Derivatives as Photostabilizers for Polymers (English, Romanian summary) 81
C. VASILE, GH. ADAMESCU, L. ODOCHIAN, I. GHICU and M. BADEA, Semi-PNIs of Polyvinylchloride and Methacrylate Esters (I) (English. Romanian summary) 87
N. OIŢĂ, M. NICU, V. NICU and E. TĂTARU, Contributions to the Study of the Acylation Reaction of Polyoles, in the Presence of Zinc Chloride (English, Romanian summary) 91
M. RUSU, S. PETROVAN and C. IBĂNESCU, Films from Ethylene—Vinyl Acetate Copolymers (English, Romanian summary) 95
BOOK REVIEWS 99

BULETINUL INSTITUTULUI POLITEHNIC DIN IAŞI
Tomul XXXVI (XL), Fasc. 1—2, 1990
Secţia II
CHIMIE ŞI INGINERIE CHIMICĂ

УДК

СИНТЕЗ И ИССЛЕДОВАНИЕ ПОЛИФОСФИНАТОВ Nb(IV)

И. РОШКА, ЕЛЕНА ШТЕФАНКУ, Н. ФОКА и М. ПАЛАМАРУ

1. Введение

В последнее время с целью получения новых термостойких материалов проводятся широкие исследования различных координационных полимеров на основе диорганофосфиновых кислот и различных катионов переходных металлов [1]...[8].

Особено интересными являются полимеры диорганофосфиновой кислоты с различными катионами, полученные Коршаком и сотр. [1] ... [3]: эти полимеры разлагаются при температурах выше 350°С.

В этом сообщений описано получение и исследование некоторых свойств координационных полиметор ниобии на основе дифенилфосфиновой и 2,8-диметилфеноксофосфиновой кислот.

2. Экспериментальная часть

Диметилфосфиновую кислоту $(C_6H_5)_2PO_2H$, получали по описанным ранее методом [11]. После перекристаллизаций из этанола т. пл. 192°...193°С (по литературным данным т. пл. 190°...192°С. [11]), 2,8 - диметилфеноксофосфиновую кислоту:

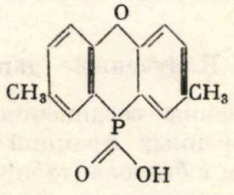

получали по методике Фридмана, Дока и Эдмистена [12].

После перекристаллизаций из этанола, т. пл. 315°...317°С (по]12] т. пл. 300°С).

Ацетилацетонат Nb(IV), $Nb(C_5H_7O_2)_4$, получали по основной описанной ранее методике [13] из холодного раствора $NbOCl_2$ ацетилацетона и раствора Na_2CO_3 10% а потом перекристаллизовывали из этанола при 40°С.

Тщательно перемешанную смесь 0,02 моля дифенилфосфиновой кислоты и 0,01 моля ацетилацетона Nb(IV) нагревали в колбе, снабжённой

прямым холодильником, охлаждаемый прмёмником для удаления ацетилацетона и трубкой для ввода чистого азота.

При 180°С смесь начинает плавиться. В тегение 30 мин. поднимают температуру от 180° до 190°С при этом происходит полное расплавление реакционной смеси и начинается выделение ацетилацетона. По мере отгонки ацетилацетона температуру постепенно повышают до 200°С приблизительно в течение 1 час, затем выдерживают при 200°С до полного прекращения выделения ацетилацетона. Полученный полимер (I) охлаждают тщательно измельчивают и последовательно экстрагируют в аппарате Сокслета спиртом, бензолом и хлороформом. Растворимая часть полимера в этих органических растворителях прибливительно 15....20% (от теоретического).

Аналогичным путём получены полидифенилфосфинат Nb(IV) (полимер *II*) из 0,4 моля дифенилфосфиновой кислоты и 0,01 моля ацетилацетоната Nb(IV).

К 0,02 моля 2,8-диметилфеноксофосфиновой кислоты растворённой в 350 мл бромбензоля добавляли при перемешиваний 0,01 моля ацетилацетоната Nb(IV) в 80 мл бромбензоля. Осадок отфильтровывали, промывали этанолом и экстрагировали в аппарате Сокслета этанолом. Очищенный таким образом продукт сушили в вакууме.

0,02 моля 2,8-диметилфеноксофосфиновой кислоты 0,01 моля ацетилацетонат Nb(IV) тщательно измельчивали и помещали в колбу снабжённую прямым холодильником и трубкой для ввода азота.

В течение 1,5 ч. температуру постепенно поднимали до 200°...240°С и реакционную смесь выдерживали при этой температуре 2 чезатем смесь охлаждали, снова тщательно измелчивали и грели в течение 4 ч. повышая температуру до 270°С. Полученные полимеры экстрагировали этанолом в аппарате Сокслета. Аналогично получали и полимер *I* из 0,04 моля 2,8-диметилфеноксосфиновой кислоты и 0,01 моля ацетилацетоната Nb(IV). Выход 85 ..,90% от теоретичсекого.

Осадок нерастворимого полимера в бензоле, этаноле или ацетоне промывали несколько раз этанолом и сушили до постоянного веса при 105° С. Растворённую фракцию полимера выделяли испарением растворителей исушили до постоянного веса. Выход 85...90% от теоретического.

3. Полученные данны

Все эти синтетизированные соединения — порошок белого цвета. Молекулярный вес растворённых фракций полимеров был определён эбуллиоскопическим методом в бензоле (таблица 1). Элементарный состав полимеров растворителей и нерастворителей идентичен (таблица 1).

Приведённые в таблице данные показывают, что элементарный состав полимеров, полученных на основе дифенил- и 2,8 диметилфеноксофосфиновых кислот, хорошо согласуется с вычисленным.

Термогравиметрический и дифференциальный термический анализ полимеров был проведён на дериватографе Ф. Паулика, И. Пауликом Л. Эрдей, при скорости нагревания 10 град/мин. в интервале температур 20°...700°С. При нагреваний на воздухе координационные полимеры разлагаются в две ступени. На рис. 1, приведены кривые ДТА и ТГА полимеров *I* и *II* при нагреваний их на воздухе.

Таблица 1

Элементарный состав и молекулярная масса растворимых фракций полимеров,

Полимер	Вычислено, [%]				Найдено, [%]				M
	Nb	C	P	H	Nb	C	P	H	
I	12,82	56,27	8,55	4,68	13,06	56,61	8,71	4,43	4 510
II	9,67	59,93	12,90	4,16	9,91	60,11	13,0	4,11	9 900
III	11,49	56,36	7,66	4,69	11,61	56,42	7,71	4,75	5 060
IV	8,23	59,52	10,98	4,25	8,36	59,71	11,10	4,31	12 050

Таблица 2

Значение порядка реакции и энергий активаций при термическом разложений координационных полимеров

Полимер	Порядок реакций		Энергия активаций разложения КДж/моль	
	стадия 1	стадия 2	стадия 1	стадия 2
I	0,76	0,83	118,4	138,9
II	0,80	0,89	123,8	145,3
III	0,82	0,88	128,1	150,2
IV	0,85	0,92	133,2	160,1

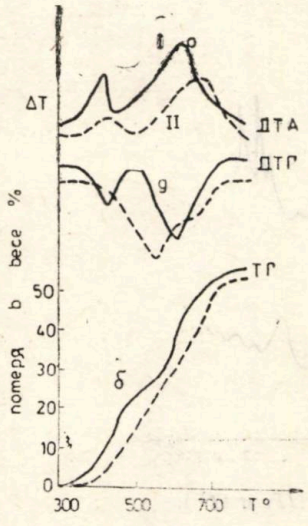

Рис. 1. — Кривые ДТА, ДТГ и ТГ полимеров *I* (—) и *II* (- - -).

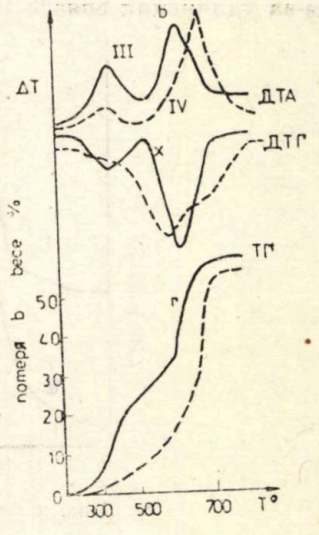

Рис. 2. — Кривые ДТА. ДТГ и ТГ полимеров *III* (—) и *IV* (- - -)

Найменьшей термостойкостью обладает полимер *I* : он начинает разлагатся при 320°C ; интенсивное разложение полимера наблюдается при 380°C.

На рис. 2 приведены кривые ДТА и ТГА полимеров *III* и *IV*.

Термостойкость этих полимеров приблизительно одинакова; оба полимера начинают интенсивно разлагаться около 300°C.

Наибольшей термостойкостью из полученных полимеров обладают полидифенилфосфинаты *I* и *II*. Первый начинает разлагаться при 380°C.

Разложение полимеров сопровождается энергичным выделением тепла (острые экзотермические пики на кривых ДТА).

Исследование координационные полимеры обладают более высокой термостойкостью чем соединения из которых они ыли получены, и это подтверждает факт образования полимеров мостикового типа с более устойчивыми хелатными циклонами. На всех стадиях порядок реакций и энергию активаций разложения определянли по методу [14].

На всех этаппах разложения порядок реакций близок к еднице (таблица 2).

Для более точной характеристики полученных полимеров были зарегистрированны ИК-спектры в области 400...4 000 $см^{-1}$ (прибор типа „Уникам").

Характерные полосы поглощения связи P—C не изменяются в полимерах по сравнению с соответствующими дифенилфосфиновой и 2,8-диметилфеноксофосфиновой кислотами, но изменяются полосы поглощения группировок PO_2.

При образование связей —P<(O, O)Nb полосы поглощения, соответствующие колебательной частоты группировок P=O, изменяются из-за удлинения связей P=O (рис. 3).

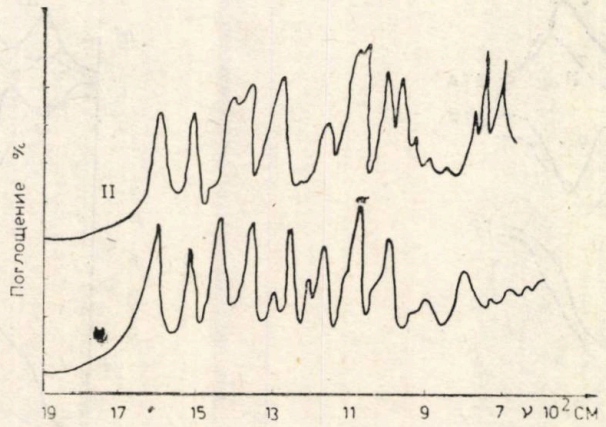

Рис. 3. — ИК-спектры полимеров (*II*) и (*IV*).

Эти колебательные частоты у полимеров меньше частот соответствующих свободных кислот.

Группировка P=O для всех использованных продуктов имеет характеристические полосы поглощения в области 1 150...1 180 $см^{-1}$.

Наиболее удобной областью спектра для определения фосфиновых кислот является область 700...900 $см^{-1}$. Полосы, лежащие в этом диапазоне, обусловлены неплоскими колебаниями ароматических групп CH фенильного ядра *I* и *II* полимеров и 1, 2, 4-тризамещённых бензольных ядер *III* и *IV* полимеров. Они узки, интенсивны и мало перекрываются.

Координационные полимеры *I* и *II* обладают свойствами полупроводников в области температур 20°...200°C Изменения удельной электропроводности этих порошковых полимеров показали, что они существенно зависят от температуры, подчиняясь закону $\sigma=\sigma_0 \exp(-E/2KT)$ (рис. 4).

Полимеры *I* и *II* имеют энергию активаций проводимости 0,68 и 0,89 эв соответственно и удельную электропроводность при 100°C равную 8.10^{-12} и 4.10^{-12} $см^{-1}$ $ом^{-1}$ соответственно.

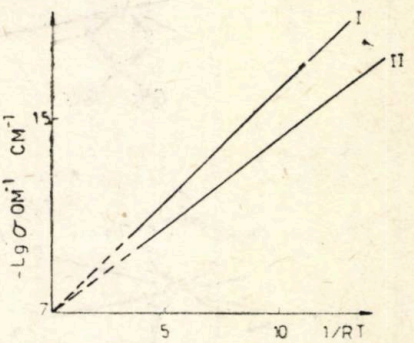

Рис. 4. — Изменение lg σ в зависимости от температуры для полимеров *I* и *III*.

Теоретически электронная конфигурация Nb (Kr), $4d^4$ $5s^1$ допускает осуществление различных координационных чисел.

Наличие Nb значительного числа свобоных орбит *4d* и *5s* обуславливают акцепторный характер его как центрального атома. Благодаря этоми Nb весьма склонен к образованию связей с кислородом и с другими донорами электронов. Отсюда, в зависимости от импользования для связей тех или иных орбит (*4d*, *5s*, *5p*), которые вэ нергитическом отношений у Nb весьма близки, последний, может выступать в качестве 2, 4, 5, 6, 7, 8 и даже 9-ковалентного центрального атома. Однако необходимо отметить определенную тенденцю Nbк повышенной координации, когда имеется избыток того или иного лиганда и отсутствуют стерические препятствия. Вследствие этой тенденции наиболее распостранены координационные числа 6 и 8 [9].

4. Выводы

Из эсперимантальных результатов следует, что на каждый ион Nb^{4+} приходится в полимерах *I* и *II* две ацетилацетонатных групп и два остатка дифенилфосфиновой или 2,8-диметилфеноксофосфиновой кислот. На каждый ион Nb^{4+} приходится в полимере *II* и *I* четыре остатка диорганофосфиновых кислот. Так, как эти радикалы имеют роль бидентатных лигандов посредством атомов кислорода, ионы Nb^{4+} могут реализовать устойчивое координационное восемь.

В соответствий с теорией поля лигандов [16] образование координационных полимеров происходит при образований молекулярных орбиталей (МО) между ионами Nb^{4+} и радикалами диорганофосфиновых кислот или ацетилацетона.

На основе из литературе и экспериментальных данных, приведённых в этой работе, очитаю что может быть оформулированна структура полимеров *I* и *II* приведена в рис. 5 .

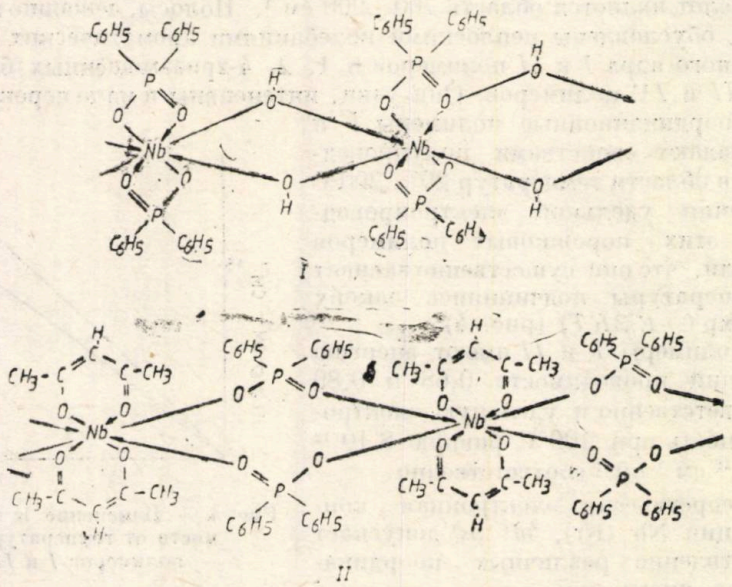

I

II

Рис. 5. — Структуры полимеров *I* и *II*.

Поступило с 15 февраля 1989 г.

Ясский политехнический институт,
Кафедра неорганической химии
и технологической и
аналитической химий

ЛИТЕРАТУРА

1. Коршак В. В., Круковский С. П., Ван Жун-Хан, Высокомол. соед., **Б9**, 583 (1967).
1. Коршак В. В., Круковский С. П., Ван Жун-Хан, Локшин Б. В., Высокомол. соед., **Б9**, 628 (1967).
3. * * * *Успехи в области синтеза элементоорганических полимеров.* Изд. Наука, Москва, 1966, 59.
4. Рошка И., Высокомол. соед., **В9**, 2086 (1973).
5. Соловкин А. С., Цветкова З. Н., Усп. химий, **11**, 1 394 (1962).
6. Blok B. P., Simikin J., Oconel L. R., J. Amer. Chem. Soc., **84**, 1 749 (1962).
7. Blok B. P., Rose L., Scouman C. W., Roth E., J. Amer. Chem. Soc., **84**, 3 200, (1962).
8. Crescenzi V., Rancotti V., Ripsmoti A., J. Amer. Chem. Soc., **88**, 391 (1966).
9. Roşca I., Bul. Inst. polit., Iaşi, **XVI (XX)**, *3—4*, s. II, 15 (1970).
10. Golgoţiu T., Roşca I., Bul. Inst. polit. Iaşi, **XVII (XXI)**, *1—2*, s. II, 1 (1971).
11. Roşca I., Bul. Inst. polit., Iaşi, **XVII (XXI)**, *3—4*, s. II, 13 (1971).
12. Golgoţiu T. Roşca I., Makromolek. Chem., **59**, 160 (1972).
13. Lewis J., Wilkins G. R., *Modern Coordination Chemistry.* Interscience Publ., N. Y., 1964.
14. Jorgensen K. C., *Absorbtion Spectra and Chemical Bounding in Complexes. Ligand Field Theory.* Interscience Publ, London, New-York, 1962.
15. Kosolapff G. M., J. Amer. Soc., **64**, 2 982 (1982).
16. Roşca I., *Compuşi termostabili ai acetilacetonaţilor de Cr (III), Mn (II), Cr (II), Ni (II), UO_2^{2+} cu acizi şi tioacizi dialchilfosfinici şi difenilfosfinic.* Докт. дисс., Ясский полит. инст., 1975.

17. Drăgulescu C., Petrovici E., *Chimie structurală modernă.* Vol. **8**, *Chimia coordinaţiei.* Ed. Acad. R.S.R., 1977.
18. Freeman, E. S., Carroll B., J. Phys. Chem., **62**, 394 (1958).
19. Orgel I., *An Introduction to Transition Metal Chemistry, Ligand Field Theory.* Interscience Publ., London, New-York, 1962.
20. Roşca, I., Bul., Inst. polit., Iaşi, **XXII (XXVII)** , *1—2*, s. II, 21 (1977).
21. Ginns N. R., Hamilton B. J., Inorg. Nucl. Lett., **6**, 245 (1972).
22. Stockelmann G., Kettrup A., Specker N., Angew. Chem., **79**, 530 (1968).
23. Липатова И. П., Семеонова Е. И., Изв. Акад. Наук СССР, ОНХ, *1*, 6 (1967).

SINTEZA ŞI STUDIUL POLIFOSFINAŢILOR DE Nb (IV)

(Rezumat)

Se studiază sinteza polimerilor de coordinaţie ai Nb(IV) cu acizii difenifosfinic şi 2,8 dimetil-fenoxofosfinic ca o continuare a preocupărilor anterioare în acest domeniu.

Datele experimentale provin de la spectrele de absorbţie în IR, termocinetica descompunerii, conductibilitatea electrică şi energia de activare.

Pe baza datelor experimentale şi a referirilor bibliografice se propune structura compuşilor sintetizaţi.

BULETINUL INSTITUTULUI POLITEHNIC DIN IAŞI
Tomul XXXVI (XL), Fasc. 1—2, 1990
Secţia II
CHIMIE ŞI INGINERIE CHIMICĂ

C.D. 546.76

COMPLEXES POLYNUCLEAIRES DU Cr(III)

PAR

I. BERDAN, AL. CAŞCAVAL et GABRIELA BUNDUC

1. Introduction

L'ion Cr (III) manifeste un caractère d'acide L e w i s de classe *a* puisque la coordination des ligands autour de lui se réalise à base de liaisons ioniques [1]. Ce caractère est illustré par sa haute capacité de former des complexes mono- et polynucléaires avec des ligands qui contiennent des atomes donneurs à forte électronégativité (O, N, F) [2].

La symétrie octaédrique caractérise la plupart des complexes hexacoordonnés du Cr (III) avec les ligands azote- et oxygène-donneurs. La configuration tétraédrique, moins importante, est caractéristique à l'ion $[CrCl_4]^-$ se trouvant dans le sel complexe $[PCl_4][CrCl_4]$ [3].

D'autre part il faut remarquer la capacité de l'ion Cr (III) de former facilement des complexes polynucléaires conformément aux équilibres (1) et (2) qui dépendent de la température, pH et de la concentration des réactifs :

$$[Cr(H_2O_6)^{3+} + H_2O \rightleftharpoons [Cr(OH)(H_2O)_5]^{2+} + H_3O^+, \quad (1)$$

$$2[Cr(OH)(H_2O)_5]^{2+} + SO_4^{2} \rightleftharpoons [Cr_2(OH)_2(H_2O)_6(SO_4)]^{2+} + 4H_2O. \quad (2)$$

Dans le but d'approfondir les connaissances concernant la capacité complexante de l'ion Cr (III,) on étudie dans ce qui suit le système de réaction Cr^{3+} (M) — [N-salicylidène]-amino-2-pyridine (HL).

2. Partie expérimentale

Comme source de Cr (III) on a utilisé $Cr(NO_3)_3 \cdot 9H_2O$ en solution aqueuse ou aqueuse — alcoolique ($H_2O - C_2H_5OH$). Le titre de la solution a été déterminé par deux méthodes : a) la méthode spectrophotométrique (courbe d'étalonage basée sur la détermination de l'absorbance des solutions de K_2CrO_4 obtenues par oxydation de l'ion Cr (III) à l'aide de H_2O_2 en milieu alcalin) : b) la méthode volumétrique (titrage de l'ion Cr^{3+} en solution neutre ou faiblement acide avec du $KMnO_4$.

Le ligand, préparé par condensation de l'aldéhyde salicylique avec de l'amino-2-pyridine:

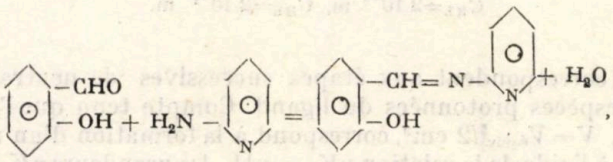

a été utilisé sous forme de solutions alcooliques (C_2H_5OH).

Les propriétés acido-basiques du ligand ainsi que le processus de formation des complexes dans le système mentionné ci-dessus ont été étudiées par voies pH-métriques et spectrophotométriques. La détermination du pH a été effectuée à l'aide du pH-mètre type MV-85 (R.D.A.). Les spectres d'absorption électroniques ont été obtenus avec les appareils de type Specol (400... 800 nm) et Spekord UV-VIS (200... 800 nm).

La formation des complexes a été suivie en faisant réagir la solution aqueuse de Cr (III) avec des quantités appropriées de ligand à température ordinaire. Au cours de la réaction la couleur du mélange devient bleue-verte qui s'enfonce au fur et à mesure qu'on ajoute de l'excès de ligand.

3. Résultats et discussions

3.1. Les propriétés acido-basiques du ligand HL

En tant que base L e w i s , le ligand HL (HL = $C_{12}H_{10}N_2O$) contient trois points basiques à savoir : le groupement —OH, l'atome d'azote pyridinique et celui du groupement azo-méthinique — tous les deux à l'état d'hybridation sp^2 avec une faible basicité due à la conjugaison $p-\pi$.

Les propriétés acido-basiques du ligand ont été suivies par le titrage de 20 cm^3 de solution 2.10^{-2} m avec une solution de HCl 2.10^{-1} m. Sur le graphique de la fonction $pH=f(V_{HCl})$ (Fig. 1) on observe l'apparition de deux points

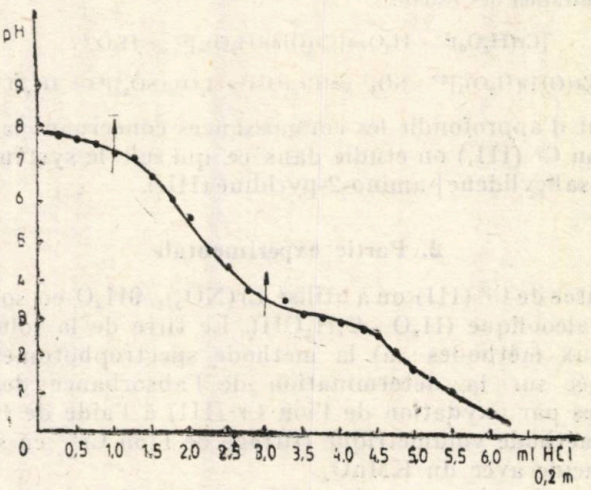

Fig. 1. — Titrage pH-métrique de la solution de HL avec de l'acide chlorhydrique ; V_{HL} =20 cm^3 ; $C_{HL}=2.10^{-2}$ m, $C_{HL}=2.10^{-1}$ m.

d'inflexion qui correspondent aux étapes successives de neutralisation avec formation des espèces protonnées du ligand. Compte tenu que l'addition d'un volume de HCl, $V=V_{équiv}/2$ cm^3, correspond à la formation d'un mélange tampon, on calcule, à l'aide de la relation $pK_{ai}=pH_i$, les grandeurs pK_{ai} et pK_{bi} dont les valeurs sont portées dans le Tableau 1.

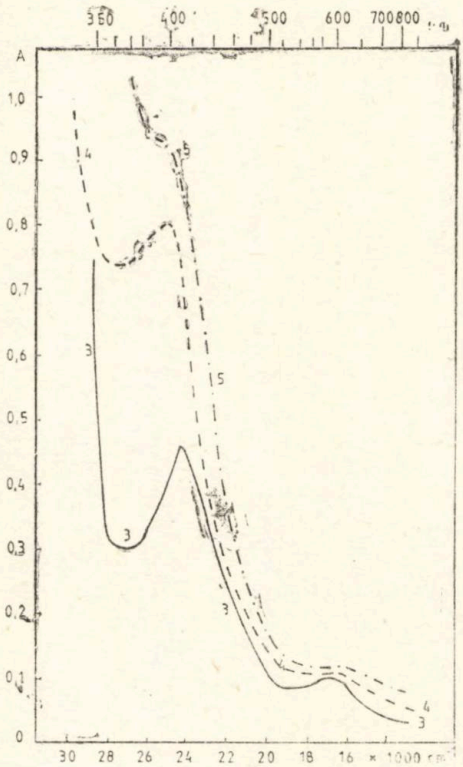

Fig. 2. — Spectres d'absorption dans le visible ; cuve : 1 cm ; —$Cr(NO_3)_3.\ 9H_2O$, $C=5.10^{-1}$ m ; solution aqueuse ; – – – $Cr(NO_3)_3.9H_2O$, $C=2.10^{-1}$ m ; solution aqaueuse; –.–.–HL, $C=2.10^{-2}$ m.

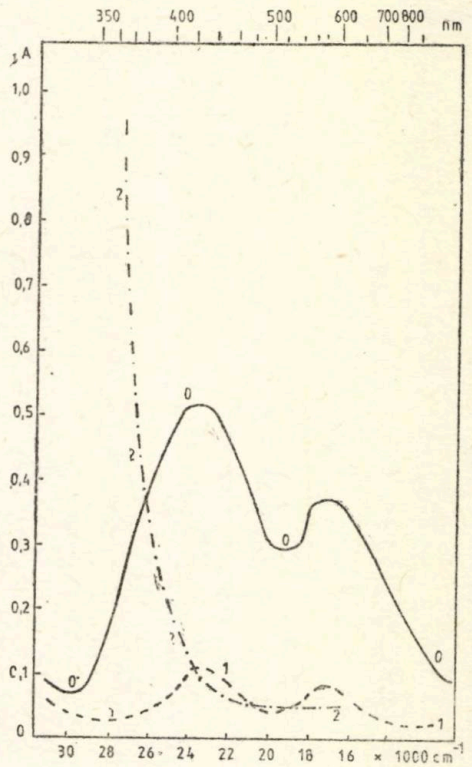

Fig. 3. — Spectres d'absorption dans le visible des mélanges Cr (III)—HL ; cuve : 1 cm; —Cr (III)/HL=1: 1; $Cr^{3+}=5.10^{-1}$ m; – – –Cr (III)/HL =1 : 2; $Cr^{3}=5.10^{-1}$ m; –.–.–Cr (III)/HL=1 : 3 ; $Cr^{3+}=5.10^{-1}$ m (en solution de $C_2H_5OH-H_2O$, 1 : 1).

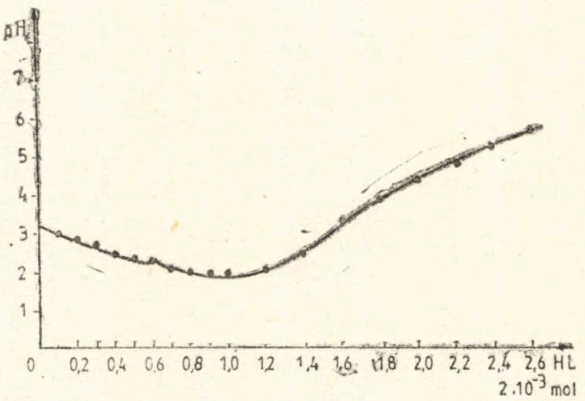

Fig. 4.—Titrage de la solution de $Cr(NO_3)_3.9H_2O$ avec la solution de HL ; $V^{3+}_{Cr}=10$ cm³, $C^{3+}_{Cr}=2.10^{-2}$ m, $C_{HL}=2.10^{-1}$ m.

La première étape de neutralisation correspond à la forme protonnée de l'atome d'azote pyridinique ($pK_{b1}=6,7$) avec une basicité plus forte que celle de l'atome d'azote du groupement azo-méthinique ($pK_{b2}=10,4$).

Le système de réaction Cr (III)—ligand, en solution alcool éthylique—eau (1 : 1), a été étudié par voies pH-métrique et spectrophotométrique. Ainsi, on a enregistré les spectres d'absorption dans le visible, de l'ion $[Cr(H_2O)_6]^{3+}$ et du ligand (Fig. 2). Dans le spectre de l'ion $[Cr(H_2O)_6^{3+}$ on retrouve deux

Tableau 1

Les valeurs expérimentales de pK_{ai} et pK_{bi} du ligand HL

	pK_{a1}	pK_{a2}	pK_{b1}	pK_{b2}
Ligand HL	7,3	3,6	6,7	10,4
Forme protonné	—	—	$[H_2L]^+$	$[H_3L]^{2+}$

des trois bandes d'absorption propres aux complexes octaédriques (d^3) du Cr(III) dont les caractéristiques sont données dans le Tableau 2.

Tableau 2

Les caractéristiques spectrales, dans le domaine visible, de l'ion $[Cr(H_2O)_6]^{3+}$

Transition électronique	Valeurs théoriques			Valeurs expérimentales		
	Bande	$\bar{\nu}$, [cm^{-1}]	ε	$\bar{\nu}$, [cm^{-1}]	λ, [nm]	ε
$^4A_{2g} \rightarrow {}^4T_{2g}(F)$	ν_1	17 400	17	17 200	580	15
$^4A_{2g} \rightarrow {}^4T_{1g}(F)$	ν_2	24 600	15	23 800	421	17
$^4A_{2g} \rightarrow {}^4T_{1g}(P)$	ν_3	37 800	4	apparait dans l'ultraviolet		

Lors de l'interaction de l'ion Cr^{3+} avec le ligand apparaissent, successivement, des espèces complexes dont les équilibres de formation sont influencés par le pH du milieu et la concentration des réactants. Les mélanges des solutions Cr(III) — L, ayant de différents rapports molaires, contiennent des complexes solubles de couleur bleue-verte, stables, dans l'intervalle de pH=6...8. À pH>8, le métal précipite sous forme de $Cr(OH)_3$.

Les spectres électroniques dans le visible des mélanges Cr(III)—ligand indiquent une série de modifications des caractéristiques spectrales par rapport aux réactants (Fig. 3). Ainsi, pour les mélanges ayant des rapports molaires Cr (III)/HL=1 : 1; 1 : 2 et 1 : 3, à pH=7,5, on observe des modifications concernant la position et l'intensité des bandes ν_1 et ν_2 du spectre de l'ion hydraté, $[Cr(H_2O)_6]^{3+}$. La bande ν_2, située à 421 nm, est deplacée par effet hypsochrômique (407 nm pour 1 : 1 ; 400 nm pour 1 : 2 et épaulement à point d'inflexion au-dessous de 400 nm pour 1 : 3), avec l'accroissement de l'absorbance

(ε_1=90 l.mol^{-1} cm^{-1}, ε_2=160 l.mol^{-1}.cm^{-1} et ε_3=180 l.mol^{-1}.cm^{-1}). La bande ν_1 est deplacée par effet bathochrôme (590 nm) avec une légère intensification de l'absorbance ($\varepsilon \simeq 70...80$ l.mol^{-1}.cm^{-1}). Les modifications des trois bandes d'absorption sont dûes à la coordination du ligand polydenté à l'ion central Cr(III).

De cette manière la formation des complexes dans le système étudié correspond à l'équilibre suivant :

$$(3) \qquad m\mathrm{Cr}^{3+} + n\mathrm{HL} \rightleftharpoons [\mathrm{Cr}_m\mathrm{L}_n]^{3m-n} + n\mathrm{H}^+.$$

La diminution du pH lors du processus (3) a été mise évidence par le titrage de la solution aqueuse de $Cr(NO_3)_3.9H_2O$ avec la solution alcoolique de ligand (Fig. 4).

Les déterminations ultérieures d'absorbance ont été effectuées à λ_{max} = =590 nm à laquelle l'absorbance du ligand est négligeable. La lois de L a m b e r t—B e e r est valable dans le domaine de concentrations compris entre 0,1.10^{-2} mol/l et 1,1.10^{-2} mol/l (Fig. 5).

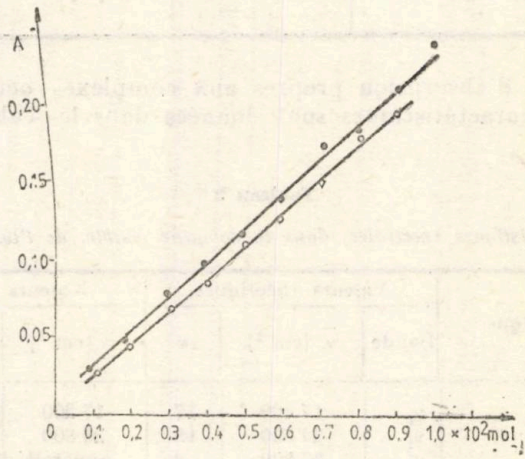

Fig. 5. — Verification de la loi de L a m b e r t— B e e r; o— Cr (III)/HL= 1 : 1; ●—Cr(III)/HL=1 : 2.

3.2. La composition et la stabilité des complexes

La composition et la stabilité des complexes ont été déterminées par deux méthodes spectrophotométriques : a) la méthode des variations continues [4] ; b) la méthode logarithmique (B e n t et F r e n c h) [5].

Dans la Fig. 6 on présente les résultats expérimentaux concernant l'application de la méthode des variations continues pour la déterminatioan du rapport molaire de combinaison Cr (III)/HL. La représentation graphique de la dépendence absorbance — composition du système met en évidence un maximum qui correspond au rapport molaire Cr^{3+}/HL=3 : 2. Le même résultat a été obtenu par l'utilisation de la méthode logarithmique (Fig. 7) qui repose sur la détermination de l'absorbance de deux séries de mélanges Cr^{3+}—HL : a) [Cr^{3+}] = const. et [HL] = variable ; b) [Cr^{3+}] = variable et [HL] = =const.

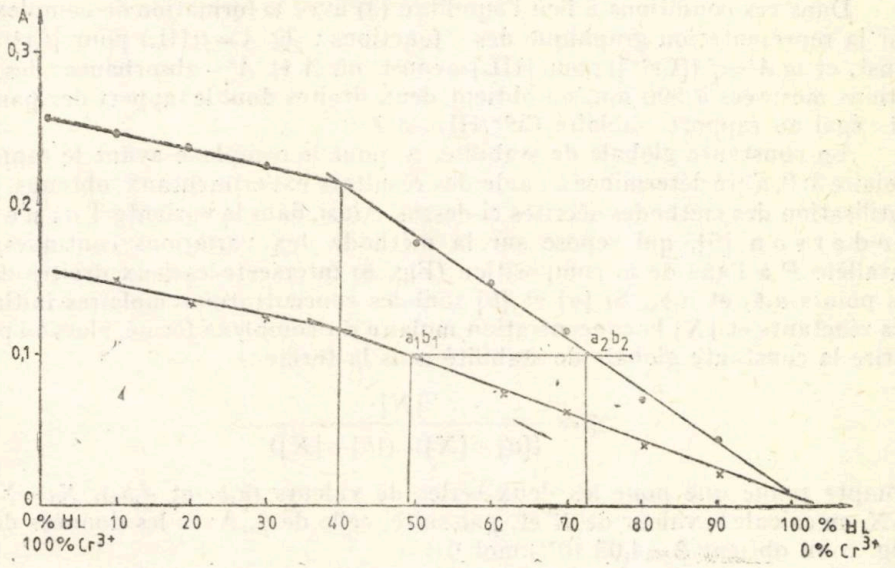

Fig. 6. — Données concernant la détermination du rapport molaire Cr(III)/HL par la méthode des variations continues.

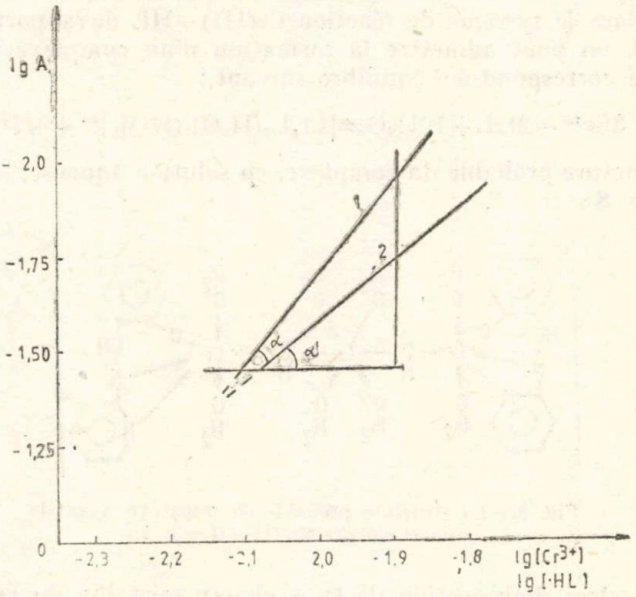

Fig. 7.— Données concernant la détermination du rapport molaire Cr(III)/HL par la méthode logarithmique ; *1* — $[Cr^{3+}]$ = const. ; *2* — [HL] = const.

Dans ces conditions a lieu l'équilibre (3) avec la formation de complexes. Par la représentation graphique des fonctions : $\lg A = f(HL)$ pour $[Cr^{3+}] = const.$ et $\lg A' = f([Cr^{3+}])$ pour $[HL] = const.$ où A et A' — absorbances des solutions mesurées à 590 nm, on obtient deux droites dont le rapport des pantes est égal au rapport molaire $Cr^{3+}/HL = 3/2$.

La constante globale de stabilité, β, pour le complexe ayant le rapport molaire 3: 2, a été déterminée à l'aide des résultats expérimentaux obtenus par l'utilisation des méthodes décrites ci-dessus. Ainsi, dans la variante Turner—Anderson [6], qui repose sur la méthode dex variations continues, la parallèle P à l'axe de la composition (Fig. 6) intersecte les deux droites dans les points a_1b_1 et a_2b_2. Si $[a]$ et $[b]$ sont les concentrations molaires initiales des réactants et $[X]$ la concentration molaire du complexe formé, alors on peut écrire la constante globale de stabilité sous la forme :

$$\beta = \frac{[X]}{([a]-[X])\ ([b]-[X])}.$$

Compte tenue que pour les deux séries de valeurs (a_1b_1 et a_2b_2), $X_1 = X_2 = X$, on calcule la valeur de X et, par suite, celle de β. Avec les données de la Fig. 6 on obtient $\beta = 4{,}05.10^3$ l.mol^{-1}.

En utilisant les données obtenues par l'application de la méthode logaritmique (Fig. 7), on obtient la valeur $\beta = 7.10^3$ l.mol^{-1}, comparable avec celle obtenue ci-dessus.

3.3. Données sur la structure du complexe 3 : 2. Spectres de type champ cristallin

En s'appuyant sur les déterminations pH-métriques et spectrophotométriques, dans le système de réaction Cr(III)—HL de rapport molaire 3 : 2, à pH = 7...8, on peut admettre la formation d'un complexe trinucléaires à ponts *ol* qui correspond à l'équilibre suivant :

(5) $$3Cr^{3+} + 2HL + 10H_2O \rightleftharpoons [Cr_3L_2(H_2O)_8(HO)_2]^{5+} + 4H^+.$$

La structure probable du complexe, en solution aqueuse, est représentée dans la Fig. 8 :

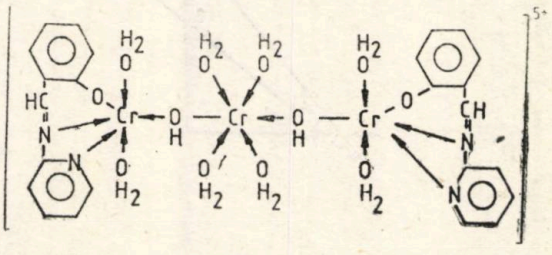

Fig. 8.—La structure probable du complexe ayant le rapport molaire Cr(III)/HL = 3 : 2.

Les spectres d'absorption de type champ cristallin du complexe $[Cr_3L_2(H_2O)_8(OH)_2]^{5+}$ ont été interpretés à l'aide du diagramme des niveaux énergétiques propres au cas $d^3(Cr^{3+})$ de la microsymétrie octaédrique (O_h). Les

trois transitions électroniques qui produisent les trois bandes d'absorption ν_1, ν_2 et ν_3, caractéristiques aux complexes du Cr (III), sont présentées dans la Fig. 9.

Dans l'hypotèse d'un champ de ligand faible, les trois bandes d'absorption du complexe 3 : 2 correspondent aux transitions suivantes :

ν_1 : $^4A_{2g} \rightarrow {}^4T_{2g}(F)$; $E_1 = 10\ Dq$; 17 200 cm^{-1} (590 nm) ;

ν_2 : $^4A_{2g} \rightarrow {}^4T_{1g}(F)$; $E_2 = 18\ Dq$; 23 800 cm^{-1} (421 nm) ;

ν_3 : $^4A_{2g} \rightarrow {}^4T_{1g}\ (P)$; $E_3 = 12Dq + 15\ B$; en ultra-violet.

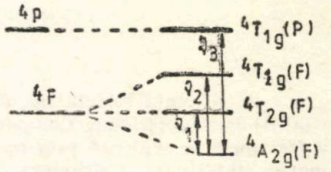

Fig. 9. — Le diagramme des niveaux énergétiques propres au cas $d^3(Cr^{3+})$ dans la symétrie octaédrique (O_h).

On a calculé aussi les caractéristiques principales des spectres champ cristallin : le paramètre de scission, le paramètre R a c a h (B) et le terme nephélauxétique (β).

Le paramètre de scission est $\nu_1 = 10\,Dq$ et donc $Dq = 1\,720$ cm^{-1}. Le paramètre B, pour l'ion libre (Cr^{2+}) est $B_{\text{ion libre}} = 918$ cm^{-1} et la valeur B_{complexe} a été déterminée par une méthode graphique [7], basée sur la représentation du type $\nu_m/\nu_n = f(Dq/B)$. En utilisant le rapport $\nu_2/\nu_1 = 1{,}38$ on obtient $B_{\text{complexe}} = 781$ cm^{-1}. Par conséquent, $\beta = B_{\text{complexe}}/B_{\text{ion libre}} = 0{,}85 < 1$. Il s'ensuit que la liaison Cr—ligand du complexe présente un caractère covalent plus faible que celui existant dans les complexes du Cr^{3+} avec des ligands N-donneurs tels que dipyridile et éthylène diamine dont les valeurs de β sont situées entre 0,55 et 0,67.

4. Conclusions

Dans le système de réaction Cr (III) — [N-salycilidène]-amino-2-pyridine, en solution d'eau—alcool éthylique, à pH = 7...8, dans la présence d'un excès de ligand (HL), se forme l'espèce complexe de rapport molaire $Cr^{3+}/HL = 3/2$ avec la constante globale de stabilité $\beta = 0{,}4.10^3$ $l.mol^{-1}$. Le spectre électronique du complexe, interprété sur la base de la théorie du champ cristallin, indique la formation d'un complexe trinucléaire de microsymétrie octaédrique dans lequel la liaison métal—ligand présente un faible caractère covalent.

Reçue le 27 octobre 1989

Institut Polytechnique, Jassy,
Chaire de Chimie et Technologie Anorganique et Chimie Analytique
et
Chaire de Chimie et Technologie Chimique Organique et Macromoleculaire

BIBLIOGRAPHIE

1. A h r l a n d S., C h a t t J., D a v i e s N. R., Quart. Rev., **12**, 265 (1958).
2. C a r l s s o n S. L., I r v i n g H., J. Chem. Soc., 4 390 (1954).
3. D u r r a n t P. I., D u r r a n t B., *Introduction to Advanced Inorganic Chemistry*. Longmans, London, 1971

4. Job P., Ann. Chim. (France), 113 (1928).
5. Bent H., French C., J. Amer. Chem. Soc., **63**, 568 (1941).
6. Turner E., E. Anderson R. C., J. Amer. Chem. Soc., **71**, 932 (1949).
7. Lever A. B. P., *Inorganic Electronic Spectroscopy*. Elsevier, Amsterdam, New-York, 1968.

COMPLECŞI POLINUCLEARI Al Cr(III)

(Rezumat)

Se prezintă rezultatele obţinute privind studiul sistemului de reacţie Cr(III) —[N-salicilidenj-2-aminopiridină. Comportarea ionului Cr(III) ca acid Lewis (M) faţă de ligand (HL) a fost pusă în evidenţă prin formarea de combinaţii complexe polinucleare de tip M_nL_m. Formarea, stabilitatea şi structura complecşilor au fost studiate prin metode pH-metrice şi spectrofotometrice. Spectrele de absorbţie de tip cîmp cristalin ale complexului de raport molar M/L= =3/2 au fost interpretate pe baza diagramei de nivele energetice proprii cazului $d^3(Cr^{3+})$ corespunzătoare microsimetriei O_h.

BULETINUL INSTITUTULUI POLITEHNIC DIN IAȘI
Tomul XXXVI (XL), Fasc. 1—2, 1990
Secția II
CHIMIE ȘI INGINERIE CHIMICĂ

D.C. 537.4 ; 547.372.35 ; 547.466.8

RADIOPROTECTION EFFECT OF RUTIN-CYSTEINE DETERMINED BY ELECTRONIC PARAMAGNETIC RESONANCE (E. P. R.)

BY

SORIN DAN MIRON, AL. CECAL and TRAIAN BARAN

1. Introduction

The living cells, as it is known, have on their structure a large quantity of water. When the ionising radiation is absorbed, the energy is given to the medium and consequently in principal, to the water. This energy brings out fundamental modifications in the absorbant medium that transformes the molecules of water in nonstabile entities, highly reactive, able to provoke chemical and biochemical irreversible modifications. Schematically those modifications are :

$$\rightsquigarrow H_2O \rightarrow H_2O^+ + e^-, \qquad \rightsquigarrow H_2O \rightarrow H_2O^* \qquad \rightsquigarrow H_2O^* \rightarrow H^\cdot + HO^\cdot$$

The radicals formed are able to react according to the following mechanism :

$$H^\cdot + H^\cdot \rightarrow H_2, \quad HO^\cdot + HO^\cdot \rightarrow H_2O_2, \quad HO^\cdot + HO^\cdot \rightarrow HO_2 + H^\cdot,$$

$$HO_2^\cdot + HO_2^\cdot \rightarrow H_2O_2 + O_2, \quad O_2 + H^\cdot \rightarrow HO_2^\cdot$$

The perhydroxil radical could initiate in blood a number of chemical reactions that transformes Fe^{2+} in Fe^{3+} and the structure of the hemoglobine is altered. The mechanism of this process is :

$$H^\cdot + O_2 \rightarrow HO_2, \quad HO_2^\cdot + H^+ + Fe^{2+} \rightarrow Fe^{3+} + H_2O_2,$$

$$H_2O_2 + Fe^{2+} \rightarrow Fe^{3+} + HO^- + HO^\cdot, \quad HO^\cdot + Fe^{2+} \rightarrow Fe^{3+} + HO^-$$

Therefore we state that the chemical action of the radiation is reduced to a competition between the oxydation and reduction reactions [4]...[6].

On the basis of experimental data the action mechanism of the chemical radioprotectors are grouped together as follows [1] ... [3], [7], [8] : a) free radicals capture; b) mixed disulphide formation ; c) biochemical shock.

We used electronic paramagnetic resonance for testing the efficiency of a cocktail of radioprotector substances (rutin-cysteine) which, in the dose

we used, is not toxic for the body. We obtain rutin-cysteine from rutozid and cysteine by a Mannich condensation [9], [10].

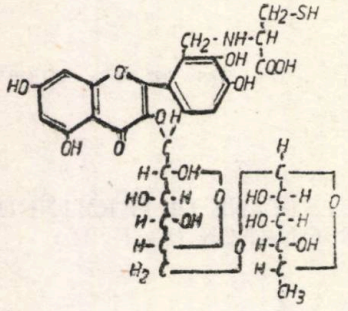

Fig. 1

The structure of rutin-cysteine is represented in Fig 1.

Rutin-cysteine is an unitary substance, yellow in colour, cristalline lens, highly soluble in water and the melting point is 118°...120°C.

The apparatus used in that experiment is a spectrograph ART-5 which equip the Biophysics Laboratory of the Institute of Medicine and Pharmacy, Jassy.

2. Experimental

The experiences had been effected on transfusion blood which was beforehand lyophilysated and represented complete blood. Plasma, red cells, leucocytes and red cells membranes were obtained from complete blood by specific methods.

X-rays irradiation was given in a unic dose of 1 000 R and respectively 10 KR. The samples were divided in three groupes : a) nonirradiated samples; b) 1 000 R and 10 KR irradiated samples ; c) samples with radioprotector rutin cysteine (800 mg /Kg body) administred 10...15 min. before being irradiated with 1 000 R and 10 KR.

The separation of the components by centrifugation has been done either after radioprotectors introduction and irradiation, or before irradiation and radioprotector administring.

3. Results and Discussion

The experimental data are presented in Tables 1...4.

Table 1

Number of Paramagnetic Centres in the Blood Samples with and without Rutin-Cysteine (800 mg/Kg Body), *1 000 RX-Rays Irradiated*

Probes	Number of paramagnetic centres, $[\times 8\times10^{16}]$			
	Normal		1 000 R X-rays administred	1 000 R X-rays administred+ rutin-cysteine
	1	2	1	2
Total blood	14.5×10^{-3}	15.0×10^{-3}	11.49×10^{-3}	9.5×10^{-3}
Plasma	10.25×10^{-3}	13.6×10^{-3}	5.98×10^{-3}	9.37×10^{-3}
Red cells	18.8×10^{-3}	19.7×10^{-3}	18.8×10^{-3}	22.2×10^{-3}
Leucocytes	6.83×10^{-3}	5.9×10^{-3}	8.54×10^{-3}	5.3×10^{-3}
Hemoglobine	17.94×10^{-3}	18.74×10^{-3}	13.35×10^{-3}	7.11×10^{-3}
Membranes	17.63×10^{-3}	25.0×10^{-3}	11.63×10^{-3}	5.3×10^{-3}

From the Table 1 it may be observed that after irradiation with X-rays in a unic dose of 1 000 R, the N.P.C. (Number of Paramagnetic Centres), in

Table 2

Number of Paramagnetic Centres in the Blood Samples Separated before the Introduction of the Radioprotector Rutin-Cysteine (800 mg/Kg Body), *before Beeing Irradiated with 10 000 R X-Rays*

Probes	Number of paramagnetic centres, [$\times 8\times10^{16}$]		
	Normal	1 000 R X-rays irradiated	1 000 R X-rays+ rutin-cysteine administrated
Total blood	16.49×10^{-3}	8.75×10^{-3}	18.88×10^{-3}
Plasma	Nearly the sensibility limit of the apparatus		
Red cells	6.625×10^{-3}	12.113×10^{-3}	15.53×10^{-3}
Leucocytes	6.25×10^{-3}	9.13×10^{-3}	9.38×10^{-3}
Hemoglobine	5.44×10^{-3}	4.63×10^{-3}	7.0×10^{-3}
Membranes	7.9×10^{-3}	4.75×10^{-3}	9.38×10^{-3}

Table 3

Number of Paramagnetic Centres in the Blood Samples Separated before Rutin-Cysteine Administred

Probes	Number of paramagnetic centres, [$\times 10^{16}$]	
	Normal	Probes+ rutin-cysteine 800 mg/Kg body
Total blood	11.5×10^{-3}	10.7×10^{-3}
Plasma	Nearly the sensibility limit of the apparatus	
Red cells	2.6×10^{-3}	3.3×10^{-3}
Leucocytes	12.14×10^{-3}	17.5×10^{-3}
Hemoglobine	11.5×10^{-3}	14.7×10^{-3}
Membranes	0.94×10^{-3}	6.39×10^{-3}

Table 4

Number of Paramagnetic Centres in the Blood Samples with and without Rutin-Cysteine (800 mg/ Kg Body) *Irradiated with 10 KR X-Rays*

Probes	Number of Paramagnetic Centres, [$\times 10^{16}$]		
	Normal	10 KR X-yays administred	10 KR X-rays+ + rutin-cysteine administred
Total blood	14.55×10^{-3}	16.0×10^{-3}	10.5×10^{-3}
Red cells	18.8×10^{-3}	26.0×10^{-3}	20.2×10^{-3}
Leucocytes	17.63×10^{-3}	24.0×10^{-3}	15.0×10^{-3}

the irradiated samples, is smaller then in the nonirradiated ones for the red and the white cells. With the samples in which we add rutin-cysteine prior, after irradiating the N.P.C. is nearly the normal value (in the absence of irradiation) for plasma and leucocytes, but for hemoglobine and red cells membranes the N.P.C. is highly decreased.

Examining the Table 2 it results, on the one hand, that the 1 000 R irradiation causes diminution of the N.P.C. for complete blood, hemoglobine and red cells membranes but on the other hand we may notice the increase of the N.P.C. for red and white cells. In the samples with radioprotector (rutin-cysteine) we may notice values of the P.C. nearly the normal ones for complete blood and red cells membranes.

In the Table 3 we intended to give emphasis to the N.P.C. in the probes with and without rutin-cysteine, noticing the fact that the N.P.C. have a significantly increase for red cells membranes for red and white cells.

The radioprotection effect of rutin-cysteine is remarkably revealed by studying the Table 4; one may observe that irradiating the samples with a 10 KR dose the values of P.C. for the samples with rutin-cysteine are nearly to the normal ones for all the cases.

If the primary physical effect is ionisation, the primary, chemical effect, is oxidation. The oxidation causes the primary biological effect. It is normal then to obtain protection against it by reducing substances. This reduction function is carried out by cysteine which has a free —SH function that gives a disulphuric bridge —S—S—, probably by protecting the enzymes which have the —SH function. The radioprotection —SH functions forms mixed disulphide with the —SH functions of the proteins. The disulphuric bridge —S—S— fulfils the role of derivation the migratory energy and stabilizes the nonpair electron.

4. Conclusions

The radioprotector effect of rutin-cysteine is positive and it is better than that of the two substances administrated separately leading to the following conclusions :

a) We have to find out mixtures of radioprotectors substances which can satisfy varied levels of the activity mechanism of the ionising radiation.

b) The probable activity mechanism of rutin-cysteine concernes the physical potential, because of the rutin which bloks the hydrolising enzymes (proteolitics enzymes), which are released after irradiation.

c) The intimate mechanism of the radioprotector process due, on the one hand, to the forming of mixed disulphid between the molecules of rutin-cisteine which has a —SH group and the enzymes with —SH groups and on the other hand, to inhibite the proteolitics enzymes, by the structure of rutozid.

Received, April 27, 1989

Institut of Medicine and Pharmacy, Jassy
and
Polytechnic Institute, Jassy,
Department of Anorganic Chemistry
and Technology and Analytical Chemistry

REFERENCES

1. Bacq Z. M., *Chemical Protection Against Ionising Radiation*. Charles C. Thomas, Publ., Springfield, Illinois, 1965.
2. Bacq Z. M., *Radiobiologia şi biologia moleculară* (transl. from. English). Ed.Med., Buc., 1967, 13.
3. Bacq Z. M., *Drugs and Enzymes*. Proc. of the 2-nd Int. Pharmacol. Meeting, 1983, 441.
4. Baran T. *Modificări biologice ale organismelor vii induse de iradiere*. Ph. D. Diss., Med. Farm. Inst., Jassy, 1974.
5. Baran T., Rusu V., Baciu I., Mîndreci I., Vasiliu I., *Determinarea radicalilor liberi prin REP în ţesuturile liofilizate*. Rev. Med. Chir., **90**, *3* (1986).
6. Bullock A. T., *Electron Spin Resonance Spectroscopy and Free Radical Reactions*. Annual Reports B, Chemical Society, London, 90—104 (1977),
7. Cecal Al., *Implicaţii ale fisiunii nucleare*. Ed. Tehnică, Bucureşti, 1989.
8. Danysz A., *Posibilités nouvelles de la radioprotection chimique*. Ed. Masson et Cie, Paris, 1969.
9. Mioque M., Ann. Pharm. Franc., **27**, 391 (1969).
10. Neniţescu C. D., *Chimie organică*. Vol. **1**, EDP, Bucureşti, 1980, 695.

EFECTUL RADIOPROTECTOR AL RUTIN-CISTEINEI DETERMINAT CU AJUTORUL REZONANŢEI ELECTRONICE DE SPIN

(Rezumat)

Efectul radioprotector al rutin-cisteinei (obţinută din rutozid şi cisteină printr-o condensare Mannich) poate fi pus în evidenţă şi prin rezonanţă electronică de spin. Mecanismul intim, probabil, al procesului radioprotector se datoreşte pe de o parte formării de disulfuri mixte între molecula de rutin-cisteină, care are o grupare —SH şi enzimele de grupări —SH, iar pe de altă parte, prin inhibarea enzimelor proteolitice de către structura rutozidului.

BULETINUL INSTITUTULUI POLITEHNIC DIN IAȘI
Tomul XXXVI (XL), Fasc. 1—2, 1990
Secția II
CHIMIE ȘI INGINERIE CHIMICĂ

D.C. 547.771.2 ; 546.215

KINETICAL AND THERMODYNAMICAL ASPECTS ON THE DECOMPOSITION OF HYDROGEN PEROXIDE IN HOMOGENEOUS CATALYSIS

BY

DOINA HRIȚCU, LUCIA ODOCHIAN and GH. IONESCU

1. Introduction

The decomposition of hydrogen peroxide in homogeneous catalysis is an important model both for theoretical and experimental studies in chemical kinetics. The reaction in aqueous solution (the so-called „catalase process") is accelerated by ions of transitional metals with various mechanisms.

A chemical process in homogeneus catalysis is provided to be a process with formation of an intermediate between the catalyst and one of the reactants [1]. Using the above reaction, Shpitalsky formulated the theory of intermediates in homogeneous catalysis. After that, Kobozev have completed and verified this theory and have resolved important aspects of the mechanism [2].

In this paper we have used as catalysts : MoO_4^{2-}, CrO_4^{2-} and WO_4^{2-} ions. Starting from the knowing theoretical informations the necessary experimental data for the simultaneous determination of three characteristics parameters of the process : the partial order of reaction with respect to hydrogen peroxide, the stability constant of intermediate and the constant of the reaction rate for the decomposition of intermediate into the products and free catalyst are obtained.

2. Theoretical Considerations and Experimental Data

2.1. Theoretical Considerations

The Shpitalsky — Kobozev differential kinetical equation is based on the following hypotheses :

1° The catalyst forms a reactive unstable intermediate with hydrogen peroxide

2° The formation of the intermediate is a relatively fast reversible process.

3° The unstable intermediate relatively slowly decomposes into the products and catalyst, the rate of this process being smaller than the rate of formation of reactant and catalyst from the intermediate.

4° The overall rate of the process is proportional to the concentration of the intermediate.

These hypotheses are similar to those for the enzymatical reactions studied by M i c h a e l i s [3].

Fot the rapid reversible reaction of the intermediate formation :

$$nH_2O_2 + C \rightleftharpoons M, \tag{1}$$

the stability constant will be expressed by the equation :

$$K = \frac{[M]}{[H_2O_2]^n ([C]_0 - [M]} \tag{2}$$

(if one considers that the equilibrium is drawn to the left : $[C] = [C]_0 \gg [M]$).

From Eq. (2) may be determined :

$$[M] = \frac{K[H_2O_2]^n . [C]_0}{1 + K[H_2O_2]^n} \tag{3}$$

The stage :

$$M \xrightarrow{k_d} \text{Products} + C \tag{4}$$

is the determinative one on the overall rate of the process (hypothesis 4°) :

$$-\frac{d[H_2O_2]}{dt} = k_d[M] = \frac{k_d K[H_2O_2]^n [C]_0}{1 + K[H_2O_2]^n} . \tag{5}$$

where : C — catalyst; $[C]$ and $[C]_0$ — the catalyst concentrations at the equilibrium of the first stage and at the initial moment ; M — intermediate; $[M]$ — the intermediate concentration ; $[H_2O_2]$ — the hydrogen peroxide concentration ; n — the partial order of reaction with respect to hydrogen peroxide ; k — the stability constant of the intermediate; $-d[H_2O_2]/dt$ — the overall rate of reaction; k_d — the constant of the overall rate of reaction.

2.2. Experimental Data

The experimental study have been realized through measuring the oxygen volume resulted from the reaction in isobar and isotherm conditions, using an installation summary described in Fig. 1. Beyond the literature informations [4], the reactor has a greater volume in comparison with the manometer, the temperature is maintained constant with precision and the stirring rate of the reaction mixture is uniform. The first condition is necessary with the aim to avoid the errors produced by the differences between the gas temperature in the reactor and the one from the manometer. The last condition provides an uniform escaping of oxygen formed in the liquid reaction mixture. The working parameters were the following : temperature 20°C and atmospheric pressure.

From these parameters, the most important is the temperature. Concerning pressure influence, it isn't necessary to be maintained constant because the measuring of escaping oxygen is relative. In the course of an experiment (1.5...2 h), the invariability of the atmospheric pressure is assured.

In this period of time the reaction was complete owing to the initial catalyst concentration (s. examples in Table 1).

The preliminary experimental data regarding the relationship oxygen volume—time were remade for obtain the dependence between hydrogen peroxide concentration and time. The kinetical curves $[H_2O_2]$—time were derivated to get the reaction rate, $-d[H_2O_2]/dt$, at different instantaneous reactant concentrations. The results are concentrated in Table 1.

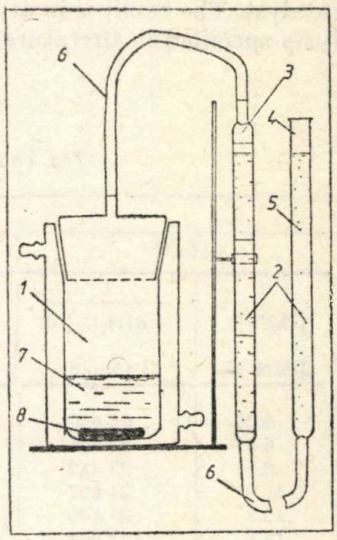

Fig. 1. — The scheme of used installation: *1* — thermostated reaction cell; *2* — burettes; *3* — graduated fixed burette; *4* — ungraduated movable burette; *5* — manometric liquid; *6* — rubber tube; *7* — reaction mixture; *8* — stirrer.

3. Experimental Data Interpretation

In order to verify the proposed physical model and the corresponding mathematical one, it was necessary to modify equation (5) in such co-ordinates to obtain a linear function:

$$(6)\qquad \frac{1}{\dfrac{d[H_2O_2]}{dt}} = \frac{1}{k_d K[C]_0}\cdot\frac{1}{[H_2O_2]^n} + \frac{1}{k_d[C]_0}.$$

Eq. (6), in co-ordinates $1/-d[H_2O_2]/dt$ and $1/[H_2O_2]^n$ will be a liniar representation only for a certain value of exponent n. This value will be found through trials knowing that it is a whole number because it represents the reactant molecules number which take part to the intermediate formation with the catalyst. With help of the straight line parameters values obtained in this way it may be calculated K and k_d magnitudes. In Table 2 are written the co-ordinate values from Eq. (6), after proving that $n=2$ (Fig. 2). In Fig. 2 is given as an example only MoO_4^{2-}

Table 1

Kinetical Magnitudes Reaction Rate—Reactant Concentration

The used catalysts					
MoO_4^{2-} $[C]_0=2.92\times10^{-3}$M		CrO_4^{2-} $[C]_0=1.79\times10^{-2}$M		WO_4^{2-} $[C]_0=9.29\times10^{-2}$M	
$[H_2O_2]$ mole/l	$-\frac{d[H_2O_2]}{dt}$ $10^5\times$ mole/l·s	$[H_2O_2]$ mole/l	$-\frac{d[H_2O_2]}{dt}$ $10^4\times$ mole/l·s	$[H_2O_2]$ mole/l	$-\frac{d[H_2O_2]}{dt}$ $10^4\times$ mole/l·s
0.390	4.464	0.252	3.700	0.354	4.400
0.335	4.264	0.193	2.240	0.271	3.770
0.302	4.049	0.154	1.530	0.203	2.720
0.271	3.937	0.129	1.100	0.150	1.890
0.237	3.636	0.111	0.725	0.101	1.130
0.207	3.375	0.0975	0.600	0.0792	0.868
0.189	3.185	0.086	0.550	0.0614	0.770
0.176	3.000	0.076	0.450	0.0555	0.700

catalyst. The result is in accordance with the value obtained for other catalysts specified in literature [5].

Table 2

The Values of Co-ordinates in Equation (6)

The used catalysts					
MoO_4^{2-}		CrO_4^{2-}		WO_4^{2-}	
$\frac{1}{[H_2O_2]^2}$ (l/mole)^2	$\frac{1}{-d[H_2O_2]/dt}$ l·s/mole	$\frac{1}{[H_2O_2]^2}$ l/mole)^2	$\frac{1}{-d[H_2O_2]/dt}$ l·s/mole	$\frac{1}{[H_2O_2]^2}$ (l/mole)^2	$\frac{1}{-d[H_2O_2]/dt}$ l·s/mole
4.00	21 550	—	—	20.05	4.60
6.57	22 401	6.264	1.266	44.92	5.291
8.91	23 452	15.80	2.702	98.61	6.99
11.0	24 697	26.98	4.464	120.8	7.93
13.6	25 400	41.95	6.536	159.5	8.85
17.8	27 503	53.55	7.895	186.4	9.69
23.0	29 630	60.09	9.090	265.0	11.52
28.0	31 397	67.80	10.25	324.1	12.98
32.3	33 333	81.53	12.3	—	—
—	—	105.2	16.0	—	—

Remade data from Table. 2 are written like linear diagrams in Figs. 3...5. Based on the obtained diagrams the straight lines parameters are determined sloping and intercepting the ordinate axis. These parameters allow to calculate the K and k_d magnitudes, indicated in Table 3.

Table 3

The K and k_d Calculated Values

The used catalyst					
MoO_4^{2-}		CrO_4^{2-}		WO_4^{2-}	
K, [l/mole]^2	k_d, [s^{-1}]	K, [l/mole]^2	k_d, [s^{-1}]	K, [l/mole]^2	k_d, [s^{-1}]
47.0	1.73×10^{-2}	2.346	159.6	153.2	2.560

As an example, for MoO_4^{2-} catalyst (Fig. 3), the calculus of K implies the following steps. Extrapolating to $1/[H_2O_2]^2 = 0$, it will be obtained: 10^{-3}:$-d[H_2O_2]/dt = 19.75 = 10^{-3}/k_d[C]_0$ and consequently $k_d = 1.73 \times 10^{-2}$ s^{-1}. From the straight line slope, tg $\alpha = PN/NM = 1/k_dK[C]_0$, one can see that $K = 1/k_d[C]_0(PN/NM)$. But : $PN/NM = 421$ mole.s/l, and $K = 47.0$ (l/mole)^2:

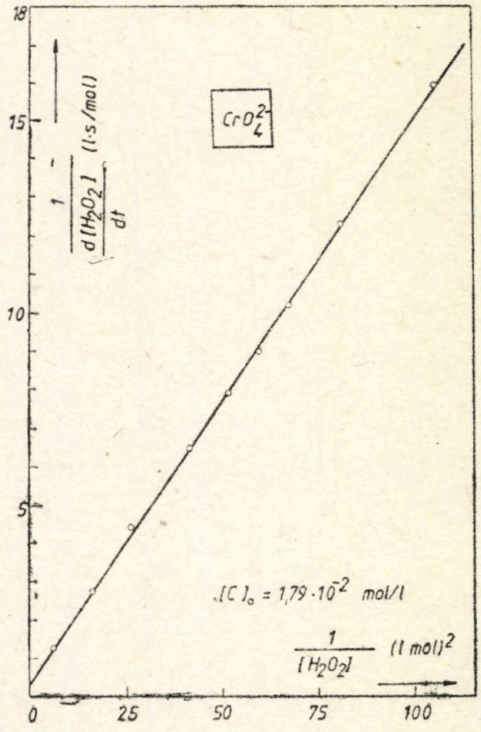

Fig. 4. — Verification of the linearity of equation (6) for CrO_4^{2-} catalyst.

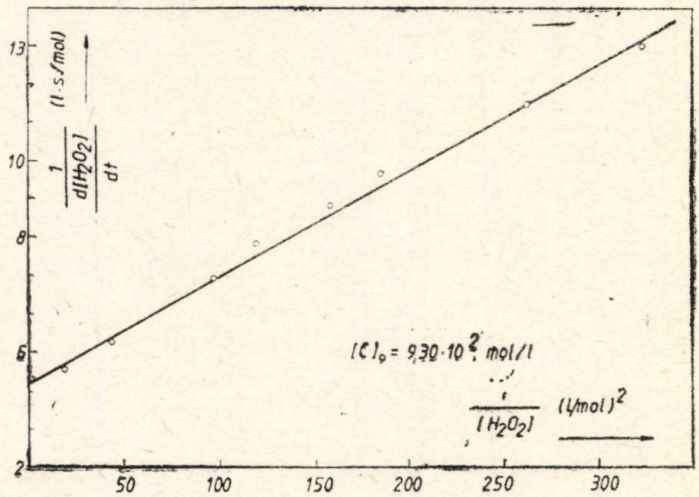

Fig. 5. — Verification of the linearity of equation (6) for WO_4^{2-} catalyst.

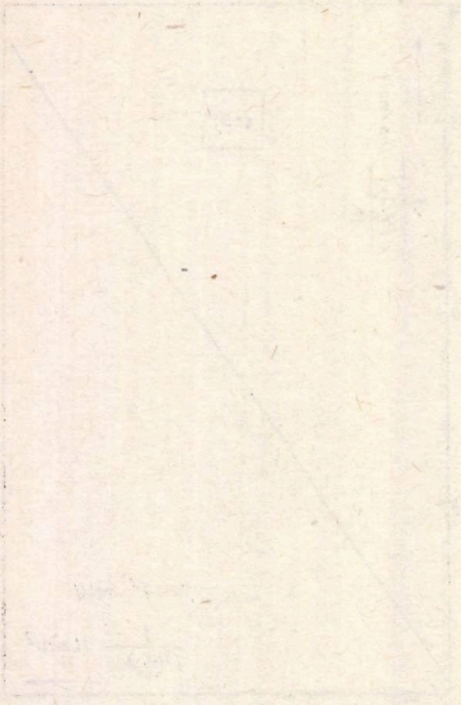

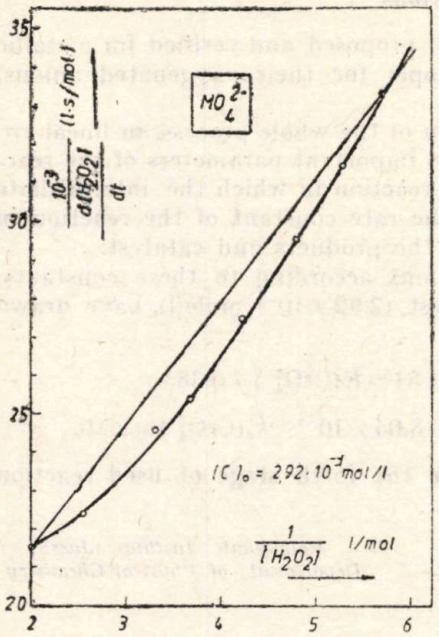

Eig. 2. — Verification of the value $n=2$ of the exponent.

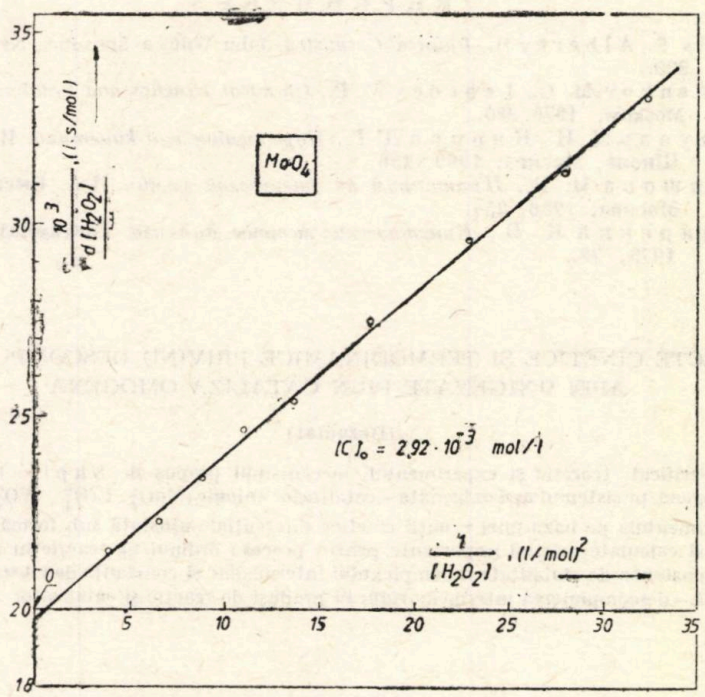

Fig. 3. — Verification of the linearity of equation (6) for MoO_4^{2-} catalyst.

4. Conclusions

1. The Shpitalsky mechanism, proposed and verified for metallic cations as catalysts, was proved to be proper for their oxygenated anions, too.

2. The differential kinetical equation of the whole process, in linear coordinates, is available for determining two important parameters of the reaction : a) the equilibrium constant for the reaction in which the intermediate catalyst/hydrogen peroxide appears; b) the rate constant of the reaction in which the intermediate decomposes into the products and catalyst.

3. The arrangement of the using ions according to these constants, for the same concentration of the catalyst (2.92×10^{-3} mole/l), have drawn to the following series:

$$K(MoO_4^{2-}) = 47.0 > K(WO_4^{2-}) = 4.81 > K(CrO_4^{2-}) = 0.383 ;$$

$$k_d(MoO_4^{2-}) = 1.73 \times 10^{-2} < k_d(WO_4^{2-}) = 8.04 \times 10^{-2} < k_d(CrO_4^{2-}) = 26.0.$$

4. The obtained two series prove the forth stage of used reaction mechanism.

Received, April 3, 1989

Polytechnic Institute, Jassy,
Department of Physical Chemistry

REFERENCES

1. Daniels F., Alberty R., *Physical Chemistry*. John Wiley a. Sons Inc., New-York, 1975, 300.
2. Panchenkov M. G., Lebedev V. P., *Chemical Kinetics and Catalysis*. Mir Publ., Moskow, 1976, 380.
3. Эмануель М. Н., Кнорре Д. Г., *Курс химической кинетики*. Изд. Высшая, Школа, Москва, 1969, 256.
4. Кудряшова И. В., *Практикум по физической химии*. Изд. Высшая Школа, Москва, 1986, 354.
5. Яшимирский К. Б., *Кинетические методы анализа*. Госхимиздат, Москва, 1973, 78.

ASPECTE CINETICE ŞI TERMODINAMICE PRIVIND DESCOMPUNEREA APEI OXIGENATE PRIN CATALIZA OMOGENĂ

(Rezumat)

S-a verificat, teoretic şi experimental, mecanismul propus de Shpitalsky pentru cataliză omogenă, pe sistemul apă oxigenată—catalizator anionic (MoO_4^{2-} CrO_4^{2-}, WO_4^{2-}). Prelucrînd datele experimentale pe baza unei ecuaţii cinetice diferenţiale ajustată sub formă de funcţie liniară au fost calculate mărimi importante pentru proces : ordinul de reacţie în raport cu apa oxigenată, constanta de stabilitate a complexului intermediar şi constanta de viteză pentru etapa determinantă—descompunerea intermediarului în produşi de reacţie şi catalizator liber.

BULETINUL INSTITUTULUI POLITEHNIC DIN IAŞI
Tomul XXXVI (XL), Fasc. 1—2, 1990
Secţia II
CHIMIE ŞI INGINERIE CHIMICĂ

D.C. 542.65 ; 546.322.26

THE STUDY OF CRISTALLIZATION EQUILIBRIUM OF POTASSIUM SULPHATE IN THE K^+, $NH_4^+ \| Cl^-$, $SO_4^{2-}-H_2O$ SYSTEM

BY

STELIAN PETRESCU, C. CALISTRU and CAMELIA PETRESCU

1. Introduction

The crystallization process of potassium sulphate in the quaternary system of double change K^+, $NH_4^+ \| Cl^-$, $SO_4^{2-}-H_2O$ implies, in the same time, the crystallization of ammonium sulphate both salts generating solid solutions of the following type $(K^+, NH_4^+)_2\ SO_4^{2-}$ [1]....[3].

The equilibrium study, in the present case, implies the simultaneous description of the equilibrium between the two phases, with phasic and chemical composition determination of each phase. The study of the equilibrium in such a complex system must to surpass real difficulties because of the big number of components and phases. To calculate the equilibrium of the system corresponding to the forming process of the potassium sulphate from KCl and ammonium sulphate is used the phase equilibrium method in systems of chemical reactions [4]... [9].

The results of the above mentioned study are synthesized under the form of material and thermic balances. Comparison between real and theoretical balances allows the correct appreciation of a situation, of the attained performances, allowing to make the process better.

In the present study is established a grapho-analytical calculus method of the solid—liquid equilibrium in K^+, $NH_4^+ \| Cl^-$, $SO_4^{2-}-H_2O$ system, in conditions of crystallization of solid solutions of the type: $(K^+, NH_4^+)_2SO_4^{2-}$. Based on this method the separation degrees of postassium and ammonium ions are calculated, in conditions of equilibrium, for different values of $X_{(K^+)_2}$ and $X^0_{H_2O}$, at 25°C and atmospheric pressure. It is to be noticed that in literature are missing equilibrium data at different values of temperature and pressure.

2. The Method Principle

The proposed grapho-analytical method allows to obtain complete data regarding both the liquid phase composition at equilibrium and the values of the theoretical separating degrees of potassium and ammonium ions. The equilibrium calculus based on the proposed method presume the use of the following steps :

a) The establishment, according to the calculus diagram graphically represented, of the co-ordinate points which characterize the initial and final state of the system .

b) Calculation of the liquid phase composition at equilibrium .

c) Calculation of the equilibrium separation degrees for potassium and ammonium ions, at different values of the system composition, initially represented by potassium ion concentration ($X^0_{(K^+)_2}$ and number of water $\dot{X}^0_{H_2O}$).

The way of composition determination of the system at equilibrium is showed in Figs. 1 and 2.

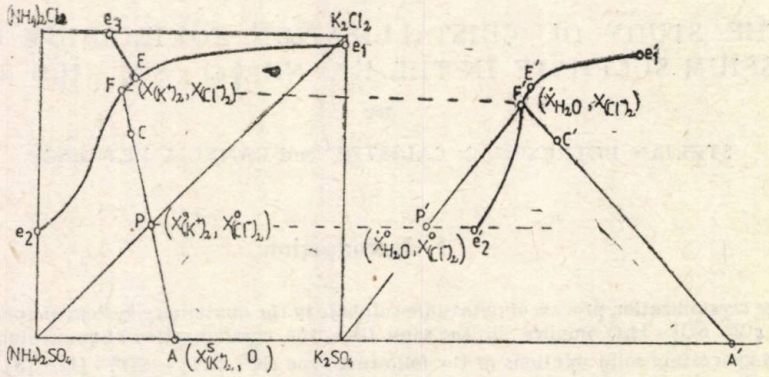

Fig. 1. — The computation method for the equilibrium variables with $\dot{X}^0_{H_2O}$ = min.

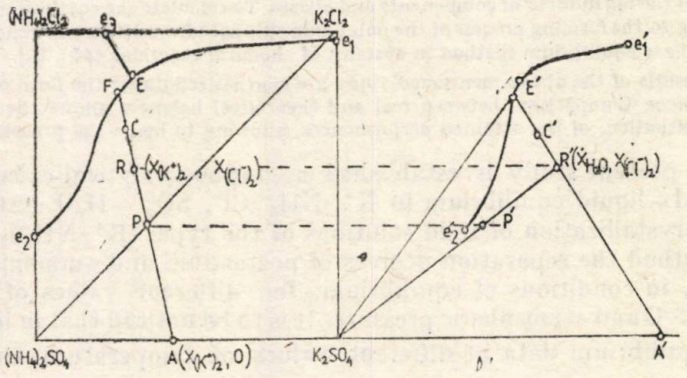

Fig. 2. — The computation method for the equilibrium for different values of $\dot{X}_{H_2O}$.

Following the notations from Fig. 1 (where only one connection line is represented) the concentration of the potassium ion is given by the abscissa of point P', the minimal water number, by the absciss of P' and the concentrations used for computing the transformation degrees $\eta^e_{(K^+)_2}$ and $\eta^e_{(NH_4^+)_2}$ are given by the coordinates of P and F.

The diagram drawn in Fig. 2 indicates the way of determination of the values required to study the dilution of the initial system and its influence upon the separation degrees of potassium and ammonium ions. The water number, for the initial system, is given by the abscissa of point P', and the values used

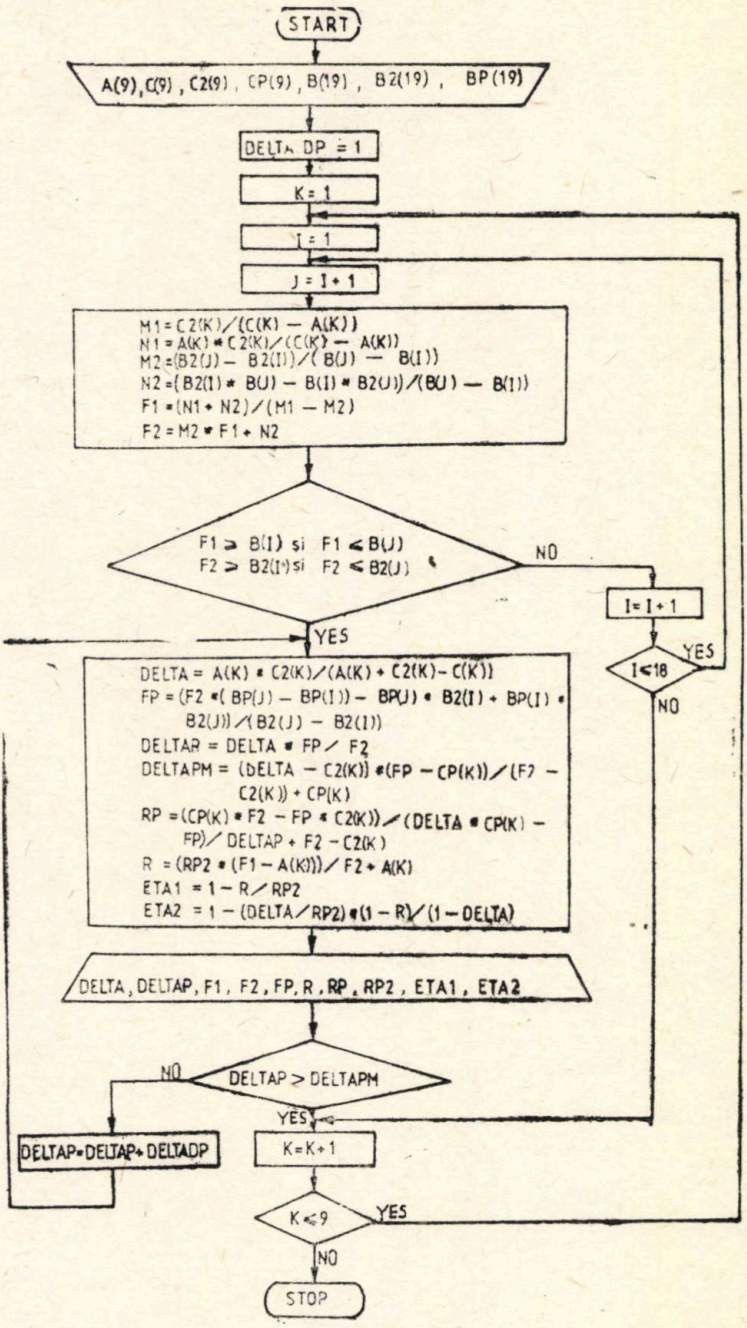

Fig. 3. — The flowchart.

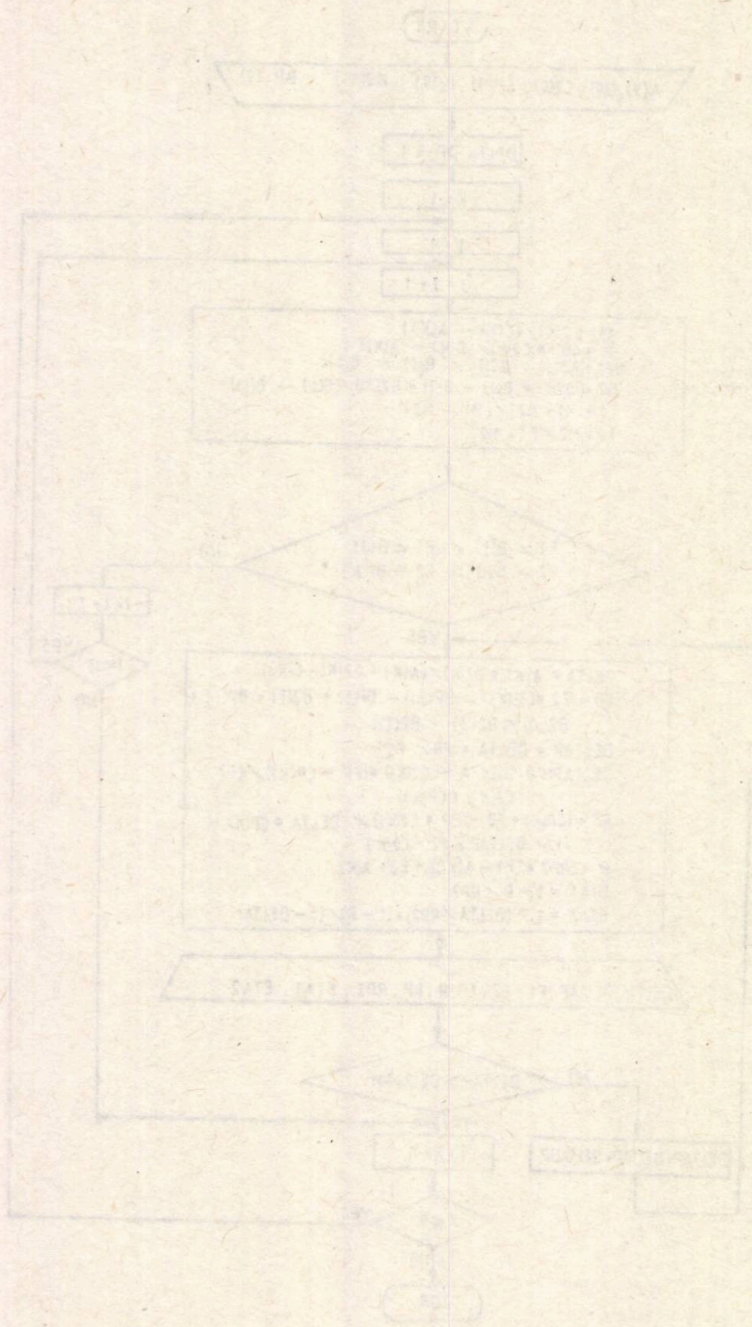

to calculate the separation degrees of above ions are given by the co-ordinate of points P and R'.

The separation degrees of K^+ and NH_4^+ are calculated by the equations showed below, obtained on the basis of their definition relations :

$$(1) \qquad \eta^e_{(K^+)_2} = 1 - \frac{n_{SA} X_{(K^+)_2}}{n_{SA} X_{(Cl^-)_2}} = 1 - \frac{X_{(K^+)_2}}{X_{(Cl^-)_2}},$$

$$(2) \qquad \eta^e_{(NH_4^+)_2} = 1 - \frac{n_{SA} X_{(NH_4^+)_2}}{n_{SA} X^0_{(NH_4^+)_2}} = 1 - \frac{X^0_{(Cl^-)_2} X_{(NH_4^+)_2}}{X_{(Cl^-)_2} X^0_{(NH_4^+)_2}},$$

In Fig. 3 is represented the logical scheme wich contains the calculation algorithm of equilibrium for the proposed grapho-analytical method. The significance of this scheme is showed in Fig. 4.

The equilibrium line is composed from straight line between two neighbouring points, in Fig. 4 being represented only one. The co-ordinates points (B1 (I), B2 (I)), (B(J), B2(J)), (BP(I), B2(I)), (BP(J), B2(J)) represents points on the equilibrium line in the square diagram, and respectively on the water diagram, whose co-ordinates, expressed by ionic molar fractions,

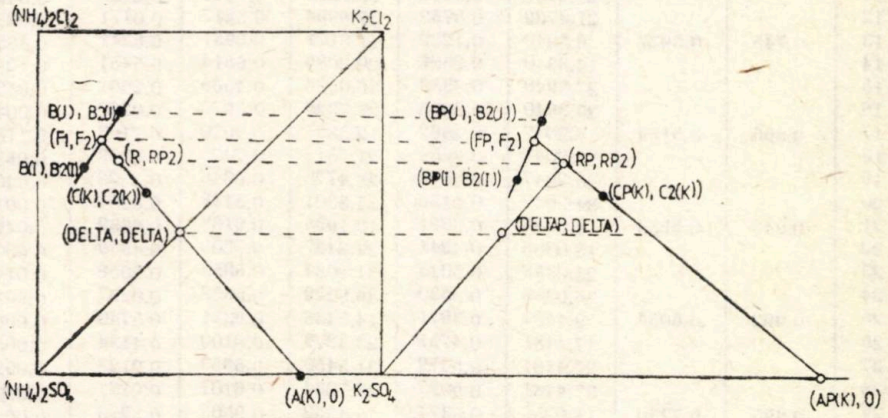

Fig 4. — Diagram of the symbols in the flowchart.

were obtained by processing the equilibrium data. The co-ordinates points (DELTA, DELTA) and (DELTA P, DELTA) express the composition of the initial system.

3. Results and Discussions

In view to solve the proposed algorithm with the aid of a computer, the equilibrium data of the K^+, $NH_4^+ \parallel Cl^-$, SO_4^{2-}—H_2O system, at 25°C and atmospheric pressure [10], [11] were used. For $X^0_{(K+)_2}$ were taken the

following values : 0.2537 ; 0.3238 ; 0.3786 ; 0.3927 ; 0.5169 ; 0.5583 ; 0.6056 ; 0.7230 and for $\dot{X}_{H_2O}$ were chosen values between 1.84 and 30.

The obtained data results are shown in Table 1.

Data from Table 1 indicate the presence of a peak, at $X^0_{(K^+)_2}=0.3238$, for the separation degree of ammonium ion.

Table 1

Computed E uilibrium Data

Nr. crt.	$X^s_{(K^+)_2}$	$X^0_{(K^+)_2}$	$\dot{X}^0_{H_2O}$	$X_{(K^+)_2}$	$\dot{X}_{H_2O}$	$X_{(Cl^-)_2}$	$\eta^e_{(K^+)_2}$	$\eta^e_{(NH_4^+)_2}$
1	0.4940	0.2537	4.9717	0.0416	9.3603	0.4777	0.9129	0.3180
2			7.9717	0.1200	12.4090	0.3949	0.6963	0.2425
3			11.9717	0.1901	15.1393	0.3208	0.4074	0.1418
4			16.9717	0.2479	17.3852	0.2599	0,0463	0,0163
5	0.8520	0.3238	6.2468	0.0465	9.5557	0.4937	0.9059	0.0751
6			12.2468	0.1615	16.0089	0.4232	0.6184	0.0513
7			18.2468	0.2477	20.8722	0.3703	0.3310	0.0272
8			24.2468	0.3149	24.6553	0.3292	0.0436	0.0035
9	0.795	0.3786	6.4739	0.0989	10.8223	0.6329	0.8437	0.1326
10			12.4739	0.2091	17.5522	0.5327	0.6075	0.0955
11			20.4739	0.3112	23.7893	0.4399	0.2926	0.0461
12			27.4739	0.3752	27.6996	0.3817	0.0171	0.0280
13	0.745	0.3927	6.3940	0.1222	11.3171	0.6951	0.8241	0.1834
14			14.3940	0.2508	20.2089	0.5514	0.5451	0.1214
15			22.3940	0.3353	26.0536	0.4569	0.2661	0.0593
16			29.3940	0.3896	29.7390	0.3973	0.0220	0.0049
17	0.866	0.5169	7.2047	0.2562	12.5857	0.9030	0.7163	0.1187
18			15.2047	0.3659	21.7817	0.7405	0.5059	0.0838
19			25.2047	0.4578	28.4775	0.6046	0.2428	0.0405
20			34.2047	0.5156	34.3301	0.5188	0.0061	0.0010
21	0.948	0.5583	8.0388	0.3081	13.1995	0.9167	0.6639	0.0460
22			18.0388	0.4241	24.2497	0.7505	0.4349	0.0301
23			28.0388	0.5045	31.9084	0.6353	0.2059	0.0142
24			36.0388	0.5530	36.5279	0.5658	0.0227	0.9014
25	0.992	0.6056	9.4481	0.3971	14.5438	0.9321	0.5740	0.0068
26			17.4481	0.4751	23.3379	0.8100	0.4134	0.0050
27			27.4481	0.5479	31.5450	0.6959	0.2128	0.0025
28			37.4481	0.6027	37.7264	0.6101	0.0121	0.0001
29	0.995	0.7230	14.0256	0.6374	18.4362	0.9503	0.3293	0.0041
30			25.2506	0.6725	29.6690	0.8570	0.2153	0.0025
31			34.0256	0.6965	37.3377	0.7933	0.1221	0.0014
32			43.0256	0.7150	43.2583	0.6442	0.0392	0.0004

It is clear that the optimal value for $X^0_{(K^+)_2}$ is 0.3238 due to the apparition of the solid phase with a high content of potassium. At higher values for $X^0_{(K^+)_2}$ are obtained very low values for $\eta_{(NH_4^+)_2}$, which leads to high concentrations of potassium ion in solid phase, but, due to relatively low values of its separation degree, the concentrations of potassium in liquid phase will have high values.

Table 2

Theoretical Material Balance, $X^0_{(K^+)_s}=0.237$, $\overline{X}^0_{(NH_4)_2SO_4}=0.30$

Phase	Component	Input		Output	
		m^0, [Kg]	$\overline{X}^0$	m, [Kg]	$\overline{\overline{X}}$
Liquid	KCl	—	—	64.32	0,0637
	$(NH_4)_2SO_4$	300	0.3000	208.60	0.2066
	NH_4Cl	—	—	36.58	0.0362
	H_2O	700	0.7000	700.03	0.6935
	Total	1 000	1	1 009.53	1
Solid	K_2SO_4	—	—	59.49	0.5627
	$(NH_4)_2SO_4$	—	—	46.22	0.4373
	KCl	115.27	1	—	—
	Total	115.27	1	105.71	1
Total		1 111.27	1	1 115.24	1

Table 3

Theoretical Material Balance, $X^0_{(K^+)_s}=0.3238$; $\overline{X}^0_{(NH_4)_2SO_4}=0.30$

Phase	Component	Input		Output	
		m^0, [Kg]	$\overline{X}^0$	m, [Kg]	$\overline{X}$
Liquid	KCl	—	—	55.46	0.0543
	$(NH_4)_2SO_4$	300	0.3000	189,66	0.1856
	NH_4Cl	—	—	76.19	0.0745
	H_2O	700	0.7000	700.03	0.6856
	Total	1 000	1	1 021.34	1
Solid	K_2SO_4	—	—	123,89	0.8820
	$(NH_4)_2SO_4$	—	—	16.30	0.1179
	KCl	161.56	1	—	—
	Total	161.56	1	140.45	1
Total		1 161.56		1 161.79	

Table 4

Theoretical Material Balance, $X^0_{(K^+)_2} = 0.3927$; $\overline{X}^0_{(NH_4)_2SO_4} = 0.30$

Phase	Component	Input		Output	
		m^0, [Kg]	$\overline{X}^0$	m, [Kg]	$\overline{X}$
Liquid	KCl	—	—	69,13	0.0691
	$(NH_4)_2SO_4$	300	0.3000	123.68	0.1237
	NH_4Cl	—	—	106.47	0.1065
	H_2O	700	0.7000	700.03	0.7007
	Total	1 000	1	999.03	1
Solid	K_2SO_4	—	—	173.14	0.7939
	$(NH_4)_2SO_4$	—	—	44.93	0.2061
	KCl	217,40	1	—	—
	Total	217.40	1	—	—
Total		1 217.40	—	1 217.38	—

Table 5

Theoretical Material Balance, $X^0_{(K^+)_2} = 0.5169$, $X^0_{(NH_4)_2SO_4} = 0.30$

Phase	Component	Input		Output	
		m^0, [Kg]	$\overline{X}^0$	m, [Kg]	$\overline{X}$
Liquid	KCl	—	—	140.1	0.1305
	$(NH_4)_2SO_4$	300	0.3000	72.47	0.0675
	NH_4Cl	—		159.73	0.1489
	H_2O	700	0.7000	700.03	0.6531
	Total	1 000	—	1 072,24	1
Solid	K_2SO_4	—	—	259,74	0.8951
	$(NH_4)_2SO_4$	—	—	30.44	0.1049
	KCl	362.44	1	—	—
	Total	362.44	1	290.18	1
Total		1 362.44	—	1 362.42	—

Having in view the equilibrium data shown in Table 1 was conceived the mathematical model of the balance of materials for the development of this process at equilibrium ; the obtained results are shown in Tables 2...5.

In this case, the balance of materials is reported to 1 000 Kg of ammonium sulphate solution concentration $\bar{X}^0_{(NH_4)_2SO_4}=0.30$, for the following values of $X^0_{(K^+)_2}$: 0.2537; 0.3238 ; 0.3927; 0.5169. From Tables 2...5 it may be seen that, at the growth of $X^0_{(K^+)_2}$ the amount of the obtained product increases and in the same time, the concentration of potassium becomes higher in final solid, but the liquid phase has a high content in potassium.

The optimal conditions are attained when is used the concentration $X^0_{(K^+)_2}=0.3238$, while in this case, the final solid phase has a high content of potasium, and in the same time, the final liquid phase has a low concentration of potassium ion.

4. Conclusions

The liquid—solid equilibrium, in the quaternary system of double change K^+, $NH_4^+||Cl^-$, $SO_4^{2-}-H_2O$ was studied.

Using a proposed grapho-analytical method are calculated the equilibrium concentrations $X_{(K^+)_2}$, $X_{(Cl^-)_2}$, $\dot{X}_{H_2O}$ and further the separation degrees of K^+ and NH_4^+, for different values of the concentration of the initial system.

Based on the obtained results, using a 30% $(NH_4)_2SO_4$ solution, it is established the theoretical balance of materials of the potassium sulphate crystallization, determining the maxima quantities of solid phase, possible to obtain and the chemical composition of the resulted liquid phase.

Notations

$X^0_{A+(-)}$ —the molar fraction of the $A+(-)$ ion with respect to the anhydrous salts in the initial system ;

$X_{A+(-)}$—the molar fraction of the $A+(-)$ ion with respect to the anhydrous salts in the liquid phase at equilibrium ;

$\dot{X}^0_{H_2O}(\dot{X}_{H_2O})$— the water number in the initial system and in the liquid phase at equilibrium, respectively;

$X^s_{(K^+)_2}$ — the molar fraction of the K^+ ion in the solid phase at equilibrium ;

$\bar{X}^0_A(\bar{X}_A)$— the mass fraction of the A component in the liquid or solid phase, in the initial and final data respectively ;

m^0 (m) — the initial and final mass, respectively ;

$\eta^e_{A+(-)}$ — the separation degree of the $A+(-)$ ion at equilibrium.

Received, February 16, 1989

Polytechnic Institute, Jassy,
Department of Inorganic Chemistry and
Technology and Analytical Chemistry

REFERENCES

1. Повин М. Е., *Технология минеральных солей*. Госхимиздат, Ленинград, 1970.
2. Filipescu L., Pincovschi E., *Echilibrul solid—lichid. Aplicații în tehnologia sărurilor minerale*. Ed. Tehn., București, 1980.
3. Petrescu St., *Cercetarea de inginerie chimică a procesului de obținere a sulfatului de potasiu prin valorificarea soluției de sulfat de amoniu rezultată la fabricarea caprolactamei*. Ph. D. Diss., Polyt. Inst., Jassy, 1987,

4. Calistru C., Loente C., *Tehnologia substanţelor anorganice*. EDP, Bucureşti, 1972.
5. Calistru C. et al., Rev. Chim., **27**, *6*, 499 (1976).
6. Calistru C. et al., *Tehnologia îngrăşămintelor minerale*. Vol. **II**, Ed. Tehn., Bucureşti, 1982.
7. Викторов М. М., *Графические расчёты в технологий неорганических веществ*. Изд. Химия, Ленинград, 1972.
8. Аносов В. И., *Краткое введение в физико-химических анализ*. Изд. АН СССР, Москва , 1959.
9. Кашкаров О. Д. *Графические расчёты солевых систем*. ГНТИХЛ, Лен инград, 1960.
10. Зданов ский А. Б. и сотр., *Справочник экспериментальных данных по растворимости водносолевых систем* Т. I, ГНТИХЛ., Ленинград, 1953.
11. Зданов ский А. Б. и сотр., *Справочник по растворимости солевых систем*. Т. II, Госхимиздат, Ленинград, 1954.

STUDIUL ECHILIBRULUI CRISTALIZĂRII SULFATULUI DE POTASIU ÎN SISTEMUL $K^+, NH_4^+ \parallel Cl^-, SO_4^{2-} - H_2O$

(Rezumat)

Se prezintă o metodă grafo-analitică de calcul a echilibrului pe baza căreia se stabileşte compoziţia fazei lichide şi solide la echilibru pentru cristalizarea sulfatului de potasiu în sistemul $K^+, NH_4^+ \parallel Cl^-, SO_4 - H_2O$ la temperatura de 25°C şi presiunea atmosferică. Rezultatele obţinute au permis întocmirea bilanţului de materiale teoretic, stabilindu-se cantităţile maxime de fază solidă şi compoziţia chimică a fazei solide rezultate.

BULETINUL INSTITUTULUI POLITEHNIC DIN IAŞI
Tomul XXXVI (XL), Fasc. 1—2, 1990
Secţia II
CHIMIE ŞI INGINERIE CHIMICĂ

D.C. 665.511.3

NATURAL GAS REFORMING AT LOW STEAM/CARBON RATIOS

BY

ILIE SIMINICEANU and CORNELIU PETRILĂ

1. Introduction

It is estimated that, in order to ensure the food security of the world population, which by the year, 2 000 will be over six billion, the consumption of mineral fertilizers will have to grow, until the end of the this century, by almost 80 million tons of nutrients ($N+P_2O_5+K_2O$) [1]. Over 50 % of this quantity will consist of nitrogen compounds.

The ammonia synthesis will still remain, in the near future, the single way of industrial fixation of the atmospheric nitrogen and the most efficient source of hydrogen necessary for the synthesis, will further be the catalytic oxidation of natural gas by steam [2], also named steam reforming. Over 99 % of the energy introduced in such a plant is in the gas natural form. This is consummed as combustion gas in the primary reformer furnace and for steam generation (approximatively 1/3 from total), as well as such as row material (2/3 from total) [3].

The possibilities of natural gas feedstock consumption reduction were studied in a previous work [4] by the method of process analysis and synthesis. The possibility of the combustion gas consumption reduction, by means of the steam/carbon ratio lowering, and the consequences of this measure on the output parameters of the overall reforming process, are analysed in this work. With that end in view a mathematical model correlating the specific heat consumption in the primary reformer, the specific consumption of combustion gas in the radiant section of the furnace, and the methane concentration in the gas leaving the secondary reformer, as a function of the steam/carbon molar ratio at the primary reformer inlet, is built. The model is checked up by comparing the computed data to those measured in a commercial plant. The influence of the steam/carbon ratio lowering, from 4.0 to 2.0, on the mentioned output parameters, is then studied utilising a computer.

2. The Mathematical Model

The overall reforming process consists of three chemical processes (primary reforming, combustion, and secondary reforming) as well as several steps of heat exchange. A simplified flowsheet for the overall reforming process is given in Fig. 1.

The reactions involved are the following:

(1) $CH_4+H_2O=CO+3H_2$, (2) $CO+H_2O=CO_2+H_2$, (3) $\frac{1}{2}O_2+H_2=H_2O$,

(4) $CH_4+2O_2=CO_2+H_2O$,

where (1) and (2) are available in the primary reforming , (1)... (3), in the secondary reforming , (4), in the combustion stage.

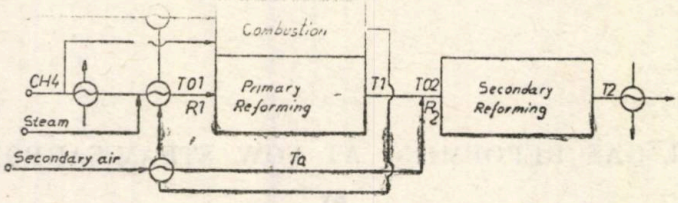

Fig. 1. — Flowsheet of the overall reforming process.

The mathematical model of the *primary reforming* is based on the asumption, experimentally proved [5], that the rate of the process is given by the rate of heat transfer from the tube wall to the reaction surface, whereas the transformations (1) and (2) take place at equilibrium. Therefore, the primary reforming may be mathematically represented by the equations:

$$K_{p1}-\frac{(\alpha_1-\beta_1)(3\alpha_1+\beta_1)^3P^2}{(1-\alpha_1)(R_1-\alpha_1-\beta_1)(1+R_1+2\alpha_1)^2}=0, \tag{5}$$

$$K_{p2}-\frac{\beta_1(3\alpha_1+\beta_1)}{(\alpha_1-\beta_1)(R_1-\alpha_1-\beta_1)}=0, \tag{6}$$

$$\log_{10}K_{p1}=-9\,861.11/T-11.87-2.0585\times10^{-3}T+0.1779\times10^{-6}T^2+8.3432\log_{10}T, \tag{7}$$

$$\log_{10}K_{p2}=2\,217.18/T-3.27467+0.3524\times10^{-3}T-0.0507\times10^{-6}T^2+0.2969\log_{10}T. \tag{8}$$

The thermal balance of the primary reforming gives the equation:

$$\begin{aligned}q=\frac{1.045}{\alpha_1}[&41\,100\alpha_1-10\,320\beta_1+(32.5\alpha_1+0.522\beta_1+3.422+7.219R_1)T_1-\\&-(17.93\alpha_1-4.13\beta_1-8.922-1.187R_1)\times10^{-3}T_1^2+\\&+(2.85\alpha_1-1.336\beta_1-1.388+0.089R_1)\times10^{-6}T_1^3-(3.422+\\&+7.219R_1)T_{01}-(8.922-1.187R_1)\times10^{-3}T_{01}^2+\\&+(1.388-0.089R_1)\times10^{-6}T_{01}^3],\end{aligned} \tag{9}$$

which allow to determine the specific heat consumption (q) as a function of the conversions α_1 and β_1, as well as of the process parameters R_1, T_{01} and T_1.

Equations for the combustion gas consumption have been derived on the basis of the material and heat balances in the *combustion process*. These rather complex equations correlate the consumption of combustion gas to the parameters of the primary reformer (T_{01}, T_1, R_1, P_1) as well as to those of the burners: inlet temperatures of the air and the gas; air/gas ratio; the tem-

perature of the combustion gases leaving the radiative section of the furnace. These equations have been presented in a previous paper [6].

The *secondary reforming* is an adiabatic—autothermic process. The heat released by the reaction (3) increases the temperature of the reaction mixture over 1 273° K. So, the equilibrium of the reaction (1) is moved to the right, increasing the methane conversion. The mathematical model of this process includes the thermodynamic equilibrium equations (7), (8), and

$$(10)\quad K_{p1}-\frac{(\dot{X}^0_{CO_2}-\dot{X}^0_{CO}\,\beta_2/\alpha_2+\alpha_2-\beta_2)(\dot{X}^0_{H_2}+\dot{X}^0_{CO}\,\beta_2/\alpha_2-2\dot{X}^0_{O_2}+3\alpha_2+\beta_2)^3P^2}{(1-\alpha_2)(\dot{X}^0_{H_2O}-\dot{X}^0_{CO}\beta_2/\alpha_2+2\dot{X}^0_{O_2}-\alpha_2-\beta_2)(S+2\alpha_2)^2}=0,$$

$$(11)\quad K_{p2}-\frac{(\dot{X}^0_{CO_2}+\dot{X}^0_{CO}\beta_2/\alpha_2+\beta_2)(\dot{X}^0_{H_2}+\dot{X}^0_{CO}\beta_2/\alpha_2-2\dot{X}^0_{O_2}+3\alpha_2+\beta_2)}{(\dot{X}^0_{CO}+\alpha_2-\beta_2-\dot{X}^0_{CO}\,\beta_2/\alpha_2)(\dot{X}^0_{H_2O}-\dot{X}^0_{CO}\beta_2/\alpha_2+2\dot{X}^0_{O_2}-\alpha_2-\beta_2)}=0,$$

where :

$$(12)\qquad S=1+\dot{X}^0_{CO}+\dot{X}^0_{CO_2}+\dot{X}^0_{H_2}+\dot{X}^0_{H_2O}+\dot{X}^0_{N_2}$$

as well as the thermal balance equations :

$$\begin{aligned}(13)\quad &[A-0.291\dot{X}^0_{O_2}+3.256\,\alpha_2+1.162\,\beta_2(1+\dot{X}^0_{CO}/\alpha_2)]\times10^{-6}T^3+[B+\\&+3.443\dot{X}^0_{O_2}-18{,}838\,\alpha_2+3.225\,\beta_2(1+\dot{X}^0_{CO}/\alpha_2)]\times10^{-3}T^2+[C-12.22\dot{X}^0_{O_2}+\\&+33.156\,\alpha_2+1.18\,\beta_2(1+\dot{X}^0_{CO}/\alpha_2)]T+40\,124.32\,\alpha_2-10\,455.484\,\beta_2(1+\\&+\dot{X}^0_{CO}/\alpha_2)-112\,252.487\dot{X}_{O_2}=10^{-6}A\,T^3_{02}+10^{-3}BT^2_{02}+CT_{92},\end{aligned}$$

where :

$$\begin{aligned}(14)\quad A&=-1.388-0.114\dot{X}^0_{H_2O}-0.153\dot{X}^0_{CO_2}-0.825\dot{X}^0_{CO_2}+0.093\dot{X}_{H_2}-\\&-0.115\dot{X}^0_{N_2}-0.269\dot{X}^0_{O_2},\\B&=8.922+1.641\dot{X}^0_{H_2O}+1.045\dot{X}^0_{CO}+4.266\dot{X}^0_{CO_2}+0.033\dot{X}^0_{H_2}+\\&+0.909\dot{X}^0_{N_2}+1.495\dot{X}^0_{O_2},\\C&=3.422+6.89\dot{X}^0_{H_2O}+6.25\dot{X}^0_{CO_2}+6.85\dot{X}^0_{CO_2}+6.88\dot{X}^0_{H_2}+\\&+6.30\dot{X}^0_{N_2}+6.13\dot{X}^0_{O_2}.\end{aligned}$$

The molar ratios, $\dot{X}^0_i$, at the secondary reformer input, are correlated to α_1, β_1, R_1, and R_2 by the equations

$$(15)\quad \dot{X}^0_{CO}=\frac{\alpha_1-\beta_1}{1-\alpha_1},\quad \dot{X}^0_{H_2O}=\frac{R_1-\alpha_1-\beta_1}{1-\alpha_1},\quad \dot{X}^0_{CO_2}=\frac{\beta_1}{1-\alpha_1},$$

$$\dot{X}^0_{H_2}=\frac{3\alpha_1+\beta_1}{1-\alpha_1},\quad \dot{X}^0_{N_2}=\frac{0.79R_2}{1-\alpha_1},\quad \dot{X}^0_{O_2}=\frac{0.21R_2}{1-\alpha_1},$$

derived on the basis of the material balance of the secondary air-primary reformed gas mixing process.

The temperature at the secondary reformer inlet (T_{02}) is obtained from the thermal balance of the same mixing process:

$$T_{02}=\frac{C_1T_1+C_aT_a}{C_1+C_a}, \tag{16}$$

where:

$$C_a=R_2(0.79C_{pN_2}+0.21C_{pO_2}), \tag{17}$$

$$C_1=(1-\alpha_1)C_{pCH_4}+(R_1-\alpha_1-\beta_1)C_{pH_2O}+(\alpha_1-\beta_1)C_{pCO}+\beta_1C_{pCO_2}+ \\ +(3\alpha_1+\beta_1)C_{pH_2}. \tag{18}$$

The molar heat capacities of the components depend on the temperature by equations

$$C_{pi}=a_i+b_iT+c_iT^2, \tag{19}$$

the coefficients a_i, b_i, c_i being tabulated in the literature [7], [8].

The molar fractions of unconverted methane in the dry gas, after primary and secondary reformers, are determined by the equations:

$$(X_{CH_4})_1=\frac{1-\alpha_1}{1+3\alpha_1+\beta_1}, \tag{20}$$

$$(X_{CH_4})_2=\frac{(1-\alpha_1)(1-\alpha_2)}{1+3\alpha_1+\beta_1+0.37R_2+(1-\alpha_1)(3\alpha_2+\beta_2+\beta_2/\alpha_2)}. \tag{21}$$

The mathematical model, consisting of equations (5) ... (21), allow to determine α_1, β_1, α_2, β_2, q, T_2, $(X_{CH_4})_1$, and $(X_{CH_4})_2$ for given values of the parameters R_1, R_2, P_1, T_1 and T_a. In order to check the accuracy of the system (5)... (21), the output values of the parameters, measured in a commercial plant, have been compared to those computed by the above equations in the same inlet conditions. It has been found by this method, that the computed conversions in the primary reformer are little grater than those measured. This deviation from the equilibrium was taken into account in the computation program by altering the temperature at the primary reforming exit, $T_1'=T_1-\Delta T$. It has been found, by trying on, that, at $P_1=3.0$ MPa, $\Delta T=18°K$. The pressure drop between the two reforming steps was also taken into account. The full scale runs have proved that $P_1-P_2=0.1$ MPa. With these corrections, the system (5).. (21) was tested by a commercial plant simulation, comparing the measured and the computed values of the $(X_{CH_4})_2$ main output parameters. The computed values of $(X_{CH_4})_2$ are by almost 13% grater then those measured. This deviation shows that the chemical transformations do not reach the equilibrium non in the secondary reformer. Although, the accuracy of the model may be considered satisfactory for this work aim.

3. Results

The model (5)... (21) was numerically solved by Newton-Raphson method, programmed in BASIC, on a FELIX M-18 microsystem. The values obtained for $R_1=2.0...4.0$, and $T_1=1\,050...1\,200$°K, at $T_{01}=797$°K, $T_a=730$°K, $P_1=3.0$ MPa, and $R_2=1.33$ are given in the Tables 1...4.

Table 1

Influence of R_1 at $T=1\,050$°K

R_1	2.0	2.5	3.0	3.5	4.0
α_1	0.4143	0.4693	0.5189	0.5640	0.6051
β_1	0.2225	0.2665	0.3075	0.3458	0.3819
$q\times10^{-4}$, [J/mol]	8.5043	8.5664	8.6451	8.7342	8.8304
$100(X_{CH_4})_1$	23.7498	19.8419	16.7950	14.3508	12.3491
α_2	0.7630	0.8159	0.8631	0.9022	0.9317
β_2	0.0711	0.0811	0.0870	0.0879	0.0836
T_2, [°K]	1 150.20	1 155.95	1 163.22	1 173.32	1 184.66
$100\times(X_{CH_4})_2$	3.1574	2.1417	1.4033	0.8896	0.5539

These data allow the analysis of R_1 and T_1 influence on α_1, β_2, α_2, β_2, q, T_2, $(X_{CH_4})_1$ and $(X_{CH_4})_2$. Among the last ones, the specific heat consumption in the primary reformer (q), and the final methane conversion (α_2) may be considered the basic performances of the overall reforming process. The values of β are less important because they refere to the secondary reaction (2). The data show that at high temperatures ($T_1>1150$°K) this reaction proceeds from the right to the left. The temperature in the two reforming steps is limited from mechanical considerations. Until 1980 the primary reformer tubes were made up only of HK-40 alloys (25 Cr—20 Ni) with an inner diameter of 0.1

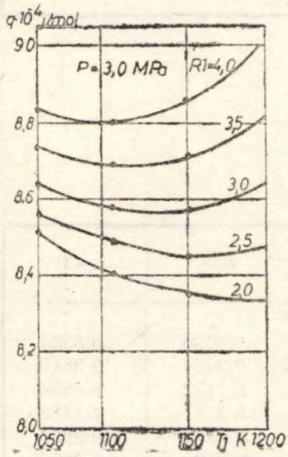

Fig. 2.— Influence of R_1 and T_1 on the specific heat consumption, at $P_1=3.0$ MPa.

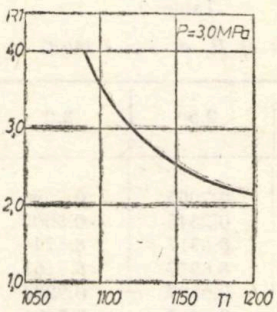

Fig. 3. — The minimum specific heat consumption curve, at $P_1=3.0$ MPa.

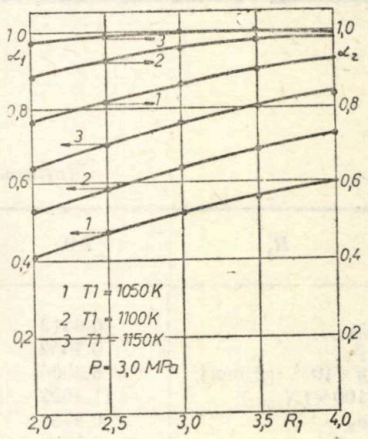

Fig. 4. — The dependence of α_1 and α_2 vs. R_1 at different temperatures: *1*— $T_1=1\,050$° K; *2*— $T_1=1\,100$°K; *3*— $T_1=1\,150$°K

m and a wall thickness of 0.018 m. These tubes had a life-time of over 10 years, at pressures of 3.0 MPa and maximum temperatures of 1 225° K [9]. The development of tubes made up of high-alloy steels (25 Cr—35 Ni), with a low thermal expansion, will allow the maximum temperature to be as high as 1 225°K [9]. So, T_1 may be increased from 1 083°K to nearly 1 123°K, and T_2 from 1 269°K to about 1 300°K.

The dependence $q-R_1-T_1$ (Fig. 2.) point out a minimum of the specific heat consumption at a temperature T_1 that increases as the ratio H_2O/C decreases. The curve from Fig. 3 represents the pairs R_1-T_1 giving the minimum specific heat consumption at $P_1=3.0$ MPa, $T_a=730°K$, $T_{01}=797°K$, and $R=1.33$. At these conditions, and $R_1=3.5$, the optimum temperature is 1 100° K. If the ratio R_1 is reduced at 3.0 the temperature T_1 must be in-

Table 2

Influence of R_1 et $T_1=1\ 100°K$

R_1	2.0	2.5	3.0	3.5	4.0
α_1	0.5240	0.5864	0.6406	0.6879	0.7293
β_1	0.2198	0.2673	0.3113	0.3521	0.3903
$q\times10^{-4}$, [J/mol]	8.4178	8.4912	8.5848	8.6920	8.8097
$100\times(X_{CH_4})_1$	17.0474	13.6646	11.1145	9.1339	7.5636
α_2	0.8811	0.9341	0.9645	0.9744	0.9865
β_2	0.0333	0.0262	0.0176	0.0070	−0.0027
T_2, [°K]	1 218.07	1 240.83	1 265.97	1 288.33	1 305.55
$100\times(X_{CH_4})_2$	1.2363	0.5790	0.2665	0.1330	0.0747

Table 3

Influence of R_1 at $T_1=1\ 150°C$

R_1	2.0	2.5	3.0	3.5	4.0
α_1	0.6413	0.7065	0.7596	0.8030	0.8384
β_1	0.2052	0.2545	0.3002	0.3424	0.3812
$q\times10^{-4}$, [J/mol],	8.3566	8.6917	8.5744	8.7122	8.8654
$100\times(X_{CH_4})_1$	11.4622	8.6917	6.7161	5.2511	4.1465
α_2	0.9733	0.9887	0.9937	0.9956	0.9964
$-\beta_2$	0.0030	0.0255	0.0491	0.0720	0.0936
T_2, [°K]	1 336.19	1 379.20	1 407.74	1 424.36	1 432.48
$100\times(X_{CH_4})_2$	0.2048	0.0696	0.0316	0.0180	0.0119

Table 4

Influence of R_1 et $T_1=1\,200°K$

R_1	2.0	2.5	3.0	3.5	4.0
α_1	0.7536	0.8140	0.8585	0.8915	0.9161
β_1	0.1842	0.2342	0.2805	0.3229	0.3615
$q\times10^{-4}$, [J/mol]	8.3391	8.4721	8.6340	8.8164	9.0141
$100\times(X_{CH_4})_1$	7.1505	5.0575	3.6670	2.7117	2.3969
α_2	0.9954	0.9974	0.9979	0.9981	0.9981
$-\beta_2$	0.0241	0.0479	0.0707	0.0915	0.1099
T_2, [°K]	1 493.19	1 526.79	1 540.21	1 541.70	1 536.29
$100\times(X_{CH_4})_2$	0.0242	0.0102	0.0059	0.0042	0.0033

creased at 1 125°K, in order to maintain q at its minimum value. In practice, this last temperature may be admitted only by replacing the conventional tubes with the new ones. Further reduction of R_1 ($R_1<3.0$) needs even greater temperatures.

The conversions α_1 and α_2 are strongly influenced by R_1 and T_1 (Fig. 4). At $T_1=1\,100°K$, for instance, the reduction of R_1 from 4.0 to 3.0 brings about the diminution of α_1 from 0.7293 to 0.6406, and the lowering of α_2 from 0.9865 to 0.9645. To avoid the harmful effect of the unconverted methane on the synthesis cycle, α_2 must be greater than 0.95. The data obtained shaw that, if $R_1\geqslant3.0$, $\alpha_2\geqslant0.95$.

4. Conclusions

The mathematical model presented in this paper allow the analysis of the basic parameters (P_1, T_{01}, T_a, T_1, R_1, R_2) on the overall reforming performances (q, α_1, α_2, T_2, X_{CH_4}).

The new data, obtained in this work with help of a computer, refers to the influence of the steam/carbon molar ratio reduction on the basic performances of the process : the specific heat consumption in the primary reformer, and the methane conversion in the secondary reformer. The optimum values of the parameters R_1 and T_1 are found by this method.

For the given values of the other parameters ($R=1.33$, $T_{01}=797°K$, $T_a=730°K$, $P_1=3.0$ MPa) the ratio R_1 may be reduced from 3.5...4.0 (presently used) to 3.0. The diminution of R_1 under 3.0 needs too great temperatures in the primary reformer and gives rise to an excessive content of residual methane in the synthesis gas which, in its turn, troubles the synthesis cycle.

It is also expected that the excess steam reduction to affect the performances of the other chemical processes coming after reforming (CO shift conversion, methanation). For that reason the working out of a more complex model is necessary in order to study the effects of the excess steam reduction on the whole ammonia synthesis plant.

Notations

A, B, C — quantities defined by Eq. (14);
C_a, C_1 — heat capacity of air, and gas mixture after primary reformer, respectively;
C_{pi} — molar heat capacity of the i component;
K_{p1}, K_{p2} — equilibrium constant of the reaction (1) and (2), respectively;

P_1, P_2^+ — total pressure in primary, and secondary reformer, respectively;
q — specific heat consumption in primary reformer, [J/mol H_2];
R_1 — steam/carbon molar ratio at the primary reformer inlet;
R_2 — secondary air/carbon molar ratio;
S — quantity defined by Eq. (12);
T_1, T_2 — exit temperature in the primary and secondary reformer, respectively;
T_a → secondary air temperature;
$\dot{X}_i^0$ — inlet molar ratios ($\dot{X}_i^0 = n_i^0/n_{CH_4}^0$);
X_{CH_4} → molar fraction of methane in the gas mixture (dry gas basis);
α_1, α_2 — methane conversion (η_{CH_4}) in primary and secondary reformer, respectively.
β_1, β_2 — the product η_{CH_4} η_{CO} in the primary and secondary reformer, respectively;

Received, May 15, 1989

Polytechnic Institute, Jassy,
Department of Inorganic Chemistry
and Technology and Analytical Chemistry
and
Department of Chemical Engineering

REFERENCES

1. * * * *Hrană pentru şase miliarde.* Ed. politică, Bucureşti, 1986.
2. Siminiceanu I., *Sinteza industrială a amoniacului la 75 ani.* The IVth National Symp. of. Chem. Proc. Eng. Piatra Neamţ, 1988.
3. Honti G. D., *Energy Conservation in the Nitrogen Industry.* Brit. Sulphur. Corp. Symp., London, 1981, Paper *1.*
4. Siminiceanu I., Rev. Chim. (Bucureşti), **40**, *2*, (1989).
5. Siminiceanu I., *Contribuţii la modelarea procesului de oxidare calalitică a metanului cu vapori de apă.* Ph. D. Diss. Polyt. Inst., Jassy., 1980.
7. Calistru C. et al., *Tehnologia îngrăşămintelor minerale.* Vol. **1**, Ed. Tehn., Bucureşti, (1984).
8. Siminiceanu I., Petrilă C., Jianu E., Rev. chim. (Bucureşti), **38**, *1*, 39 (1987).
9. Schillmoller C. M., Hydrocarbon Processing, **9** (1986).

REFORMAREA GAZULUI NATURAL LA UN RAPORT SCĂZUT ABUR/CARBON

(Rezumat)

Se stabileşte un model matematic al procesului global de reformare catalitică a gazului natural din instalaţiile de fabricare a amoniacului. Modelul corelează consumul specific de căldură (q), temperatura (T_1) şi gradul de transformare a metanului (α_1) în reformerul primar, precum şi temperatura (T_2) şi gradul de transformare (α_2) în reformerul secundar, în funcţie de parametrii de intrare: raportul molar abur/carbon (R_1), raportul molar aer/carbon (R_2), temperatura aerului (T_a), temperatura amestecului abur—metan (T_{01}) şi presiunea în reformerul primar (P_1). Pentru R_2=1,33; T_{01}=797°K; T_a=730°K; P_1=3,0 MPa se studiază, cu ajutorul calculatorului, influenţa variaţiei raportului R_1 în intervalul 2,0...4,0 la T_1=1 050... 1 200°K. Se găsesc astfel perechi al parametrilor R_1, T_1 la care consumul specific de căldură este minim. Datele obţinute arată că este posibilă reducerea lui R_1 de la 3,5...4,0 (actual) la 3,0 fără a afecta esenţial gradul final de transformare a metanului (α_2) şi alte performanţe ale procesului tehnologic.

BULETINUL INSTITUTULUI POLITEHNIC DIN IAŞI
Tomul XXXVI (XL), Fasc. 1—2, 1990
Secţia II
CHIMIE ŞI INGINERIE CHIMICĂ

C.D. 631.893 ; 62.004.8

RECHERCHES SUR LE COMPORTEMENT DES DÉCHETS D'OS CALCINÉS DANS LE PROCESSUS D'OBTENTION DES ENGRAIS COMPLEXES

PAR

CAROLINA HAGIU et GRETA YAHIA

1. Introduction

La production d'engrais complexes dans notre pays est basée sur des matières premières phosphatées qui proviennent exclusivement de l'importation. Dans ces conditions, la valorification de toute source autochtone de phosphore présente un intérêt particulier. Parmi celles-ci, la farine d'os — produit secondaire de la fabrication de la colle d'os — ayant une teneur élevée en P_2O_5, constitue une matière première adéquate à l'obtention des engrais complexes. La qualité des déchets d'os et donc leur comportement dans le processus technologique dépendent de leur provenance et des opérations de mise en oeuvre préliminaire. Pour apprécier le mode de comportement des dechets d'os dans le processus de décomposition nitrique et pour intervenir avec efficacité dans l'orientation du processus technologique, il est nécessaire de connaître au préalable leurs caractéristiques.

Le présent travail réunit les résultats obtenus concernant les propriétés chimiques, physiques et technologiques des déchets d'os calcinés, propriétés dont la connaissance est indispensable au calcul de l'installation et à la direction du processus technologique.

2. Caractérisation par des propriétés chimiques et physiques

La composition chimique des déchets d'os calcinés, déterminée à l'aide méthodes analytiques connues [1]...[3] et exprimée en composants fictifs, est la suivante : $P_2O_5=35,9\%$; $Ca=36,2\%$; $N=0.19\%$; $Fe=0,625\%$; $Cu=3,53.10^{-3}\%$; $Pb=5,6.10^{-3}\%$; $Cr=4,5.10^{-3}\%$; $Ni=1,3.10^{-3}\%$; $Mg=0,13.10^{-3}\%$; $Zn=0,77.10^{-3}\%$. Les composants réels les plus probables sont : $Ca_3(PO_4)_2=80\%$; $Mg_3(PO_4)_2=2\%$; $CaCO_3=13\%$; $CaF_2=1,5\%$; sels alcalins$=3,5\%$. La farine d'os calcinée a une teneur élevée en P_2O_5 comparativement à celle des phosphorites de Maroc et de Togo et de l'apatite de Kola; la valeur élevée du rapport CaO/P_2O_5 et son influence défavorable sur la qualité de l'engrais obtenu exige l'adoption d'une variante de mise en oeuvre avec séparation partielle du calcium ou bien avec fixation de celui-ci sous forme d'autres composants La teneur relativement faible en fluor (0,73%) ne justifie pas des installations spéciales de récupération de celui-ci mais simplement l'introduction dans le flux technologique d'une opération de lavage des gaz au fluor afin d'éviter la polluation. Les microélements présents dans le déchet d'os améliorent la qualité de l'engrais.

Le traitement avec des acides provoque des réactions de décomposition des phosphates, du carbonate et du fluorure de calcium et des substances organiques présentes avec formation de CO_2, H_2 et d'autres gaz, qui déterminent l'apparition du phénomène d'écumage.

Le déchet d'os calcinés est un mélange de composants solides ; les propriétés physiques de l'ensemble matériel sont déterminées par expérimentation directe.

3. Caractérisation par des propriétés technologiques

La caractérisation technologique du déchet d'os implique la connaissance d'un ensemble de propriétés qui en totalité permettent d'apprécier le comportement de la matière première dans le processus technologique et d'établir les mesures nécessaires pour obtenir certaines performances technologiques.

Parmi les propriétés technologiques générales, la forme des particules, le facteur de forme et l'état de la surface, les dimensions des particules et leur distribution par ordre de grosseur, l'angle de talus naturel et la densité en vrac intéressent tout particulièrement dans l'orientations du processus chimique principal aussi bien que dans le calcul des installations de stockage, de transport et de dosage. Pour le déchet d'os calcinés ayant la composition présentée au §2, les valeurs expérimentales de ces propriétés sont :

a) Densité en vrac . . . . . 1 342 kg/m³
b) Angle de talus naturel . . . . . 37,98°

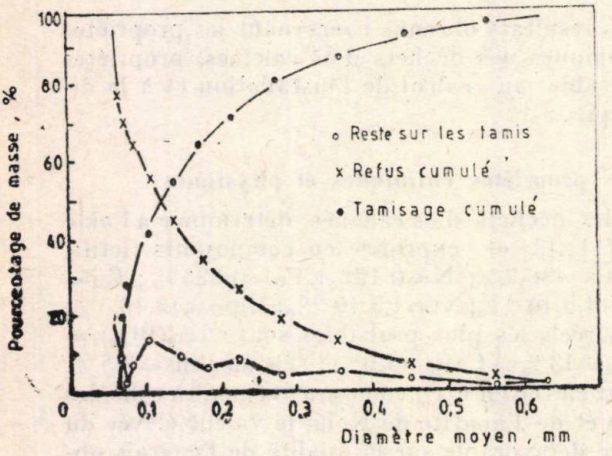

Fig. 1. — Distribution de la grosseur des particules.

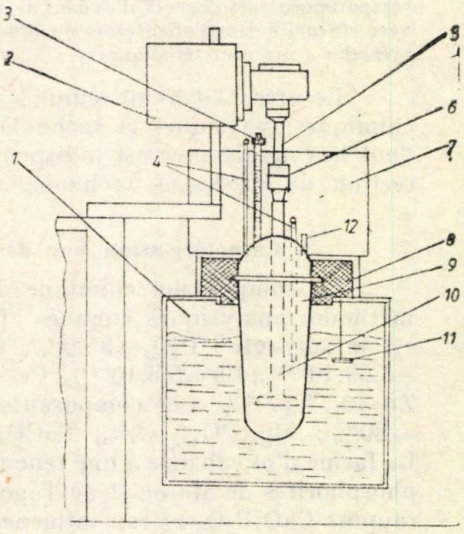

Fig. 2 — Installation de laboratoire pour la détermination des propriétés technologiques spécifiques : *1* — thermostat ; *2* — variateur de rotation ; *3* — thermomètre de contact ; *4* — thermométre de contrôle ; *5* — axe agitateur ; *6* — fermeture hydraulique ; *7* — bloc régulateur ; *8* — collier d'étanchement ; *9* — réacteur ; *10*, *11* — agitateurs.

c) La distribution de la grosseur des particules, qui est représentée dans la Fig. 1.

Il résulte de la Fig. 1 que le spectre granulométrique du déchet d'os calcinés correspond, sous rapport des dimensions, à une mise en oeuvre par décomposition nitrique: la plupart du matériel ($\sim 73\%$) est formeé de particules ayant le diamètre moindre que 0,225 mm et seulement $\sim 7\%$ des particules ont le diamètre dépassant 0,45 mm.

Parmi les propriétés technologiques spécifiques, celles qui déterminent au plus haut degré le comportement du déchet d'os dans le processus de fabrication sont : la norme expérimentale d'acide, la durée d'atteinte du degré maximum de transformation et l'intensité d'écumage. On peut déterminer les propriétés technologiques spécifiques, avec de bons résultats, à l'aide de l'installation de laboratoire présentée dans la Fig. 2.

a) *La norme d'acide azotique* représente la masse de HNO_3 100 % nécessaire à la décomposition d'une unité de masse de matière première solide. La norme stoéchiométrique calculée à partir des réactions chimiques avec de l'acide azotique de tous les composants du déchet d'os, représente la quantité de HNO_3 100% nécessaire à la décomposition de 1 Kg de déchets d'os.

Les réactions chimiques à partir des quelles on calcule la norme stoéchiométrique sont :

$$Ca_3(PO_4)_2+6HNO_3=3Ca(NO_3)_2+2H_3PO_4,$$
$$CaCO_3+2HNO_3=Ca(NO_3)_2+CO_2+H_2O,$$
$$Mg_3(PO_4)_2+6HNO_3=3Mg(NO)_2+2H_2PO_4,$$
$$CaF_2+2HNO_3=Ca(NO_3)_2+2HF.$$

La norme stoéchiométrique d'acide est calculée à l'aide de l'équation:

$$(1) \qquad N_{st}=1{,}216\bar{X}^0_{Ca_3(PO_4)_2}+1{,}442\bar{X}^0_{Mg_3(PO_4)_2}+1{,}26\bar{X}_{CaCO_3}+1{,}615\bar{X}^0_{CaF_2}.$$

Pour le déchet d'os calcinés ayant la composition présentée au §2 on obtient $N_{st}=1{,}1896$ Kg HNO_3 100%/1 Kg déchet.

La norme expérimentale d'acide azotique représente la masse d'acide azotique 100% pratiquement consommée pour la décomposition de 1 Kg de déchet d'os. La norme expérimentale est déterminée dans l'installation de laboratoire présentée dans la Fig. 2 ; en principe, la méthode est basée sur la désagrégation de la farine d'os à un rapport des réactants qui assure une consommation totale des composants de la phase solide.

La norme expérimentale d'acide est calculée à l'aide de la relation :

$$(2) \qquad N_{exp}=\frac{V^0_{\square i}C^0_{HNO_3}-V_{\square i}C_{HNO_3}}{m^0_{\square_s}}, \quad [Kg/Kg],$$

où : $V^0_{\square i}$, $V_{\square i}$ —volume de la phase liquide initiale et finale, [l] ; $C^0_{HNO_3}$, C_{HNO_3} — concentration de l'acide azotique dans la solution initiale et finale, [Kg/l] ; $m_{\square_s}$ —masse de la phase solide initiale, [Kg].

La concentration de l'acide azotique dans la solution initiale est déterminée par la méthode standardisée [4] ; la détermination de la teneur en acide azotique dans la phase liquide finale est effectuée par double titrage avec de la solution de hydroxyde de sodium de normalité connue, en présence d'indicateurs sélectifs [2].

En travaillant avec 400 ml d'acid azotique de 46%, une quantité de déchet d'os polygranulaire homogène, représentant 40% de la quantité stoéchiométrique nécessaire, à la température de 75°C, 120 tours/min., durant 6 heures, on obtient $N_{exp.}=1{,}433$ Kg NHO_3 100% /l Kg déchet.

b) *La durée d'atteinte du degré final de transformation* représente le temps de stationnement de la masse de réaction dans le réacteur où l'on atteint le degré maximum de transformation du P_2O_5. Cette durée dépend des conditions de réalisation du processus : température, concentration de l'acide, fraction granulométrique, rapport des phases, etc. Le degré de transformation du P_2O_5 est calculé à l'aide de la relation

$$\eta_{P_2O_5}=\frac{\overline{X}_{H_3PO_4}(R+0{,}56\overline{X}^0_{CaCO_3})}{\overline{X}^0_{P_2O_5}(1{,}38-2{,}18\overline{X}_{H_3PO_4})}, \tag{3}$$

établie à l'aide des équations de bilan de masse, où : $\overline{X}^0_{Ai}$, $\overline{X}_{Ai}$ — fractions de masse composants, initial et final ; $R=m^0_{[]_l}/m^0_{[]_s}$ — rapport des phases.

Les déterminations expérimentales effectuées à des températures situées dans l'intervalle 60°...80°C en utilisant de l'acide azotique de 46% en quantité variant depuis la valeur stoéchiométrique jusqu'à un excès de 20% et de la farine d'os calcinée sous la forme de l'ensemble polygranulaire, on obtient le degré maximum de transformation à des temps variant entre 5 et 15 minutes.

c) *Capacité d'écumage.* La formation de l'écume durant le processus de décomposition nitrique des dechéts d'os calcinés est déterminée par le dégagement de CO_2 et d'autres gaz formés par la décomposition des substances organiques. L'apparition intense de l'écume est indésirable pouvant provoquer l'entrainement du matériel solide qui n'a pas réagi, l'obturation des trajects, etc. On peut évaluer la capacité d'écumage par l'indice d'écumage défini à l'aide de la relation :

$$I_{écum.}=\frac{H_{écum.}}{H_{masse\ de\ réact.}}. \tag{4}$$

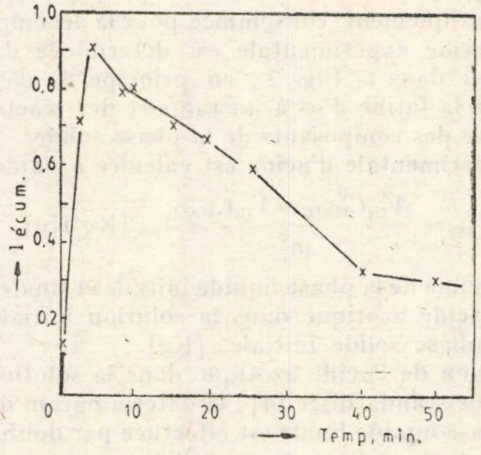

Fig. 3. — Variation de l'indice d'écumage par rapport au temps.

Déterminé par voie expérimentale dans l'installation de la Fig. 2, à l'aide du réacteur au quel on attache une règle graduée pour mesurer l'hauteur de l'écume et la masse de réaction, l'indice d'écumage varie conformément aux données présentées dans la Fig. 3 ; la valeur maxima de l'indice d'écumage est atteinte en 5 minutes.

4. Conclusions

L'appréciation du comportement des déchets d'os calcinés dans le processus d'obtention des engrais N—P—K par décomposition nitrique implique la connaissance d'un ensemble de propriétés physiques, chimiques est technologiques qui permettent la caractérisation complète du déchet en discussion. On présente les résultats expérimentaux relatifs à la composition chimique, aux propriétés technologiques générales concernant l'ensemble des granules et les propriétés technologiques spécifiques.

Les déchets d'os calcinés ont une teneur élevée en P_2O_5 (35,9%), constituant ainsi une matière première adéquate à l'obtention des engrais. La présence du carbonate de calcium et des substances organiques déterminent la propriété d'écumage à la désagrégation avec de l'acide azotique.

Les propriétés technologiques générales (densité en vrac, angle de talus natural, distribution granulométrique) et les propriétés spécifiques (norme d'acide azotique, durée d'atteinte du degré maximum de transformation, intensité d'écumage), sont utilisées au calcul des consommations spécifiques et des installations ainsi qui'à l'établissement des conditions optima, d'opération de celles-ci.

Reçue le 15 septembre 1988

Institut Polytechnique, Jassy,
Chaire de Chimie et Technologie
Anorganique et Chimie Analytique

BIBLIOGRAPHIE

1. Demetrescu A. N., Tutoveanu A., Ionescu M., *Analiza tehnică a minereurilor* Ed. Tehn., Bucureşti, 1966.
2. Liteanu C., *Chimie analitică cantitativă. Volumetria.* EDP, Bucureşti, 1969.
3. * * * STAS 3047/1974.
4. * * * STAS 447/1974.

CERCETAREA COMPORTĂRII DEŞEULUI DE OASE CALCINATE ÎN PROCESUL OBŢINERII ÎNGRĂŞĂMINTELOR COMPLEXE

(Rezumat)

Utilizarea resurselor indigene de fosfor prezintă un deosebit interes pentru industria îngrăşămintelor complexe care se bazează pe materii prime fosfatice provenite exclusiv din import. Deşeul de oase calcinate, prin conţinutul ridicat de P_2O_5, constituie o materie primă adecvată industriei îngrăşămintelor complexe. Pentru a aprecia comportarea acestuia şi a interveni eficient în conducerea procesului tehnologic este necesară cunoaşterea prealabilă a unui ansamblu de proprietăţi chimice, fizice şi tehnologice.

Se prezintă rezultatele cercetărilor experimentale privind testarea deşeului de oase calcinate ; se determină compoziţia chimică, proprietăţile tehnologice generale (distribuţia mărimii particulelor, densitatea în vrac, unghiul de taluz natural) şi proprietăţile tehnologice specifice (norma experimentală de acid, durata atingerii gradului maxim de transformare, intensitatea de spumare).

BULETINUL INSTITUTULUI POLITEHNIC DIN IAȘI
Tomul XXXVI (XL), Fasc. 1—2, 1990
Secția II
CHIMIE ȘI INGINERIE CHIMICĂ

D.C. 536.5 ; 532

TEMPERATURE DISTRIBUTION IN FLOW OF THIN FILMS OF NON-NEWTONIAN FLUIDS WHICH RESPECTS ELLIS MODEL

BY

RADU Z. TUDOSE and FĂNICĂ MUSTAȚĂ

1. Introduction

The flow of thin films of non-Newtonian fluids is extensively used in industrial equipment for heat and mass transfer.

The heat transfer in flow of thin films of non-Newtonian fluids was less investigated [1]...[3].

In the pesent paper, the theoretical and experimental distribution of the temperature in smooth input region is studied

2. Theory

The physical model of the flow in thin film in the smooth input region is depicted in Fig. 1. The axis origin is taken on the metallic surface, where the z-axis is oriented in the flow direction and the y-axis is normal to the surface.

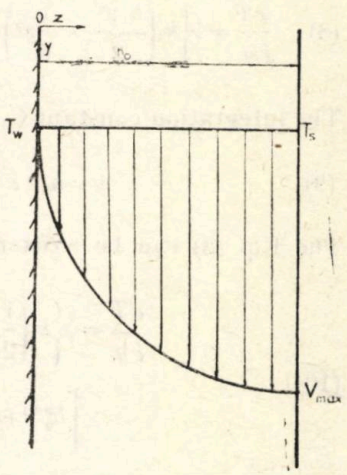

Fig. 1. — Physical model of the flow in thin films.

The rheological equation which describe the non-Newtonian behaviour for E l l i s model has the form :

$$\frac{dV_z}{dy} = k_1\tau + k_2\tau^n. \tag{1}$$

Form non-Newtonian fluids in the smooth input region, the equation of the momentum conservation, after simplification, can be written as follows :

$$\frac{d\tau_{yz}}{dy} = \rho g. \tag{2}$$

By integration of Eq. (2), taken in to considerations the boundary conditions:

(3) $$y=0,\ V_z=0 \text{ and } y=h_0,\ \mathrm{d}V_z/\mathrm{d}y=0,\ \tau_{yz}=0,$$

leads to:

(4) $$V_z=k_1\rho g\left(h_0 y-\frac{1}{2}y^2\right)+k_2\frac{1}{n+1}(\rho g)^n[h_0^{n+1}-(h_0-y)^{n+1}].$$

For the steady state, the equation of energy simplified, for this type of flow, in condition of a constant flux of the heated surface, is :

(5) $$\rho C_p V_z\frac{\partial T}{\partial z}=\lambda\frac{\partial^2 T}{\partial y^2},$$

By introducing the expression (4) into the Eq. (5) we obtain :

(6) $$\frac{\partial^2 T}{\partial y^2}=\frac{\rho C_p}{\lambda}\cdot\left.\frac{\partial T}{\partial z}\right|_{\text{const.}}(\rho g)\left\{k_1\left(h_0 y-\frac{1}{2}y^2\right)+k_2\frac{1}{n+1}(\rho g)^{n-1}[h_0^{n+1}-(h_0-y)^{n+1}[\right\}.$$

If we introduce the notation :

(7) $$\psi=\frac{\rho C_p}{\lambda}\cdot\left.\frac{\partial T}{\partial z}\right|_{\text{const.}}(\rho g),$$

after integration Eq. (6) becomes:

(8) $$\frac{\partial T}{\partial y}=\psi\left\{k_1\left(\frac{h_0 y^2}{2}-\frac{1}{6}y^3\right)+k_2\frac{1}{n+1}(\rho g)^{n-1}\left[(h_0^{n+1}y+\frac{1}{n+2}(h_0-y)^{n+2}\right]\right\}+C_1.$$

The integration constant C_1 can be determined from the boundary condition:

(9) $$y=h_0,\ \partial T/\partial y=0 \text{ (flux zero at interface).}$$

The Eq. (8) can be written as follows :

(10) $$\frac{\partial T}{\partial y}=\psi\left\{k_1\left(\frac{1}{2}y^2h_0-\frac{1}{6}y^3-\frac{1}{3}h_0^3\right)+\frac{k^2}{n+1}(\rho g)^{n-1}\times\right.$$
$$\left.\times\left[h_0^{n+1}(y-h_0)+\frac{1}{n+2}(h_0-y)^{n+2}\right]\right\}.$$

After a second integration Eq. (10) becomes :

(11) $$T=\psi\left(k_1\left(\frac{1}{6}h_0y^3-\frac{1}{24}y^4-\frac{1}{3}h_0^3y\right)+\frac{k_2}{n+1}(\rho g)^{n-1}\times\right.$$
$$\left.\times\left\{h_0^{n+1}(y^2-h_0y)+\frac{1}{n+2}\left[-\frac{1}{n+3}(h_0-y)^{n+3}\right]\right\}\right)+C_2.$$

The integration constant C_2 can be determined having in view the following boundary condition:

$$y=0,\quad T=T_w. \tag{12}$$

It results finally:

$$T-T_w=\psi\left(k_1\left(\frac{1}{6}h_0y^3-\frac{1}{24}y^4-\frac{1}{3}h_0^3y\right)+\frac{k_2}{n+1}(\rho g)^{n-1}\times\right.$$
$$\left.\times\left\{h_0^{n+1}\left(\frac{1}{2}y^2-h_0y\right)-\frac{1}{n+2}\cdot\frac{1}{n+3}\left[(h_0-y)^{n+3}-h_0^{n+3}\right]\right\}\right). \tag{13}$$

The surface temperature is determined with the following boundary condition:

$$y=h_0,\quad T=T_s. \tag{14}$$

The Eq. (14) is converted now into:

$$T_s-T_w=\psi\left[-k_1\frac{5}{24}h_0^4+\frac{k^2}{n+2}(\rho g)^{n-1}\left(-\frac{1}{2}h_0^{n+3}+\frac{1}{n+2}\cdot\frac{1}{n+3}h_0^{n+3}\right)\right]. \tag{15}$$

By denoting the dimensionles temperature with:

$$\theta=\frac{T_w-T}{T_w-T_s}, \tag{16}$$

the ratio of the Eqs. (13) and (15) has the following form:

$$\theta=\frac{k_1\left(\frac{1}{6}y^3-\frac{1}{24}y^4-\frac{1}{3}h_0^3y\right)}{-k_1\frac{5}{24}h_0^4+\frac{k_2}{n+1}(\rho g)^{n-1}\left(-\frac{1}{2}h_0^{n+3}+\frac{1}{n+2}\cdot\frac{1}{n+3}h_0^{n+3}\right)}+$$
$$+\frac{\frac{k_2}{n+1}(\rho g)^{n-1}\left\{h_0^{n+1}\left(\frac{1}{2}y^2-h_0y\right)-\frac{1}{n+2}\cdot\frac{1}{n+3}\left[(h_0-y)^{n+3}-h_0^{n+3}\right]\right\}}{-k_1\frac{5}{24}h_0^4+\frac{k^2}{n+1}(\rho g)^{n-1}\left(-\frac{1}{2}h_0^{n+3}+\frac{1}{n+2}\cdot\frac{1}{n+3}h_0^{n+3}\right)}. \tag{17}$$

For Newtonian liquid $k_2=0$ and Eq. (17) becomes:

$$\theta=\frac{\frac{1}{6}h_0y^3-\frac{1}{24}y^4-\frac{1}{3}h_0^3y}{-\frac{5}{24}h_0^4}. \tag{18}$$

3. Experimental

The experimental equipment, described in a previous paper [4], is mainly constituted from a heat exchange tube with $\varnothing=44\times3$ mm diameter and 2 000 mm length.

The non-Newtonian fluids flow as thin films on the external surface of the tube and the hot water flows in the tube. The two fluids flow in countercurrent. The temperature distribution across the film was measured by a miniature thermocuple introduced into the liquid by means of a micrometric device at intervals of 10 μm.

The solutions of polietilenoxid 4 000 has been used as non-Newtonian liquids. These solution respect E l l i s model and were characterized in a previous paper [5].

The temperature profile has been measured at distances of 30 and 130 mm from the input zone, in a smooth input region for R e y n o l d s numbers of the film between 250 and 2 500 and for temperature of hot water between 40° and 60°C.

4. Results and Discussion

In Figs. 2 and 3 is depicted the experimental distribution of the wall temperature as well as the film surface for various R e y n o l d s numbers of non-Newtonian fluids.

In Figs. 4...6 is depicted the temperature gradient across film thickness for different R e y n o l d s numbers of non-Newtonian fluids.

The dimensionless distribution of the temperature across films is represented in Figs. 7...9.

The Eq. (17), which show the dimensionless distribution of the temperature across film, theoretically derived, is plotted in Fig. 10.

The largest variation of the temperature in the film is found at a distance of 10 μm from the metallic surface.

5. Conclusions

The theoretical equation of the temperature distribution in the film have a general character. It depends on the rheological characteristics, the distance from interface and the film thickness. There is a main opposition to thermic transfer showed by metallic surface in a layer smaller that 10 μm.

Notations

C_p — thermal capacity, [J/kg °K];
g — gravity acceleration, [m/s²];
h_0 — film thickness, [m];
$k_{1,2}$ — constant in rheological model;
n — constant in rheological model;
T — temperature, [°K];
T_w — wall temperature, [°K];
T_s — temperature of the film surface, [°K];
V_z — the flow rate of fluid in the sens of flow, [m/s];
y — coordinate normal to the flow direction, [m];
z — coordinate in the flow direction, [m];
ρ — density, [Kg/m³];
λ — thermal conductivity, [W/m °K];
ψ — constant;
θ — dimensionless temperature.

Received, June 1, 1989

Polytechnic Institute, Jassy,
Department of Chemical Engineering
and
Institute for Macromolecular Chemistry
„Petru Poni", Jassy

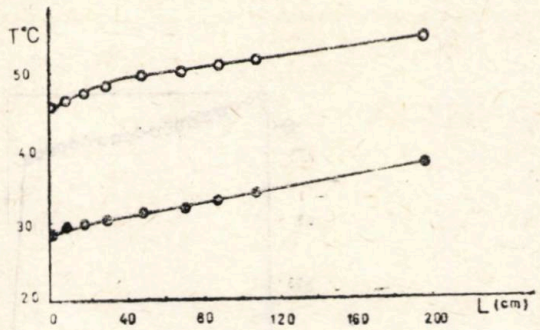

Fig. 2. — Experimental distribution of the wall temperature(○) as well as the film surface (●) for $T_{inlet}=60°C$, $\mathcal{R}_{e inlet}=24\,000$, $T_{film}=28\pm0.5°C$, $\mathcal{R}_{e film}=550$, $c=56\%$.

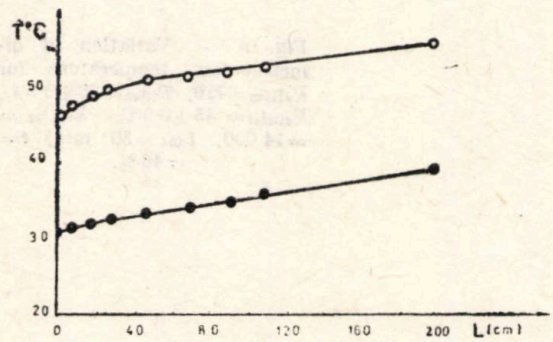

Fig. 3. — Experimental distribution of the wall temperature (○) as well as the fils surface (●) for $T_{inlet}=60°C$, $\mathcal{R}_{e inlet}=18\,000$, $T_{film}=30\pm0,5°C$, $\mathcal{R}_{e film}=290$, $c=56\%$.

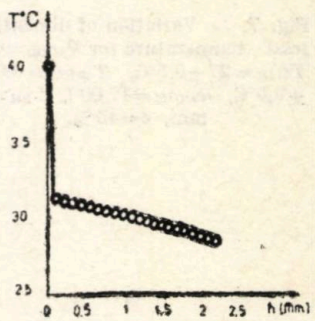

Fig. 4. — Temperature gradient across film thickness for $T_{film}=27\pm0.5°C$, $\mathcal{R}_{e film}=670$, $T_{inlet}=60\pm0.5°C$, $\mathcal{R}_{e inlet}=17\,000$, $L_{int}=30$ mm, $c=46\%$.

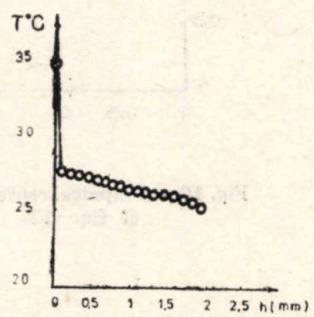

Fig. 5. — Temperature gradient across film thickness for $T_{film}=23\pm0,5°C$, $\mathcal{R}_{e film}=710$, $T_{inlet}=45°C$, $\mathcal{R}_{e inlet}=14\,000$, $L_{int}=30$ mm, $c=46\%$.

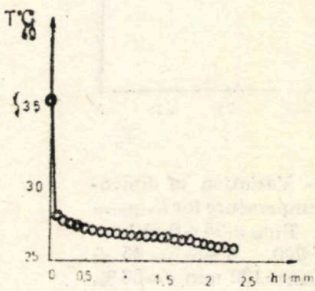

Fig. 6. — Temperature gradient across film thickness for $T_{film}=25\pm0.5°C$, $\mathcal{R}_{e film}=690$, $T_{inlet}=45\pm0.5°C$, $\mathcal{R}_{e inlet}=7\,800$, $L_{int}=130$ mm, $c=56\%$.

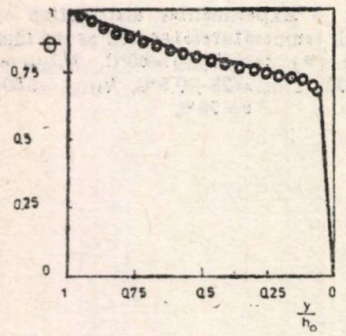

Fig. 7. — Variation of dimensionless temperature for $\mathcal{R}_{e\,film}=670$, $T_{film}=27\pm0.5°C$, $T_{inlet}=60\pm\pm0,5°C$, $\mathcal{R}_{e\,inlet}=17\,000$, $L_{int}=30$ mm, $c=46\,\%$.

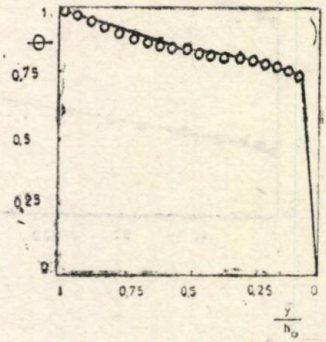

Fig. 8. — Variation of dimensionless temperature for $\mathcal{R}_{e\,film}=710$, $T_{film}=23\pm0,5°C$, $\mathcal{R}_{e\,inlet}=45\pm0.5°C$, $\mathcal{R}_{e\,inlet}=\\=14\,000$, $L_{int}=30$ mm, $c=\\=46\,\%$.

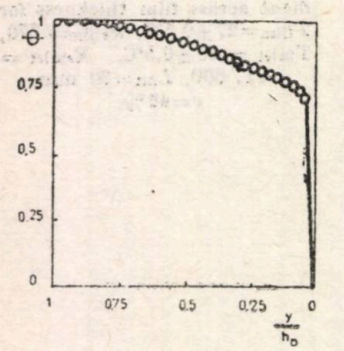

Fig. 9. — Variation of dimensionless temperature for $\mathcal{R}_{e\,film}=\\=690$, $T_{film}=25\pm0,5°C$, $\mathcal{R}_{e\,inlet}=7\,800$, $T_{inlet}=45\pm\pm0.5°C$, $L_{int}=130$ mm, $c=56\,\%$.

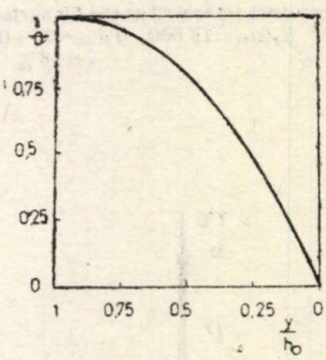

Fig. 10. — Graphical representation of Eq. (17).

REFERENCES

1. Davies J. T., Shawki A., Chem. Eng. Sci., **29**, 1 081—1 088 (1974).
2. Tudose R. Z., Mustaţă F., Bul. Inst. polit. Iaşi, **XXXIV (XXXVIII)**, *1—4*, s. II, 33—38 (1988).
3. Tudose R. Z., Mustaţă F., Mat. Plast., **25**, *1*, 33—36 (1988).
4. Mustaţă F., Tudose R. Z., Costea E., Bul. Inst. polit., Iaşi, **XXXV (XXXIX)**, *1—2*, s. II, 53—58 (1989).
5. Tudose R. Z., Mustaţă F., Stoleriu A., Costea E., Mat. Plast., **24**, *4*, 201—205 (1987).

DISTRIBUŢIA TEMPERATURII LA CURGEREA ÎN FILME SUBŢIRI DE LICHIDE NENEWTONIENE CARE RESPECTĂ MODELUL ELLIS

(Rezumat)

Se studiază transferul termic la curgerea în filme subţiri de lichide nenewtoniene de viscozitate mare care respectă modelul Ellis în condiţiile unui flux termic constant la perete. Pornind de la un profil parabolic al vitezei este obţinută distribuţia adimensională a temperaturii în film.

BULETINUL INSTITUTULUI POLITEHNIC DIN IAŞI
Tomul XXXVI (XL), Fasc. 1—2, 1990
Secţia II
CHIMIE ŞI INGINERIE CHIMICĂ

D.C. 66.093.6; 678.746.22—136.22

STUDIES ON DRYING KINETICS OF STYRENE—DIVINYL-BENZENE COPOLYMER

I. FIXED BED DRYING

BY

GH. CRISTIAN, RALUCA STAICU and I. VEREŞ

1. Introduction

The styrene — divinylbenzene copolymer is obtained by the suspension copolymerization of styrene and divinylbenzene with radicalic initiators. The product is obtained as beads of 0.2... 0.1 mm diameter containing 90 % styrene and 10 % divinylbenzene. Due to their porous structure, the copolymer beads are used as a skeleton in obtaining some ion-exchangers, as supports in gas- and gel-permeation chromatography.

The non-crystalline copolymer has a three-dimensional molecule, is insoluble in aqueous and common organic solvents such as : benzene, carbon tetrachloride, etc. It shows thermal stability up to 300°...350°C. By sulphonation the copolymer is converted into a cationite of a great practical importance due to its high exchanging capacity, thermal stability and mechanical resistance. These cationites are superior to those obtained on the basis of polycondensation resines.

During the obtaining process as well as after some practical uses the question arises of removing the moisture retained both between the copolymer beads and within its pores, which may be performed by evaporation with air as a thermal agent. The thermal agent may be passed either over the material surface or through the copolymer layer, the drying being thus carried out in fixed bed or in fluidized bed, respectively.

The drying process involves thermochemical phenomena of mass and heat transfer and the technological aspects of finding the optimum parameters of the drying agent are particularly important.

The drying is a complex phenomenon and the design of the dryier requires studies on the drying rate and duration.

In the present paper the experimental results on the fixed bed drying of the beads of styrene—divinylbenzene copolymer are reported. The moisture distribution within the copolymer fixed bed was settled and an equation for calculating the moisture migration coefficient derived.

2. Experimental Results

The experimental runs were performed on a laboratory equipment consisting of a tunnel drying provided with a drying chamber and one chamber for air heating [1]. The drying was performed by passing the drying agent over the material surface. The variation of the material moisture in time at different temperatures and flow rates of the air used as a drying agent was followed.

2.1. Influence of Drying Agent Parameters on Process Kinetics

In order to know the behaviour of the moistened materials during the drying process, experimental studies are required to make evident the in-

fluence of the drying agent parameters on the process kinetics and to lead finally to the determination of the drying duration and energy consumption.

The drying agent parameters which influence the process are the temperature, the flow rate and the relative humidity.

The drying regime must be optimized to find a minimum drying duration with a low energy consumption and the best technological properties of the material.

The influence of the temperature and air flow rate on the process kinetics of drying the copolymer beads was studied.

The temperature influence was investigated with constant flow rates of the drying agent of 3.6 m/s, by working at 40°, 50° and 60°C. The obtained results are plotted in Fig. 1 as the drying curves namely, variation of material moisture in time and variation of drying rate versus moisture.

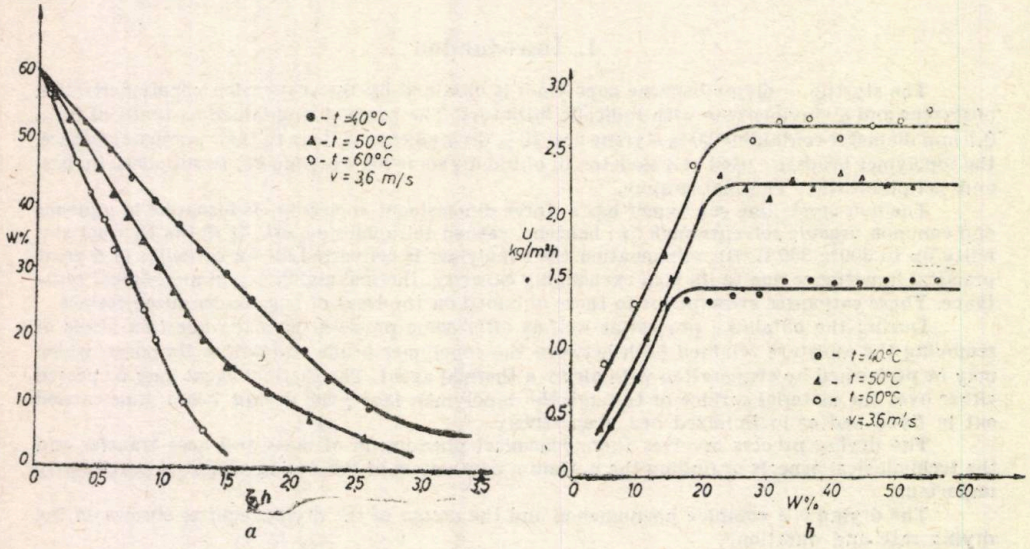

Fig. 1. — Influence of temperature on drying kinetics ; *a* — material moisture versus time ; *b* — drying rate versus material moisture.

The curves depicted in Fig. 1 show the drying rate to increase 1.6 times and the process duration to decrease two times with increasing temperature from 40° to 50°C. From the curves of drying rate variation versus moisture the conclusion may be draw that the copolymer drying proceeds in two stages, namely one of a constant drying rate and the other of a continously decreasing rate. These stages are separated by a critical point corresponding to a critical material moisture.

During the drying at a constant rate the partial pressure of the vapours on the material surface is equal to the corresponding pressure over a liquid with free surface. The drying rate depends neither on the thickness of the material layer nor on the initial moisture value if it is greater than the critical moisture, depending instead on the heat and mass transfer between the material and the sorrounding medium. The rate of moisture migration from inside is high enough to assure the passing of a moisture amount to the material surface.

This determines a nonuniform moisture distribution through the material thickness.

When the evaporation rate exceeds the moisture migration rate, the evaporation surface shifts to inside which results in a decrease in the drying rate. During this period the process is controlled by the evaporation rate, the resistance toward the vapour diffusion through the dried material layer and the resistance of the boundary layer at the surface. The resistance to diffusion through the material layer is much higher than that through the air boundary layer at the material surface. This fact is made evident by the factor of resistance to diffusion introduced by K r i s c h e r [2], which shows how many times the diffusion of water vapour is lower than that through the air layer of the same section and thickness under the same conditions of pressure and temperature.

The curves in Fig. 1 *b* indicate the existance of a single drying period of decreasing rate. During this period a dry zone exists at the material surface, whose thickness increases continuously, a moist zone and the evaporation one. The thickness of the evaporation zone is a function of the ratio between the evaporation rate and those of the moisture migration through the moist material. The moisture migration inside the material is determined by the moisture content and the temperature variation within the material. The material temperature within the dry zone increases and the moisture at the surface decreases tending to the equilibrium moisture. In this stage the process kinetics are not determined by the surface conditions but by the moisture distribution within the material.

In order to study the influence of the air flow rate on the process kinetics the experiments were carried out at two different values : 1.92 and 3.6 m/s. The temperature of the thermal agent was kept constant at 50°C.

The experimental results are shown in Fig. 2.

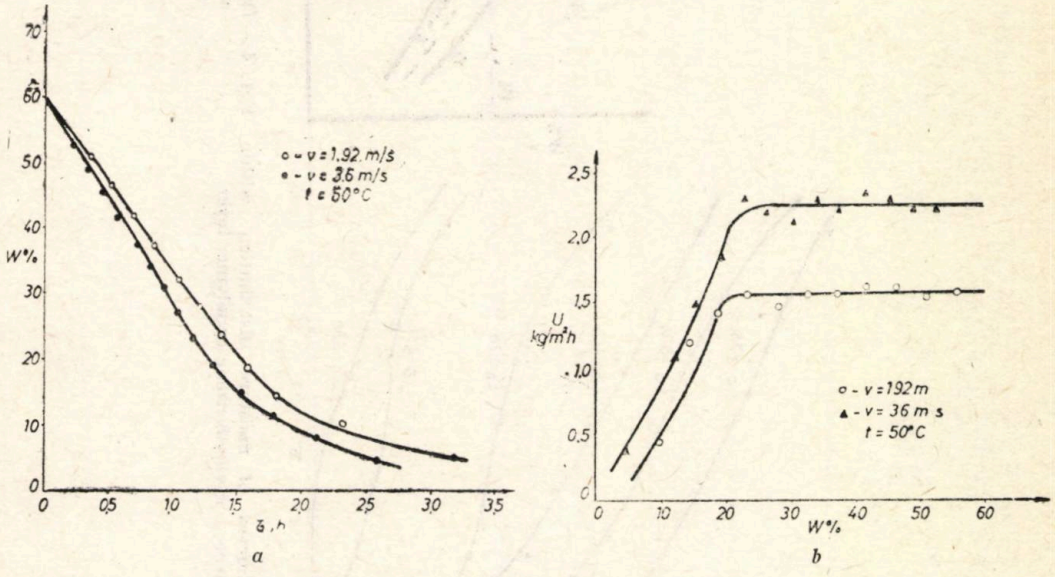

Fig. 2. — Influence of air rate on the drying kinetics : *a* — variation of material moisture in time ; *b* — variation of drying rate as a function of material moisture.

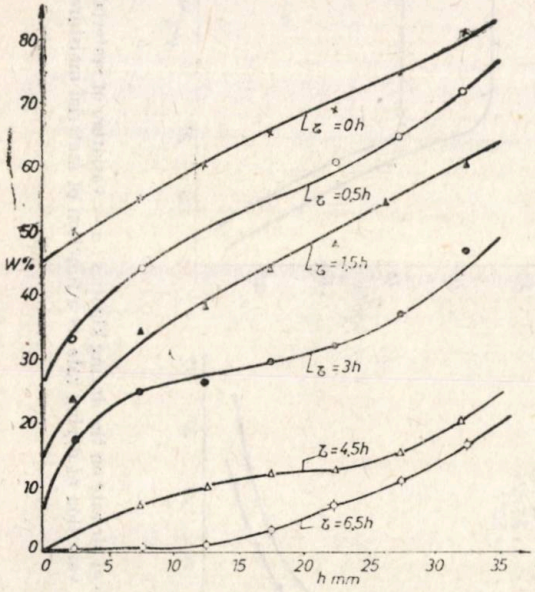

Fig. 3. — Curves of moisture distribution within the styrene — divinylbenzene copolymer layer.

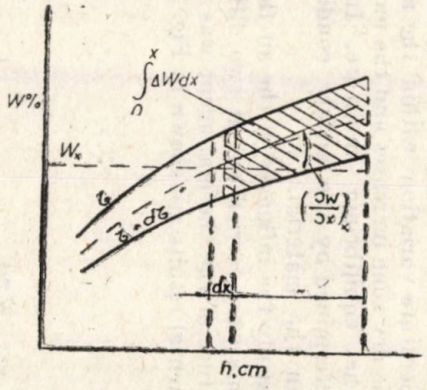

Fig. 4. — Determination of the moisture migrati on coefficient.

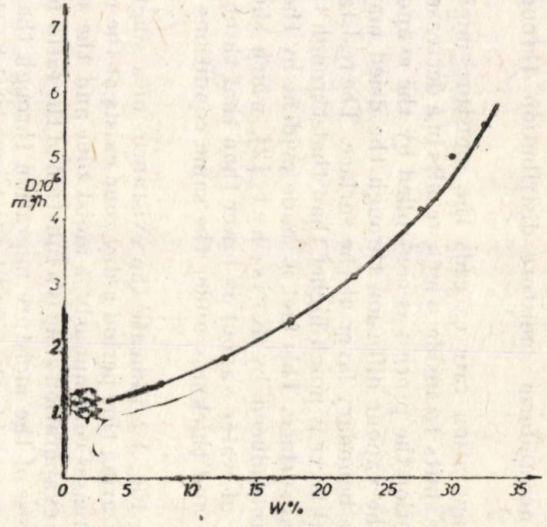

Fig. 5. — Variation of coefficient of moisture migration versus material moisture.

The curves in Fig. 2 show the increase in the air flow rate over the material surface resulting in a sensible increase in the drying rate during the first stage. The flow rate of the thermal agent influences on the drying rate by means of the surface boundary layer. During the second stage the influence of the air flow rate is lower since the evaporation surface shifts inside the material. The resistance of the boundary layer begins to decrease in comparison with that of the dry material layer toward the vapour diffusion.

2.2. Moisture Distribution within the Material Layer

Due to the moisture evaporation at the material surface, a moisture gradient occurs which determines the moisture migration to the evaporation surface. This process is influenced by the structure of the material submitted to drying, the parameters of the drying agent, moisture content, etc. The moisture migration during drying determines its distribution over the material layer thickness. The curves of moisture distribution were drawn by means of a gravimetrical method [1], [3]. The experimental results are depicted in Fig. 3.

The curves from Fig. 3 show the moisture to be non-uniformly distributed within the material thickness at the process beginning, probably due to the high moisture content of the sample. During drying the moisture variation takes place over the whole material thickness and after about 4 hours the equilibrium moisture is obtained at the surface.

For the moist material a coefficient of moisture migration was defined [1] which is a function of the moisture content, the capillary — porous structure of the material, etc.

The coefficient of moisture migration was determined as a function of moisture content by a grapho-analytical method [3] using also the moisture distribution curves in Fig. 3.

The equation of mass transfer in a single direction integrated with the condition $(\partial w/\partial \tau)_{x=0}=0$ leads to the equation ;

$$D_m = \frac{\int_0^x (\partial w/\partial \tau)\, dx}{(\partial w/\partial x)_x}. \tag{1}$$

The therms in Eq. (1) were determined from the moisture distribution curves by applying the grapho-analytical method. The principle of this calculation method is presented in Fig. 4.

The following relationship was finally derived for the coefficient of moisture migration ;

$$D_m = \frac{1}{\Delta\tau} \cdot \frac{\int_0^x \Delta w\, dx}{(\partial w/\partial x)_x} = \frac{1}{\Delta\tau} \cdot \frac{\sum A_i}{(\partial w/\partial x)_x}. \tag{2}$$

To determine the values of the moisture migration coefficient by means of Eq. (2) small moisture intervals, Δw, were chosen so that the migration

coefficient to be assumed constant. For such an interval the A_i surface on the sample thickness was calculated and the moisture amount which migrated within the time interval, $\Delta\tau$, through the cross section of the sample obtained. The moisture gradient was calculated in different points and by means of Eq. (2) the moisture migration coefficient estimated. The obtained results are presented in Fig. 5.

The results in Fig. 5 show an exponential variation of the moisture migration coefficient as a function of the moisture content. The equation describing this variation is of the following form :

$$D_m = 9.66 \times 10^{-7} e^{0.0518w}. \quad (3)$$

The experimental values, represented by points in Fig. 5, were found to be in a good agreement with the theoretical ones.

3. Conclusions

The following conclusions may be drawn from the experimental results on the fixed-bed drying of the styrene—divinylbenzene copolymer beads:

1. The drying process proceeds in two stages ; the first, having a constant drying rate and the second, with a continuously decreasing rate.

2. The parameters of the drying agents influences both the drying rate and duration process. The increase in the temperature and flow rate of the drying agent determines the increase in the drying rate and shortening of the process duration.

3. The curves of moisture distribution over the material thickness during the process allowed the calculation of the moisture migration coefficient. For the investigated range of moisture content an equation for calculating the migration coefficient varying exponentially with the moisture content was derived.

Notations

D_m — coefficient of moisture migration, [m^2/s] ;
U — drying rate, [$Kg/m^2 h$] ;
h — thickness of material, [m] ;
t — temperature, [°C] ;
v — flowing rate of the drying agent, [m/s] ;
w — humidity, [%] ;
x — current length, [m] ;
τ — drying time, [h].

Received, December 10, 1989

Polytechnic Institute, Jassy,
Department of Chemical Engineering

REFERENCES

1. Cristian Gh., Oprea V. Cl., Toth C., Toth I., Acta Polymerica, **35**, *8* (1984).
2. Krischer O., *Die Wissenschaftlichen Grundlagen der Trocknungstechnik*. Springer-Verlag, Berlin, Göttingen, Heidelberg, 1963.
3. Cristian Gh., Tudose R. Z., Revista de Chimie, **27**, *10* (1976).

STUDII DE CINETICA USCĂRII COPOLIMERULUI STIREN—DIVINILBENZEN

I. Uscarea în strat fix

(Rezumat)

Sînt prezentate rezultatele experimentale obţinute în cazul uscării în strat fix a perlelor de copolimer stiren — divinilbenzen prin trecerea agentului de uscare peste suprafaţa materialului. S-a studiat influenţa temperaturii şi vitezei aerului asupra vitezei de uscare. Experimental s-au obţinut curbele de distribuţie a umidităţii pe grosimea materialului iar pe baza lor s-a determinat coeficientul de migrare a umidităţii. Pentru acest coeficient s-a stabilit o ecuaţie de calcul.

BULETINUL INSTITUTULUI POLITEHNIC DIN IAŞI
Tomul XXXVI (XL), Fasc. 1—2, 1990
Secţia II
CHIMIE ŞI INGINERIE CHIMICĂ

УДК 678.5 ; 661.183.48

ПОВЫШЕНИЕ КАЧЕСТВА ПЛАСТИЧЕСКИХ МАСС ПРИ ВНЕДРЕНИИ ЦЕОЛИТОВ

ФЕЛИЧИЯ ЯКОМИ, Г. И. РУСУ, ЕВЕЛИНА ПОПОВИЧ, МИХАЕЛА РУСУ, ФЛОРИКА ИОАН, Ш. КУРКЭНЯНУ и И. Д. БУРСУК

1. Важной и перспективной областью применения цеолитов является промышленость пластических масс и синтетических волокон.

Было установленно, что при внедрении цеолитов в этих материалов их физико-механические характеристики не изменяются, но получается существенное возрастание равновесной влажности, а также уменьшение электростатического заряда.

Опыты показали, что внедрение некоторых молекулярных сит в прядильном растворе полиакрилонитрила определяет резкое уменьшение электросопротивления образцов [1], [2[.

В настоящей работе изученны электрические свойства некоторых материалов из поливинилхлорида с содержанием синтетических и природных цеолитов. Было установленно, что исследование температурной зависимости электропроводности этих материалов позволяет определить антистатизационные свойства соответствующих цеолитов.

2. Как известно, электропроводность на постоянном токе является найболее часто измеряемым параметром органических веществ. Тем не менее точное измерение этого параметра было проведено лишь нескольких случаях. Расхождение результатов различных авторов указывает на трудность таких измерении [3].

Что касается природа механизма электрической проводности в твердых полимерах, это очень спорная область. До сих пор, не было разработана унитарная теория о механизмах генерации носителей заряда в этих материалах, о кинетических явлении и т. д.

Для измерения электрической сопротивления были использованы образцы в виде таблеток с толщиной 1...2 мм, которых были изготовлены из пластинок пластических масс и цеолитов. Были использованы серебряные электроды. Проверка смичности контактов осуществлялась путём снятия вольтамперных характеристик.

Экспериментальные установки и методика измерения были описаны в [4] [5].

Некоторые электрические свойства синтетических цеолитов типа NaA были изучены в [5]. Для этих цеолитов, энергия активации вычисленная из температурной зависимости электропроводности лежит в интервале 0,70....1,70 эв и возрастает с увеличением отношения SiO_2/Al_2O_3 из исследованных образцов.

Для получения свидения о влиянии цеолитов на электрические свойства поливинилхлорида, были изготовлены образцы с разной концентрацией синтетического цеолита типа NaA и природного клиноптилолита. Гранулы цеолита зернением 120...150 микрометров были проникнуты в полимерных материалах во время их приготовления. Исследованные образцы также содержали пластификаторы и некоторые класители.

Для большого каличества образцов с разной концентрацией цеолитов (табл. 1), была изучена зависимость удельной электропроводности от температуры.

Наши опытки, показали, что все образцы изменени температуры обладают невоспроизводимыми электрическими свойствами. Ход зависимости удельной электопроводности от температуры в прямом и обратном направлении образует своево рода „петлю гистерезиса". Термическая обработка (некоторые последовательные нагревания и охлаждения в определенном температурном интервале ΔT приведён в таблице 1) приводит к установлению равновесной структуры образцов и, в результате измерение температурной зависимости электропроводимости дает совпадение прямого и обратного хода.

3. Из проведенных опытов можно сделать следующие выводы :

а) Для всех образцов, в исследованном интервале температур, ΔT, зависимость электропроводности от температуры имеет типически полупроводниковый характер. Следовательно, электропроводность меняется по экспоненциальному закону.

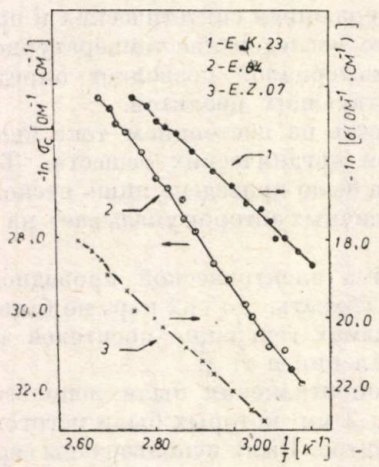

Рис. 1. — Зависимостя электрнпроводности от $10^3/T$.

б) Энергия активации ΔE (ширина запрещенной зоны), вычисленная из наклонов кривых $\ln\sigma=(10^3/T)$ имеет меньшие значения в образцах содержающих цеолиты. В результате этого, концентрация носителей заряда резко изменяется в зависимости от температуры.

в) Присутствие цеолитов орпеделяет увеличение электропроводности образцов. Следовательно, использованные цеолиты имеют хорошое антистатизационное действие.

γ) Установлено, что существует определенная концентрация цеолита при которой получается самое лущее действие антистатизации материалов. Можно предположить, что повышение концентрации цеолитов в образцах создает структурные дефекты которые являются лобушками для носителей заряда.

д) При использовании синтетических цеолитов типа NaA содержающих ионы Fe^{3+}, можно получить большое возрастание электропроводности образцов.

е) Хорошие антистатизационные эффекты получаются и при использовании клиноптилолита (использованный клиноптилолита содержает примерно 1,3% вес железо).

В таблице 1 приведены значения некоторых параметров, характеризующих исследованные образцы : d — толщина образцов, c — содержание цеолита, [% вес], σ_e —электропроводность при комнатой температуре после термического обработки.

Для три образцов зависимость электропроводности от температуры показана на рис. 1.

Таблица 1

Образец	Тип цеолита	c % вес	d мм	ΔT °K	σ_e $ом^{-1}.см^{-1}$	ΔE эв
E.21	—	—	1,7	290...370	$2,25.10^{-14}$	2,40
E.84	—	—	1,5	295...370	$8,33.10^{-14}$	2,20
E.Z.70	NaA	0,75	1,0	293...375	$2,45.10^{-12}$	1,90
E.Z.09	NaA	3,75	1,7	290...370	$6,50.10^{-10}$	1,80
E.Z.15	NaA	12,87	1,0	293...370	$7,35.10^{-9}$	1,50
E.Z.07	NaA	13,50	1,5	293...375	$2,50.10^{-10}$	1,75
E.Z.35	NaA	18,25	1,7	290...370	$8,75.10^{-11}$	1,80
E.ZF.6	NaA, Fe^{3+}	3,75	1,2	290...375	$8,25.10^{-9}$	1,50
E.ZF.3	NaA, Fe^{3+}	12,30	1,0	290...370	$1,15.10^{-8}$	1,40
E.K.12	Кл.	3,75	1,5	293...365	$8,33.10^{-10}$	1,80
E.K.23	Кл.	12,50	1,2	290...360	$7,80.10^{-9}$	1,60
E.K.07	Кл.	15,20	1,4	290...365	$1,23.10^{-9}$	1,65
E.A.17	—	—	1,3	295...375	$6,50.10^{-9}$	1,70
E.A.23	—	—	1,4	297...360	$5,45.10^{-9}$	1,75

В таблице 1 также приведены значения параметров для двух образцов, содержающих классические антистатизаторы (E.A.17 и E.A.23).

Поступило с 9 февраля 1990

Ясский политехнический институт
Кафедра общий химий и технологий
и
Ясский Университет им. „Ал. И Кузы"

ЛИТЕРАТУРА

1. Брек Д. *Цеолитовые молекулярные сита.* Изд. Мир, Москва, 1976.
2. Townsed R. P., *The Properties and Applications of Zeolites.* The Chem. Soc. London, 1980.
3. Pope M., Swenberg C., *Electronic Process in Organic Cristals.* Clarendon Press, Oxford, 1982.
4. Rusu G. I. et al., Makromol. Chem., **107**, 33 (1982).
5. Rusu G. I., Iacomi F., Rusu M., Proc. of Symp. on Meth., Mod. and Technol. in Phys. and Related Fields, Cluj-Napoca, 1986, 74.

CREŞTEREA CALITĂŢII MASELOR PLASTICE PRIN ÎNCORPORARE DE ZEOLIŢI

(Rezumat)

Se analizează conductivitatea maselor plastice conţinînd policlorură de vinil alături de NaA, FeNaA, clinoptilolit şi alte materiale antistatice. Pulberile zeolitice naturale sau sintetice încorporate în mase plastice sporesc conductivitatea acestora, favorizînd lărgirea gamei lor de de utilizare în procese tehnologice.

BULETINUL INSTITUTULUI POLITEHNIC DIN IAŞI
Tomul XXXVI (XL), Fasc. 1—2, 1990
Secţia II
CHIMIE ŞI INGINERIE CHIMICĂ

УДК 661.183.48

ДЕГИДРИРОВАНИЕ МЕТАНОЛА НА ПРИРОДНОМ ЦЕОЛИТЕ И НА ЕГО МОДИФИЦИРОВАННЫХ ФОРМАХ

ЕВЕЛИНА ПОПОВИЧ, ФЕЛИЧИЯ ЯКОМИ, ЕЛЕОНОРА ТРИФ, И. МЫНДРЕЧ и АЛ. НИКУЛА

1. В настоящее время уже не вызывает сомнения, что цеолиты, содержащее ионы переходных металлов, обладают высокой каталитической активностью во многих окислительных процессах [1].

Изучение каталитических свойств цеолитов в реакциях окисления показало, что обычно каталитическая активность выше в присутсвии ионов переходных металлов, на которых процесс протекает либо с изменением валентности иона металла, либо с диссоциативной адсорбцией и активированием кислорода и его последующим взаимодействием с углеводородом в газой фазе.

В реакции окислительной дегидрогенизации метанола в формальдегиде, имеющей важное практическое значение, цеолитные катализаторы изучались в их Fc^{+3} Co^{+2}, Cu^{+2}, Ni^{+2}, ионообменных формах [2] ... [5].

До сих пор не существует однозначного мнения а том, могут ли клиноптилолиты служить катализаторами мякого окисления.

Целью настоящей работы являлось приготовление и прелиминарное исследование каталитических свойств модифицированных природных цеолитов-клиноптилолитов, в реакции окислительной дегидрогенизации метанола.

2. Приготовление катализатора было сделано с помощью подходящего изменения природного клиноптилолита (69,20% SiO_2; 11,65% Al_2O_3; 1,30% Fe_2O_3 ; 0,67% MgO ; 3,74% CaO ; 0,72% Na_2O ; 3,30% K_2O ; 9,14% потери топливо) преследуя, в первую очередь, получение цеолитной подложки кислотно-термически-стабильный и с высокой чистотой, и потом пропитывание с Mo и Fe окисями.

В качестве исходного цеолита применяли природные цеолиты с соотношением $SiO_2/Al_2O_3 = 5,8$, имеюшим степень кристалличности 60%.

Предыдущее исследование показало, что термическая обработка при температуре 400°C, в течение 4 часов, определяет увеличение химического сопротивления природного клиноптилолита.

Для очищения, образцы клиноптилолита предварительно подвергались кислотной обработке 2 H растворами соляной кислоты при температуре 90°C, два раза в течение 10 часов (образец *1*).

Природные катализаторы содержащие окиси Mo, Fe во внутренних адсорбционных каналах природного клиноптилолита, было сделано путем проколенного цеолита с Mo—Fe комплексных раствотами в воде металл-аминным катионом, который вводился в адсорбционным канал цеолита (образец *5*).

После смещения, пластическим дроблением получаются зерны с 2×4 мм. Полученный катализатор после высущивания при температуре 120...200°C, был проколован при 400°C.

Для установления некоторых выводов была приготовлена модифицированная форма клиноптилолита с помощью ионообмена с Mo и Fe ионами (образец *2* содержит 1,81 мэкв Fe^{+3}/г, образец *3* содержит 0,82 мэкв Mo^{6+}/г).

Каталитические исследования проводятся в проточной установке непрерывного действия при концентрации метанола—воздушной смеси 3...6 об. % в интервале температур 200°...450°C с навесной катализатора 0,5 г.

Диффракционным анализам радиации X образцов были обнаружены небольшое снижение кристалличности образцов и модификация интенсивности пиков диффракции. Это наводит на мысль, что комплексные окиси, образованные в каналах цеолита, нарушают решетку клиноптилолита.

Исследования ЭПР на образцах *1...5* дают сведения о непосредственном соседстве парамагнитных ионов в цеолите. Спектр образца-свидетеля (образец *1*) указывает присутствие небольшого количества железа в ионообменных позициях ($g=2$; $\Delta H=300$ G) и в каркасе цеолита ($g=4{,}3$; $\Delta H=150$ G) (рис. 1) [6].

Образцы *2*, *3* не представляют модификации сигнйла ЭПР. Предполагаем, что Mo^{6+} и $Fe^{3+}(H_2O)_6$ не дают сигналы ЭПР.

Согреванием в вакууме до 150°C образца *2* сигнал от $g=4{,}3$ (рис. 1) увеличивается, что указывает на модификацию симметричности соседства иона в катионных позициях удалением воды.

Образцы, термически обработанные в вакууме, указывают повышение сигнала, характерно для Mo^{5+} иона в ионообменных позициях (образец *3*, рис. 2) [7], [8].

Сигналы ЭПР образцов *4*, *5* широкие, характерные для окисных фаз, образованных в каналах цеолита.

Спектры ИК образцов *1...5* представляют полосу от 1 390 $см^{-1}$, характерную для внешних колебаний $(Si, Al)O_4$. Полосы от 970 $см^{-1}$ и 1 000 $см^{-1}$ принадлежат комплексам окиси образцов *4* и *5* (рис. 3) [9].

В рис. *4* представлена каталитическая активность исследуемых образцов в окислительной реакции метанола в формальдегиде (образец *1*). Эти результаты выявляют то, что и начальный клиноптилолит, благодаря присутствия окисей железа в своем канале, проявляет небольшую каталитическую активность (самую высокую при 400°C).

Исследование образцов *2...5* показывает что самые хорошие результаты получаются для образцы *4* и *5*.

Ионообмен с Mo и Fe каталитическая активность растет и отходит к более низким значеням реакции (образец *4*). Прокалыванием окисями (Mo/Fe=2) каталитическая активность растет проявляясь преимущественно в сфере 350°....400°C (образец *5*).

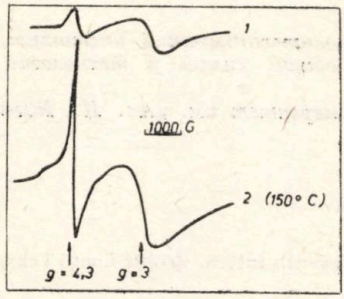

Рис. 1. — Спектры ЭПР при комнатой температуре (Fe^{3+}).

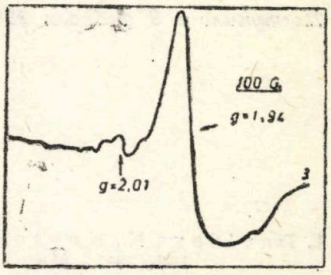

Рис. 2. – Спектр ЭПР Mo^{6+}, при комнатой температуре (после термическая обработка в вакууме при 400°С).

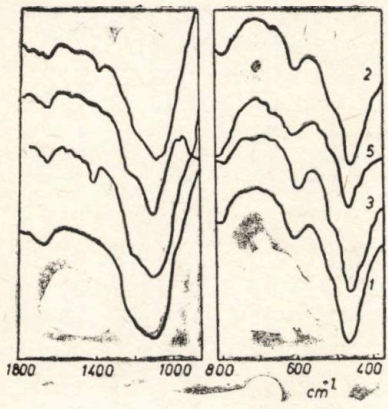

Рис. 3.— ИК спектры образцов.

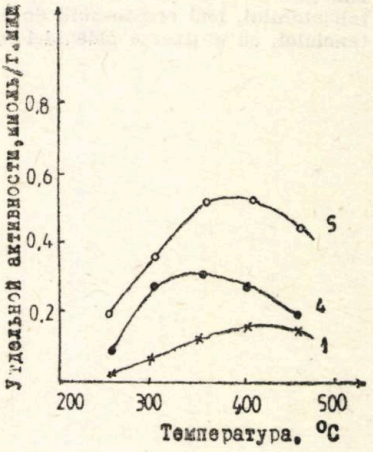

Рис. 4. — Удельной активность образцов.

Эти прелиминарные результаты наводят на мысль, что надо продолжать исследование каталитическую активность клиноптилолита-катализатора.

Поступило с 9 февраля 1990

Ясский политехнижческий институт,
Кафедра общий химий и технологий
и
Ясский университет им. „Ал. И. Кузы"

ЛИТЕРАТУРА

1. Davidova N., Kovacheva P., Shopov D., Seventh Intern. Zeolite Conf., Tokyo, 1986, 811—818.
2. Cucherov A. V., Slinkin A. A., Zeolites, **7**, 38—42 (1987).
3. Cucherov A. V., Slinkin A. A., Zeolites, **6**, 175 (1986).
4. Johns J. R., Howe R. F. Zeolites, **5**, 251—256 (1985).
5. Ward M. B., Lunsford J. H., Proc. of 6th Intern. Zeolite Conf., Butterworths, 1984 (Eds. D. H. Olson and A. Bisio).
6. Dai P. E., Lunsford J. H. Catal. J., **64**, 173 (1980).
7. Kovacheva P., Davidova N., Shapov D., Zeolites, **3**, 92 (1983).
8. Sato M., Anderson R. B., J. Catal., **67**, 296 (1981).
9. Rooney J. J., Stewart A., Catalysis (Chem. Soc. Spec. Per. Rep.), **1**, 277 (1977).

DEHIDROGENAREA METANOLULUI PE ZEOLIŢI NATURALI ŞI PE FORMELE LOR MODIFICATE

(Rezumat)

Se prezintă propietăţile catalitice ale clinoptilolitului şi a formei modificate Mo—Fe clinoptilolit. Studiile RES, IR precizează localizarea ionilor Fe^{3+} şi Mo^{5+} în structura catalizatorului, ioni responsabili de activitatea catalitică în procesul de dehidrogenare a metanolului, cu obţinerea aldehidei formice.

BULETINUL INSTITUTULUI POLITEHNIC DIN IAŞI
Tomul XXXVI (XL), Fasc. 1—2, 1990
Secţia II
CHIMIE ŞI INGINERIE CHIMICĂ

C.D. 667.211 ; 668.474

PRÉPARATION DE QUELQUES COLORANTS AZOÏQUES UTILISANT LA LIGNINE COMME COMPOSANT DE COPULATION

PAR

SAVEL IFRIM

1. Introduction

La nécessité toujours croissante de matières premières utiles pour l'industrie chimique a déterminé l'orientation des recherches vers la mise en valeur des différentes sources et sous-produits, apparaissant en certains processus technologiques. Un tel sous-produit est la lignine, résultant pendant la désincrustation du bois pour séparer la cellulose.

Compte connu que le pourcentage de lignine dans la composition du bois dépasse 20...25 % [1] et que les quantités de bois utilisées annuellement sont immenses, il résulte que les quantités de lignine qui apparaissent sont de même très grandes. Ces quantités de lignine doivent trouver une mise en valeur.

Il y a des recherches scientifiques qui indiquent la possibilité d'utiliser la lignine en multiples directions [2], [3], par exemple la fabrication de quelques produits chimiques ayant une petite molécule ou bien de produits macromoléculaires [4].

Un nombre réduit de travaux scientifiques indiquent la lignine comme matière première dans le but d'obtenir de colorants organiques.

Quoique la méthode de séparation de la lignine influence ses propriétés physiques et chimiques [5], toutefois son caractère aromatique et la présence des groupements phénoliques sont toujours gardés dans sa structure chimique.

Compte tenu de cette structure chimique, dans ce travail on indique la possibilité de mise en pratique de la lignine comme composant de copulation pour obtenir de colorants azoïques.

2. Partie théorique

On peut soumettre la macromolécule de la lignine à différentes opérations qui modifient sa structure chimique et également ses propriétés physico-chimiques.

Il y a des travaux scientifiques qui indiquent la possibilité d'utiliser la lignine comme composant de diazotation afin d'obtenir de colorants azoïques [6] ; dans ce but la lignine a été tout d'abord nitrée, ensuite réduite et puis transformée par diazotation dans un sel de diazonium. Dans un autre travail [7] on a indiqué l'utilisation de la lignine hydrolytique comme composant de copulation.

Puisque la lignine est un produit macromoléculaire, par son utilisation dans la synthèse des colorants organiques, les produits colorés qui peuvent résulter auront de même une structure macromoléculaire, leur solubilité réduite et par conséquent leur solicitation dans la pratique sera limitée.

Par activation de la lignine, c'est-à-dire par son traitement dans un milieu alcalin, sous pression et à chaud, apparaissent certains processus hydrolytiques et la lignine traitée de cette manière devient plus réactive. L'hydrolyse et l'activation de la lignine sont fondées sur sa propriété de se dissoudre dans une solution alcaline.

Dans le présent travail on utilise la lignine séparée de la lessive noire, qui résulte à la fabrication de la cellulose par le procédé „sulfate". Après sa purification et activation, la lignine a été couplée avec quelques sels de diazonium, obtenus par la diazotation de l'acide *p*-aminobenzoïque, de la *p*-nitroaniline, de l'α-naphtylamine et de la β-naphtylamine, en obtenant des colorants à diverses nuances, ayant les suivantes formules chimiques générales :

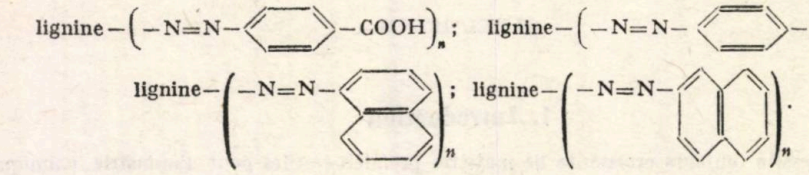

C'est facile de comprendre qu'on dispose de possibilités d'utiliser également d'autres composants diazotables afin d'obtenir de colorants organiques, qui aient différentes propriétés de teindre.

3. Partie expérimentale

L'activation de la lignine a été réalisée de la manière suivante: on introduit 30 g lignine purifiée en 300 ml de l'eau et on ajoute 12 g hydroxyde de sodium. Pratiquement il apparait une solution aqueuse de 4% NaOH et d'une concentration de 40% NaOH par rapport à la lignine. L'hydromodule de cette solution rapporté à la lignine est 1/10. Dans ces conditions la lignine est totalement dissoute.

On introduit la solution de lignine ainsi obtenue dans une autoclave d'acier inoxydable et on la chauffe à 180°C, pour une durée de 5 h. Pendant le chauffage la pression dans l'autoclave augmente à six atmosphères. Après le chauffage on refroidit l'autoclave à l'eau, puis on introduit la solution dans un verre Berzelius et on acidifie avec de l'acide chlorhydrique jusqu'au pH=3.

En milieu acide, la lignine activée précipite. On filtre et ensuite on lave à l'eau distillée pour éloigner les traces d'acidité.

La lignine activée obtenue de la sorte a été utilisée comme composant de copulation.

La diazotation des composants diazotables a été réalisée, pour tous les cas, à l'aide de l'acide chlorhydrique et de l'azotite de sodium, en travaillant toujours selon la méthode connue. Pour obtenir une diazotation totale les quantités d'acide et d'azotite, calculées théoriquement, ont été choisies en pratiques avec un excès de 5%.

Pour calculer la quantité du composant de copulation on a considéré la moyenne arithmétique résultant par la totalisation des poids moléculaires des alcools se trouvant dans la composition de la lignine, à savoir : l'alcool *p*-hydroxycinamique (I), l'alcool coniferilique (II) et l'alcool sinapique (III):

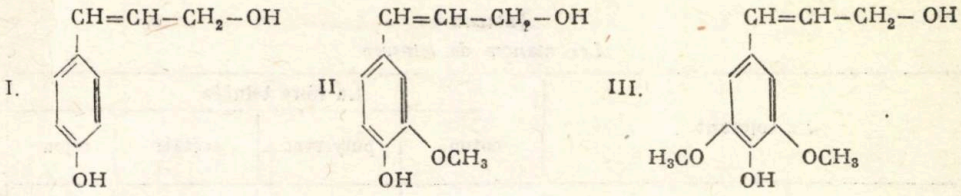

Il résulte par calcul que ce poids moléculaire moyen est 180.

Pour préparer les colorants on a pesé dans tous les cas 2 g lignine activée et par rapport à cette quantité on a calculé celle du composant diazotable ; il résulte respectivement 1,5 g de l'acide *p*-aminobenzoïque, 1,5 g *p*-nitroaniline, 1,6 g α-naphtylamine et 1,6 g β-naphtylamine.

On a dissout le composant de copulation en utilisant une très petite quantité de solution d'hydroxyde de sodium 32,5% ; ensuite on a dilué à l'eau et on a refroidit jusqu'à 2° ...3°C.

La copulation a été effectuée en milieu alcalin, par l'introduction de la solution de diazonium, sous agitation, sur la solution de lignine. Après l'achèvement de la réaction de copulation, on filtre le colorant sous pression réduite et puis on le lave sur filtre à l'eau distillé. Dans tous les cas les rendements sont très bons, dépassant 80%.

4. Applications

Les colorants obtenus ont été utilisés pour teindre du coton, de l'acétate de cellulose, des fibres synthétiques polyestériques et synthétiques type „relon" (polycaprolactame). On a effectué les teintures dans une solution aqueuse de carbonate de sodium 2...3%, à l'ébullition, pour une durée de 10 min., en utilisant un hydromodule de 1/50 et un concentration en colorant de 3% par rapport à la quantité de fibre teintée.

La solubilité des colorants préparés, dans la solution de carbonate de sodium, n'est pas la même ; les produits obtenus à partir de l'acide *p*-aminobenzoïque et de la β-naphtylamine manifestent une bonne solubilité, tandis que le colorant obtenu à partir de l'α-naphtylamine se dissout difficilement.

Les nuances des teintures sont présentés dans le Tableau 1.

On constate tout d'abord que les colorants préparés manifestent une meilleure affinité pour les fibres cellulosiques que pour ceux synthétiques. Cette propriété n'est pas une surprise, puisque la lignine est très compatible avec la cellulose. On observe de même que tous les coloriages sont claires, mais par utilisation d'autres composants diazotables on peut obtenir également des nuances différentes.

5. Conclusions

Les épreuves expérimentales démontrent que la lignine constitue un matériel organique de grande valeur, qui par activation en milieu alcalin est transformée dans un produit plus réactif qui peut être utilisé comme composant de copulation afin d'obtenir de colorants organiques.

Tableau 1

Les mances de teinture

Le colorant	La fibre teintée			
	coton	polyester	acétate	relon
Lignine–(–N=N– 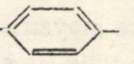 –NO_2)$_n$	beige	—	cognac	jaune
Lignine–(–N=N– 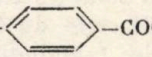 –COOH)$_n$	crème	—	jaune	—
Lignine–(–N=N– 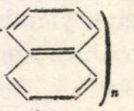)$_n$	rose-claire	rose-claire	bordeaux	rose-claire
Lignine–(–N=N– 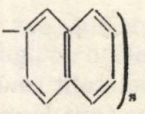)$_n$	beige	beige-rosé	orange-claire	crème

On peut utiliser les colorants azoïques ainsi obtenus au coloriage des fibres cellulosiques et synthétiques. Leur utilisation dans le processus de teinture ne présente pas de difficultés pratiques. Les résultats expérimentaux prouvent que ces colorants sont plus indiqués pour teindre les fibres cellulosiques.

Reçue le 27 février 1987

Institut Polytechnique, Jassy,
Chaire de Chimie Générale et Technologique

BIBLIOGRAPHIE

1. Diaconescu V., Obrocea P., *Tehnologia celulozei şi hîrtiei.* Vol. I, Ed. Tehn., Bucureşti, 1974, 19.
2. Simionescu Cr., Diaconescu M., Andriescu P., Popa-Stoicescu M., Cernătescu-Asandei A., Celuloză şi hîrtie, **33**, *4*, 166 (1984).
3. Simionescu Cr., Cernătescu-Asandei A., Andriescu P., Diaconescu M., Celuloză şi hîrtie, **33**, *4*, 166 (1984).
4. Popa V., *Tehnologii de valorificare a ligninei.* Inst. Polit., Iaşi, 1983.
5. Glasser W. G., Forest Product Journal, **31**, 24 (1981).
6. Rozmarin Gh., Ifrim S., Popa V., Celuloză şi hîrtie, **36**, *1*, 3 (1987).
7. Draganova R., Nenkova S., Draganov Al., Celuloză şi hîrtie, **33**, *4*, 198 (1984).

PREPARAREA UNOR COLORANŢI AZOICI FOLOSIND LIGNINA DREPT COMPONENTĂ DE CUPLARE

(Rezumat)

Se indică posibilitatea folosirii ligninei în calitate de componentă de cuplare, pentru obţinerea unor coloranţi azoici. În acest scop lignina a fost supusă unui proces de activare, prin tratare la cald, în mediu alcalin, cînd au loc, probabil, fenomene hidrolitice iar lignina devine mai reactivă.

Coloranţii azoici obţinuţi au fost folosiţi pentru vopsirea unor fibre sintetice şi celulozice rezultînd vopsiri în tonuri deschise. Utilizarea acestui tip de coloranţi pentru vopsire nu prezintă dificultăţi practice.

Probele experimentale arată că fibrele celulozice au o mai bună afinitate faţă de aceşti coloranţi, aşa precum era de aşteptat, ţinînd seama de provenienţa ligninei.

BULETINUL INSTITUTULUI POLITEHNIC DIN IAŞI
Tomul XXXVI (XL), Fasc. 1—2, 1990
Secţia II
CHIMIE ŞI INGINERIE CHIMICĂ

C.D. 547.261.1

SYNTHÈSE DE QUELQUES NOUVEAUX DÉRIVÉS PYRIDAZINIQUES DOUÉS D'ACTIVITÉ PHYSIOLOGIQUE

PAR

MARIA CAPROŞU, ŞT. CILIANU, RALUCA BOZGA, IOANA CIOCOIU, MAGDA PETROVANU et ELENA BÎCU

1. Introduction

Dans des recherches antérieures [1], ..., [3] on a synthétisé de nouveaux dérivés pyridaziniques doués d'activité anticonculsivante et analgétique du type (I) et (II).

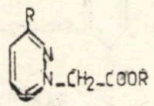

I

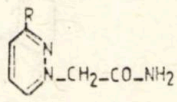

II

Poursuivant les recherches visant l'obtention de nouvelles structures pyridaziniques plus actives et moins toxiques dans le domaine des produits sédatifs, anticonvulsivants, etc., on a étudié d'une part la réaction de cyanoéthylation en série pyridaziniques et d'autre part quelques possibilités de transformation du groupement nitrile.

2. Résultats et discussions

Vu que pour obtenir les estères (I) et les amides (II) on doit utiliser le bromoacétate d'éthyle, qui est une substance assez toxique et difficile à manipuler et, en même temps, les rendements sont assez faibles, on a essayé de réaliser la cyanoéthylation des pyridazones (III), tenant compte du fait que ces structures possèdent un hydrogène mobile attaché à l'un des atomes d'azote du noyau 1.2 diazinique.

En effet, en traitant les solutions dioxaniques avec de l'acrylonitrile en présence de Triton B comme catalyseur, on a réussi à obtenir les nitriles du type (IV) (*a*: R=Br, *b*: R=CH_3). Pour l'obtention des pyridazones (III) on a utilisé les indications de la littérature [2], [3].

Les nitriles (IV), dissouts dans l'acide sulphurique et abandonnés à la température ambiante, ont conduit aux amides (V).

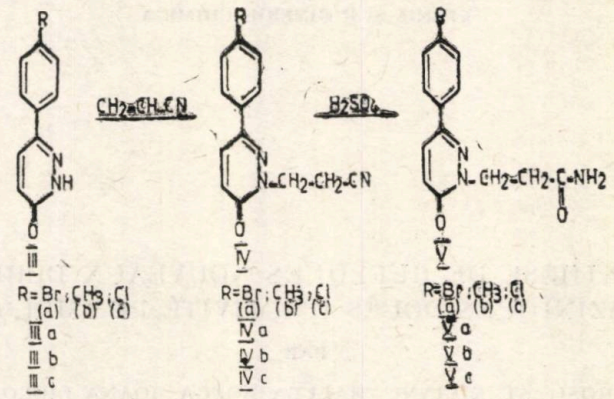

Dans une autre série de réactions on a étudié la saponification des nitriles (IV) en portant à reflux les nitriles en solution alcaline 10%. On a réussi à obtenir les acides (VI), selon la réaction :

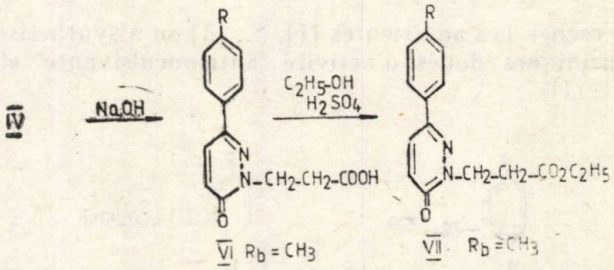

En traitant les acides (VI) avec de l'alcool éthylique et de l'acide sulphurique, on a obtenu les esters (VII) (R=CH_3, Br) [4].

Les produits obtenus ont été caractérisés par dés analyses chimiques et spectrales (IR).

3. Partie expérimentale

3.1. 3-(p.bromophényle)-pyridazonyle-1-(β-cyanoéthylène) (IV *a*)

On dissout 4 g de 3-(p. bromophényle-pyridazone (III *a*) dans 40 ml de dioxane. On ajoute 10 ml d'acrylonitrile et 2,5 ml de Triton B. On porte à reflux le mélange réactionnel pendant 4 h. On le laisse se refroidir et on précipite avec de l'eau le produit obtenu. On filtre, on lave avec de l'eau et on recristallise dans un mélange alccool méthylique—eau. On obtient un produit à p. f. 168°C.

Analyses ($C_{13}H_{10}N_3OBr$)

	N%
Calculé	13,81
Trouvé	13,04

P.M.=304.

Spectre IR (KBr) : ν_{CH_3}=2 880 cm^{-1}; ν_{CN}=2 200 cm^{-1} ; $\nu_{C=O}$=1670 cm^{-1}; $\nu_{\varphi\ aromatique}$ = =3 040 cm^{-1} ; $\nu_{C=C(aromatique)}$ =1 620, 1 587, 1 510, 1 455 cm^{-1}.

Par la même méthode on a obtenu le 3-(p. tolyle)-pyridazonyle-1-(β-cyanoéthylène) (IV *b*), à partir de la 3-(p. tolyle)-pyridazone (III *b*).

Produit blanc à p.f.=170°...171°C.

Analyses

N%

Calculé 17,57
Trouvé 17,12

3.2. Amide de l'acide 3-(p. bromophényle)-pyridazonyle-1-propionique

On abandonne à la température ambiante, pendant 24 h, un mélange de 2 g 3-(p. bromophényle)-pyridàzonyle-1-(β-cyanoéthylène) (IV *a*) et 8 ml H_2SO_4. On agite de temps en temps. On verse le mélange sur de la glace ; il se forme un produit blanc. On recristallise l'amide formé dans un mélange alcol éthylique—eau. Produit incolore à p. f. 209°...210°C.

Analyses ($C_{13}H_{12}N_2O_2Br$)

N%

Calculé 13,04
Trouvé 13,18 ; 13,25
P. M.=322

Spectre IR (KBr) : ν_{N-N}=3 290 cm^{-1} ; ν_{CH_2}=2 880 cm^{-1} ; $\nu_{C=O(cycle)}$=1 667 cm^{-1} ; $\nu_{C=O}$=1 659 cm^{-1} ; ν_{N-N} = 1 633 cm^{-1} ; $\nu_{C=C(aromatique)}$ = 1 588, 1 510, 1 486 cm^{-1} ; $\nu_{C-H(aromatique)}$ =730 cm^{-1}.

3.3. Acide 3-(p.tolyle)-pyridazonyle-1-propionique (VI *b*)

On traite 2 g de 3-(p. tolyle)-pyridazonyle-1-(β- cyanoéthylène) (IV *b*) par une solution de 1 g NaOH dans 200 ml d'eau. On porte à reflux le mélange réactionnel pendant 3 h; on laisse refroidir la solution et on acidule. Il se sépare un produit incolore. On recristallise dans un mélange d'alcool éthylique — eau. On obtient un produit blanc à p. f. 183°C.

Analyses ($C_{14}H_{14}N_2O_3$)

N%

Calculé 10,85
Trouvé 11,02
P.M.=258

Spectre IR (KBr) : ν_{C-H}=2 370...2 810 cm^{-1} ; $\nu_{C=O(acide)}$=1 746 cm^{-1} ; $\nu_{C-HO(acide)}$= =1 180, 1 194, 1 214 cm^{-1}.

3.4. Ester éhylique de l'acide 3-(p. tolyle)-pyridazonyle-1-propionique (VII *b*)

On traite 2 g d'acide 3-(p. tolyle)-pyridazonyle-1-propionique (VI *b*) avec 9 ml d'alcool éthylique anhydre et 1 ml d'acide sulphurique. On chauffe au bain-marie le mélange réactionnel pendant 10 h. Après refroidissement on verse la solution sur de la glace ; il se précipite un produit blanc. On recristallise dans de l'acétate d'ethyle. Produit blanc à p. f. 82°C.

Analyses ($C_{16}H_{18}O_3N_2$)

N%

Calculé 9,79
Trouvé 10,01
P.M.=286

Reçue le 13 mars 1989

Institut Polytechnique, Jassy,
Chaire de Chimie et Technologie
Organique et Macromoléculaire

BIBLIOGRAPHIE

1. Wermuth G. G., Revue Agressologie, **VI**, *4*, 383 (1965).
2. Ciocoiu I., Cilianu St., Cârstea Al., Caproşu M., Ştefănescu E., Petrovanu M., Rev. Med. Chirurg., **91**, *1*, 137 (1987).

3. Ciocoiu I., Cilianu St., Cârstea Al., Bozga R. Caproşu M., Ştefănescu E., Petrovanu M., Bul. Inst. polit., Iaşi, **XXXIV (XXXVIII)**, *1—4*, s. II, (1988).
4. Stachelin A., Eichenberg K., Druey J., Helv. Chim. Acta, **XXXIX**, *V—VIII* 1 741 (1956)

SINTEZA UNOR NOI DERIVAŢI PIRIDAZINICI CU EVENTUALĂ ACTIVITATE FIZIOLOGICĂ

(Rezumat)

Continuind cercetările în vederea obţinerii de noi produşi cu structură piridazinică cu eventuală acţiune sedativă, anticonvulsivantă etc., au fost sintetizaţi cinci produşi noi.
Structura produşilor obţinuţi a fost confirmată de analizele chimice şi spectrale.

BULETINUL INSTITUTULUI POLITEHNIC DIN IAȘI
Tomul XXXVI (XL), Fasc. 1—2, 1990
Secția II
CHIMIE ȘI INGINERIE CHIMICĂ

C.D. 547.53.024 ; 615-015

STRUCTURES AMIDIQUES AVEC ACTION SUR LE SYSTÈME NERVEUX CENTRAL

III. N-Benzyl—carbamates de méthyle et N-(aminométhyl)-amides*)

PAR

LEONTE CANDIANO, EUGENIA CARP, SAVA DUMITRESCU, Șt. CILIANU et RODICA BOZGA

1. Introduction

Dans une série de travaux antérieurs [1] on a montré que certains diacyl-dérivés non symétriques de la méthylène-diamine, les N-(amidométhyl—carbamates d'alkyle (I) :

$$\underset{\text{(I)}}{R-CO-NH-CH_2-NH-COOR'} \qquad \underset{\text{(II)}}{(p)\ R-C_6H_4-CH_2-NH-CO-C_6H_4-R'\ (p)}$$

possèdent de remarquables propriétés anticonvulsivantes. L'analogie de ces composés avec d'autres structures actives nous a conduit aux N-benzyl-benzamides (II) [2], qui se sont montrées intéressantes en ce qui concerne leur action pharmacologique.

En simplifiant les structures d'une manière encore plus drastique, dans ce travail nous avons obtenu, en vue d'une étude pharmacologique, les N-benzyl-carbamates de méthyle (III) ci-dessous :

$$\underset{\text{(III)}}{(p)X-C_6H_4-CH_2-NH-COOCH_3}$$

$(X=H,\ Cl,\ NO_2)$.

2. Résultats théoriques

Les produits (III) ont été préparés par le traitement des benzylamines correspondantes avec le chloroformiate de méthyle en opérant dans un système à deux phases : benzène (chloroformiate) — eau (amine, carbonate alcalin) ; cette variante de carbalkoxylation, qui est en quelque sorte différente de celles utilisées d'habitude, a permis l'obtention des produits bruts d'un degré avancé de pureté et avec des rendements plus élevés, conséquence de la prévention, dans une mesure importante, de la réaction concurrente d'hydrolyse du chloroformiate (v. le Tableau 1).

---

*) Communication présentée au III-ème Congrès National de Chimie, Bucarest, 21—24 septembre 1988.

Tableau 1

N-Benzyl-carbamates de méthyle (III)

No.	X	Rendement en produit brut (par rapport à l'amine), [%]	Formule moléculaire	*F* °C (solvant)[a)]
1	H	97	$C_9H_{11}NO_2$	62 ... 64 (cyclohéxane)[b)]
2	Cl	93	$C_9H_{10}ClNO_2$	83 (cyclohéxane)
3	NO_2	95	$C_9H_{10}N_2O_4$	108 ... 110 (méthanol)[c)]

a) La recristallisation n'a pas modifié les températures de fusion des produits bruts.

b) Litt. [3] : 64° ... 65°C (éther de pétrole), produit obtenu par la dégradation de Hofmann de la phenylacétamide en milieu méthanolique.

c) Litt. [4] : 109,5°C (éthanol), produit obtenu par la nitration du N-benzyl-carbamate de méthyle et par l'acylation de la *p*-nitrobenzylamine avec du chloroformiate de méthyle dans l'éther, litt. [5]: 104° ... 105°C (corr.) (ligroïne), obtenu par la dégradation de la *p*-nitrophenylacétylazide selon Curtius, en milieu méthanolique.

La structure du composé (III) (X=Cl) a été confirmée par les analyses élémentaires (C, H, N) et les spectres en IR et, dans le cas des produits décrits dans la littérature, par comparaison avec des échantillons authentiques. Dans le travail antérieur [2], nous avons aussi obtenu le produit (III) (X= $=NO_2$) par la nitration du composé (III) (X=H) dans des condition différentes et plus précises que celles indiquées en [4], qui n'ont pas offert des résultats reproductibles.

Les essais pharmacologiques préliminaires des produits (III) ont mis en évidence leur action préventive envers les convulsions provoquées par la strychnine, plus prononcée dans le cas du dérivé *p*-chlorosubstitué, ainsi qu' une forte activité anti-amphétamine du produit non substitué. On a aussi constaté un certain effet sédatif et la potentialisation du sommeil provoqué par le hexobarbital, plus marquée chez le dérivé *p*-nitrosubstitué.

Les résultats obtenus avec ces structures relativement simples conduisent à l'idée que les nombreux esters N-benzylcarbamiques décrits dans la littérature représentent une importante source, encore insuffisamment explorée, de produits intéressants du point de vue pharmacologique.

Le caractère lipophile des structures (I) représente probablement l'une des conditions de leur action anticonvulsivante. Ce point de vue est soutenu par l'absence de cette action chez les dérivés *mono*acyclés du type (IV) :

$$R-CO-NH-CH_2-NHét.$$

(IV)

que nous avons aussi synthétisé dans ce travail.

Ces N-(aminométhyl)-amides, représentant des N-bases de Mannich, ont été obtenues selon la méthode générale de condensation entre les amides, le formaldéhyde et les amines secondaires [6], [7]. Les restes acyle des structures (IV) (*n*-butyryle, *p*-fluoro- et *p*-chloro-benzoyle) correspondent à des structures actives du type (I). Comme amines secondaires on a utilisé la pipéridine, la morpholine et la N-méthyl-pipérazine (v. le Tableau 2) :

$$R-CO-NH_2+CH_2O+NHét.\xrightarrow{-OH_2}(IV)$$

Tableau 2

N-(Aminométhyl)-amides (IV)

No.	R	HNHét*)	Formule moléculaire	*F* °C (solvant)	Sel, *F* °C (solvant)
1	n-C_3H_7	P	$C_{10}H_{20}N_2O$ [8]	36 ... 37[a])	picrate : 184 (acétone)
2	n-C_3H_7	M	$C_9H_{18}N_2O_2$	58	picrate : 169 (avec décomp.) (acétone)
3	n-C_3H_7	N	$C_{10}H_{21}N_3O$	50 ... 54	dipicrate (?) : décomp.
4	(*p*) ClC_6H_4	P	$C_{13}H_{17}ClN_2O$ [9]	141 ... 142[b]) (acétate d'éthyle)	chlorhydrate : 177 [b,c])
5	(*p*) FC_6H_4	P	$C_{13}H_{17}FN_2O$[10]	150 (avec décomp.) (acétate d'éthyle)	chlorhydrate : 175 ... 176[c])
6	(*p*) FC_6H_4	M	$C_{12}H_{15}FN_2O_2$ [10]	119 ... 120 (avec décomp.) (acétate d'éthyle)	picrate : 185 ... 187 (avec décomp.) (acétone)

*) P = pipéridine ; M=morpholine, N=N-méthyl-pipérazine.
a) Produit distillé à 145°C/10^{-1} ... 10^{-2} mm.
b) Litt. [9] : 149,5°C ; B.HCl, *F*=177°C.
c) Précipité de la soluion dans l'éthanol avec de l'éther.

Les structures des produits (IV) ont été confirmées par les analyses élémentaires (C, H, N) et les spectres en IR. Les bases ont été aussi caractérisées sous forme de sels (picrates ou chlorhydrates).

Pour la N-(*p*-chlorobenzamidométhyl)-pipéridine ((IV), R=(*p*)ClC_6H_4, —NHét.=—$N(CH_2)_5$), le seul de ces produits qui est décrit dans la littérature, on a mentionné une action antinicotinique [9].

Les produits (IV) indiqués dans le Tableau 2, possèdent en général une action myorélaxante et sont relativement toxiques. Exceptant le produit dérivé de la butyramide et de la pipéridine ((IV), R=*n*-C_3H_7, —NHét.=—$N(CH_2)_5$) qui, dans les essais préliminaires sur des rats, a démontré une bonne protection anti-amphétamine et aussi une activité tranquillisante et sédative, les produits (IV) n'ont pas manifesté, dans le cadre du screening effectué, d'autres activités intéressantes.

3. Partie expérimentale

3.1. N-Benzyl-carbamates de méthyle (III)

a) *Mode opératoire général d'acylation des benzylamines avec le chloroformiate de méthyle en système à deux phases benzène — eau* [11]. Dans un flacon contenant une solution de 12 g de carbonate de sodium dans 120 ml d'eau on ajoute 0,1 mol de la benzylamine correspondante (éventuellement le chlorhydrate, en utilisant dans ce cas des quantités doubles d'eau et de soude) et puis, en refroidissant avec de l'eau glacée, une solution de 0,12 mol de chloroformiate de méthyle dans 120 ml de benzène ; si le produit d'acylation est peu soluble dans ce solvant, pareil à (III) (X=NO_2), on a réduit la quantité à 40...50 ml. On adapte ensuite un bouchon perforé muni d'un tuyau de verre qui pénètre jusqu'à quelques centimètres au-dessus du niveau du liquide et on secoue vigoureusement pendant 15...20 min. Le produit (III) (X=NO_2) précipite dans la phase organique, d'où on l'isole finalement en état pur par filtration sous vide sur une frite, lavage avec de l'eau et séchage à l'air. Dans le cas des produits (III), solubles dans le benzène (X=H, Cl), la couche benzénique séparée est lavée avec de l'eau, séchée sur Na_2SO_4 et eva porée. Les rendements (par rapport aux benzylamines) et les températures de fusion (inchangées après recristallisation) sont indiquées dans le Tableau 1.

3.2. N-(Aminométhyl)-amides (Tableau 3)

Tableau 3

Conditions de synthèse des N-bases de Mannich (IV)

No.	R	HNHét.*)	Solvant ml**)	Température de réaction °C	Temps de réaction min.	Rendement %
1	*n*-C_3H_7	P	eau : 20	60 ... 70	45	quant.
2	*n*-C_3H_7	M	eau : 20	60 ... 70	45	quant.
3	*n*-C_3H_7	N	eau : 20	60 ... 70	45	quant.
4	(*p*) ClC_6H_4	P	éthanol absolu : 93	reflux	60	75
5	(*p*) FC_6H_4	P	éthanol : 95	reflux	60	86
6	(*p*) FC_6H_4	M	—	100	60	75

*) v. le Tableau 2.
**) quantité utilisée pour 0,1 mole de chaque réactif.

a) *N-Bases de Mannich dérivées de la butyramide*, (IV) (R=$n-C_3H_7$). La condensation est accomplie en milieu aqueux, selon les indications du Tableau 3 (No. 1, 2, 3), en ajoutant à la solution aqueuse de la butyramide le formol 35% et l'amine secondaire (rapport molaire de 1 : 1 : 1). Après chauffage le solvant est éloigné sous vide à 15 mm et puis à 5...6 mm (à une température du bain de distillation de 50°...60°C et respectivement de 40°...50°C).

Les produits de la condensation avec la morpholine et la N-méthyl-pipérazine cristallisent à l'état pur avec un rendement quantitatif. Le composé brut dérivé de la pipéridine se présente comme un sirop jaunâtre qui cristallise après distillation à 145°C/10^{-1}...10^{-2} mm. Les substances sont incolores, solubles dans l'eau et dans de divers solvants organiques, non solubles dans l'éther de pétrole.

b) *N-Bases de Mannich dérivées de la p-fluoro- et p-chloro-benzamide* ((IV), R=(p)F-C_6H_4 et (*p*)Cl—C_6H_4). Les produits de ce type dérivés de la pipéridine (v. le tableau 3, No. 4, 5) sont préparés par l'addition successive de l'amine secondaire et du formol 35% à une solution éthanolique de l'amide (rapport molaire 1 : 1 : 1), suivie de chauffage à reflux. Les produits sont précipités en ajoutant graduellement à la solution résultée (éventuellement filtrée aussi chaude que possible) un volume à peu près double de l'eau distillée. Après séchage on recristallise dans l'acétate d'éthyle. Le produit dérivé de la morpholine avec R=(*p*)F—C_6H_4 (v. le Tableau 3, No. 6) est obtenu sans solvant en ajoutant sous agitation le formol 35% (1,2 mol) et puis l'amide finement pulvérisée (1 mol) à l'amine (1 mol). Après une heure de chauffage à 100°C, la masse visqueuse est séchée sous vide sur $CaCl_2$ et le solide brut qui en résulte est recristallisé dans l'acétate d'éthyle.

Les picrates des bases, indiqués dans le Tableau 2, ont été obtenus sous forme de précipités en mélangeant les solutions éthanoliques des réactifs et puis recristallisés dans l'acétone. On n'a pas réussi la recristallisation du sel provenant de la N-méthylpipérazine (probablement e dipicrate), qui se décompose sans fusion à une température élevée.

Les chlorhydrates des bases (v. Tableau 3, No. 4, 5) ont été préparés en ajoutant de l'éther à la solution éthanolique obtenue par traitement de la base, dissoute dans l'éthanol absolu, avec la quantité correspondante d'acide chlorhydrique dilué avec de l'éthanol.

Reçue le 26 janvier 1989

Institut Polytechnique, Jassy,
Chaire de Chimie et Technologie Organique
et Macromoléculaire

BIBLIOGRAPHIE

1. Leonte C., Carp E., Dumitrescu S., Cilianu Șt., Bozga R., Bul. Inst. polit., Iași, **XXXV (XXXIX)**, *3—4*, s. II, 67 (1989); on y trouve d'autres informations.
2. Carp E., Leonte C., Dumitrescu S., Cilianu Șt., Bozga R., Bul. Inst. polit., Iași, **XXXV (XXXIX)**, *1—4*, s. II, 73 (1989)
3. Weermann R. A., Jongkees W. J. A., Rec. trav. chim., **25**, 243 (1906).
4. Baker J. W., Soc., 568, 570 (1927)
5. Shriner R. L., Cross J. M., J. Am. Chem. Soc., **60**, 2 338 (1938).
6. Einhorn A., Ann., **343**, 207 (1905).
7. Zaugg H. E., Martin W. B., Org. Reactions, **14**, 111 (1965).
8. Leonte C., Carp E., Cilianu Șt., Neubauer G., Dumitrescu S., Bobulescu V., Brevet R.S.R., Nr. *79 257*, 24. 02.1982.
9. Földeák S., Matkovics B., Pórsász J., Acta Phys. et Chem., Szeged, **8**, 88 (1962).
10. Carp E., Leonte C., Cilianu Șt., Bozga R., Brevet R.S.R., Nr. *87 212*, 25.01.1985.
11. Carp E., Leonte C., Cilianu Șt., Bozga R., Dumitrescu S., Bobulescu V., Brevet enreg. OSIM, R.S.R., Nr. *126 259*, 29. 12. 1986.

STRUCTURI AMIDICE CU ACŢIUNE ASUPRA SISTEMULUI NERVOS CENTRAL

III. N-Benzil-carbamaţi de metil şi N-(aminometil)-amide

(Rezumat)

S-au preparat N-benzil-carbamaţi de metil cu structura (III) prin carbometoxilarea benzilaminelor corespunzătoare după un procedeu de acilare în sistem bifazic benzen — apă ce permite obţinerea de produşi puri şi cu randamente ridicate. Prin condensarea dintre amide, formaldehidă şi amine secundare heterociclice s-au sintetizat N-bazele M a n n i c h de tipul (IV). S-a cercetat acţiunea compuşilor (III) şi (IV) asupra sistemului nervos central.

BULETINUL INSTITUTULUI POLITEHNIC DIN IAŞI
Tomul XXXVI (XL), Fasc. 1—2, 1990
Secţia II
CHIMIE ŞI INGINERIE CHIMICĂ

D.C. 541.141 ; 54-92

NEW 4-CHROMANONE DERIVATIVES AS PHOTOSTABILIZERS FOR POLYMERS

BY

HARTMUT SELIGER, ERWIN HAPP and AL. CAŞCAVAL

1. Introduction

Coumarins, chromanones and flavones which exists in plants protect the plant cells from ultraviolet rays [1]. It was shown in the past few years that 4-chromanon skeleton acts as UV-absorber and inhibits photodegradation of polymers. A poly(vinyl chloride) film containing 6.7% 5-hydroxy-7-methoxy-2,2-dimethyl-8-octyl-4-chromanone (I) was found to be most stable agaist photooxidation [2].

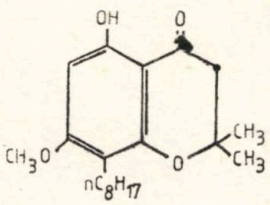

I

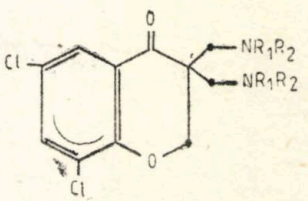

II a-e

One of us has obtained also in 1983 [3] a series of polysubstituted 4-chromanones (II_{a-e}) and tried these bis-M a n n i c h bases as stabilizers for PVC. Unfortunately, these experiments were not successfull because (II) are so sensitive to UV-light that they decomposed on their applications to PVC film.

We wish to report here the preparation of some 4-chromanone derivatives without dialkylamino groups in the heterocyclic part of the molecule hoping that these derivatives will be useful as UV-absorbers.

2. Results. Discussions

During the screenings, some water-soluble dihydrochlorides of new 3, 3, 6, 8-tetrasubstituted 4-chromanones (III_{a-e}) in a „deamination" inverse M a n n i c h reaction gave the same 3-methylene-6, 8-dichloro-4-chromanone (IV) [4] :

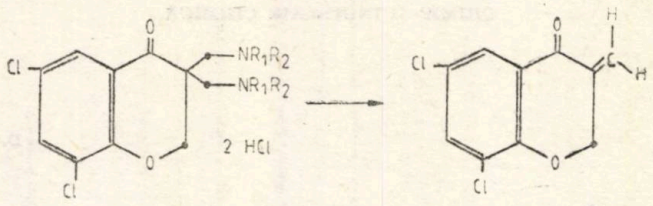

III a–e IV

By a modified M a n n i c h reaction of 2-substituted 4-chromanones with bis (dimethylamino) methane and acetic anhydride, E. C. T a y l o r and Y. S h v o [5] and more recently F. E. W a r d et al. [6] obtained 3-methylene derivatives of 4-chromanones with very promising antifungal and antibacterial activities as a consequence of their ability to covalently bind some nucleophilic receptor by conjugate addition to the unsaturated ketone.

By refluxing of (IV) in DMF solution for 10 min. we obtained a cyclic dimer (V) by a heterodien syntheses :

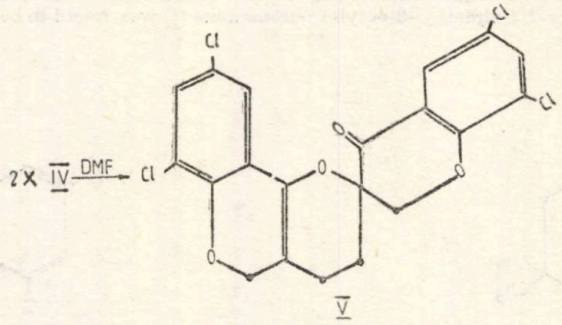

V

This compound absorbs strongly in the UV-range (240...255 nm) and, like spirochroman-chromane, can possess useful photochromic properties [7].

Now, we obtained the compound (V) in the reaction between (II_{a-d}) and T a y l o r - S h v o reagent very probably *via* (IV). Formation of spiro-4-chromanone ring as the final step of the reaction as reported in Fig. 1 was found to be generally a more convenient method of the preparation of this type of 4-chromanone derivatives :

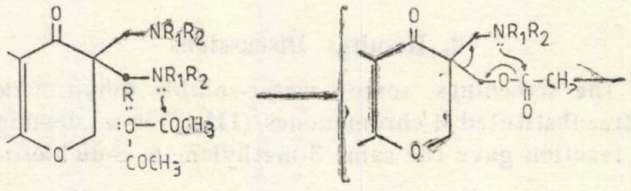

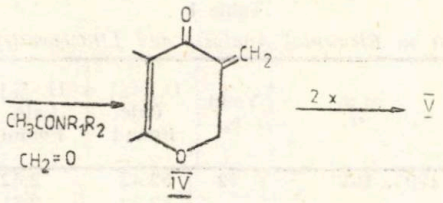

Similar amine dealkylation were reported in the literature in a single case. C. D. L u n s f o r d et al. [8] isolated acetate product when treated 2-(1-isopropyl-3-pyrrolidinyl) 2,2-diphenylacetic acid with acetic anhydride, *via* postulated mixed anhydride and acetate salts.

Trying to generalize this new reaction we have prepared a series of substituted 4-chromanones by well-known ring closures of *ortho*-hydroxyphenyl alkyl ketones and a ketone in the presence of a base [9] and submitted these compounds in the reaction with T a y l o r—S h v o -reagent:

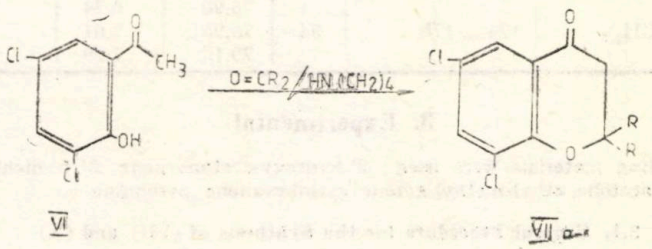

(VII), (VIII), (IX)	R
a	CH_3
b	CH_3 ; C_2H_5
c	$(CH_2)_5$

With this reagent we obtained 3-methylene derivatives ($VIII_{a-c}$); they afforded by cyclodimerization bis-spiro-compounds (IX_{a-c}). Also with *ortho*-hydroxyacetophenone we obtained unsubstituted spirochromanone in the aromatic parts of the molecule (XI_{a-c}) from the corresponding 2, 2-disubstituted 4-chromanones (X_{a-c}) by refluxing with T a y l o r-S h v o-reagent; it is possible then to avoid a step in the synthesis of spiro-4-chromanones.

Physico-chemical data of some synthesized products are given in Table 1.

Table 1

Data on Elemental Analysis and IR-Characterization

Compound	R	M.p. °C	Yield %	C, [%] Calc. Found	H, %] Calc. Found	Cl, [%] Calc. Found	IR ν, [cm^{-1}]
(V)	H	190 ... 191	42	52.42 52.90	2.62 2.31	30.97 30.65	1 690
(VII$_a$)	CH_3	49 ... 50	57	53.89 54.11	4.08 4.02	28.95 29.10	1 680
(VII$_b$)	$CH_3+C_2H_5$	b.p.$_1$: 125 ... 127	48	55.62 55.90	4.63 4.70	27.38 27.50	1 685
(VII$_c$)	$(CH_2)_5$	88 ... 89	87	58.97 59.14	4.91 4.76	24.88 24.80	1 685
(VIII$_c$)	$(CH_2)_5$	93 ... 94	60	60.62 60.97	4.71 4.56	23.88 23.62	1 650
(IX$_c$)	$(CH_2)_5$	224 ... 225	61	60.62 60.75	4.71 5.00	23.88 24.02	1 690
(X$_a$) [10]	CH_3	90 ... 91	53	—	—	—	1 690
(X$_b$)	$CH_3+C_2H_5$	b.p.$_1$: 96	90	75.79 75.92	7.37 7.80	—	1 690
(X$_c$)	$(CH_2)_5$	b.p.$_1$: 117	61	77.78 77.97	7.41 7.56	—	1 690
(XI$_a$)	CH_3	123 ... 124	70	76.59 76.90	6.38 6.74	—	1 680
(XI$_c$)	$(CH_2)_5$	174 ... 175	54	78.95 79.13	7.01 7.19	—	1 685

3. Experimental

As starting materials were used ; 2'-hydroxy-acetophenone, 3', 5'-dichloro-2'-hydroxy-acetophenone, acetone, ethyl-methyl-ketone, cyclohexanone, pyrolidine.

3.1. General Procedure for the Synthesis of (VII) and (X)

A mixture of 20 mmol of *ortho*-hydroxyacetophenone and 40 mmol of alyphatic ketone was refluxed with 20 mmol pyrrolidine in methanol for 5 h., is poured with stirring in crushed ice; hydrochloric acid is added to precipitate 4-chromanone (VII) or (X) which is purified by recrystallization or distillation in vacuum.

3.2. Synthesis of 6,8-dichloro-3-methylene-2,2,pentamethylene-4-chromanone (VIII^c)

3 g of (VII$_c$) in 10 ml bis-dimethylaminomethane was treated with stirring by room temperature with 10 ml acetic anhydride ; a exotermic reaction took place, and, after 2 h, is poured water; in the white precipitate is finered out and purified by twice recrystallization from methanol. Elemental analysis, IR-spectra also NMR-spectra for this type of compounds confirm their structure.

3.3. Synthesis of Cyclodimere of (VIII$_c$) by Diels-Alder Reaction

a) 5 g of 3-methylene derivative (VIII$_c$) in 15 ml DMF was refluxed for 10 min. and the reaction product was poured in ethanol (100 ml) to separate a white product characterized also by mass spectrum.

b) 10 mmol of (VII$_c$) in 10 ml bis-dimethylaminomethan was refluxed together with 10 ml acetic anhydride for 30 min.; working out as before we obtained also cyclic dimere (IX$_c$).

3.4. Synthesis of Cyclic Dimere (V) from (II$_{a-c}$) or (III$_{a-c}$)

a) 10 mmol of (II) in 10 ml bis-dimethylaminomethan with 10 ml acetic anhydride was refluxed for 45 min; the reaction was poured in water to separate (V) which purified by recrystallization from methanol then acetone.

b) 10 mmol of (III) in water (100 ml) refluxed for 2 h when separated an oil which by recrystallization from dichloromethane is also (V).

Acknowledgement. Generous support of this work by Deutsche Forschungs-Gemeinschaft (Sonderforschugsbereich 239) and the University of Ulm, West Germany, is gratefully acknowledged.

Received, October 30, 1989

University of Ulm,
West Germany
and
Polytechnic Institute of Jassy,
Department of Organic and Macromolecular Chemistry and Technology

REFERENCES

1. Swawzonek S., *Chromanols, Flavanones, Chromanols and Flavanols.* In Elderfield R. C., *Heterocyclic Chemistry.* Vol. **2**, ch. **10**, John Wiley and Sons Inc., New York, 1951, 343.
2. Ninagawa A., Iseki T., Matsuda H., Makromol. Chem., *184*, 71 (1983).
3. Caşcaval A., Synthesis, 579 (1983).
4. Caşcaval A., Cantow H.-J., Wegner G., Bul. Inst. polit., Iaşi, **34** (**38**), *1—4*, s. II, 81 (1988).
5. Taylor E.C., Shvo Y., J. Org. Chem., **33**, 1719 (1968).
6. Ward F.E., Garling D. L., Buckler R. T., Med. Chem., **24**, 1 073 (1981).
7. Merlini, L., *Photochromism* In Katritzky A. R., *Advances in Heterocyclic Chemistry.* Vol. **18**, 1975 187.
8. Lunsford C. D., Cale A. D. Jr., Ward J. W., Franko B. V., Jenkins H., J. Med. Chem., **7**, 302 (1964).
9. Kabbe H. J., Widdig A., Angew. Chem., **94**, 254 (1982).
10. Baker W., Floyd A. J., McOmie J. F., Pope G., Weeaving A. S., Wild J. H., J. Chem. Soc., 2010 (1956).

NOI DERIVAŢI AI 4-CROMANONEI CA FOTOSTABILIZATORI PENTRU POLIMERI

(Rezumat)

Este descrisă ciclodimerizarea unor derivaţi 3-metilenici ai 4-cromanonelor polisubstituite cînd se obţin bis-spirocromanone care pot prezenta interes farmacologic (antimicrobieni care nu au structură antibiotică) precum şi de natură protectoare faţă de radiaţiile UV ale polimerilor. Se propune un mecanism de dezaminare a bis-bazelor Mannich (II) sub acţiunea reactivului Taylor—Shvo cu obţinerea ciclodimerului (V). Produşii sintetizaţi au fost caracterizaţi analitic şi spectral (IR, RMN, MS).

BULETINUL INSTITUTULUI POLITEHNIC DIN IAŞI
Tomul XXXVI (XL), Fasc. 1—2, 1990
Secţia II
CHIMIE ŞI INGINERIE CHIMICĂ

D.C. 678.744 ; 547.26

SEMI-IPNs OF POLYVINYLCHLORIDE AND METHACRYLATE ESTERS

I. KINETIC ASPECTS OF THE PREPARATION

BY

CORNELIA VASILE, GH. ADAMESCU, LUCIA ODOCHIAN, IGNAT POINESCU, LUCREŢIA GHICU and MARIANA BADEA

1. Introduction

The preparation of the semi-Interpenetrated Polymer Networks (semi-IPN) on poly(vinyle chloride), (PVC), as basis using emulsion or suspension type polymer, is widely used with the aim to improve the resistance and elongation at break, the impact-resistance, the adesiveness, the thermal stability, the plasticizing agent migration decrease, etc.

It is well-known that ethylene glycol dimethacrylate ester by the radicalic polymerization reaction leads to the networks which possess a high chemical, thermal and water stability.

A good compatibility of these macromolecular compounds with PVC offer the possibility to develop some new research ways, and a lot of papers concerning theoretic and applied aspects were published [1]...[6].

Owing to the network structure and the texture complexity yielded during the polymerzation reaction of ethylene glycol dimethacrylate ester a few papers concerning the polymerzation reaction kinetics have been published, yet.

This paper deals with the reaction kinetic study concerning the preparation of the semi-interpenetrated polymer networks (semi-IPN) basis on PVC with different ethylene glycol dimethacrylic esters.

2. Experimental

PVC (K_w=70), industrial polymer made by the Petrochemical Works Agregate of Borzeşti, was purified by extraction with MeOH in a Soxhlet apparatus and then dried. Finaly PVC was solved in tetrahydrofurane (THF) yielding 10% solution.

Three alkylene glycol dimethacrylic esters (mono-, di-, and three ethylene glycol dimethacrylates with the structure $CH_2=C(CH_3)\ COO\ (CH_2CH_2O)_n\ COC(CH_3)=CH_2$, where $n=1, 2, 3$, called MED, DED and TED, prepared by I.C.P.A.O, Mediaş, were polymerized in the presence of PVC. Polymerization was carried out in the presence of benzoyl peroxide (Bz_2O_2), 1.0%, 87° ; 100°, 120° and 140°C.

The polymerization reaction development was investigated by IR spectroscopy following the absorption of the monomer double bonds in function of time. The PVC-solution was mixed with the dimethacrylic ester wich contained 1.0% Bz_2O_2 at a component ratio of 6 : 4. The homogeneous mixture was

laid as a thin layer on a glass plate. The solvent which has a high volatility leaves the solution after 2...3 h, at room temperature. IR-spectra were recorded on the same film (constant thickness), kept various period of time in an owen at the mentioned temperature in order to get semi-IPN samples.

3. Results and Discussion

Fig. 1 shows the IR-spectrum of the 61.0% PVC : 38.0% TED : 1.0% Bz_2O_2 mixture performed at various polymerization temperatures. One can easily notice the intensity decrease of the absorption band, particular by of the bonds corresponding to 815 cm^{-1}, 940 cm^{-1}, 1 290 cm^{-1}, 1 630 cm^{-1} and 1 710 cm^{-1}. From the mentioned absorption bands, the picks corresponding to 815 cm^{-1} and 1 630 cm^{-1} as signed to the double bands of the dimethacrylic esters, disappear during the polymerization reaction. But the band corresponding to the C—Cl (610...690 cm^{-1}) does not change, and in consequence it can be used as a reference one in calculations as follows ; the intensity of each band which changed is refered to C—Cl absorption band. i.e. 690 cm^{-1} or 640 cm^{-1}.

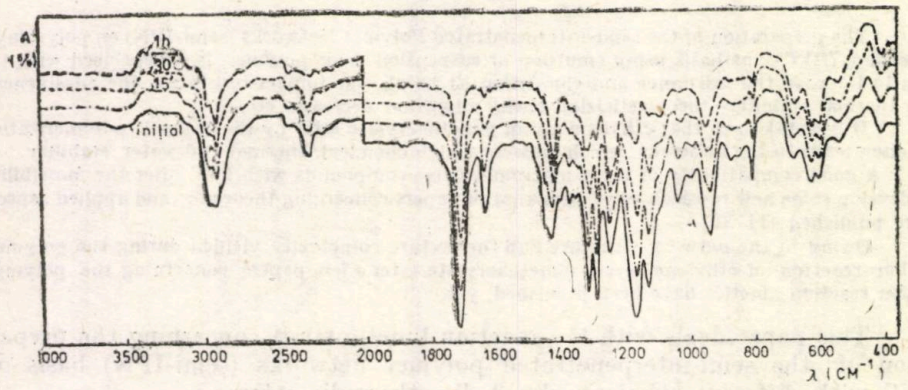

Fig. 1.—IR-spectra of 61.0% PVC : 38.0% TED at 120°C and various times of the polymerization reaction.

The kinetic curves shown by Fig. 2 were plotted as $A_{\lambda t}/A_{\lambda ref}$ vs. time for various wave lengths. The absorption at 815 cm^{-1} and 1 630 cm^{-1} were particularly investigated because the ratio $A_{\lambda t}/A_{\lambda ref}$ can be used, by similitude, to measure the double bond concentration (C_{DL}).

Hence, one can easily notice that the two curves are ronghly parallels.

The derivation of these curves leads to the estimation of a value proportional to the reaction rate. By means of these data, the kinetic parameters were calculated applying the graphical plotting differential method. Initially, the rate constants and the reaction order at various temperatures on the plottings similar to those from Fig. 3 have been obtained where ln k is the ordinate and from the curve slope results the reaction order (n).

The Arrhenius plot (Fig. 4) can be used to estimate the activation energies for the polymerization of the three dimethacrylic esters. The kinetic parameters are listed in Table 1.

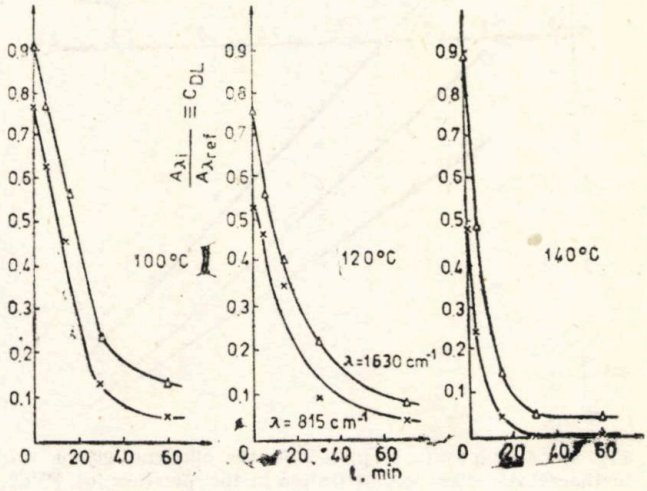

Fig. 2. — Polymerization kinetic curves of TED performed in the presence of PVC (the absorption bands are indicated).

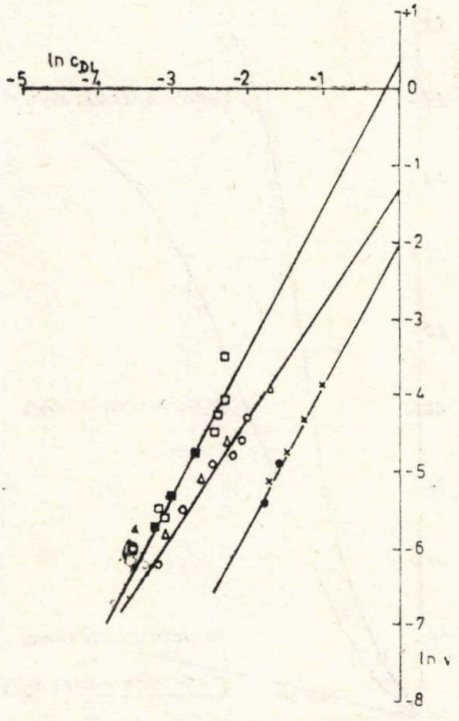

Fig. 3. — The reaction rate logarithm variation vs. the DED polymerization concentration logarithm performed in the presence of PVC at various temperatures: ●,× —100°C ; ○, Δ—120°C; □, ■ —140°C for 815 and 1630 cm^{-1}.

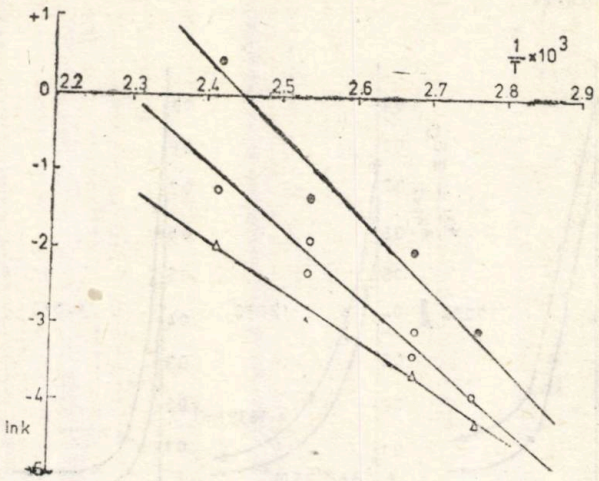

Fig. 4.—Arrhenius plots for the alkylene glycol dimethacrylate ester polymerization in the presence of PVC. ●—MED ; ○—DED ; Δ—TED.

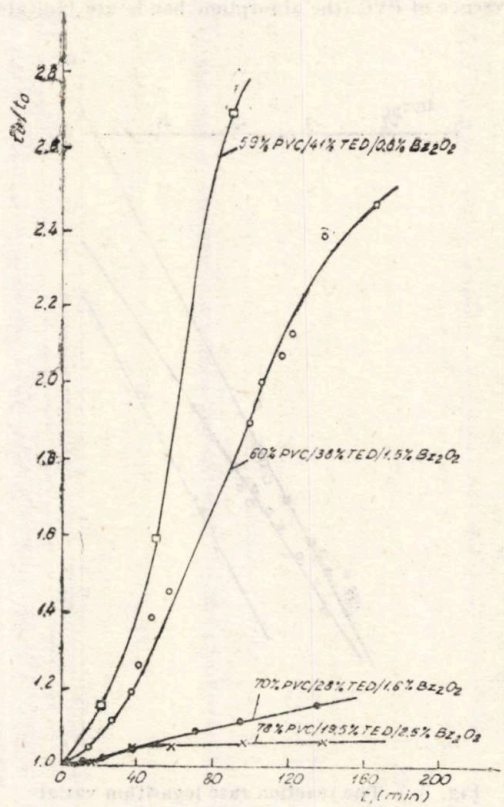

Fig. 5.—The modification vs. time of the 10.0 % PVC viscosity (cyclohexanone as solvent) in the presence of various amounts of TED and Bz_3O_2; the measurements were carried out with a Ubbelhode viscometer at 87° ±0.2°C.

Table 1

Kinetic Parameters for Ethylene Glycol Dimethacrylate Esters Polymerization in Presence of PVC

Sample	T_p °C	t_p min	k $sec^{-1} \times 10^4$	n	E_a KJ/mol.
60% PVC/40% MED	100	20	22.55	1.875	83.14
	120	15	43.20	1.46	
	140	10	261.3	1.89	
60% PVC/40% DED	100	30	7.00	1.06	72.74
	120	15	24.43	1.125	
	140	10	47.75	1.00	
60% PVC/40% TED	100	40	5.03	1.320	53.21
	120	35	8.72	1.05	
	140	20	22.56	0.975	

4. Conclusions

The following conclusions can be established;

a) the time necessary for the ending of the polymerization reaction (t_p) decreases with the temperature and increases with the monomer molecular weight.

b) The rate constants increase with the polymerization temperature and decrease with the monomer molecular weight diminution.

c) In the case of TED the reaction order decrease with the polymerization temperature increase, which proves that higher temperatures faster network polymerization of the dimethacrylic ester, i.e. the diffusion phenomenon prevails as determining rate stage. By this way is possible to explain the activation energy diminution when the monomer molecular weight increase.

The results are in good agreement with the data quoted by literature concerning the double bond consumption yielding networks [7], for which the reaction order decrease from 1.4. to 1.0, having as result the conversion degree increase. These result was proved by many polymerization reaction stages namely: a) polymerization in solution before the gelatinization point; b) the 2nd stage takes place by the polymerization between the gelatinization points; c) the polymerization end by the unreacted monomer consumption.

The activation energies also correspond to ones mentioned by literature concerning acrylic ester polymerization [7], [8]. In the case of the TED polymerization (slower reaction rate) in the presence of PVC, particular at lower temperature (87°C), it was possible to investigate the first reaction stage searching the viscosity changes in function of time of the PVC solutions which contained various quantities of TED and Bz_2O_2 (Fig. 5).

One can notice that the viscosity depends on the TED amount and Bz_2O_2 percent. This means that the crosslinked structure yielded by the polymerization of methacrylic ester in the presence of PVC will depend on these parameters. It will result a semi-interpenetrated polymer network. The distances between the knots of the network vary with the dimethacrylic ester type and Bz_2O_2 concentration.

Higher temperatures are favourable to the chemical bond formation between ester and PVC macromolecular chains having as consequence the

kinetic and thermodynamic stability increase of the system because yielded IPN structures are nearer to the true ones.

The study concerning the morphological and features of these systems will published later on.

Received, December 19, 1989

Institute of Macromolecular Chemistry „P. Poni", Jassy,
Research Institute for Rubber and Plastic Processing, Bucharest
and
Polytechnic Institute, Jassy, Department of Physical Chemistry

REFERENCES

1. Ломоносова Н. В. и сотр., Пласт. массы, *12*, 17 (1984); Ibid., *4*, 9 (1986); Ibid., *3*, 28 (1988).
2. Червяков В. Л., Гусеев В. В., Москухин В. Б., Самарин Е. Ф., Чудинова В. В., Пласт. массы, *12*, 25 (1987).
3. Bair H. E., Matsuo M., Solmon W. A., Kwei T. W., Macromolecules, **5**, *2*, 114 (1972).
4. Davis D. D., Slichter W. P., Macromolecules, **6**, *5*, 728 (1973).
5. Котова А. В., Талых А. Е., Авдеев Н. Н., Межиковский С. М., Высокомол. соед., **A 24**, 460 (1982).
6. Ланцов В. М., Котова А. В., Абдрахманова Л. А., Кустовская Л. И., Задонцев Б. Г., Ярошевский С. А., Дериновский В. С., Абрамова Е. И., Талых А. Е., Межиковский С. М., Высокомол. соед., **28**, *6*, 1197 (1986).
7. Rosenberg Y. E., Flodin P., Macromolecules, **21**, 2041 (1988); Ibid., **22**, 155 (1989).
8. Korus R., Driscoll K. F. O., *Polymer Handbook*. Vol. **II**, Eds. J. Brondrup a. Iumergut, Academic Press, 1980, 451.

REŢELE SEMIINTERPĂTRUNSE ALE PVC ŞI ESTERILOR METACRILICI

I. Aspecte cinetice ale sintezei

(Rezumat)

S-a studiat cinetica reacţiei de obţinere a reţelelor semiinterpătrunse constituite din policlorură de vinil şi esteri alchil glicol dimetil dimetacrilici.
S-a stabilit dependenţa parametrilor cinetici de structura chimică.

BULETINUL INSTITUTULUI POLITEHNIC DIN IAŞI
Tomul XXXVI (XL), Fasc. 1—2, 1990
Secţia II
CHIMIE ŞI INGINERIE CHIMICĂ

D.C. 542.951.1 ; 661.847.31

CONTRIBUTIONS TO THE STUDY OF THE ACETYLATION REACTION OF POLYOLES, IN THE PRESENCE OF ZINC CHLORIDE

BY

N. OIŢĂ, M. NICU. VIORICA NICU and ELENA TĂTARU

1. Introduction

Generally, esters are known as substances having large utilizations, such as monomers, suspension stabilizers, plastifiers, antistatic agents, thermal and photostabilizers, organic intermediates, films, drugs, etc. [1]...[3].

From the great variety of esters and polyesters a special place is taken by acetates (cellulose acetates, polyvinylacetates, the acetyl-salicylic acid etc.).

In the process of esters of the acetic acid obtention, starting from alcohols or polyoles, acetic anhydride is usually employed as acetylation agent, while minerals acids (mainly, H_2SO_4), coordination acids, amines, etc. [4], [5], [10], [11]. Due to its special activity, to its low cost and reduced toxicity, one of the most widely used catalysts is zinc chloride [6]...[11], recommendations being made in literature as to its utilization in an anhydrized form, avoiding in these way the hydrolysis of the acetic anhydride. This reaction system has been thouroughly investigated both from the kinetic and from the thermodynamic viewpoint [10, [11].

Our syntheses, performed in view to obtain penta-acetylglucose and hexaacetyl-manitol, evidenced the possibility of getting higher yields with lower reaction times, if zinc chloride is not wholly anhydrized. This observation urged us to study the influence of the catalyst's hydration degree upon the process of manitol acetylation.

2. Experimental

Acetic anhydride, containing 96% anhydride (the rest of 4% being acetic acid), manitol, containing 0.2% water, and anhydrous zinc chloride (Merk) were used in the experiments.

Nevertheless, zinc chloride has been subjected to another anhydrization process up to obtaining a spectrally (IR) pure product. Considering also the water from manitol's composition, the solution of zinc chloride has been hydrated through contact with water vapours, up to attaining the following molar ratios :

$$H_2O/ZnCl_2 = 1\ ;\ 1.5\ ;\ 2\ ;\ 2.5\ ;\ 3\ ;\ 3.5\ ;\ 4.$$

The working method involved the introduction of the calculated amount of acetic anhydride, together with 0.2 g $ZnCl_2$, in a three-bull plate flask, equipped with a stirrer refrigerator and contact thermometer setting the temperature of the water both in which the flask was placed. After solubilization

of the catalyst and reaching a temperature of 70°C, 10 g manitol were introduced into the flask.

2.1. Determination of the Reacts' Molar Ratio to Obtain a Maximum Acetylation Degree, for 4 Hours

Anhydrous zinc chloride was employed, using the manitol/anhydride molar ratios listed in Table 1.

Table 1

Variation of the Acetylation Degree and of the Yield, versus the Reactants' Molar Ratio

Manitol/anhydride molar ratio	1 : 6	1 : 7	1 : 8	1 : 9
Acetylation degree	5.54	5.65	5.8	5.98
Yield versus manitol	90.5	95.1	98.3	99.6

The determination of the yield was performed after separating the acetylation product from the reaction medium, by filtration, washing and drying. At the end, the dry product was weighed and the yield was calculated. In the case in which acetylation degrees > 5 are not to be obtained, some amount of the partially acetylated product will remain soluted in the reaction medium, while yield calculation will introduce significant errors.

For the determination of the acetylation degree, expressed as number of acetyl groups corresponding to one mole of manitol, 5 g of acetylated product were weighed, to which 0.1 N solution of NaOH was added in excess. The mixture was then brought to boiling temperature, hydrolysis of the ester groups occurring. After boiling for one hour, the mixture is cooled, and the excess of NaOH is titrated with a solution of 0.1 N acetic acid. Reporting the number of ester equivalents to one mole of manitol allow the calculation of the acetylation degrees.

Date in Table 1 evidence that, as a matter of fact, total acetylations are to be obtained with good yields, at a 1 : 9 ratio of reactants, which justify the utilization, in subsequent experiments, of this molar ratio, only.

2.2. Kinetic Determinations of Acetylation with Hydrated $ZnCl_2$

The reaction media were the same as above, with the difference that hydrated zinc chloride was introduced, in amounts calculated to contain the same quantity, i.e. 0.2 g of anhydrous $ZnCl_2$. The zero time of the reaction was considered the moment of the manitol introduction. Syntheses have been performed at reaction times of 30, 60, 90 and 120 min. and a temperature of 70°C.

Following the reaction times established, the water bath was decoupled and emptied, water being replaced by a mixture of ice, water and salt. When temperature decreased to 15°C, the nonreacted acid and anhydride were also titrated with a solution of 0.1 N NaOH. The results thus obtained were expressed as equivalents of non-reacted acetyl groups. Considering the difference versus the acetyl groups introduced, the number of esterified acetyl

group equivalents was calculated, which, reported to the number of manitol moles, lead to the value of the acetylation degree at the reaction time considered.

The results of these determinations are represented in Fig. 1.

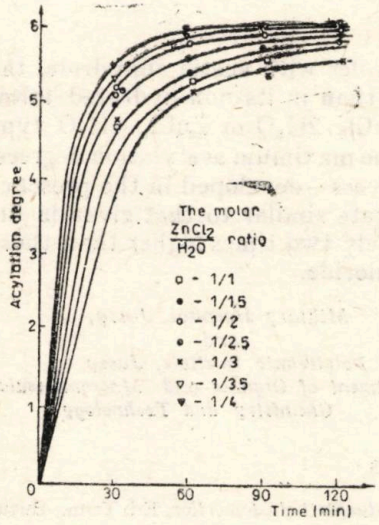

Fig. 1. — Time variation of the acetylation degree.

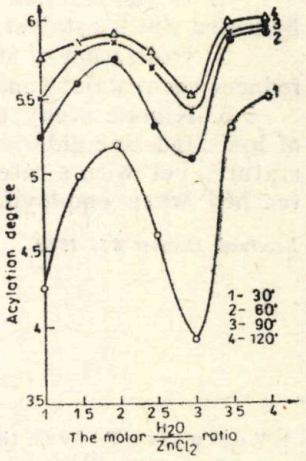

Fig. 2. — Variation of the acetylation degree vs. the molar $H_2O/ZnCl_2$ ratio, at various reaction times

3. Results and Discussion

One can see from Fig. 1 that the time required to obtain a maximum acetylation degree varies with the catalyst's hydration degree and that at hydration degrees ranging between 2 and 4, it shows values between 90...120 min., being therefore two times lower that when using anhydrous zinc chloride.

Kinetic curves plotted in Fig. 1 have been drown for the determination of the partial reaction orders of manitol (whose concentration has been expressed through the number of hydroxy groups moles/ volume), as well as of acetic anhydride, of the total reaction order and of the rate constant. In this respect, the grapho-analytical method and the method of the least squares [12] have been applied, on reaching the following rate equation :

$$v = 0.1[OH]\ [CH_3CO],$$

where 0.1 is the value of the rate constant (l/mol. min).

The reaction rate depends upon the concentrations of manitol (OH) and anhydride (CH_3CO) of the first order, the total reaction order being 2. When using hydrated zinc chloride, the value of the rate constant is observed as being about two time higher than in the case of employing anhydrous zinc chloride. The explanation of such a situation could be the following. Analyzing the variation of the acetylation degree vs. the catalyst's hydration degree at various reaction times, the curves plotted in Fig. 2 are obtained.

The conclusion to be drawn is that maximum rates are to be obtained for catalysts having the composition $ZnCl_2 . 2H_2O$ and $ZnCl_2 . H_2O$; consequently the catalytic activity of the catalyst depends on its acidic strength, being known that such hydrates have an acidic character [13].

4. Conclusions

1. In the reaction of acetylation of polyoles with acetic anhydride, the hydrated $ZnCl_2$ catalyst is much more active than in its non-hydrated form.

2. Utilization of such catalysts of the $ZnCl_2 . 2H_2O$ or $ZnCl_2 . 4H_2O$ type reduces the reaction time necessary to obtain the maximum acetylation degrees.

3. Kinetic study of the acetylation process—developed in the presence of hydrated zinc chloride—led to a reaction rate similar to that given in literature, yet with a rate constant approximately two times higher than those reached when employing anhydrous zinc chloride.

Received, October 25, 1989

Military Hospital, Jassy,
and
Polytechnic Institute, Jassy,
Department of Organic and Macromolecular Chemistry and Technology

REFERENCES

1. Volintiru T., Ivan Gh., *Bazele tehnologice ale prelucrării elastomerilor*. Ed. Tehn., Bucureşti, 1974.
2. Feldman D., *Tehnologia compuşilor macromoleculari*. Ed. Tehn., Bucureşti, 1974.
3. Horun S., *Aditivi pentru prelucrarea polimerilor*. Ed. Tehn., Bucureşti, 1978.
4. Blaga A., Robu C., *Chimia şi tehnologia polimerilor pentru pelicule*. Ed. Tehn., Bucureşti, 1977.
5. Olteanu D., *Tehnologia plastifianţilor esteri*. Ed. Tehn., Bucureşti, 1980.
6. * * * *Farmacopeea română*. Ed. IX, Ed. Militară 1975
7. Oiţă N., Brevet R.S.R., *87 311* (1987).
8. Mungiu O. C., Oiţă N., Bozgan L., Petrescu O., Rev. medico-chirurg., Iaşi, *2*, 320 (1982).
9. Mungiu O. C., Popa V., Vulturescu M., Popescu M., Grigorescu S., Oiţă N., Rev. medico-chirurg., Iaşi, *1*, 83 (1983).
10. Neniţescu C. D., *Chimie organică*. Vol. **I** and **II**, EDP, Bucureşti, 1968.
11. Becker H., *Organicum*, (transl. from. German). Ed. şt. şi encicl., Bucureşti, 1982.
12. Levenspiel O., *Tehnica reacţiilor în inginerie chimică*, (transl. from. English). Ed. Tehn., Bucureşti, 1967.
13. Neniţescu C. D., *Chimie generală*. EDP, Bucureşti, 1979.

CONTRIBUŢII LA STUDIUL REACŢIEI DE ACETILARE A POLIOLILOR ÎN PREZENŢA CLORURII DE ZINC

(Rezumat)

S-a studiat, sub aspect cinetic, reacţia de acetilare a poliolilor (manitol) cu anhidridă acetică, în prezenţă de clorură de zinc cu diverse grade de hidratare. S-a constatat că pentru catalizatori de tipul $ZnCl_2.2H_2O$ şi $ZnCl_2.4H_2O$ se obţin viteze de reacţie de două ori mai mari decît în cazul utilizării catalizatorului anhidru. S-a determinat expresia vitezei de reacţie.

BULETINUL INSTITUTULUI POLITEHNIC DIN IAŞI
Tomul XXXVI (XL), Fasc. 1—2, 1990
Secţia II
CHIMIE ŞI INGINERIE CHIMICĂ

D.C. 678.746.22

FILMS FROM ETHYLENE-VINYL ACETATE COPOLYMERS

BY

M. RUSU, SIMION PETROVAN and CONSTANŢA IBĂNESCU

1. Introduction

Ethylene—vinyl acetate (EVA) copolymers, containing up to 10 % vinyl acetate, have about the same characteristics as low density polyethylene (LDPE) and may be used, as this, for the film manufacture [1], [2]. But, as compared with the low density polyethylene films, those obtained from EVA copolymers show some different characteristics, namely a higher flexibility, better optical properties and clearness, higher crack resistance and a more reduced gas permeability [3]. EVA copolymers are easier to process for films production than LDPE [4].

All these have made the films from EVA copolymers more competitive in the field of fresh food packages, especialy meat.

This paper presents the results concerning the correlation between some technological parameters and the characteristics of the tubular films obtained by extrusion blowing of EVA copolymers with 10% vinyl acetate.

2. Experimental Part

In order to study the influence of the main technological parameters on the tubular film characteristics, an EVA copolymer type B23 FA 117B was used, produced by PCP, Piteşti, Romania, by the copolymerization at high pressure of the ethylene with vinyl acetate. The characteristics of this copolymer are presented in Table 1.

Table 1

The Characteristics of the EVA Copolymer

Characteristic	Value
Vinyl acetate content, [%]	10 ± 3
Aspect	Uniform granules
Density at 23°C, [g/cm^3]	0.926 ± 0.002
Melt index, [g/10 min.]	21 ± 1
Tensile strength, [MN/m^2]	min. 15
Elongation at break, [%]	min. 60
Gloss (film of 0.03 mm), [units]	min. 40

The tubular films were obtained with an extrusion equipment made up of a MEA 25 extruder and a take-off device LISFA-800.

The following independent technological parameters were taken into account: 1° blow-up ratio (x_1) ; 2° take-up velocity (x_2) ; 3° the distance between the die and the air ring (x_3).

In order to carry out the experiments a second order, composed, centrate, rotatable design was used. The obtained films were tested for following characteristics: a) tensile strength on longitudinal direction ; b) tensile strength on transversal direction; c) elongation at break on longitudinal direction; d) elongation at break on transversal direction; e) tear strength on longitudinal direction ; f) tear strength on transversal direction; g) contraction on longitudinal direction ; h) contraction on transversal direction ; i) impact strength ; j) film thickness.

The experimental design and the experimental results are presented in Table 2.

The experimental data were processed by regression method on a computer in order to obtain a regression equation of the following form :

$$(1) \qquad y=a_0+\sum_i a_i x_i+\sum_{i,j} a_{ij}x_i x_j, \qquad i \leqslant j,$$

where : y — a physico-mechanical property ; a_i, a_j — regression coefficients; x_i — independent variable.

The computer was programed also to draw constant level curves for all the properties.

3. Discussion

Constant level curves, for all the properties, against the three independent variables taken in the study, are presented in the Figs. 1...5. From these figures, information on the simulaneous influence of the three parameters may be obtained.

In Fig. 1, constant level curves for tensile strength in the longitudinal and transversal directions are presented. It is seen that in the case of the first property there exists a minima values domain centred at about 2.2 blow-up ratio, 14.2 m/min. take-up velocity and 152 mm distance to air ring. Also, a minimum domain exists for transversal direction tensile strenght but shifted towards lower blow-up ratio and take-up velocity and maxima values for the distance to the air ring.

As the blow-up ratio increases and the distance to air ring decreases and maintaining constant the take-up velocity, a decrease followed by an increase in the values of the two properties is recorded. This trend is more evident for tensile strength in the longitudinal direction. It may be shown that this is the important feature of influence, mainly at lower take-up velocities. Also, the Fig. 1 shows the domain where films with the best values for the tensile strength are obtained. This domain is determined by the highest blow-up ratio values and minima values for the other two variables.

The constant level curves for the elongation at break for the two directions are presented in Fig. 2. For this property too, one observes the existence of a minimum domain for longitudinal elongation at break. The center

Table 2

The Experimental Design and the Properties of the Obtained Films

Exp. no.	Blow-up ratio	Take-up velocity m/min.	Distance to air ring mm	Tensile strength on longitudinal direction Kgf/cm²	Tensile strength on transversal direction Kgf/cm²	Elongation at break on longitudinal direction %	Elongation at break on transversal direction %	Tear strength on longitudinal direction Kgf/cm	Tear strength on transversal direction Kgf/cm	Contraction on longitudinal direction %	Contraction on transversal direction %	Impact resistance g	Thickness mm
1	3.21	17.5	80.0	243.24	247.76	412	596	86.38	90.28	60.66	37.83	135	0.0196
2	2.48	13	104.33	217.04	212.68	424	768	87.84	89.76	52.66	15.5	160	0.0286
3	3.88	13	104.33	225.06	242.48	384	768	87.78	90.30	55.00	34.66	125	0.0203
4	3.94	21.5	104.33	239.94	223.08	404	576	75.58	85.44	60.33	35.50	85	0.0128
5	2.54	21.5	104.33	221.62	228.64	336	632	77.04	88.30	62.66	24.80	130	0.0192
6	2.006	17.5	140.0	184.20	170.18	364	596	69.07	71.48	63.00	5.33	110	0.0298
7	3.21	10.0	140.0	196.80	205.70	536	568	70.40	76.34	55.00	26.33	150	0.0372
8	3.24	17.5	140.0	194.56	152.22	432	680	67.92	80.40	63.90	33.33	120	0.0196
9	3.18	24.0	140.0	204.76	231.12	384	700	77.16	80.22	65.00	21.20	85	0.0116
10	3.18	17.0	140.0	193.42	183.92	316	600	78.09	80.24	58.00	28.66	100	0.0201
11	3.18	17.0	140.0	175.84	197.72	300	508	72.38	69.44	65.83	31.50	110	0.0184
12	3.18	17.5	140.0	221.22	263.64	300	672	76.40	60.18	59.83	29.16	125	0.0223
13	3.18	17.0	140.0	212.74	239.26	316	664	80.48	81.64	55.55	24.66	125	0.0226
14	3.15	17.0	140.0	222.52	242.70	328	592	87.56	86.36	58.00	23.50	130	0.0188
15	2.51	12.75	175.7	218.38	218.26	440	624	83.26	88.20	60.00	23.66	155	0.0320
16	3.89	13.50	175.7	200.24	231.92	472	636	64.42	62.20	55.50	39.16	110	0.0202
17	2.54	21.5	175.7	243.50	235.40	400	600	82.64	80.40	52.50	20.50	110	0.0190
18	3.91	21.5	175.7	215.22	240.70	288	380	72.54	80.78	63.16	36.33	85	0.0114
19	3.24	17.1	200.0	201.96	211.62	388	680	77.14	87.54	53.26	21.76	110	0.0200

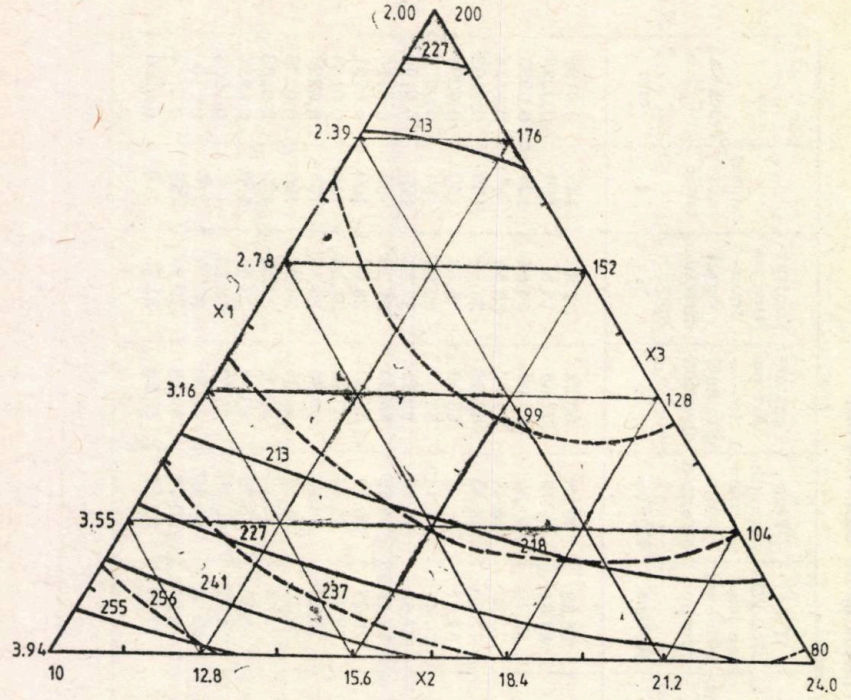

Fig. 1. — Tensile strength (Kgf/cm²) vs. the studied parameters (— in the longitudinal direction ; — — — in the transversal direction).

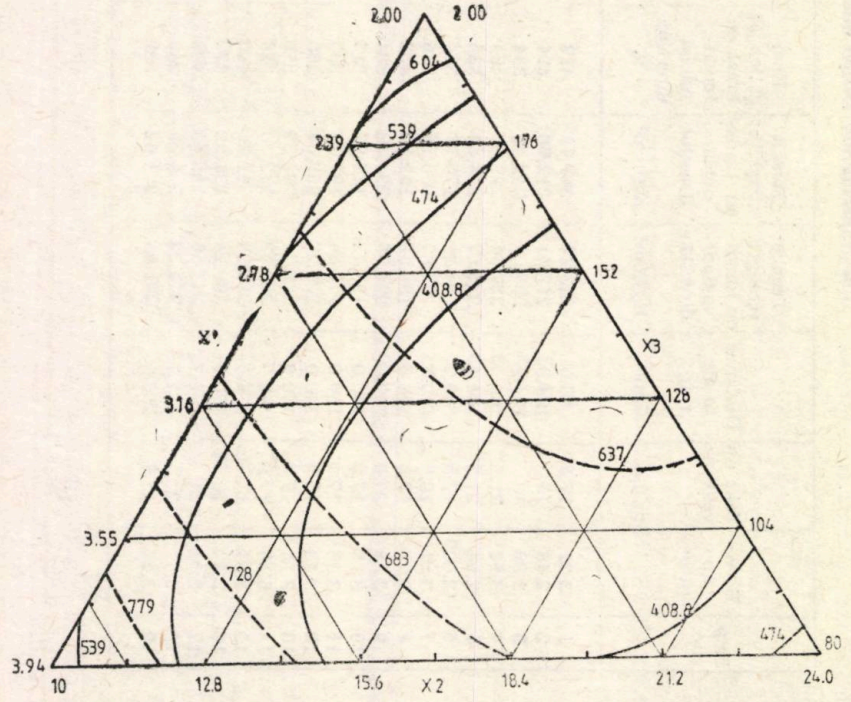

Fig. 2. — Variation of elongation at break (%) vs. the three parameters (in the longitudinal direction ; — — — in the transversal direction).

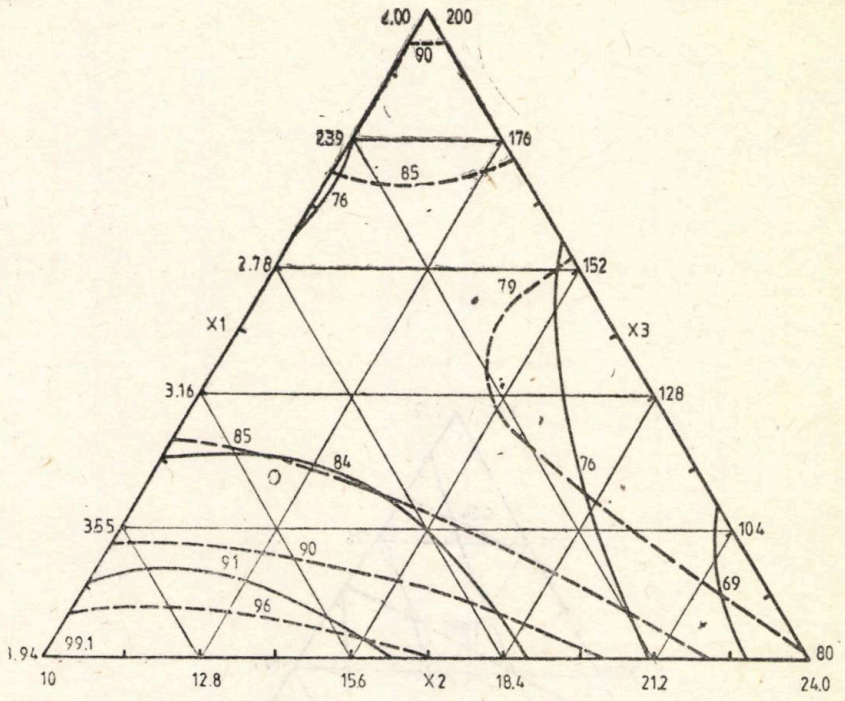

Fig. 3.— Variation of tear strength (Kgf/cm²) vs. the studied parameters (— in the longitudinal directicn : — — — in the transversal direction).

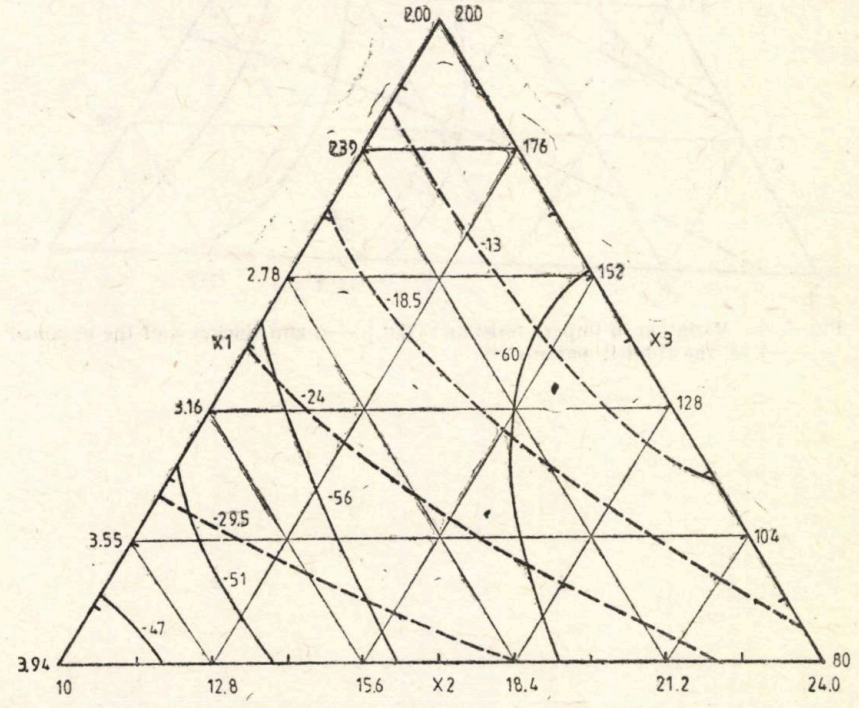

Fig. 4. — Variation of contraction (%) vs. the three parameters (— in the longitudinal direction ; — — — in the transversal direction).

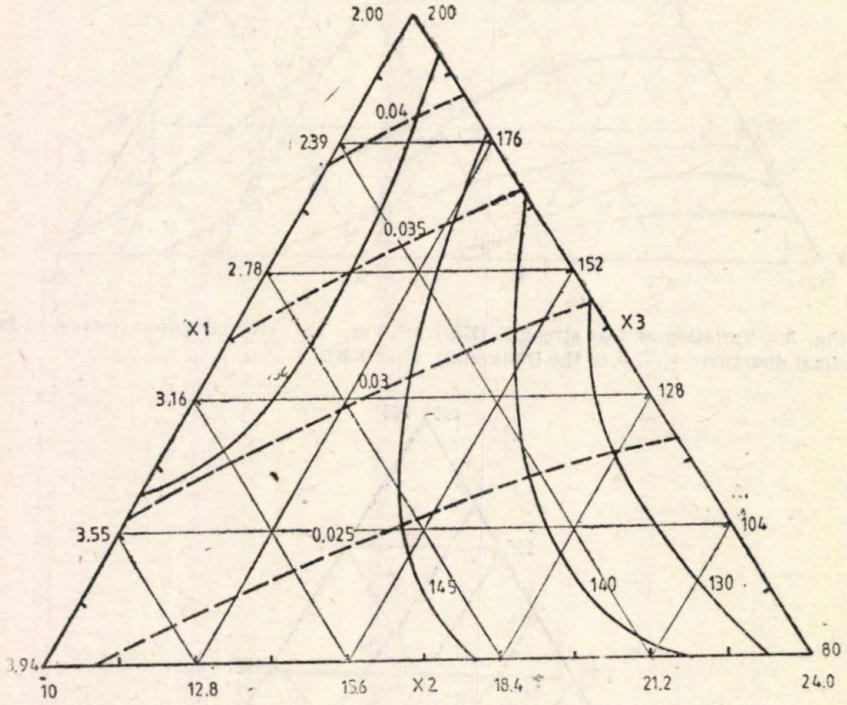

Fig. 5. — Variation of impact resistance ([g,] ——) and thickness of the obtained flims ([mml, — — —) vs. the studied parameters.

of this domain may be localized at 2.2. blow-up ratio, 17 m/min. take-up velocity and 116 mm distance to air ring. But the transversal elongation at break continuously increases as the blow-up ratio increases and the distance to air ring and take-up velocity decrease. Maxima values for longitudinal elongation at break are obtained in a band domain corresponding to take-up velocity betwen 10...13 m/min., with minor influence of the blow-up ratio. Also, in this domain, the largest influences of the distance to air ring are recorded. The direction of the influence of the independent variables on the transversal elongation is perpendicular on that of longitudinal elongation. Maxima values of the transversal elongation are recorded at high blow-up ratio and minima values for both other parameters.

The influence of the three independent variables on the tear strength on the two directions is represented in Fig. 3. By analysing the constant level curves it is seen that the response surface is in a form of a saddle, this shape being more evident for the transversal direction. Also, a zone of process stability is noticed ; it is a domain where the influence of the independent variables on the tear strength is lower. The center of this domain is located at 2.6. blow-up ratio, 11.4 m/min. take-up velocity and 140 mm distance to air ring. This tendency of variation determines an increase of the tear strength on both directions. This means that maxima values of this characteristic may be obtained for take-up velocities between 10...13 m/min., maximum blow-up ratio and minimum distance to air ring.

In Fig. 4 there are presented the constant level curves for the contraction of the films in the two directions. This characteristic continuously changes as the blow-up ratio increases and the other two parameters decreases so that an increase of transversal and a decrease of longitudinal tear strength are recorded. Taking into account the need to obtain films of about the same value of the tear strength on both directions, this goal is fulfilled if the extrusion line is operated at maximum blow-up ratio and minima values of the other two parameters.

The influence of the three independent variables on the impact resistance and thickness of the obtained films is shown in Fig. 5. As relating the impact resistance, a complex influence of the studied variables is seen. So, the increase of the values of this property is obtained on a curved trend, from a point located at 2 for blow-up ratio, 19 m/min. take-up velocity and 116 mm distance to air ring, towards another point placed about at 2.8. blow-up ratio, 10 m/min. take-up velocity and 152 mm distance to air ring, respectively. In order to achieve the largest increase of the values of this characteristic, the changes of the operating conditions, that is the operating curve, must be normal to the constant level curves. Maxima values of the impact resistance are recorded in a domain between 2...3.4 blow-up ratio, 10...12 m/min. take-up velocity and about 120...200 mm distance to air ring. For this property too, it may be evidenced a domain of minor influence of the three parameters taken in the study, at maximum blow-up ratio and minima values of the other two parameters.

The thickness of the obtained films decreases continuously with the increase of the blow-up ratio and take-up velocity and decrease of the distance to the air ring.

4. Conclusions

It is demonstrated the possibility of obtaining blown films from EVA copolymers on a common extrusion blowing equipment. It was studied the influence of the blow-up ratio, take-up velocity and the distance from the die to air ring on the physico-mechanical characteristics of the obtained films.

By using an experimental design and by computer processing of the experimental data, the optima conditions for the obtaining of imposed characteristics of the films were determined.

Received, November 7, 1989

Polytechnic Institute, Jassy,
Department of Organic and
Macromolecular Chemistry and Technology

REFERENCES

1. Goldenberg N., Deaconescu I., Butucea V., Dobrescu V., *Poliolefine.* Ed. Tehn., Bucureşti, 1976.
2. Dobrescu V., Andrei C., *Progrese în chimia şi tehnologia poliolefinelor.* Ed Şt. şi Encicl., Bucureşti, 1987.
3. Палех И. В., Пластические массы, *9*, 32 (1979).
4. Han C. D., *Rheology in Polymer Processing.* Academic Press, New York, 1976, 238.

FILME DIN COPOLIMERI ETILENĂ—ACETAT DE VINIL

(Rezumat)

S-a demonstrat posibilitatea realizării, folosind o instalaţie obişnuită de formare, a unor folii contractibile subţiri din copolimer etilenă—acetat de vinil.

Prin utilizarea metodei programării experienţelor şi prelucrării pe calculator a datelor s-au determinat condiţiile optime pentru obţinerea de folii cu caracteristici impuse.

BULETINUL INSTITUTULUI POLITEHNIC DIN IAŞI
Tomul XXXVI (XL), Fasc. 1—2, 1990
Secţia II
CHIMIE ŞI INGINERIE CHIMICĂ

RECENZII

BOOK REVIEWS РЕЦЕНЗИЙ

FANGHÄNEL E., EBISCH R., HABICHER W.-D., HANN R., UNDERFERTH K., *Chemische Kinetik*. Arbeitsbuch **6**, VEB Deutscher Verlag für Grundstoffindustrie, Leipzig, 1987, ISBN 3-342-00184-4.

Having in view the increasing importance of better knowing of the notions of chemical kinetics, involved in the kinetic study, so necessary for training specialists in the field of chemistry, the book under review, entitled *Chemische Kinetik*, is addressed to university assistants and students, representing a valuable reference material that contributes to a better understanding of the notions in this field.

The material is structured according to the curriculum of this high education discipline.

Chemische Kinetik, volume **6** of the series, consists of six chapters, discussing in the form of question problems solved and unsolved numerical applications, as well laboratory studies applying the theoretical knowledge of the most important chapters of the course on chemical kinetics. Thus, chapter 1 is devoted to *Simple Laws and Activation Parameters*, discussing thoroughly such notions as: the reaction rate, the reaction order, specific rate, activation energy and the preexponential factor, different theoretical problems and practical studies referring both to organic and anorganic chemistry being proposed. Special mention must be made of the fact that this chapter also includes the calculation of errors from kinetic investigation which is essential for the obtainment of precise results. The importance of this aspect is also justified by the fact that the authors have given it a considerable space (59 pages out of 199).

Chapter 2, *Complex Reactions*, deals with notions referring to reversible, parallel, succesive, as well as chain reactions. After a tabular presentation of the kinetic, differential and integral laws, specific to these reactions for various reaction orders, representative problems and practical studies are proposed. Chapter 3, entitled *Influence of the Reactants Structure and of the Reaction Medium upon the Reaction Rates*, discusses some theoretical aspects, presented again as question problems, as well as some unsolved problems and practical studies, to be performed in laboratories, all meant at evidencing the influence of the reaction medium upon kinetic parameters.

Chapter 4, *Heterogeneous Reactions*, analyses the two phenomena occurring within these reactions — diffusion and adsorbtion; further on, several practical applications regarding various types of heterogeneous reactions both in gaseous and liquid phase are proposed.

Chapter 5, *Influence of Catalysts upon the Reaction Rate*, discusses some problems regarding homogeneous and heterogeneous catalysis supported by practical examples from this field, such as: catalytic decomposition of H_2O_2, saccharose inversion, aniline ioduration, hydrolysis of the ethyl acetate in acidic medium, a. s. o.

Chapter 6, entitled *Photochemical Reactions*, introduces by means of question the basic photophysical and photokinetic values, also followed by significant practical applications.

The book also contains a list of the symbols employed and a table of the most important universal constants, as well as the International System of Units, also the results of the numerical applications proposed in the book, an alphabetic index and the periodic system.

All in all, the reviewed book is logically and rigorously structured, being based on a rich bibliography which is a proof of the authors'long and competent experience in this field of investigation, thus offering to students the opportunity of developing and enriching both their practical skills and the theoretical knowledge.

Natalia Hurduc, Lucia Odochian, Elena Mihai

WOLF G., SCHNEIDER W., *Chemische Thermodynamik*. Arbeitsbuch 4, VEB Deutscher Verlag für Grundstoffindustrie, Leipzig, 1983, 272 S., ISBN 3-342-00385-5.

The book, called *Chemische Thermodynamik*, deals with Chemical Thermodynamics experiments, more precisely with applied works.

The book is writen on 272 pages and divided in eight chapters which are very well developed with experiments and specific exercises for each important chemical thermodynamic phenomenon.

Chapter 1, *Chemical Thermodynamic Ground*, listes the general working techniques characteristics to be thermodynamics, for instance : thermal state equations of pure substances and thermodynamic studies of mixtures.

Chapter 2, *The First Thermodynamic Law*, deals with the following aspects : internal energy and enthalphy ; caloric state equations for the constant quantities and variables quantities of substances.

Chapter 3, *Calorimetry*, presents the calorimetry basis and calorimetric proceedings in order to measure the thermal effects.

Chapter 4, *The 2nd Thermodynamic Law*, treats the basis of the 2nd thermodynamic law and the entropy as a state function.

Chapter 5, *General Laws of Equilibrium and non-Equilibrium of the States*, has the following content : free energy and enthalpy ; chemical potential.

Chapter 6, *Phase Esuilibrium* includes : G i b b s phase law ; phase equilibrium in monocomponent systems, in binary and ternary systems.

Chapter 7, *Chemical Reactions and Non-Equilibrium Chemical Reactions*, contains the following main parts : the mass action law ; the dependence on the equilibrium constants vs. temperature.

Chapters 8, develops *Superficial Equilibriums* as follows : superficial tension of the liquids ; adsorbtion phenomenon on the liquid and solid surfaces. The authors give exemples for the adsorption phenomenon on the solid surfaces concerning, particularly, the isotherms in several layers (BET).

All chapters contain the most specific laboratory experiments (2 ... 8 laboratory works). Also, each chapter and underchapter contains exercises and tests with the purpose to make easier the understanding of the treated phenomenon.

The book *Chemische Thermodynamik*, contains, besides the above chapters, additional two paragraphs which present the exercise results, as well several tables with physical and chemical constants very usefull to calculate different thermodynamical magnitudes resulted from experimental measurements and exercises.

The whole content of the book is presented at a high scientific level by the authors and it is very usefull to understand the treated phenomena. In order to solve the exercises, the International System Units are used.

The content of the book as well as the laboratory experiments and exercises are extremely usefull for all students who have to study the physical chemistry, particularly, the chemical thermodynamic, in order to get a better training in the theoretical and experimental physical chemistry.

I warmly recommend this book for the students who are studing the chemistry and the engineering chemistry.

Cameluța Beldie

MÖBIUS H. H., DÜRSELEN W., *Chemische Thermodynamic.* Lehrbuch 4, VEB Deutscher Verlag für Grundstoffindustrie, Leipzig, 1988, 292 S., ISBN 3-342-00294-8.

The book called *Chemische Thermodynamic* deals on 292 pages, the chemistry thermodynamic basis elements, as well as its relationships with other physical chemistry chapters.

The book contains eight chapters as follows ; the first chapter deals with the general considerations on the thermodynamic and molecular kinetic ; thermodynamic systems ; processes and states ; state equations of pure bodies ; mixt phases ; elemental processes.

The second chapter, entitled *The 1st Thermodynamic Principle,* gives information on the following aspects ; the 1st thermodynamic principle bases ; different ways to ground the 1st thermodynamic principle through the internal energy and enthalpy ; caloric sizes of the pure bodies ; energy variation when the bodies are compressed or expanded.

The chapter is concerned primarily with the elements of *Thermochemistry* as follows ; thermochemistry basis, reaction energy and enthalpy, Hess law, pressure and temperature influence on the reaction enthalpy, thermochemistry of the most important interface processes.

The chapter called *The 2nd Thermodynamic Principle,* treats the basic elements of the 2nd thermodynamic principle as follows : entropy as a state function, statistic interpretation of entropy and the 2nd thermodynamic principle.

The fifth chapter discusses *General Laws of Equilibriums and Non-equilibriums,* which are well concisely treated as follows ; the application of the thermodynamic principle in the closed systems and the chemical potential.

The sixth chapter deals with *Phase Equilibriums,* which were developed as follows : phase equilibriums in pure bodies ; equilibriums in solutions ; solubility equilibriums ; equilibriums between liquids and gases ; systems with liquids and pure phases.

The seventh chapter, called *Chemical Reactions and Chemical Equilibrium,* is concisely developed on the reaction chemical affinity, masses law and its application, deduction of equilibrium constants.

The eight chapter is concerned with the *Interface Equilibrium* and treates the following main aspects : surfaces and state parameters, adsorption of gases, adsorption of dissolved substances.

The whole content of book is very clear treated, with the physical meaning well developed and mathematic relationships not very complicated, but adequately to express the basic elements of the chemical thermodynamic.

Each chapter is closed with the test questions which are very well selected and quite useful. The book is recommendable to those who wish to study the ground elements of Chemical Thermodynamic in connection with other physical chemistry chapters.

Cameluța Beldie

ASEEVA R. M., ZAICOV G. E., *Combustion of Polymer Materials.* Ed. Hanser Publishers, Münich, Vienna, New York, 1986, 389 pp.

The book *Combustion of Polymer Materials* by R. M. Aseeva and G. E. Zaikov, translated in English by Hanser Publisher, Münich, Vienna, New York (1985), treats the combustion of natural and synthetic polymers as well as involved chemical and physical processes that represent a subject of particular theoretical and practical importance. Indeed, the utilisation of polymeric materials in daily life and industry is closely connected with their inflammability problem. As a results, the manufactures and consumers give a great attenntion to this problem that involves the knowing of combustion process of polymers and conditions in which these have place.

The work is dedicated to combustion of polymeric materials and methods of reduction of their inflammability in connection with requirement of their use in different domains of application.

The problem involves studies related to chemical kinetics (chain reactions, thermooxidative degradations and the properties of same additives for polymers with a reduced inflammability), as well as by some branch of physics and technological processes.

The book is composed from an introduction and 5 chapters. In *Introduction* are presented the fundamental concepts of polymer combustion processes. The first chapter contains theoretical general and experimental studies about combustion of polymers. In the second chapter the most important characteristics of polymer combustion are considered in detail.

The third chapter is dedicated to chemical aspects of polymer combustion, problem of smoke formation during combustion and slowing means of these processes.

The determination methods of combustibility and the studies of polymer combustion are included in chapter IV.

The chapter V presents a general material about methods of reduction of polymeric inflammability.

The authors make a critical presentation of extended experimental data refered to the combustion of different polymer classes exposing the development of theories which result from study of this research domain that have evolved through utilisation of some rigorous kinetic criterion.

The presented informations in this book are useful for chemists, researchers and engineers that work in synthesis of polymeric non-inflammable materials, with reduced inflammability as well as for users of these materials.

Ana Onu, Gh. Nemțoi

ADAM G., LÄUGER P., STARK G., *Physikalische Chemie und Biophysik.* Zweite, völlig neu bearbeitete und erweiterte Auflage, Springer-Verlag, Berlin, Hedelberg, New York, London, Paris, Tokyo, 1988, 532 S.

The present development of biology, especially of some of its main branches, such as biochemistry, molecular biology, cell biology, genetics and others, inevitably involves a through knowledge of the main concepts and rules of physical chemistry and biophysics. One of the numerous attempts made in this direction is the book written by professors dr. Gerold Adam, dr. Peter Läuger and dr. Günther Stark (from the University of Konstanz, Federal Republic of Germany), entitled *Physical Chemistry and Biophysics;* it represents a most valuable synthesis of the fundamental problems of physical chemistry and biophysics, as applied to biological and biochemical processes.

The book contains 11 chapters, each of them accompanied by comprehensive reference lists, as well as by a number of problems, to be solved by the reader.

The first chapter discusses the thermodynamical bases of macroscopic systems, special stress being laid upon the behaviour of ideal and real gases.

Chapter two is devoted to the laws of thermodynamics. The first principle of thermodynamics is presented, in parallel with the introduction of notions such as internal energy, enthalpy, calorimetry ; there follows the presentation of second principle of thermodynamics, of the notion of enthropy and, finally, the application of the thermodynamical laws to biological processes.

Chapter three deals with thermodynamical potentials and equilibria, special mention being made of free enthalpy, the Gibbs equation, thermodynamical equilibria in monocomponent systems, etc.

Chapter four treats about systems with several components. After specifying the notions of partial molar volume and chemical potential, the chemical potential for ideal gases and solutions is discussed. The chapter ends with phase equation of the two-component systems.

Chapter five describes several aspects related to chemical equilibria, such as the law of the action of weigts and the energetics of chemical reactions, the solubility product, the acid—base equilibrium, protolysis and hydrolysis, ionic produce of the water, the pH, the Henderson—Hasselbalch equation, buffer solution, protolytic equilibria of aminoacids. Several examples of chemical reac-

tions discussed within this chapter are taken from the field of biochemistry.

Chapter six is devoted to problems of electrochemistry, such as: Faraday's law, ion migration in an electric field, redox processes, redox potentials, the Nernst equations, redox processes in biological systems, ionic equilibria at electrodes and membrane ionic equilibria.

Chapter seven discusses surface phenomena such as: capilarity, adsorption, monomolecular and bimolecular lipidic layers, their properties and their implications in biology and membranology.

Chapter eight treats about transport phenomena in continuous systems: viscosity, diffusion, sedimentation in a gravitational field and centrifugation, ion diffusion, surface electrical potential and electrophoresis.

Chapter nine, one of the most ample in the book, refers to biological membranes. After the presentation of the aspect regarding the structure of biological membranes, the properties of plasmatic membranes, the mechanisms of membrane transport, accompanied by several concrete examples (Na—K pump, the chemiosmotic theory of oxidative phosphorylation and photophosphorylation), electrically excitable membranes (the axon membrane) and the natrium canal of the nerve membrane are discussed.

Chapter 10, the most ample in the book, presents some notions of kinetics of the chemical processes, enzymatic kinetics included. Thorough analysis is devoted to reaction rates, formal kinetics of reactions of different orders, compartmental analysis, population dynamics, physical interpretation of the reaction rate, practical performance of the kinetic analysis. In the closing of the chapter, ample space is given to enzymatic kinetics.

The last chapter (11) of the book discusses notions about highly energetical radiations, radiations—matter interaction, radiation estimation, radioactive isotopes, radiation dosimetry, biological effects of energy-rich radiations and man's exposure to radiations.

The book also includes, in its final part, the answere to the problems offered to be solved by the reader, a subject index, a table of the chemical elements in alphabetical order and the periodic system of the elements.

The graphical conditions of the book are excellent, while its content, clearly and systematically explained is accompanied by several tables, diagrams and suggestive schemes. The mathematical apparatus, necessary for a thorough understanding of the problems treated, is quite accessible.

All in all, the book under review, *Physikalische Chemie und Biophysik*, is an interesting, original study, addressed not only to students in biology, chemistry and medicine, but also to specialists and researchers in the field of chemistry and biology.

Lucia Odochian, Vlad Artenie

SCHWEITZER A. P. (Editor-in-Chief), *Handbook of Separation Techniques for Chemical Engineers*. Second Edition, Mc Graw-Hill Book Company, New York, 1988, 1 200 pp.

Chemical engineering processes of primary importance are those of mixing, conversion, and separation involving gases, liquids, and solids. The handbook includes all the major separation techniques industrially used not only in chemical manufacturing operations but also in the design of pollution control equipment. The separation techniques covered in this text are those defined as „operations which isolate specific ingredients of a mixture without a chemical reaction taking place". One exception has been made by including *ion exchange* (Section 1.12).

The material in this handbook is divided into six *parts* and thirty eight *sections*. Each part includes sections dealing with the separation techniques available for a given type of mixture (liquid—liquid, solid—liquid etc.).

Part 1 *Liquid—Liquid Mixtures* (538 pp.) includes: Distillation (section 1.1...1.8); Extraction (1.9 and 1.10); Decantation (1.11); Ion-exchange Separation (1.12); Separation by Activated-carbon (1.13); Dialysis and Electrodialysis (1.14); Parametric Pumping (1.15), and High-performance Liquid Chromatography (1.16).

Part 2. *Liquids with Dissolved Solids* (196 pp.) has five sections dealing with : Membrane Filtration (2.1), Hydrometallurgical Extraction (2.2), Evaporation (2.3), Crystallization from Solutions (2.4) and Foam Separation (2.5).

Part 3. *Gas (Vapor) Mixtures* (116 pp.) has only three chapters : Gas-phase Adsorption (3.1) ; Design of Gas Absorption Towers (3.2) ; Mass Transfer using Fluidized Bed Techniques (3.3).

Part 4. *Solid—Liquid Mixtures* (203 pp.) includes : Filtration (sections 4.1 ... 4.4, 4.6 and 4.7), Centrifugation (4.5), Sedimentation (4.8), Hydrocyclone Separation (4.9), and Drying of Wet Solids (4.10).

Part 5. *Solid Mixtures* (42 pp.), referes to Leaching (5.1) and Glotation (5.2).

Part 6. *Gas—Solid Mixtures* (55 pp.) includes two sections. The first, Gas—Solid Separations (6.1), presents the separation methods for gas—solid systems. These are gravitational, inertial, filtration, sprays, and electrical methods. The second section (6.2) is devoted only to the electrostatic precipitators. The text ends with a *subject index*.

The editor has adopted a plan similar to that of the first edition. Some chapters of the first edition still give reasonably definitive accounts of their subjects. On other topics there has been much progress and the corresponding sections have been either updated (1.1 ... 1.8) or completely rewritten (1.9, 1.10, 1.15, etc.). In addition, there are two completely new sections (1.16 and 3.3).

The thirty eight sections of the book are written by fourty six experts in chemical engineering from U.S.A., most of them members of A.I.Ch.E. This is the only handbook providing in a single source all the information needed to help a practicing engineer to evaluate which is the most suitable separation technique for a given application.

Ilie Siminiceanu

SEYMOUR R. B., CARRAHER C. E. Jr., *Polymer Chemistry — An Introduceion*. Second Edition, Marcel Dekker, New York, 1988, 688 pp., ISBN 0-8247-7781-6.

The work represents one of the newest monographs which synthesize the basic notions in the field of polymer science, in a very clear and accessible manner.

Both R. B. Seymor and C. E. Carraher Jr. are very experienced in teaching polymer chemistry, being famous scientists both in USA and abroad.

The book, published in the second edition, includes the newest data from literature of subject and from own data of the authors, judicious distributed on chapters.

Keeping pace with the development of polymer using in various domains, the authors treat aspects referring to the genetic engineering, the mechanism of mechanical energy absorbtion and the transformations which are produced on different structural levels, the polymeric mixtures.

A separate chapter is destined to inorganic polymers, being emphasized their importance for life and technics.

Every chapter ends with a glossary of terms and number of suggested checking questions.

In the first chapter of the book are reviewed chronologically the main events that have marked the development of polymer science. Then, the data referring to production of plastics, fibers and elastomers in USA are presented.

The following chapters present the basic notions connected with polymer structure and structure-properties relation, being presented practical data referring to the apparatus and to the mode of performing of some determinations (concerning the average molecular weight and molecular weight distribution).

In the next chapter are presented polymer testing and characterisation. Then are treated the naturally occuring polymers (polysaccharides, starch, chitin, nucleic acids, naturally rubbers) apart section being reserved to some notions of genetic engineering.

The main aspects of polycondensation reactions (or step polymerization), ionic, ionic-coordinative and radicalic polymerization, with reference to copolymerization reactions, are presented in the following chapters.

Further on, data referring to inorganic and inorganic—organic polymers are presented.

The subsequent section of the work is concerned with basic aspects of polymer technology, being given notions about the main additives used in polymer industry, methods of monomers and polymers synthesis, as well as processing technologies, One subchapter treats the absorbtion mechanism of mechanical energy by macromolecular compounds.

To every chapter is annexed a representative up-to-date bibliography.

This book, appeared in excellent graphically conditions, was written with a focus on the polymer chemistry and technology, beeing a valuable material for students and teaching staff and to engineers and scientists interested by these domains.

Cleopatra Vasiliu-Oprea, Al. Constantinescu

CARBERRY J. J., VARMA A. (Ed.), *Chemical Reaction and Reactor Engineering.* Marcel Dekker, New York, 1987, 1 069 pp., ISBN 0-8247-7543-0.

We are presenting to our readers a very valuable work that was realised by contributions of some prestige specialists in domain of chemical reaction engineering and of reactors theory.

The work is structured in 15 chapters that treats about the fundamental problems in domain as : numerical methods in chemical reaction engineering, the use of stationary and contact time of catalytic surfaces and catalysts. The book deals with diffusion—reaction interactions under the form of pellets ; non-catalytic gas—solid reactions ; design of gas—solid reactors with catalyst in fixed bed and fluid bed ; reactors for gaseification of coal ; reactors gas—liquid and gas—liquid—solid ; polymerization reactors ; biological reactors, analysis and design of photo-reactors ; engineering of electro-chemical reactions ; stability and multiplicity of stationary reactors.

The selected topics by the authors on the basis of an exhaustive bibliography include the basic notions referring to the engineering of chemical reactions, especially to reactors theory, in particular for different processes with an accent regarding the phase composition of reaction systems. Thus, is employed a rich mathematical apparatus that comprises numerical methods which allow the use of the computer assisted design.

In the context of the appearance of some new fields (biotechnologies, unconventional energies, etc.) are presented data referring to biological reactors, photoreactors and engineering of electrochemical reactions.

This book, appeared in excellent graphical conditions, represents a valuable contribution in domain, being addressed especially to the specialists from design for chemical industry, but not in the last place to students and professors from profile faculties.

Cleopatra Vasiliu-Oprea, Al. Constantinescu

HUBER O., SZEJTLI J. (Eds.), *Proceedings of the Fourth International Symposium on Cyclodextrins.* Munich, West Germany, April 20—22, 1988, Kluwer ducts resulted from acid hydrolisis of cyclodextrins, hydroxyethylester, beta-cyclo- Academic Publishers, Dordrecht-Boston-London, 1988, 576 pp.

In April 1988 there was held in Munich the IVth International Symposium on Cyclodextrins dedicated to the 65th birth anniversary of Professor Friedrich Cramer from Max Plank Institute for Experimental Medicine of Göttingen.

The Symposium gathered 32 contributions and 54 posters ; 71 of the papers delievered — written by over 200 authors from 21 countries — have been included in a volume, edited by O. Huber and J. Szejtli.

The volume of the symposium is structured into 7 chapters, logically organized, refering mainly to the study of cyclodextrins, their derivatives and their complexes, as well as to their practical application. After a short preface of the editors, chapter 1 *(Chemistry Enzymology and Productions of Cyclodextrins)*, including 13 papers, deals with the obtainment, characterization and immobilization of enzymes

catalizing the synthesis of cyclodextrins, branched cyclodextrins included, as well as cloning of these enzymes genes ; production of pure state cyclodextrins in the presence of organic solvents, their acid hydrolysis, isolation and purification of gamma-cyclodextrins through affinity chromatography are also discussed. The second chapter, entitled *Cyclodextrin Derivatives*, gathers 10 papers devoted to the preparation and properties of some cyclodextrins derivatives, such as the products resulted from acid hydrolisis of cyclodextrins, hydroxyetylester, beta-cyclodextrins, methylated cyclodextrins, Schiff bases and thioglicosides obtained from cyclodextrins, as well as compounds having position 6 from cyclodextrins substituted with hydrophobic and hydrophillic groups, cyclodextrins-cellulose complexes, cyclodextrins substituted to oxygen 3 and their complexes with metals. The 15 papers of chapter 3 *(Chemical and Physical Properties of CD-Complexes)* analyse the preparation of various inclusion compounds and complexes, obtained from the reaction of cyclodextrins with other substances, by employing ^{13}C—RMN and ^{1}H—RMN spectroscopic methods, IR spectroscopy and neutron diffraction, as well. The fourth chapter, entitled *Cyclodextrins in Pharmaceuticals*, contains 15 papers analyzing some practical applications of cyclodextrins in pharmaceuticals ; special mention has to be made here of the studies upon the menadione inclusion compounds with mixtures of natural cyclodextrins, cyclodextrins interaction with antimycotic imidazole derivatives, increasing the solubility characteristics of iomeglamic acid with betacyclodextrin, inclusion complexes of tolbutamide with maltosyl-beta-cyclodextrin, complexes of polyene antibiotics with gammacyclodextrin, molecular encapsulation of retinoic acid by betacyclodextrins, a.s.o.

Chapter 5, *Cyclodextrin Derivatives in Pharmaceuticals*, consists of 8 papers revealing the possibilities of utilizing cyclodextrins in the solubization, stabilization and absorption of some drugs, the hemolytic effect of the cyclodextrins derivatives, a.s.o.

The 6th chapter, *Cyclodextrins in Catalysis and Analytical Chemistry*, exemplifies the utilization of cyclodextrins in chromatography and isotachophoresis in the creation of artificial hydrolases as a model for alpha-chimotrypsin, as well as functionalization of cyclodextrins as an oxydo-reductasic enzyme, occurrence of some reactions in the presence of cyclodextrins, a.s.o.

The last chapter of the volume, *Cyclodextrins in Foods and Agriculture*, is devoted to the applications of cyclodextrins in foods, cosmetics, toiletries, meat industry, in improving the action of some fungicides a.s.o.

Although very different as topics and style, the papers of the volume may be all characterized by the fact that they do not only go deeply in the investigation of some less known aspects, but also launch new questions and, possibly, new scientific approaches to be followed.

Worth mentioning are the excellent graphical conditions of the book ; the main text in accompanied by several tables, graphs, diagrams, schemes and figures, significantly contributing to a better and easier understanding of the problems considered. Rich, impressive references are given at the end of each chapter, the volume ending with a necessary subject index.

The diversity of the themes tackled in the studies of the reviewed volume recommends it to a large area of specialists, such as chemists, biochemists, biologists, pharmaceutical chemists, chemical engineers, farming experts, a.s.o.

D. C. Cojocaru, Vlad G. Artenie

Tipărit la Întreprinderea Poligrafică Iaşi
sub comanda nr. 17/1990

1991 APR 17

40822

ISSN 0254-7104

F 1503/2

BULETINUL INSTITUTULUI POLITEHNIC DIN IAŞI

Tomul XXXVI (XL)

Fasc. 3–4

Secţia II

CHIMIE ŞI INGINERIE CHIMICĂ

1990

BULETINUL INSTITUTULUI POLITEHNIC DIN IAŞI

Tomul XXXVI (XL)

Fasc. 3–4

Secţia II

CHIMIE ŞI INGINERIE CHIMICĂ

1990

EDITORIAL STAFF

Prof. dr. doc. D. I. MANGERON (Honorary President)

Prof. dr. ing. VITALIE BELOUSOV (President)

Conf. dr. ing. MIRCEA MANOLOVICI (Secretary)

Conf. dr. ing. MATEI MACOVEANU

Prof. dr. doc. ALFRED BRAIER (Editor)

Prof. dr. ing. HUGO ROSMAN (Editor)

Prof. dr. ing. MIHAIL VOICU (Head of the Echange Service)

Prof. dr. AUREL BEJANCU

Prof. dr. ing. VICTOR BULACOVSCHI

Prof. dr. ing. MIHAI LUCANU

Prof. dr. ing. SPIRIDON CREȚU

Prof. dr. ing. ADRIAN RADU

Conf. dr. ing. AURELIA GRIGORIU

BULETINUL INSTITUTULUI POLITEHNIC DIN IAŞI
BULLETIN OF THE POLYTECHNIC INSTITUTE OF JASSY
ИЗВЕСТИЯ ЯССКОГО ПОЛИТЕХНИЧЕСКОГО ИНСТИТУТА
Tomul XXXVI (XL), Fasc. 3–4 1990

Secţia II

CHIMIE ŞI INGINERIE CHIMICĂ

S U M A R

Pag.

T. ONOFREI, V. DULMAN şi T. POP, Sorbţia şi separarea Tl(IV), Zr(IV) şi Th(IV) pe 1(4-azobenzilceluloza)2-naftol (engl. rez. rom.) 1
I. ROŞCA şi E. ŞTEFANCU, Studiul sintezei şi posibilităţi de utilizare a metasilicatului de sodiu (engl., rez. rom.) 5
C. BELDIE, GH. NEMŢOI, N. AELENEI şi IG. POINESCU, Studiul poly(metilmetacrilat-co-stiren) şi a homopolimerilor săi în soluţie (engl., rez. rom.) 11
O. VICOL, N. FOCA şi L. ALDINI, Studiul spectrofotometric al echilibrelor din sistemul $K_2[PdCl_4]$—DL nor leucină (engl., rez. rom.) 19
GH. IONESCU, D. HRIŢCU şi I. M. POPA, Studiul proprietăţilor intrinseci ale curgerii viscoase în sistemul 1,2-propandiol (1,2-PD)—metanol (MeOH) (engl., rez. rom.) 23
I. M. POPA şi AL. SAVIN, Determinarea fenil-glicidil-eterului prin cromatografie în faza lichidă de înaltă presiune (engl., rez. rom.) 31
N. HURDUC, L. ODOCHIAN, C. LUCA, E. MIHAI, ŞT. UNGUREANU şi E. IONESCU, Cinetica reacţiei de sinteză a monometiladipatului (engl., rez. rom.) 35
R. Z. TUDOSE, E. MERICĂ şi I. MĂMĂLIGĂ, Transferul de masă la curgerea suspensiilor în filme subţiri (I) (engl., rez. rom.) 39
GH. CRISTIAN, R. STAICU, C. ŞFABU şi D. IONESCU, Studii de cinetica uscării copolimerului stiren-divinilbenzen (II) (engl., rez. rom.) 45
M. CAPROŞU, I. DRUŢĂ, I. FULGER, M. PETROVANU şi D. DOROHOI, Piridaziniumilide. Acţiunea bromurei de *p.*-metoxi-fenacil asupra piridazinei şi a unor 3-aril-piridazine (franc. rez. rom.) 51
V. ŞUNEL şi AL. CECAL, Sinteze de substanţe anticanceroase (engl., rez. rom.) 57
A. AZZOUZ, D. BOUTARFA, D. NIBOU, B. ABBAD (Algeria), E. DUMITRIU şi V. HULEA, Dependenţa dintre activitatea şi selectivitatea catalizatorilor NaLaY şi NaCeY în disproporţionarea catalitică a toluenului (engl., rez. rom.) 63
C. ONISCU, E. HOROBA, I. M. POPA, C. ŞOLDEA şi O. NĂSTASĂ, Modelarea procesului de extracţie a atropinei din *Radix Atropa Belladonna* (engl., rez. rom.) 69
C. VASILIU-OPREA, N. HURDUC şi I. VLAD, Comportarea firului de poliamidă-6 la temperaturi scăzute (engl., rez. rom.) 75
S. PETROVAN, Prelucrarea datelor experimentale. 3. Corelaţie şi regresie polinomială (engl., rez. rom.) 83
V. BULACOVSCHI, A. IOANID, N. HURDUC şi P. ONU, Compozite macromoleculare pe bază de cauciuc şi policaprolactamă (engl., rez. rom.) . . 89
C. VASILE, GH. ADAMESCU, L. CHICU, A. IOANID, M. MIHĂIEŞ, C. DURNESCU şi A. STOLERIU, Reţele semi-interpătrunse constituite din policlorură de vinil şi esteri metacrilici (II) (engl., rez. rom.) 95
RECENZII 101

BULETINUL INSTITUTULUI POLITEHNIC DIN IAŞI
BULLETIN OF THE POLYTECHNIC INSTITUTE OF JASSY
ИЗВЕСТИЯ ЯССКОГО ПОЛИТЕХНИЧЕСКОГО ИНСТИТУТА
Tome XXXIV (XL), Fasc. 3—4 1990

Section II

CHEMISTRY AND CHEMICAL ENGINEERING

CONTENTS

Pp.

T. ONOFREI, V. DULMAN and T. POP, Ti(IV) and Th(IV) Sorption and Separation on 1(4'-Azobenzylcellulose) 2-naphtol (English, Romanian summary) 1

I. ROŞCA and E. ŞTEFANCU, Studies concerning the Synthesis and Possibilities of Using Sodium Metasilicate (English, Romanian summary) 5

C. BELDIE, GH. NEMŢOI, N. AELENEI and IG. POINESCU, Study of Poly (methyl methacrylate-co-styrene) and its Homopolymers in Solution (English, Romanian summary) 11

O. VICOL, N. FOCA and L. ALDINI, Spectrophotometric Study of the Equilibria in the System $K_2(PdCl_4]$—DL-nor-Leucine (English, Romanian summary) 19

GH. IONESCU, D. HRIŢCU and I. . POPA, Study of the Intrinsic Properties of Viscous Flow in the 1 2, -Propandiol (1, 2-PD)—Methanol (MeOH) System (English, Romanian summary) 23

I. M. POPA and AL. SAVIN, Analysis of Phenyl-glycidyl - ether by High-pressure Liquid Chromatography (English, Romanian summary) 31

N. HURDUC, L. ODOCHIAN, C. LUCA, E. MIHAI, ŞT. UNGUREANU and E. IONESCU, Kinetics of the Reaction of Monomethyladipate Synthesis (English, Romanian summary) 35

R. Z. TUDOSE, E. MERICĂ and I. MĂMĂLIGĂ, Mass Transfer in Flow of Thin Films of Suspensions (I) (English, Romanian summary) 39

GH. CRISTIAN, R. STAICU, C. ŞFABU and D. IONESCU, Studies on Kinetics of Styrene-Divinylbenzene Copolymer Drying (II) (English, Romanian summary) 45

M. CAPROŞU, I. DRUŢĂ, I. FULGER, M. PETROVANU et D. DOROHOI, Pyridaziniumylures. Action du bromure de *p*. méthoxy-phénacyle sur la pyridazine et quelques 3-aryle-pyridazines (French, Romanian summary) 51

V. ŞUNEL and AL. CECAL, Synthesis of Anticancerous Substances (English, Romanian summary) 57

A. AZZOUZ, D. BOUTARFA, D. NIBOU, B. ABBAD (Algier), E. DUMITRIU and V. HULEA, Dependence between the Activity and Selectivity of NaLaY and NaCeY Catalysts in the Catalytic Disproportionation of Toluene (English, Romanian summary) 63

C. ONISCU, E. HOROBA, I. M. POPA, C. ŞOLDEA and O. NĂSTASĂ, Modeling of Process of Atropine Extraction from *Radix Atropa Belladonna* (English, Romanian summary) 69

C. VASILIU-OPREA, N. HURDUC and I. VLAD, Study about the Polyamid-6 Technical Yarn in Conditions of Low Temperatures Processing (English, Romanian summary) 75

S. PETROVAN, Experimental Data Processing. 3. Polynominal Correlation and Regression (English, Romanian summary) 83

V. BULACOVSCHI, A. IOANID, N. HURDUC and P. ONU, Polymer Blends of Policaprolactam with Elastomers (English, Romanian summary) 89

C. VASILE, GH. ADAMESCU, L. CHICU, A. IOANID, M. MIHĂIEŞ, C. DURNESCU and A. STOLERIU, Semi-Interpenetrating Networks Based on Polyvinyl Chloride and Metacrylic Esters (II) (English, Romanian summary) 95

BOOK REVIEWS 101

BULETINUL INSTITUTULUI POLITEHNIC DIN IAȘI
Tomul XXXVI (XL), Fasc. 3—4, 1990
Secția II
CHIMIE ȘI INGINERIE CHIMICA

D. C. 661.882 ; 661.883.1 ; 661.884 ; 547.659.3

Ti(IV), Zr(IV) AND Th(IV) SORPTION AND SEPARATION ON 1(4'-AZOBENZYLCELLULOSE)2-NAPHTOL

BY

TINCA ONOFREI, VIORICA DULMAN and TAMARA POP

1. Introduction

The 1(4'-azobenzylcellulose) 2-naphtol chelating sorbent is selective towards some elements in group II. In a series of previous notes [1]...[4] the sorption mechanism of these elements and the possibility of their chromatographic separation have been investigated.

The present paper presents the data concerning Ti(IV), Zr(IV) and Th(IV) sorption and separation on the same modified cellulose.

2. Experimental

1(4'-azobenzylcellulose)2-naphtol was synthetised from PAB-cellulose diazotized and coupled with 2-naphtol [5].

The mechanism of Ti(IV), Zr(IV) and Th(IV) sorption on 1(4'-azobenzylcellulose)2-naphtol has been investigated by means of the following determinations : a) Ti(IV), Zr(IV) and Th(IV) distribution coefficients (K_D) dependence on pH at 25°C ; b) Zr(IV) and Th(IV) sorption isotherms at 25°C ; c) Zr(IV) and Th(IV) isobars between 0°...100°C ; d) determination of the apparent free enthalpy : e) IR spectra of the sorbent before and after Ti (IV), Zr (IV), Th (IV) sorption between 400... 4 000 cm^{-1}.

The distribution coefficients have been determined by the static method stirring 0.5 g of sorbent under the form H with 25 ml of standard solution of $TiCl_4$ (4.46 μg Ti(IV)/ml), $Zr(NO_3)_4$ (8.52 μg Zr(IV)/ml) and $Th(NO_3)_4$ (22.22 μg Th(IV)/ml) with a given pH at 25°C.

After the equilibrium has been reached the phases have been separated by filtration. The equilibrium pH (pH_e) has been determined in the aqueous phase. In an aliquot part of the filtrate the excesses of Ti (IV) with sulphosalicylic acid [6], Zr(IV) with alizarin *S* [7] and Th (IV) with thoron [8] have been spectrophotometrically determined.

3. Results and Discussions

From the study of the dependence of the distribution coefficients on pH results that Ti(IV) sorption increases gradually from $pH_e=1$ ($K_D=0.75$) tp $pH_e=2$ ($K_D=0.3\times10^2$), while Zr(IV) sorption increases considerably between

$pH_e = 1.7$ ($K_D = 0.5 \times 10^2 ... 2 \times 10^3$) and Th(IV) sorption between $pH_e = 1.2 ... 2.9$ ($K_D = 2.03 ... 1.51 \times 10^3$). From this investigation there can be infered that the order of selectivity towards the sorbent is as follows :

$$Zr(IV) > Th(IV) \gg Ti(IV).$$

The Zr(IV) and Th(IV) sorption isotherms (Fig. 1) assume shapes that plead in favour of a combined adsorption and chemosorption process, the later being prevalent. The same conclusions could be drawn from the analysis of the sorption isobars (Fig. 2).

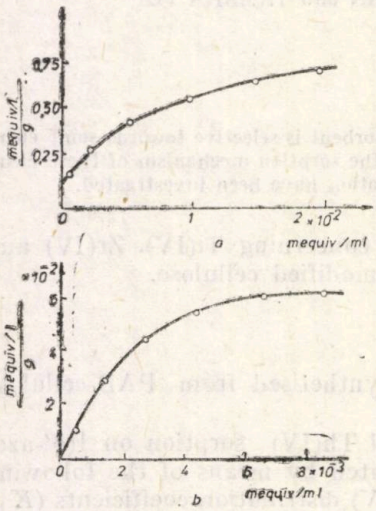

Fig. 1. — The sorption isotherms at 25°C ; *a* — for Zr(IV) at $pH_e = 1.4 ... 1.6$; *b* — for Th(IV) at $pH_e = 2.7 ... 2.9$.

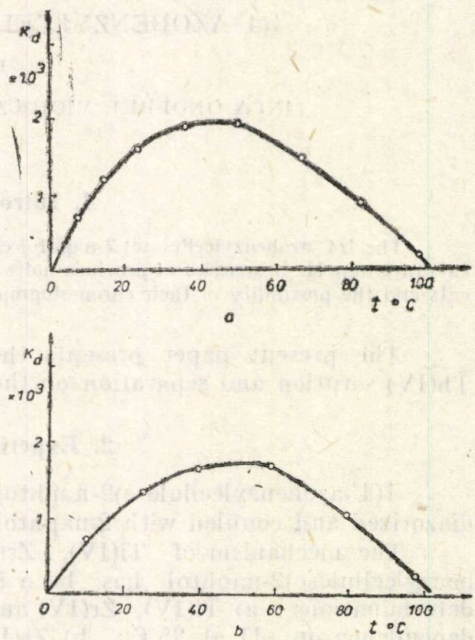

Fig. 2.—The sorption isobars between 0°...100°C ; *a* — for Zr(IV) at $pH_e = 1.4..1.6$; *b* — for Th(IV) at $pH_e = 2.7...2.9$.

Between 0°...60°C Zr(IV) and Th(IV) distribution coefficients increase gradually which is indicative of a chemical reaction that overlaps the physical sorption. At a temperature higher than 60°C there occurs a decrease in sorption, probably due to the partial degrading of the sorbent.

The apparent free enthalpy has been determined with the help of relation :

$$\Delta G = -RT \ln K,$$

where K is the exchange reaction constant.

The K values have been infered from the isotherms by Nikolski's relation [9].

The apparent free enthalpy has the values —1 731 cal/mol for Zr(IV) and — 1 363 cal/mol for Th(IV), fact which points out to an ionic exchange phenomenon that is more prominent for Zr(IV).

Conclusions can be drawn as to the chemical sorption from IR spectra. In the spectrum of the sorbent there appear two small peaks characteristic of the azo group, one at 1 580 cm^{-1} and the other one at 1 080 cm^{-1}. The —OH group from β-naphtol is not evident in the spectrum since it overlaps the band from 3 300...3 600 cm^{-1} attributed to the unmodified cellulose —OH groups. In the presence of metallic ions the two peaks disappear which points to the azo groups being implied in the formation of chelate type compounds between the sorbent and cations.

The pH decrease during the sorption as well as the modifications that occur in the IR spectra led to the conclusion that the physical sorption of Ti(IV), Zr(IV) and Th(IV) is accompanied by formation of chelates :

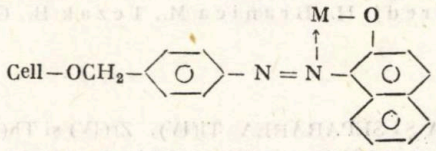

where : M = $Ti(OH)_2/2$, $Zr(OH)_2/2$ and Th/4.

There exists the possibility that the sorpted species might be the above mentioned ones since in an aqueous solution at considered pH values, Ti(IV) is to be found under the form of $[Ti(OH)_2]^{2+}$ [10], Zr(IV) as $[Zr(OH)_2^{2+}$ [11] and Th (IV) under the form of tetravalent ions [12].

The experimental data obtained under static conditions have suggested the possibility of separating the three elements on a column filled with 1(4'-azobenzylcellulose)2-naphtol. By using a column of 150 mm long and 10 mm

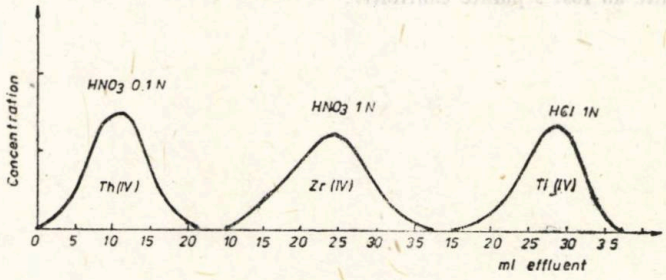

Fig. 3. — The separation of Th(IV) — Zr(IV) —Ti(IV) .

in diameter filled with 6 g of sorbent the three elements have been separated quantitatively (Fig. 3) by succesive elution with 0.1 N HNO_3, 1 N HNO_3 and 1 N HCl.

Received, May 16, 1980

Polytechnic Institute, Jassy,
Department of Analytical Chemistry

REFERENCES

1. Fișel S., Ungurenașu-Onofrei T., Gabe I., An. Șt. Univ. „Al. I. Cuza", Iași, **13**, 19 (1967).
2. Fișel S., Ungurenașu-Onofrei T., Cellulose Chem. Technol., **3**, 383 (1969)
3. Fișel S., Ungurenașu-Onofrei T., 3rd Analytical Conf., August 24—29, 1980, Budapest, 99.
4. Ungurenașu-Onofrei T., Fișel S., Rev. Chim. (București), **24**, 926 (1973).
5. Fișel S., Ungurenașu-Onofrei T., Gabe I., An. Șt. Univ. „Al. I. Cuza", Iași. **11**, 51 (1965).
6. Ziegler M., Glemser O., v. Baeckmann A., Z. Analyt. Chem., **160**, 324 (1958).
7. Ледков М., Рабчиков Д. Н., Савин С. Б., ЖАХ, **20**, 574 (1965).
8. Athavale V. T., Oke K. P., Tillu M. M., Analyt. Chim. Acta, **21**, 528 (1959).
9. Никольский В. П., ЖПХ, **8**, 1935 (1939).
10. Liberti A., Chiantella V., Corijliano F., J. Inorg. Nucl. Chem., **25**, 415 (1963).
11. Соловкин А. С., Цветкова З. Н., Усп. хим., **31**, 1394 (1962).
12. Bilinski H., Füredi H., Branica M., Tezak B., Croat Chem. Acta, **35**, 19 (1963).

SORBȚIA ȘI SEPARAREA Ti(IV), Zr(IV) și Th(IV) PE 1(4-'AZOBENZILCELULOZA) 2-NAFTOL

(Rezumat)

S-a cercetat sorbția și separarea Ti(IV), Zr(IV) și Th(IV) pe 1(4′-azobenzilceluloza) 2-naftol.

Din cercetarea dependenței coeficienților de distribuție față de pH rezultă că ordinea selectivității este următoarea :

$$Zr(IV) > Th(IV) \geqslant Ti(IV).$$

Studiul izotermelor și izobarelor de sorbție arată că sorbția Zr(IV) și Th(IV) are loc ca urmare a suprapunerii sorbției chimice peste cea fizică, chemosorbția fiind predominantă.

Modificările care au loc în spectrele IR conduc la concluzia că sorbția chimică a Ti(IV), Zr(IV) și Th(IV) are loc printr-o reacție cu formarea de chelați.

Folosind o coloană cu umplutură de 1(4′-azobenzilceluloză) 2-naftol și eluenți adecvați cele trei elemente au fost separate cantitativ.

BULETINUL INSTITUTULUI POLITEHNIC DIN IAȘI
Tomul XXXVI (XL), Fasc. 3—4, 1990
Secția II
CHIMIE ȘI INGINERIE CHIMICĂ

D C. 661.683 ; 366.095.6

STUDIES CONCERNING THE SYNTHESIS AND POSSIBILITIES OF USING SODIUM METASILICATE

BY

I. ROȘCA and ELENA ȘTEFANCU

1. Introduction

Through the sodium silicates are known from old times, being firstly signaled even in 1577 [1], [2], they continue to be of interest for many researchers which investigate their structure and uses.

Usually natrium silicates are classified according to their structure and SiO_2/Na_2O mol ratio. According to this criterion can be distinguished sodium silicates in which the SiO_2/Na_2O mole ratio is 1...1.5. The sodium metasilicate (Na_2SiO_3 crude formula) with a more complicated structure like an infinite chain of SiO_4^{4-} tetrahedrons belongs to this class.

At present, the anhydrous or hydrated sodium metasilicate is not produced in Romania ; it is imported in small amounts from USA, FRG or France, in crystalline form. The technological process for obtaining the imported product is not described in literature being kept constant by the producers.

2. Critical Review of the Methods of Natrium Metasilicate Obtaining

The sodium metasilicate is usually obtained from sodium hydroxide and quartz sand by melting. The sand has to be free of impurities since the latter are regained in the final product natrium metasilicate.

Thus, the presence of Fe^{2+} and Fe^{3+} results in a blue green colour of the final product or a yellow one, respectively while the iron sulphides iron give colours varying from yellow to brown [2].

For obtaining high purity silicates Deguse aerosil and Na_2O or NaOH are used [2].

The sodium metasilicate can also be obtained from sodium sulphate and sand using coal as reducing agent, at 1 300...1 400°C, according to the reactions [2] :

$$Na_2SO_4 + 2C \rightarrow Na_2S + 2CO_2,$$

$$Na_2S + 3Na_2SO_4 \rightarrow 4Na_2O + 4SO_2,$$

$$4Na_2O + 4SiO_2 \rightarrow 4Na_2SiO_3.$$

To avoid the presence of sodium sulphide in the final product the sodium sulphate has to be added but in a small excess only.

To obtain the sodium metasilicate in solution a concentrated solution of sodium silicate can be used with a SiO_2/Na_2O mole ratio >1, which is mixed with a concentrated sodium hydroxide or with solid sodium hydroxide in a 1/1 mole ratio.

By cooling the solutions individual hydrates can be separated by introducing the crystallization germs. For obtaining the anhydrous product the liquid solution can be submitted to a drying process.

According to a german patent [5] the sodium metasilicate can be obtained by treating NaCl with NO_2, the obtained sodium nitrate reacting with SiO_2. The process can be described by the following reaction scheme :

$$2NaCl + 4NO_2 \rightarrow 2NaNO_3 + 2NOCl,$$

$$2NOCl + O_3 \rightarrow 2NO_2 + Cl_2,$$

$$2NaNO_3 + SiO_2 \rightarrow Na_2SiO_3 + 2NO_2 + \frac{1}{2} O_2.$$

The NaCl and SiO_2 are raw materials while NO_2 is recycled.

According to some american patents [6], [7] anhydrous and hydrated sodium metasilicates can be obtained by mixing sand and 50% NaOH solution at 200°C, in an autoclave, under pressure.

At the reaction end the solid sodium metasilicate is separated and washed firstly with 28% ammonia solution and then with methanol to remove the retained water.

By warming the separated product at various temperatures, anhydrous silicates or hydrated, with various amounts of water, can be obtained.

The direct method of sodium hydrate and sand melting is among the simplest procedures for metasilicate obtaining. Thus, an anhydrous product is obtained but with a rather high content of impurities.

The sodium metasilicate obtained by this method can fulfil the requirements of the machine building industry but its quality is not adequate for using in the food or electronic industries and for the galvanizing baths.

In addition to the pure quality of the product obtained in this way the problem of corrosion also arises (the corrosion is rather strong due to the high sodium hydrate content). The method is adventageous since the raw materials are cheap and the technological process rather simple.

The method of lawering the mole ratio of a sodium silicate solution with a solution of sodium hydroxide exhibits the following advantages : a) the raw materials are liquids and can be easily handled ; b) the use of a high temperature is not required ; c) the final product results directly in a granulated form which removes the product crushing and grinding.

The main disadvantage of the process arises from the high price of raw materials compared to the direct metting procedure.

The method based on the direct transformation of sodium chloride into nitrozil chloride and the obtaining of sodium nitrate which by treating with SiO_2 passes into sodium metasilicate is rather complicated, exhibits a permanent danger of explosion and cannot assure a high purity of the product.

3. Experimental

During the studies referring to metasilicate obtaining, the sodium silicate of SE type and solid sodium hydroxide produced by C. C. Rîmnicu Vîlcea have been used as raw materials. From these materials solutions of sodium metasilicate, with a SiO_2/Na_2O mole ratio = 1 have been obtained.

The composition of raw materials used is the following :

Sodium Silicate of SE type

a) Density . . . . . 1 320 Kg/cm³
b) SiO_2 . . . . . 23.98%
c) Na_2O 7.78%
d) NaCl 0.05%
e) RM 3.18%

Solid Sodium Hydroxide

NaOH 98.0%
Na_2CO_3 . . . . . 1.3%
NaCl 0.4%
Fe_2O_3 . . . . . 0.008%.

The sodium silicate solution of SE type with a SiO_2/Na_2O mole ratio = = 3 : 1 is mixed with the amount of sodium hydroxide solution required for obtaining a solution with a SiO_2/Na_2O mole ratio = 1 : 1. The obtained metasilicate solution is filtered for removing the existing solids suspended in the raw matarials and centrifuged on a centrifuge rotating with 5...7 000 rot/min. A clear sodium metasilicate solution is acquired which is submitted to the crystallization when the obtaining of a hydrated crystalline products is desired or is evaporated in an adequate apparatus to obtain anhydrous metasilicate.

The sodium metasilicate solution obtained according to the above described method at a minimum concentration of 270 g/l Na_2SiO_3 is introduced in a crystallizer cooled at 20°C (on water bath) and crystallizing germs introduced (crystalline sodium metasilicate). After keeping for six hours at this temperature partly of the sodium silicate found in solution (30...40% crystallizes as white sodium metasilicate crystals with nine water molecules per one Na_2SiO_3 mole).

The suspension obtained during the crystallization process is filtered for removing the mother liquor. The filtration is carried out on a Büchner filter funnel under a vacuum of 0.5 Kgf/cm².

The sodium metasilicate hydrates loose water on heating according to the equations :

$$\underset{\text{M.p}=37.2^\circ\text{C}}{Na_2SiO_3 \cdot 10H_2O} \xrightarrow[-H_2O]{31^\circ\text{C}} \underset{\text{M.p.}=47.2^\circ\text{C}}{Na_2SiO_3 \cdot 9H_2O} \xrightarrow[-3H_2O]{41.9^\circ\text{C}} \underset{\text{M.p.}=62.3^\circ\text{C}}{Na_2SiO_3 \cdot 6H_2O}$$

The sodium metasilicate is dissolved in water but at temperatures above 70°C decomposes with the occurence of a sediment of acid orthosilicate ($Na_2H_2SiO_4$).

The solubilities are given below : a) at 13°C....281 g/l Na_2SiO_3 ; b) at 30°C...380 g/l Na_2SiO_3 ; c) at 50°C...483 g/l Na_2SiO_3.

Table 1

Characterization of the Obtained Metasilicate Compared with the Sodium Metasilicate Reported in Literature [3], [16]

Characteristics	Product obtained in the laboratory		German patent [3]		American patent [6]	
	Anhydrous	Hydrated	Anhydrous	Hydrated	Anhydrous	Hydrated
Na_2O, [%]	50...51	15...18	15...52	29...30	50	28.5...30
SiO_2 [%]	48	15..17	45	28.5...29	45	27.5...29
SiO_2/Na_2O	1...1.03	1	1.075...1.123	1	1 ... 1.05	1
Insoluble, [%]	2...7	0.2	0.8	0.2	0.2... 0.5	0.2
CO_2, [%]	0.9..2.5	0.6...0.8	2.0	1.2	1.2... 2.0	1.2
pH sol.	12.6...12.8	13.0	12.6	12.3	12.6...12.9	
Crist. water, [%]	—	61...69	—	40...42	—	40...42

The chemical analyses have been carried out according to literature methods namely : STAS 3 068-61 for natrium hydroxide and STAS 2 902-67 for sodiumsilicate.

As can be seen in Table 1 the quality of anhydrous and crystalline metasilicates obtained in the laboratory correspond to the foreign standards with small differences regarding the insoluble content and the amount of crystallization water.

4. The Uses of Sodium Metasilicate

Though the sodium metasilicate is not produced in our country we use it as detergent, especially in the machine building industry for treating the pieces submitted to galvanization, in the textile and food industries.

The sodium silicate can also be used for water dedurization and as foaming agent when added to soap or detergents solutions.

The sodium metasilicate stabilizes the foam so that an addition of 80... 100 g of the obtained product to 1 000 g detergents improve the washing power by 2...2.5 times.

The sodium metasilicate acts as a stabilizing agent for the hydrogen peroxide used in bleaching the cotton, wool and silk.

The bleaching degree estimated in photocolorimetric units is about 5.4 for a solution containing sodium metasilicate compared to 2.5 for a bleaching solution containing sodium carbonate.

The sodium metasilicate exhibits some properties such as the emulsifying soaking and defloculating abilities. Due to its structure (a weak acid and a string base) forms buffer solutions which recommend it for various uses in this direction.

The sodium metasilicate can also be used for consolidating the grounds. The grounds are impenetrated with a solution of these product and treated then with $CaCl_2$. It can also be used as fire proofing agent and in the manufacture of antiacide putties.

The sodium metasilicate obtained in the laboratory fulfil the requirements for use above mentioned and the procedure can be extended to pilot and then to industrial scale for diminishing the amount of imported product.

Received, November 30, 1988

Polytechnic Institute, Jassy,
Department of Inorganic Chemistry

REFERENCES

1. Solacolu S., *Chimia fizică a silicaţilor tehnici.* Ed. Tehn., Bucureşti, 1963.
2. * * * *Enzyclopädie der technischen Chemie.* Bd. **16**, Ed. Springer-Verlag. Berlin. 1964.
3. * * * German Patent nr. *1 567 272*, 2. XI. 1972.
4. * * * German Patent, *1 567 573*, 2. XI. 1972.
5. * * * German Patent, *1 236 488*, 16. III. 1967.
6. * * * USA Patent, *3 532 458*, 6. X. 1970.
7. * * * USA Patent, *3 471 253*, 7. X. 1969.

STUDIUL SINTEZEI ŞI POSIBILITĂŢI DE UTILIZARE A METASILICATULUI DE SODIU

(Rezumat)

Se prezintă studii de laborator şi posibilităţile de utilizare ale metasilicatului de sodiu. Se scot în evidenţă avantajele şi dezavantajele metodelor de sinteză existente în condiţii de laborator.

Studiile au fost efectuate aplicînd metode chimice, fizico-chimice şi fizice de analiză.

Utilizările deosebite ale metasilicatului de sodiu sînt, în principal: în industria detergenţilor la decaparea suprafeţelor metalice, în turnătorie, pentru obţinerea celulelor de determinarea a umidităţii solurilor etc.

BULETINUL INSTITUTULUI POLITEHNIC DIN IAȘI
Tomul XXXVI (XL), Fasc. 3—4, 1990
Secția II
CHIMIE ȘI INGINERIE CHIMICĂ

D. C. 678.746.22—136.22

STUDY OF POLY(METHYL METHACRYLATE-co-STYRENE) AND ITS HOMOPOLYMERS IN SOLUTION

BY

CAMELIA BELDIE, GH. NEMȚOI, N. AELENEI and IGNAT POINESCU

1. Introduction

The copolymer behaviour assumption on the experimental measurement basis corresponding to its homopolymers presents a great theoretical and practical importance. Such relationships lead to the characterization of the copolymer samples.

This paper deals with the study of poly(methyl methacrylate-co-styrene) by analogy with its homopolymers, poly(methyl methacrylate), and polystyrene, which were prepared in the same experimental conditions.

Dilute solutions of polymers (0.2...1.0 g/dL) at which the equation

$$\frac{\pi}{C} = \frac{RT}{\overline{M}_n} + RTA_2C, \tag{1}$$

can be applied were used [1] where: π — the osmotic pressure, $\overline{M}_n$ — the number-average molecular weight, C — the concentration of the polymer solution, A_2 — the second virial osmotic coefficient, T — the temperature, [K].

In order to estimate the intrinsic viscosity of dilute polymer solutions (0.1...1.0 g/dL), the graphic double extrapolation method of the Huggins and Fuoss—Mead equation was applied [2]...[3].

The evaluation of the structural parameters of a certain solvent—polymer system can be done applying the most known equations as follows ;

a) Stockmayer — Fixman's equation [4] :

$$\frac{[\eta]}{M^{1/2}} = K_0 + 0.51\,\Phi_0 B M^{1/2}\,; \tag{2}$$

b) Schaefgen — Flory's equation [5]:

$$\frac{[\eta]^{2/3}}{M^{1/3}} = K_0^{2/3} + 4.085\,\Phi_0 B \frac{M}{[\eta]}\,; \tag{3}$$

c) Kurata — Stockmayer — Roig's equation [6] :

$$\frac{[\eta]^{2/3}}{M^{1/3}} = K_0^{2/3} + 0.363\,\Phi_0 B g(\alpha_\eta) \frac{M^{2/3}}{[\eta]^{1/3}}, \tag{4}$$

where : M — the molecular weight of the fractionated polymers, B — the second virial coefficient, which is correlased with A_2 through the equation ;

(5) $$B=\frac{2\bar{v}_2^2}{N_m v_1}\left(\frac{1}{2}-\chi\right)=\frac{2A_2}{N_m},$$

with : $\bar{v}_2$ — the partial specific volume of the polymer sample from solution ; χ — the F l o r y 's interaction parameter, N_m - the A v o g a d r o's number,

(6) $$g(\alpha_\eta)=\frac{8\alpha_\eta^3}{(3\alpha_\eta^2+1)^{3/2}};$$

here α_η is the hydrodynamic expansion factor given by the equation ;

(7) $$\alpha_\eta^3=\frac{[\eta]}{[\eta]_\theta}=\frac{[\eta]}{K_\theta M^{1/2}},$$

where : $[\eta]_\theta$ — the intrinsic viscosity at θ conditions ; K—a characteristic constant for the investigated polymer — solvent system, directly connected with the unperturbed dimensions of macromolecules in -solution [7], [8] ;

(8) $$K_\theta=6^{3/2}\Phi\left(\frac{<R^2>_\theta}{M}\right)^{3/2},$$

with: Φ_0—F l o r y's hydrodynamic constant whose value for homogeneous polymers is 2.87×10^{21} dl.mol^{-1}. cm^{-3} [9]...[11], $<R^2>_\theta$ — the mean square radius of gyration of the unperturbed chain at θ conditions; $<R^2>_\theta$ can be calculated applying the relationship (8), and the mean square radius of gyration of the true macromolecular chain in a good solvent can be directly determined using the F l o r y—F o x equation [11] ;

(9) $$[\eta]=6^{3/2}\Phi_0\frac{<R^2>^{3/2}}{M}.$$

Taking into account that the macromolecular dimensions and implicitly $[\eta]$ and α_η are dependent on the intermolecular forces these parameters can be corelated with the second virial osmotic coefficient resulting the possibility to estimate A_2 on the basis of viscosity measurements. Hence, applying Eqs. (2)...(4), it is possible to calculate the second virial coefficient using the viscosity data as follows ;

a) S t o c k m a y e r — F i x m a n's equation :

(10) $$A_2=205.5\frac{[\eta]}{M}\left(1-\frac{1}{\alpha_\eta^3}\right);$$

b) S c h a e f g e n —F l o r y's equation :

(11) $$A_2=138.13\frac{[\eta]}{M}\ln\left[1+0.866(\alpha_\eta^2-1)\right];$$

c) K u r a t a —S t o c k m a y e r — R o i g's equation ;

(12) $$A_2=187.6\frac{[\eta]}{M}\cdot\frac{(\alpha_\eta^2-1)\left(1-\frac{1}{3}\alpha_\eta^2\right)}{\alpha_\eta^2}.$$

The hydrodynamic expansion factor used within these equations can be calculated by means of the equation (7) and K_θ was estimated applying the equations (2)...(4).

3. Experimental

The polymer and copolymer samples were fractionated as follows :

a) Seven fraction of polystyrene were obtained by precipitation with methanol from a 1.29 g/dL benzene solution at 15°C.

b) Seven fractions of poly(methyl methacrylate) were obtained by precipitation with an acetone—water mixture (1 : 1 ; v/v) from a 1.0 g/dL acetone solution at 15°C.

c) The copolymer samples were fractionated by precipitation of a solution using the benzene—petroleum ether at 15°C.

The fractions of PS and PMMA were thoroughly washed with methanol and then reprecipitated from a benzene solution. The copolymer fractions were washed with petroleum ether and then reprecipitated from a benzene solution. Finaly, all samples were vacuum-dried at 55°C for 48 h.

In order to check the fraction chemical composition of the polymer and copolymer samples, the St-MMA molar composition was determined using NMR analysis. It resulted that unfractionated samples contained 44.04% mole styrene, while the fractionated samples had 41.0...44.0% mole styrene.

Benzene (B) and tetrahydrofurane (THF) were then distilled. THF was stabilized with hydroquinone (0.05%).

The osmotic pressure measurements were performed on a Hewlett-Packard membrane osmometer, type 502, using regenerated cellulose membrane which had a good selectivity for solute, and benzene as solvent, at 28°C [12].

At least five osmotic pressure measurements were performed for each sample solution whose concentrations varied between 0.20 g/dL and 1.0 g/dL and the data were processed by means of expression (1) applying the linear regression method.

The solution viscosity measurements (at least 6...7) were performed on a Ubbelohde viscometer, and the solution concentrations were varied between 0.15 g/dL and 1.0 g/dL using THF as solvent at 25° ±0.05°C. Haggenbach—Couette's corrections were applied.

The number average molecular weights, ($\bar{M}_n$), and the intrinsic viscosity, [η], values, measured in C_6H_6 and THF for polymer and copolymer samples, are listed on Table 1.

4. Results and Discussion

According to the Mark—Houwink 's equation, the dependence

$$\ln[\eta]=\ln K+a\ln\bar{M}_n \tag{13}$$

of the intrinsic viscosity vs. the molecular weight was established. The thermodynamical structural parameters were calculated using the expressions (2)... (4). The equation (13) was interpreted applying the linear regression method and the results were listed on Table 2. These table shows that the linear dependence of $\ln[\eta]$ vs. $\ln\bar{M}_n$ is very good. The literature quotes a lot of studies which dealt with the calculation of K and a coefficient value from Mark—Houwink 's equation for tne investigated systems. But, these values are not always in agreement, particular by the PS—C_6H_6/THF and PMMA—C_6H_6/THF systems [6], [8], [13]...[15]. For the PS—C_6H_6 system,

Table 1

$\overline{M}_n$ and $[\eta]$ of the Homopolymers and Copolymer Fractions in Benzene and THF

Sample	Fraction	$\overline{M}_n$ g. mol^{-1}	$[\eta]$, [dL.g^{-1}]	
			C_6H_6	THF
Polystyrene	1	68,400	0.4080	0.3276
	2	55,800	0.3271	0.2937
	3	42,200	0.2638	0.2466
	4	39,600	0.2543	0.2285
	5	27,100	0.1944	0.1851
	6	19,700	0.1522	0.1563
	7	12,200	0.1069	0.1147
nonfractionated	—	26,000	0.2460	0.2320
Poly(methyl methacrylate)	1	274,800	0.8500	0.7450
	2	176,000	0.6320	0.5600
	3	120,600	0.4875	0.4400
	4	111,500	0.4353	0.4230
	5	99,600	0.4100	0.3840
	6	72,400	0.3250	0.3400
	7	32,400	0.1763	0.1976
nonfractionated	—	99,300	0.4320	0.4150
Poly (methyl methacrylate—co-styrene)	4	147,400	0.5950	0.6200
	7	86,400	0.4520	0.4620
	9	64,800	0.3600	0.3950
	10	57,800	0.3290	0.3530
	11	49,000	0.2980	0.3150
nonfractionated	—	63,800	0.3980	0.3850

Table 2

Mark—Houwink's Coefficients

Solvent	Sample	a	10^4K dL/g	Linear correlation coefficient
Benzene	PS	0.757	0.851	0.9986
	PMMA	0.741	0.813	0.9992
	Copolymer	0.639	3.039	0.9955
THF	PS	0.608	0.378	0.9991
	PMMA	0.613	3.417	0.9985
	Copolymer	0.606	4.595	0.9961

the measured value of a coefficient lies on the upper position of the value domain quoted by literature as a consequence of a broader polydispersity of the first fractionated samples. In exchange, the measured value of a for the PMMA —C_6H_6 system lies within the domain qouted by literature. But the values of a, of the PS — THF and PMMA—THF systems, measured by the authors, are lower than one mentioned by the literature [14], [15]. The values of a, de-

Table 3

Thermodynamic-structural Parameters in C_6H_6 Measured at 25°C

Fraction	$\bar{M}_n$ g. mol^{-1}	$[\eta]$ dL. g^{-1}	R_G Å	Stockmayer–Fixman			Schaefgen–Flory			Kurata–Stockmayer–Roig		
				α_η	R_G	10^4A_2	α_η	R_G	10^4A_2	α_η	R_G	10^4A_2
				Polystyrene								
1	68,400	0.4080	87.14	1.4020	62.15	7.81	1.9351	45.03	10.03	1.4557	59.86	20.53
2	55,800	0.3271	75.64	1.3474	56.14	7.12	1.8597	40.67	9.24	1.3990	54.06	15.57
3	42,200	0.2638	64.15	1.3139	48.82	7.18	1.8136	35.37	9.44	1.3643	47.02	13.98
4	39.600	0.2543	62.04	1.3118	47.29	7.35	1.8106	34.26	9.67	1.3621	45.55	14.20
5	27,100	0.1944	49.99	1.2777	39.12	7.67	1.7667	28.34	10.30	1.3267	37.67	13.14
6	19,700	0.1522	41.43	1.2419	33.36	7.59	1.7142	24.17	10.52	1.2895	32.12	11.42
7	12,200	0.1069	31.39	1.1957	26.25	7.47	1.6504	19.02	11.06	1.2416	25.28	9.52
				Poly(methyl methacrylate)								
1	274,800	0.8500	176.92	1.3277	133.26	3.64	1.6643	106.31	3.97	1.3704	129.10	7.14
2	176,000	0.6320	138.16	1.2955	106.65	3.99	1.6239	85.08	4.38	1.3372	103.32	6.97
3	120,600	0.4875	111.71	1.2654	88.28	4.21	1.5862	70.43	4.68	1.3061	85.53	6.59
4	111,500	0.4353	104.79	1.2345	84.88	3.76	1.5475	67.72	4.27	1.2743	82.24	5.26
5	99,600	0.4100	98.93	1.2331	80.23	3.95	1.5457	64.00	4.49	1.2729	77.79	5.49
6	72,400	0.3250	82.32	1.2035	68.40	3.93	1.5087	54.57	4.62	1.2423	66.27	4.90
7	32,400	0.1763	51.35	1.1223	45.76	3.27	1.4068	36.50	4.62	1.1584	44.33	3.05
				Poly (methyl methacrylate-co-styrene)								
1	147,400	0.595	127.64	1.1285	113.11	2.52	1.1514	110.85	1.39	1.1341	112.54	1.78
2	86,400	0.452	97.47	1.1286	86.59	3.21	1.1484	84.87	1.76	1.1312	86.16	2.23
3	64,800	0.360	82.09	1.0946	74.99	2.71	1.1168	73.50	1.49	1.1000	74.62	1.63
4	57,800	0.329	76.68	1.0826	70.83	2.48	1.1046	69.42	1.37	1.0880	70.48	1.42
5	49,000	0.298	70.21	1.0767	65.21	2.49	1.0986	63.92	1.38	1.0821	64.89	1.38

Table 4

Thermodynamic - structural Parameters Measured in THF at 25°C

Fraction	$\overline{M}_n$ g. mol^{-1}	$[\eta]$ dL.g^{-1}	R_G Å	Stockmayer–Fixman			Schaefgen–Flory			Kurata–Stockmayer–Roig		
				α_η	R_G	10^4A_2	α_η	R_G	10^4A_2	α_η	R_G	10^4A_2
				Polystyrene								
1	68,400	0.3276	80.99	1.1183	72.42	2.81	1.1390	71.11	1.52	1.1232	72.11	1.87
2	55,800	0.2937	72.97	1.1155	65.41	3.02	1.1362	64.23	1.63	1.1204	65.13	1.99
3	42,200	0.2466	62.72	1.1026	56.89	3.05	1.1229	55.85	1.64	1.1074	56.64	1.89
4	39,600	0.2285	59.86	1.0864	55.11	2.61	1.1064	54.11	1.41	1.0911	54.86	1.50
5	27,100	0.1851	49.18	1.0788	45.59	2.86	1.0987	44.76	1.56	1.0835	45.39	1.59
6	19,700	0.1563	41.79	1.0753	38.87	3.19	1.0952	38.16	1.75	1.0800	38.70	1.74
7	12,200	0.1147	32.13	1.0506	30.59	2.66	1.0699	30.03	1.53	1.0552	30.45	1.31
				Poly(methyl methacrylate)								
1	274,800	0.745	169.32	1.1360	149.05	1.77	1.1597	145.99	0.98	1.1417	148.30	1.29
2	176,000	0.560	132.70	1.1125	119.28	1.79	1.1358	116.84	0.98	1.1181	118.68	1.17
3	120,600	0.440	107.95	1.0933	98.74	1.76	1.1162	96.72	0.97	1.0988	98.24	1.06
4	111,500	0.423	103.80	1.0933	94.94	1.83	1.1161	93.00	1.01	1.0987	94.47	1.10
5	99,600	0.384	96.79	1.0787	89.73	1.61	1.1012	87.89	0.90	1.0841	89.28	0.90
6	72,400	0.340	83.57	1.0923	76.50	2.25	1.1152	74.94	1.24	1.0978	76.12	1.34
7	32,400	0.1976	53.34	1.0423	51.18	1.47	1.0641	50.13	0.91	1.0476	50.92	0.71
				Poly(methyl methacrylate-co-styrene)								
1	147,400	0.620	129.40	1.0944	118.24	2.05	1.1056	117.04	1.02	1.0974	117.92	1.19
2	86,400	0.462	98.18	1.0846	90.52	2.38	1.0957	89.61	1.18	1.0875	90.28	1.31
3	64,800	0.395	84.66	1.0799	78.40	2.58	1.0910	77.60	1.28	1.0829	78.19	1.40
4	57,800	0.353	78.50	1.0602	74.04	2.02	1.0711	73.29	1.01	1.0631	73.84	1.00
5	49,000	0.315	71.53	1.0492	68.17	1.77	1.0599	67.48	0.90	1.0521	67.99	0.83

termined by the authors for the six polymer—solvent systems, led to the conclusion that C_6H_6 is a better solvent for PS and PMMA than THF which is a less good solvent for these polymers.

Concerning the copolymer samples it was noticed that both solvents are less good, although it led to the remark that C_6H_6 might be a little better than THF.

The evaluation of the thermodynamic structural parameters of the polymer solutions above was performed applying the expressions (1)...(4). But K_θ and B were calculated applying the linear regression method. As it was already mentioned K_θ is a constant characteristic for the investigated polymer—solvent pair and it defines the dimensions of the macromolecular coil for theta conditions, i.e., in the absence of polymer—solvent interactions. If K_θ is known, the mean square radius of gyration of the unperturbed macromolecular coil, $R_0=(<R^2>_0)^{1/2}$, can be calculated by means of the expression (8).

The mean square radius of gyration of a true chain, $R_G=(<R^2>)^{1/2}$; in a good solvent, was calculated by means of the expression (9).

The hydrodynamic expansion factor, α_η, was calculated by means of the equation (7), and the second virial coefficient applying the equations (10)... (12). The data concerning the thermodynamic parameters are given in Table 3 (C_6H_6 as solvent), and Table 4 (THF as solvent).

According to the theoretical assumptions, the solution viscosity measurements can lead to the estimation of a mean value for the second coefficient $\overline{A}_2$, within the used molecular weight range, which is subsequently used to establish the most suitable equation for the description of the thermodynamic structural behaviour, applying the value of $\overline{A}_2$ obtained from the expression:

$$B=\frac{2\overline{A}_2}{N_m}=3.32\times10^{-24}\overline{A}_2 \cdot \tag{14}$$

Table 5 shows the values calculated for K_θ, $\overline{A}_2$ and B applying equations (2) ... (4) and (14).

From the analyses of K_θ values, listed on Table 5, one can notice that for the homopolymer—solvent system, the Stockmayer—Fixman's and Kurata—Stockmayer—Roig's equations give values in good agreement, while the Schaefgen—Flory's expression for the PS—THF and PMMA—THF systems lead to the close values of ones determined by means of the other two relationships. Therefore, THF is less good than C_6H_6, because that the Schaefgen—Flory's expression according to the assumed premises, is not applicable to the polymer-good solvent systems. The results determined by means of application of this theory get near the true values as the polymer—solvent system is near the theta point.

In the case of the copolymer samples, for both solvents, a good agreement of the K_θ values was obtained applying Kurata—Stockmayer—Roig's and Schaefgen—Flory's expressions. This is a prove that C_6H_6 and THF are less good solvents for the copolymer samples. As a conclusion it results that the hydrodynamic constant value K_θ is larger for the copolymer samples than for any of the investigated homopolymer solutions took into account. The agreement of the B values, determined applying the equations (2) ... (4) as well as the expression (14), lead us to the conclusion that the

Table 5

The Data of K, B and $\overline{A}_2$

Equation	Solvent—polymer system	$10^4 K_\theta$ dL.mol$^{3/2}$. . g$^{-3/2}$	$10^{27} B$ dL.mol^2. . g$^{-1/2}$	$10^4 \overline{A}_2$	$10^{27} B$ dL.mol^2. . g$^{-1/2}$ Eq. (17)
Stockmayer—Fixman	PS—C_6H_6	5.66	2.65	7.46	2.48
	PS—THF	8.96	0.103	2.89	0.96
	PMMA—C_6H_6	6.93	0.014	3.82	0.13
	PMMA—THF	9.69	0.064	1.78	0.59
	Copolymer—C_6H_6	1.08	9.57	2.68	0.89
	Copolymer—THF	1.23	7.71	2.15	0.72
Schaefgen—Flory	PS—C_6H_6	2.15	0.049	10.04	0.45
	PS—THF	8.48	0.0012	1.58	0.52
	PMMA—C_6H_6	3.52	0.0026	4.43	0.15
	PMMA—THF	9.11	0.00079	0.99	0.33
	Copolymer—C_6H_6	10.20	0.0013	1.48	0.49
	Copolymer—THF	11.95	0.0010	1.08	0.36
Kurata—Stockmayer—Roig	PS—C_6H_6	5.06	5.20	14.05	4.81
	PS—THF	8.84	1.46	1.70	0.56
	PMMA—C_6H_6	6.30	2.23	5.63	1.87
	Copolymer—C_6H_6	10.62	1.37	1.07	0.34
	PMMA—THF	9.55	0.91	1.69	0.56
	Copolymer—THF	12.22	1.027	1.14	0.38

applied equation is the most adequate to characterize a certain polymer—solvent system. Therefore, for the PS—C_6H_6 system, one can use both equations (2) and (3), while for the rest of the systems, by the comparison of the B values, the most adequate equation able to characterize the thermodynamic structural point of view is the expression (4).

Mean square end-to-end distance of the macromolecular chain, in theta conditions, can be also calculated when $<R^2>_\theta$ is known, applying the relationship

$$<L^2>_\theta = 6<R^2>_\theta ; \tag{15}$$

if $L_\theta = (<L^2>_\theta)^{1/2}$, then the expression (15) can be written :

$$L_\theta = 6^{1/2} R_{G\theta}. \tag{16}$$

Taking into account the equations (8) and (15), it will result :

$$\frac{L_\theta}{M^{1/2}} = \left(\frac{K_\theta}{\Phi_\theta}\right)^{1/3}. \tag{17}$$

Also, the ratio $L_\theta/M^{1/2}$ represents a characteristic value of the macromolecular dimensions. Table 6 presents the ratio values of $L_\theta/M^{1/2}$ for the studied systems.

According to the previous assumptions concerning the thermodynamic structural characterization of the copolymer—solvent system, it is advisable to apply the Kurata—Stochmayer—Roig's equation and therefore

Table 6

Calculated Values of $L_0/M^{1/2}$

Polymer Equation		Solvent	PS	PMMA	Copolymer
Stockmayer–Fixman	$L_0/M^{1/2} \times 10^{11}$ cm. mol$^{1/2}$.g$^{-1/2}$	Benzene	583	623	343
		THF	678	696	358
Schaefgen–Flory		Benzene	422	497	724
		THF	666	682	764
Kurata–Stockmayer–Roig		Benzene	561	603	734
		THF	675	693	769

the true value of the $L_0/M^{1/2}$ ratio, it will be one determined by the interpretation of the data applying this equation. The value is larger than one corresponding to the homopolymer–solvent systems. This behaviour might be explained by the existance within tne copolymer sample of some repulsive forces between the methyl methacrylate and styrene structural units, that lead to an internal swelling of the macromolecular coil.

5. Conclusions

Samples of polystyrene, poly(methyl methacrylate) and poly(styrene-co-methyl methacrylate), synthetized in the same conditions, both fractionated and nonfractionated, were studied. The styrene content of the copolymer samples, determined by the NMR analysis, was 40...44%.

A fractionation technique for the poly(styrene-co-methyl-methacrylate) samples was developed.

The relationsnip of $[\eta]$ vs. $\bar{M}_n$, for six polymer–solvent systems, were obtained and the calculated constants of the Mark–Houwink's expression were compared with ones quoted by the literature.

Stockmayer–Fixman's, Schaefgen–Flory's and Kurata–Stockmayer–Roig's equations were applied with the aim to thermodynamic characterization of the samples. On the obtained value basis, it was established which of the three equations was the most adequate to characterize from the thermodynamic structural point of view the studied systems.

The calculated values for the unperturbed dimensions of the macromolecules show the existence of some repulsive forces between the structural units contained by the macromolecular chain.

Received, September 18, 1990

Polytechnic Institute, Jassy,
Department of Physical Chemistry
and
Macromolecular Chemistry Institute
„P. Poni", Jassy

REFERENCES

1. Flory P. J., *Principles of Polymer Chemistry*. Vol. **14**, Cornell Univ. Press, Ithaca, New-York, 1953, 613.
2. Huggins L., J. Am. Chem. Soc., **64**, 2 716 (1942).
3. Mead D., Fuoss R., J. Am. Chem. Soc., **64**, 277 (1942).
4. Stockmayer W. H., Fixman M., J. Polymer Sci., Part C, **1**, 137 (1963).
5. Schaefgen J. R., Flory P. J., J. Am. Chem. Soc., **70**, 2 709 (1948).
6. Kurata M., Stockmayer W. H., Roig A., J. Chem. Phys., **53**, 151 (1960).
7. Flory P. J., Makromol. Chem., **98**, 128 (1966).
8. Yamakawa H., *Modern Theory of Polymer Solutions*. Harper and Row, New York, 1971, 419.
9. Brandup I., Immergut E. H., *Polymer Handbook*. Interscience Publishers, New York 1965, IV—13, IV — 26.
10. Ескин В. Е., *Рассеяние света растворами полимеров*. Изд. Наука, М., 1973, 353.
11. Miyaki Y., Einaga Y., Tujity H., Fukuda M., Macromolecules, **13**, 588 (1980).
12. Flory P. J., Fox T. G., J. Phys. Colloid. Chem., **53**, 21 (1949).
13. Aelenei N., Eur. Polym. J., 533 (1981).
14. Brandup I., Immergut E. H., *Polymer Handbook*. 2-nd Ed., J. Wiley, New York, 1974.
15. Spychaj T., Lath D., Berek D., Polymer, **20**, *4* 437 (1979).
16. Stickler M., Pauke D., Wunderlich W., Makromol. Chem., *188*, 2651 (1987)

STUDIUL POLI(METILMETACRILAT-co-STIREN) ȘI A HOMOPOLIMERILOR SĂI ÎN SOLUȚIE

(Rezumat)

S-a studiat comportarea în soluție a copolimerului poli(metilmetacrilat-co-stiren) și a homopolimerilor săi preparați în aceleași condiții. Pe baza măsurătorilor de presiune osmotică și a măsurătorilor viscozimetrice s-au determinat masele molare medii numerice și viscozitatea intrinsecă cu ajutorul cărora s-au evaluat coeficienții ecuației Mark—Houwink și para-.metrii structural-termodinamici ai macromoleculelor în soluție de benzen și tetrahidrofuran.

BULETINUL INSTITUTULUI POLITEHNIC DIN IAȘI
Tomul XXXVI (XL), Fasc. 3—4, 1990
Secția II
CHIMIE ȘI INGINERIE CHIMICĂ

D. C. 535.243 ; 661.898 ; 547.466.2

SPECTROPHOTOMETRIC STUDY OF THE EQUILIBRIA IN THE SYSTEM $K_2[PdCl_4]$ — DL NOR-LEUCINE

BY

OLGA VICOL, N. FOCA and LIGIA ALDINI

1. Introduction

The capability of transitional metals, found in different oxidation states, to form complex combinations with ligands containing donor atoms, such as nitrogen, sulphur, oxygen, e.a., is well-known.

The literature offers many examples of complex combinations of some metals from the platinum family with ligands such as amines, olefines, aminoacids, etc.

A special mention deserve complex combinations of Pd(II) and Pt(II) with aminoacids. Many of them present both theoretical and special applied interest (e. g., biology, medicine, biocatalysis, etc.).

It is known that simple and complex salts of Pd(II), respectively $PdCl_2$ and $K_2[PdCl_4]$, react in neutral or weak alkaline medium with the majority of the aminoacids, generating complexes having the combination ratio of metal to ligand equal to 1 : 1 or 1 : 2. In this context we must also remark the formation of some complexes, of the V a u q e l i n type, specific to Pt(II) and Pd(II) [1]..,[4].

In the present paper, the interaction between $K_2[PdCl_4]$ and DL nor-leucine in solution, was investigated, in order to both establish the metal — ligand combination ratio and to determine the stability constants of the resulted complexes.

2. Experimental Part

The study of the interaction of Pd (II) with DL nor - leucine was spectrophotometrically effected using a Spekol apparatus (G.D.R.).

The reaction of Pd(II) with DL nor-leucine in aqueous solution is a fast one, resultig in the formation of some precipitates, which generally are hard-soluble in water or most organic solvents. For this reason, in the present study, the generator of Pd(II) complexes was approached through a complex species of $K_2[PdCl_4]$. The use of $PdCl_2$ is not recommended, as this combination is stable in strong acid medium (pH <2), where is to be found as $H_2[PdCl_4]$. The strong acid feature of the medium influences in a negative manner its reaction with DL nor-leucine.

The interaction of this two partners, quoted above, is easier in neutral or weak alkaline solutions, due to the amphionic structure of the aminoacids, which in the above mentioned conditions behave themselves as buffer solutions.

After the interaction of $K_2[PdCl_4]$ with Dl nor-leucine the *M*-ligand combination ratio was determined. Also, the evolution in time of the system was studied and the formation constants of the studied complexes were calculated.

3. Results and Discussions

In the spectrophotometric study of the system $K_2[PdCl_4]$ with DL nor-leucine, we worked with solutions of $K_2[PdCl_4]$ in a mixture of solvents (DMF $-H_2O$) and leucine in aqueous alkaline solutions (H_2O + KOH).

Taking into account that $K_2[PdCl_4]$ is water-soluble and that a decomposition takes place during the solving process, produced by a hydrolysis one, in our study this complex was dissolved in a mixture of 80...85% DMF and 15...20% H_2O.

The solutions we obtained are long-term stable. The ligand solution was prepared in water with an addition of KOH 1N.

The initial solutions of $K_2[PdCl_4]$ and DL nor-leucine had equal concentrations of $1 \cdot 10^{-3}$ moles$\cdot 1^{-1}$.

Later, it was established that the separated combinations in solid state are DMF-soluble and water-insoluble. This was taken into consideration in deriving the electronic spectra choosing as solvents DMF for $M : L = 1 : 1$ and $1 : 2$ and distillated water for $K_2[PdCl_4]$ and DL nor-leucine.

The UV-visible spectra of the above mentioned species were recorded using a Specord (G.D.R.) spectrophotometer and are illustrated in Figs. 1 and 2.

The leucine, as expected, does not show absorbtion bands in the visible range. For $K_2[PdCl]_4$ a well-defined absorbtion band in the visible range at $\lambda = 435$ nm was evidenced.

The UV-visible spectra of Pd : leucine 1 : 1 and 1 : 2 complexes in a mixture of DMF — H_2O were also recorded. It is to mention in that in the combination ratio $1M : 2L$ *cis—trans* isomers were evidenced.

The mentioned complexes show absorbtion bands in the transition range between UV and visible and also a well-defined maximum at 380 nm (Fig. 3).

3.1. Determination of Combination Ratio Pd(II)— DL Nor-leucine

The combination ratio $K_2[PdCl_4]$: DL nor-leucine in a mixture of DMF — H_2O solvents was determined with a Spekol apparatus, choosing the best defined absorbtion maximum, respectively $\lambda = 380$ nm.

The determination of the combination ratio was effected using some spectrophotometric methods. The values of the absorbance were read at the moment of mixing the reactives and later, at time intervals of 15, 30, 45 min. and after 24 hours.

The molar ratio method [5] was used in two variants : a) keeping constant the metal concentration and varying the ligand concentration ; b) varying the metal concentration and keeping constant the ligand concentration.

The obtained results are presented in Figs. 4 and 5. From the analysis of the data in these figures the same combination ratio of 1 : 1 results.

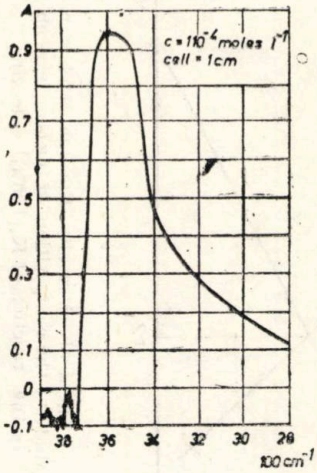

Fig. 1. — Absorbtion spectrum of leucine in UV—VIS: solvent : DMF ; $C = 1 \times 10^{-4}$ mol·l^{-1} ; volume = 1 cm^3.

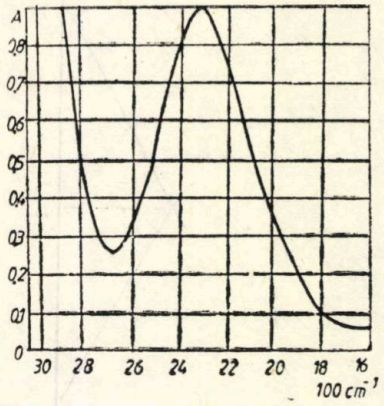

Fig. 2. — Absorbtion spectrum in visible range of $K_2[PdCl_4[$ in aqueous solution : $C = 1 \times 10^{-3}$ mol · l^{-1} ; volume = 1 cm^3.

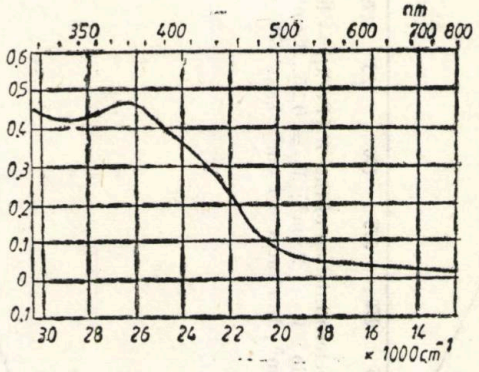

Fig. 3. — Electronic spectra of some Pd(II) — — leucine complexes ($1M$: $1L$; $1M$: $2L$).

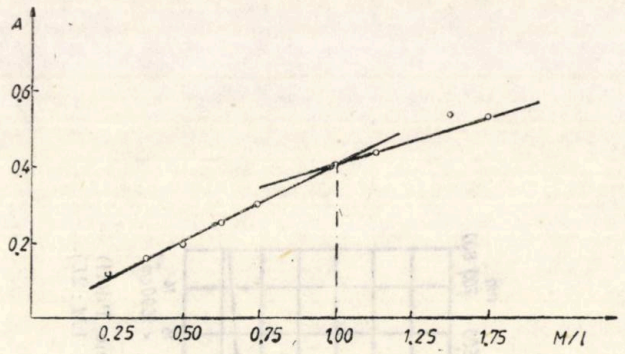

Fig. 4. — Determiniation of the $K_2[PdCl_4]$ — leucine combination ratio : $V_L = 2$ cm^3 ; $V_M = 0.25...3$ cm^3 ; $V_{final} = 5$ cm^3 ; thickness = 1 cm^3 ; $\lambda_{max} = 380$ nm.

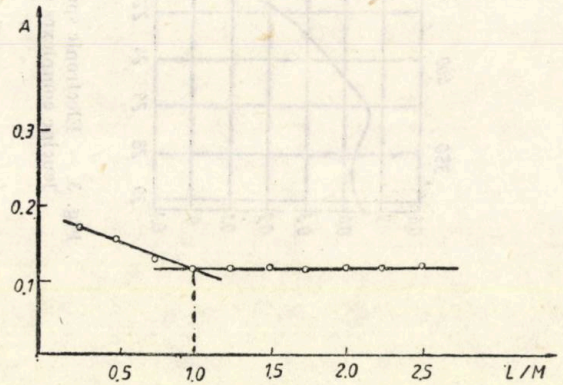

Fig. 5 — Determination of the $K_2[PdCl_4]$ — leucine combination ratio : $V_L = 0.25..3$ cm^3 : $V_M = 1$ cm^3 ; thickness = 1 cm^3 ; $\lambda_{max} = 380$ nm^3.

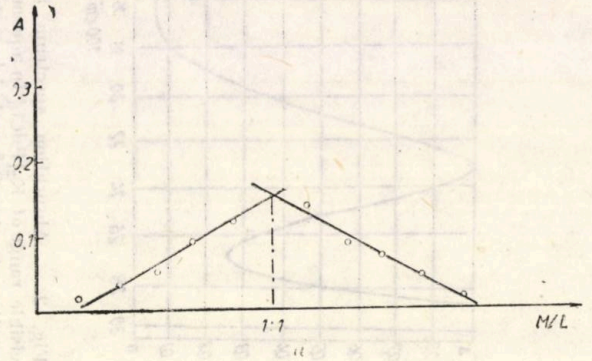

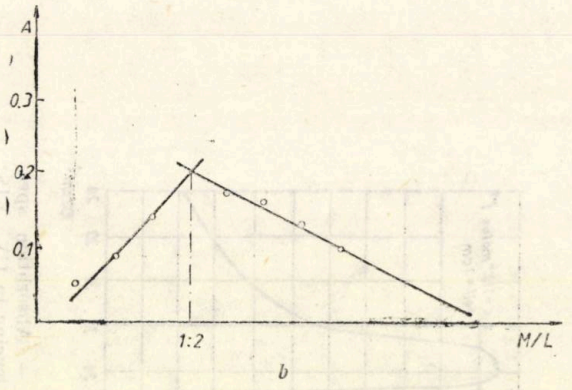

Fig. 6 — The derived results through J o b 's method in the study of the composition of the complexes obtained in the reaction of $K_2[PdCl_4]$ — leucine.

The combination ratio $K_2[PdCl_4]$ — leucine was also determined with the continuous variations method [6], where the M/L ratio varies continously, but $V_M + V_L = \text{const.}$ (5 cm^3 in our case).

As $K_2[PdCl_4]$ has a sharp maximum in the visible range and its absorbtion band in this range overlaps with that of the complexes in solution, the absorbance was determined using as a witness the mixture $H_2O - K_2[PdCl_4]$ in DMF, where $C_{K_2[PdCl_4]}$ was equal to the value in the complex solution.

Thus, we eliminated the absorbance excess due to $K_2[PdCl_4]$. The results derived through this method are given in Fig. 6 *a* and *b*.

Based upon the results derived in the present study, we concluded that the combination ratios of Pd(II) — DL nor-leucine are 1 : 1 and 1 : 2.

The spectrophotometric study of the equilibrium in the $K_2[PdCl_4]$ — DL nor-leucine system confirms the results we obtained in a previous paper [7], referring to the synthesis of some Pd(II) — leucine complexes.

3.2. Determiniation of Formation Constants

The formation constants for Pd — leucine $1M : 1L$ and $1M : 2L$ complexes were calculated using the spectrophotometric data.

For the complex 1 : 1, the Turner—Anderson method [8] was applied, while for the 1 : 2 complex, the method of Edmonds and Birnbaum [19] was used.

The values we obtained are :

$$K_1\ (1M : 1L) = 2.38 \times 10^{12}\ \text{l} \cdot \text{mol}\ ;\ K\ (1M : 2L) = 3.45 \times 10^{16}\ \text{l} \cdot \text{mol}^{-2}.$$

The values of the formation constants show that both complexes resulted from the interaction $K_2[PdCl_4]$ with DL nor-leucine (1 : 1) and 1 : 2) have a great stability. This means that the equilibria in solution are shifted to the right (complex).

Received, April 10, 1990

Polytechnic Institute, Jassy,
Department of Analytical Chemistry

REFERENCES

1. Вольштейн Л. М., ЖНХ, **X**, 542 (1965).
2. Hooper R. J., Lane T. L., Inorg. Chem., **III**, 11, 1 568 (1964).
3. Vicol O., An. șt. Univ. „Al. I. Cuza", Iași **XVI**, s. I., (1970).
4. Vicol O., An. șt. Univ. „Al. I. Cuza", Iași **XIX**, s. I., 21 (1973) ; Ibid., **XXV**, 309— 315 (1979).
5. Job A. Jones A., Ind. Eng. Chem. Anal., **16**, 111 (1944).
6. Job A., Ann. Chem., 113 (1928).
7. Vicol O., Palie M., Bul. Inst. polit., Iași, **XXXII (XXXVI)**, *1—4*, s. II, 37 (1986).
8. Turner S. E., Anderson R. J., J. Amer. Chem. Soc., **71**, 912 (1949).
9. Edmonds N. S. Birnbaum N. J., Amer. Chem. Soc., **63**, 1 471 (1941).

STUDIUL SPECTROFOTOMETRIC AL ECHILIBRELOR DIN SISTEMUL $K_2[PdCl_4]$— DL NOR LEUCINĂ

(Rezumat)

Se prezintă un studiu spectrofotometric al echilibrelor în sistemul Pd(II) — DL nor leucină. S-au determinat raportul de combinare metal — ligand și s-au calculat constantele de formare ale complecșilor.

BULETINUL INSTITUTULUI POLITEHNIC DIN IAȘI
Tomul XXXVI (XL), Fasc. 3—4, 1990
Secția II
CHIMIE ȘI INGINERIE CHIMICĂ

D. C. 532 ; 547.213 ; 547.412.1

STUDY OF THE INTRINSIC PROPERTIES OF VISCOUS FLOW IN THE 1,2-PROPANDIOL (1,2-PD)-METHANOL (MeOH) SYSTEM

BY

GH. IONESCU, DOINA HRIȚCU and IONEL MARCEL POPA

1. Introduction

The parameters characterizing viscous flow represent indispensable characteristics for solutions, in various physical and chemical processes in which they are involved.

Thus, the 1, 2-propandiol (1, 2-PD)—methanol (MeOH) solution is involved, as a practical system, in polyesteric fiber industry, such as the process of synthesis and subsequent recovery of some components. Establishment of the flow, stirring, rectification regimes require thorough knowledge of the parameters of viscous flow.

In this respect, the present paper aims at determining the viscosity of the above mentioned solution, for several industrial-type concentrations and for some temperature values lower than the normal one of MeOH boiling. Starting from such experimental data the following steps have been performed : checking of the Guzmán—Andrade equation applicability, establishment of the values of E_{vis} and B parameters from this equation, the value of the activation parameters of the viscous flow, expressed by $\Delta H_m^{\neq}$, $\Delta S_m^{\neq}$ and $\Delta G_m^{\neq}$ and the value of the potential component of the internal energy $(\partial U_m/\partial V_m)_T$.

2. Reactives and Equipments

The 1, 2 - PD MeOH and ethyleneglycol (EG) employed have been of p. a. purity and anhydrous versus the Karl-Fischer reactive. Ostwald-type viscosimeter was employed, equipped with capillary tube assuring flow times of minimum 200 sec., the correction necessary for the perturbation of the laminar flow at the capillary's ends being thus eliminated. The thermostating temperature has been maintained with a degree of precision of 0.1°C. The pycnometer, equipped with an internal thermometer, has been thermostated under the same conditions. Solution preparation employed weighings on an analytical balance having a 10^{-4} precision.

3. Measurement Methods and Experimental Data Obtained

Viscosity has been determined as a relative value employing 1, 2 - PD as reference liquid. As, in literature [1] dynamic viscosity of 1, 2 - PD is

given only at one temperature value from the working domain, determination of this parameter for other values of temperature too became necessary. For such determinations, the reference liquid selected was EG, for which information of this type already exist [2]...[3]; starting from such data, the equation of the $\eta = \eta(T)$ function has been established, in ln η...$10^3/T$ coordinates:

$$\ln\eta_{EG} = -4.0724 \pm 1.5826 \quad (10^3/T)\,; \quad (\eta_{EG}, [\text{cP}]). \tag{1}$$

1, 2-PD viscosity has been calculated from the equation:

$$\eta_{PD} = \frac{\eta_{EG}\tau_{PD}\rho_{PD}}{\eta_{EG}\rho_{EG}}, \tag{2}$$

while ρ_{EG} and ρ_{PD} values have been estimated from experimental relations of the form:

$$\rho_{EG} = 1.1277 - 7.0433 \times 10^{-4}t,$$
$$\rho_{PD} = 1.0520 - 7.4233 \times 10^{-4}t \quad (\rho_{EG}, \rho_{PD}, [\text{g.cm}^{-3}];\ t, [^\circ\text{C}]). \tag{3}$$

The deduction of such relations required previous establishment of the dependence of the pycnometer volume vs. temperature, by means of water, for which there exist detailed data upon density's variation w.r.t t parameter [4]. The equation to be employed has the form:

$$V = 25.3\,668 \pm 1.896 \times 10^{-4}t \quad (V, [\text{cm}^3];\ t, [^\circ\text{C}]). \tag{4}$$

For 1,2-PD—MeOH solutions, viscosity has been calculated with the relation:

$$\eta = \frac{\eta_{PD}\tau_{\rho}}{\tau_{PD}\rho_{PD}}. \tag{5}$$

The flow times for (τ) solutions and for 1, 2—PD (τ_{PD}), as well as the solutions' densities constituted the primary data, measured during the experiments performed.

Table 1 gives the experimental data on the solutions' molar fractions their viscosities and working temperatures.

Table 1

Viscosity Values of 1, 2-PD-MeOH Solutions

x_{PD} \ t, [°C]	20	25	30	37	45
0.4902	7.8649	7.1116	5.4141	4.2136	3.1445
0.5508	10.0488	9.0246	6.8589	5.2938	3.9644
0.6920	18.2458	15.9023	11.7399	8.7593	6.1602
0.8502	36.7826	30.4540	21.7498	15.2189	10.1760
1	65.6337	54.3565	37.4949	25.3246	16.7654

4. Checking of the Guzmán—Andrade Equation Applicability and Determination of the E_{vis} and B Parameters

For electrolitically non-dissociable liquids, as well as for their solutions, the dependence of viscosity vs. temperature is expressed, in the majority of cases, by the semi-empiric equation proposed by Guzmán and Andrade [5], [6]:

$$\ln \eta = \ln B + E_{vis}/RT, \tag{6}$$

where: B — viscosity value for $T \to \infty$, E_{vis} energy barrier at flow, known as molar activation energy of the viscous flow.

Table 2

Values of the $\ln \eta ... 10^3\ T^{-1}$ *Coordinates*

$10^3\ T^{-1}$ K^{-1}	x_{PD}				
	0.4902	0.5508	0.6920	0.8502	1
3.4112	2.0624	2.3074	2.0939	3.6050	4.2141
3.3540	1.8517	2.1999	2.7664	3.4162	3.9955
3.2987	1.6890	1.9255	2.4269	3.0796	3.6242
3.2242	1.4383	1.6665	2.1701	2.7225	3.2317
3.1432	1.1457	1.3773	1.8181	2.3200	2.8193

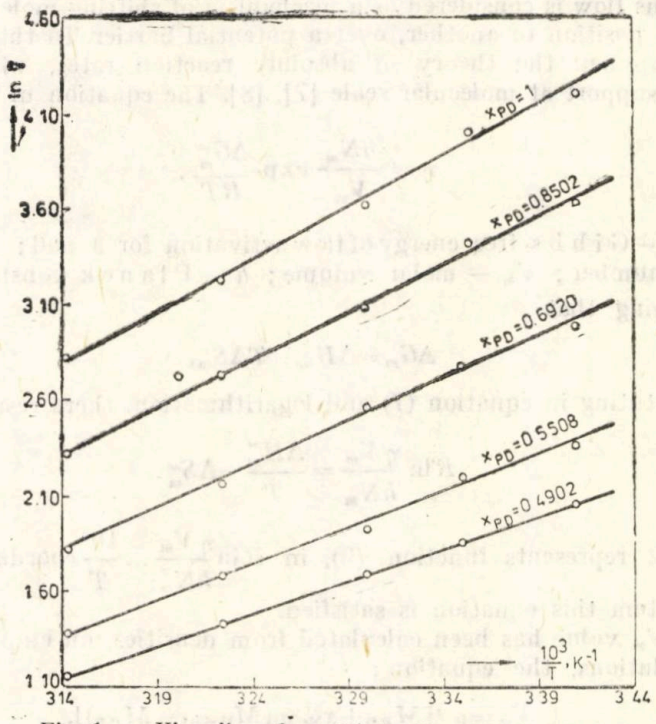

Fig. 1. — Viscosity values of 1, 2 - PD—MeOH solutions.

Table 3

Values of the Guzmán—Andrade Equation Parameters

x_{PD}	$10^4 E_{vis}$, [J/mol]	$10^5 B$, [cP]
0.4029	2.784	9.420
0.5508	2.939	5.925
0.6920	3.658	0.605
0.8502	4.235	0.110
1	4.413	0.093

Eq. (6), having an experimental origin, has to be checked for demonstrating its applicability in the case of the investigated solution. In this respect, experimental data from Table 1 have been processed in $\ln\eta$ vs. $1/T$ coordinates, in which the equation represents, after logarithmation, a linear function. Satisfaction of this condition indicates the equation applicability. Table 2 records the numerical values of the above mentioned coordinates.

The diagram plotted in Fig. 1 evidences that the equation is satisfied in the concentration and temperature domains employed in the experiment.

The parameters of these linear functions, E_{vis} and B, are given in Table 3.

5. Calculation of Viscous Flow Parameters According to Eyring

Viscous flow is considered as a mechanism of shifting molecules from an equilibrium position to another, over a potential barrier. To this mechanism. Eyring applied the theory of absolute reaction rates, with the same theoretical support at molecular scale [7], [8]. The equation of such phenomenon is :

$$\eta = \frac{hN_m}{V_m} \exp \frac{\Delta G_m^{\neq}}{RT}, \tag{7}$$

with : $\Delta G_m^{\neq}$ — Gibbs free energy of flow activation for a mol; N_m — Avogadro's number; V_m — molar volume; h — Planck constant.

Knowing that

$$\Delta G_m = \Delta H_m - T\Delta S_m,$$

after substituting in equation (7) and logarithmation, there results :

$$R \ln \frac{\eta V_m}{hN_m} = \frac{\Delta H_m^{\neq}}{T} - \Delta S_m^{\neq}. \tag{9}$$

Fig. 2 represents function (9), in $R \ln \frac{\eta V_m}{hN_m^{\neq}} \ldots \frac{10^3}{T}$ coordinates; for the studied system this equation is satisfied.

The V_m value has been calculated from densities, on employing, in the case of solutions, the equation :

$$V_m = \rho^{-1}[M_{PD} + x_{MeOH}(M_{MeOH} - M_{PD})], \tag{10}$$

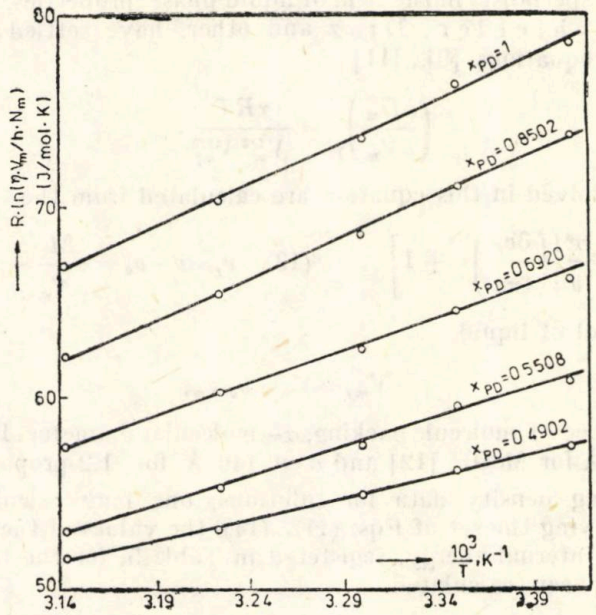

Fig. 2. — Graphical checking of Eyring's equation applicability.

Table 4

Values of Eyring's Parameters

x_{PD}	$\Delta H_m^{\neq}$, [J/mol]	$\Delta S_m^{\neq}$, J/mol.K	$\Delta G_m^{\neq}$, [J/mol]
0.4902	24.138	24.436	16.734
0.6920	30.000	41.532	17.416
0.6920	33.333	48.010	18.786
0.8502	41.379	68.153	20.729
1	44.118	72.056	22.285

where : M_{PD} and M_{MeOH} —molar weights of the components ; ρ — solutions' density.

Calculation of the straight lines' parameters and application of Eq. (8) led to drawing up Table 4, containing the Eyring's parameters.

6. Determination of the Potential Component of the Internal Energy

Generally, liquids may be treated according to the following physical model : the molecules having a volume of their own, v_0 move, within a free volume, v_f, in the field potential energy created by the intermolecular forces. Consequently, potential energy constitutes an intrinsic value of a liquid, belonging to its internal energy and being identified with the potential component, $(\partial U_m/\partial V_m)_T$. 1

Reputed specialists in the field of liquid phase properties, such as G l a s t o n e, H i r s c h f e l d e r, D i a z and other, have settled for $(\partial U_m/\partial V_m)_T$ the following equations [9]...[11]:

$$\left(\frac{\partial U_m}{\partial V_m}\right)_T = \frac{\alpha RT}{V_m^{1/3} V_{mf}^{1/3}}. \tag{11}$$

The values involved in this equation are calculated from the relations :

$$\alpha = \frac{\sigma^3}{v}\left[\left(\frac{3v_f}{4\pi\sigma^3}\right)^{1/3} + 1\right], \tag{12}$$

$$v_f = v - v_0 = \frac{M}{\rho N_m} - \frac{\pi\sigma^3}{6}. \tag{13}$$

For 1 mol of liquid,

$$V_{mf} = V_m - v_0 N_m, \tag{14}$$

where: α — degree of molecule packing, σ — molecular diameter. In our particular case, $\sigma = 3.76$ Å for MeOH [12] and $\sigma = 6.146$ Å for 1,2-propandiol [13],[14].

Employing density data for solutions, one may calculate $V_m = M/\rho$. Further on, having the set of Eqs. (11)...(14), the values of the potential component of the internal energy, registered in Table 5, for the temperature $t = 30°C$, have been calculated.

Table 5

Values of the $10^6(\partial U_m/\partial V_m)_T$, [J/mol], *Parameter*

x_{PD}	0.4902	0.5508	0.6920	0.8502	1
$(\partial U_m/\partial V_m)_T$	230.2	234.7	248.6	280.2	417.0

7. Conclusions

η and E_{vis} values, as well as the activation parameters of the viscous flow, are determinated numerically by the intensity of the intermolecular forces. In the system under study, i.e., 1, 2-PD — MeOH, there appear, additionally, hydrogen bonds whose number depends on the concentration of the OH grups.

1. Viscosity and the activation energy of the viscous flow, E_{vis}, increase with increasing the concentration of 1,2-PD, following the increase of the OH groups concentration.

2. $\Delta G_m^{\neq}$ and $\Delta H_m^{\neq}$ have positive values, as the occurrence of the activated state involve breaking of hydrogen bonds.

3. The $\Delta H_m^{\neq}$ and $\Delta S_m^{\neq}$ values are high, with solutions formed from compounds possessing OH-groups, as compared with solutions having the same

concentration, yet made up of compounds that do not form stable molecular associations.

4. $\Delta G_m^{\neq}$ evidences a slower increase, as compared with the other values $\Delta H_m^{\neq}$ and $\Delta S_m^{\neq}$, as a consequence of the reciprocal compensation of the terms with opposite signs, $\Delta H_{ii}^{\neq}$ and $T\Delta S_m^{\neq}$.

5. The $(\partial U_m/\partial V_m)_T$ parameter, having high values, evidences the existence of intense intermolecular forces, consequently, of the hydrogen bonds. The sensible dependence vs. the 1, 2-PD concentration also supports this idea.

6. With the system under study, on employing the above mentioned concentrations and domain of temperature, the Guzmán—Andrade and Eyring equations may be applied.

Received, March 28, 1990

Polytechnic Institute, Jassy,
Department of Physical Chemistry

REFERENCES

1. Weissberger A., *Organic Solvents.* Vol. **VII**, Intersci. Publ. Inc., New York, 1955.
2. Landolt-Börnstein, *Eigenschaften der Materie in ihren Aggregatzuständen.* **5.** Teil, Bandteil *a*, *Transportphänomene.* **I** (*Viskosität und Diffusion*). Springer Verlag, Berlin—Heidelberg—New York, 1969.
3. Hriţcu D., Ionescu Gh., Popa I. M., *Study of the Intrinsic Properties of Viscous Flow in the Ethylene Glycol—Methanol System* (in press).
4. * * * *Manualul Inginerului Chimist.* Vol. **2**, Ed. Tehn., Bucureşti, 1956.
5. De Guzmán J., Anales Soc. Esp. Fiz. Quim. **11**, 353 (1913).
6. De C. Andrade E. N., Phil. Mag., **17**, 497, 698 (1934).
7. Eyring H., J. Chem. Phys., **4**, 283 (1936).
8. Eyring H., Ewell R. H., J. Chem. Phys., **5**, 726 (1937).
9. Glastone S., *Theoretical Chemistry.* Van Nostrand, Princeton, 1966, Chap. IX.
10. Hirschfelder J. O., Curtis C. F., Bird R. B., *Molecular Theory of Gases and Liquids.* John Wiley, New York, 1954, Chap. 4...6.
11. Diaz M., Roig A., *Quimica Fisica.* Ed. Alhambra, Madrid, 1975, Chap. 16.
12 Мищенко К. П., *Краткий курс справочник физико-химических величин.* Изд. Химия, Ленинград 1967.
13. Bastiansen O., Acta Chimica Scandinavica, **2**, 415 (1949).
14. * * * Acta Cryst., **3**, 46 (1950).

STUDIUL PROPRIETĂŢILOR INTRINSECI ALE CURGERII VÎSCOASE ÎN SISTEMUL 1,2-PROPANDIOL (1,2-PD)—METANOL (MeOH)

(Rezumat)

Cunoaşterea parametrilor intinseci pentru curgerea viscoasă prezintă importanţă deosebită în studiul fizico-chimic al soluţiilor. În această ordine de idei s-a determinat, ca date primare, viscozitatea soluţiei de 1, 2-PD—MeOH, la diverse concentraţii şi temperaturi de uz practic. Asemenea date au fost apoi interpretate în vederea verificării ecuaţiilor Guzmán—Andrade şi Eyring. Calculul parametrilor acestor ecuaţii, liniarizate, au permis determinarea numerică a mărimilor caracteristice curgerii viscoase : E_{vis}, B, $\Delta H_m^{\neq}$, $\Delta S_m^{\neq}$ şi $\Delta G_m^{\neq}$, precum şi a componentei potenţiale a energiei interne, $(\partial U_m/\partial V_m)_T$.

BULETINUL INSTITUTULUI POLITEHNIC DIN IAŞI
Tomul XXXVI (XL), Fasc. 3—4, 1990
Secţia II
CHIMIE ŞI INGINERIE CHIMICĂ

D. C. 545.844 ; 547.431.3 ; 547.426.2

ANALYSIS OF PHENYL-GLYCIDYL-ETHER BY HIGH-PRESSURE LIQUID CHROMATOGRAPHY

BY

IONEL MARCEL POPA and AL. SAVIN

1. Introduction

The phenyl-glycidyl-ether (PGE) is used in the following purposes : decrease in the concentration of the carboxyl end groups in the technical polyester fibres [1], [2], obtainment of some thermal agents resistant to high temperatures [3], and of lubricants for refrigerating machines [4].

The synthesis of PGE is based on the addition of phenol to epichlorhydrin, followed by the dehydrohalogenation of halohydrin in alkali medium.

The reaction results in the formation of a complex mixture of products from which the PGE can be separated by distillation under vacuum. The crude product submitted to distillation also contains traces of phenol, PHPC, DPP. The purity of PGE for polyester fibres must be no less than 99%.

The methods based on the epoxy group dosing cannot be applied for analysis of PGE resulted by synthesis due to the interferences with the epoxy groups in epichlorhydrin.

Besides, the titrimetric methods of epoxy group dosing are rather laborious [5]. On the other hand, the gas-phase chromatography cannot be applied in PGE analysis due to the complexity of the mixture containing products of different high boiling points [6].

In what follows the substances accompanying PGE in the crude product as well in that resulting by distillation under vacuum were determined by high-pressure liquid chromatography.

2. Materials and Method

The following materials were used : a) epichlorhydrin, dried on $CaCl_2$ and distilled under vacuum, $n^{20}=1.4380$; b) phenol , distilled under vacuum, m. p.=40.8°C ; c) phenyl-glycidyl-ether, dried on $CaCl_2$ and distilled under vacuum, b. p.=80°C/1 mm Hg, $n^{20}=1.5302$; d) 3-phenoxy-2-hidroxypropyl cloride, dried on $CaCl_2$ and distilled under vacuum, b. p.=112°C/1 mm Hg ; e) 1, 3-diphenoxy-2-propanol, recristallized from methanol, m. p.=81°C ; f) perchloric acid, Merck reagent ; g) methanol, purified by the method given, in [8].

The samples of the reaction mixture and of the purified product were solved in methanol (1 mg/ml conc.) and then analysed by high-pressure liquid chromatography, on a Varian Model 5 020 chromatograph under the following conditions : a) column : Micro-Pak, CN—10.250 ×4.7 mm ; b) mobile phase : mixture methanol—water brought to pH =2.5 by perchloric acid, under iso-

cratic conditions or with solvent gradient ; c) flow rate : 0.6 mL/min. ; column temperature 40°C ; d) detector : Varichrom UV—VIS, sensibility=0.5 AUFS ; e) pressure : 68 atm ; f) volum of injected sample : 10 μL.

3. Results and Discussions

The following reactions take place during the process of PGE synthesis :

a) Addition of phenol to the oxiranic ring in epichlorhydrin :

(1) 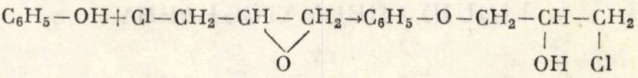

(I) (II) (III)

b) Elimination of hidrogen chloride from 1, 3-phenoxy-2-hydroxypropyl chloride and PGE formation :

2) 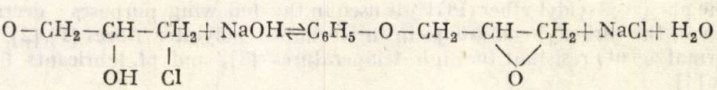

(III) (IV)

c) Addition of phenol to PGE and DPP formation :

(3) 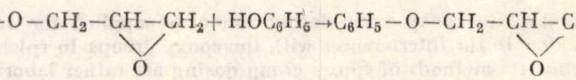

(IV) (V)

The organic mixture submitted to distillation contains all compounds involved in the reactions (1)...(3).

The PGE solved in hexane shows maxima in the UV spectrum at 220 nm (ε=8 128.3) ; 267 nm and 277 nm (ε=1 258.9) and 271 nm (ε=1 548.8) [7].

The PGE may be identified by means of two wavelengths of the detector namely at 220 and 271 nm, where the extinctions shows the highest values. For the detection the wavelength of 271 nm was chosen where all the compounds in the reaction mixture show absorptions.

The separation under isocratic conditions of PGE in the other products, by using a mixture methanol/water, 80/20, as a mobile phase, is not possible (Fig. 1). Under the working conditions with solvent gradient at $t=0$ water (pH=2.5)/methanol=70/30 (by vol.) and after 15 min. water (pH =2.5)/methanol =20/80 (by vol.), the PGE is well separated from the other compounds (Fig. 2).

By analysing mixture of different contents of the products (I)...(V) the following retention times were settled : phenol : 6.2 min.; PGE : 7.8 min. ; PHPC : 10.9 min. ; DPP : 11.9 min. (Fig. 3).

The chromatographic analysis of the product resulting by distillation under vacuum (130°C/5 mm Hg) did not reveal other products in PGE (Fig. 4).

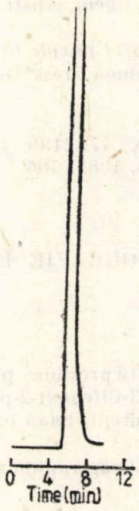

Fig. 1. — The chromatogram of reaction mixture under isocratic condition (mobile phase methanol/water= 80/20).

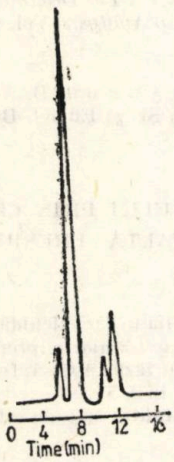

Fig. 2. — The chromatogram of reaction mixture by working with solvent gradient: (mobile phase at $t = 0$ min., water (pH=2.5)/methanol=70/30 (by vol.) and after 15 min. water (pH=2.5)/methanol=20/80 (by vol.)).

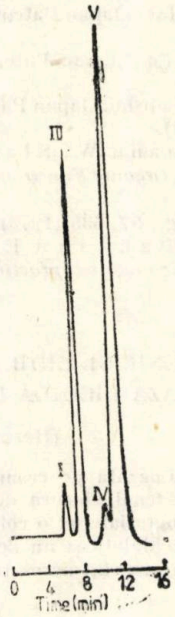

Fig. 3. —The chromatogram of (I), (III), (IV), (V) compounds in sinthetic mixture by working with solvent gradient ; retention times : (I) — 6.2 min. ; (III)— 7.8 min. ; (IV)— 10.9 min. ; (V) — 11.9 min.

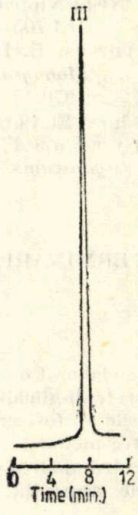

Fig. 4.— The chromatogram of the product resulting by distillation under vacuum (130°C/5 mm Hg), by working with solvent gradient ; retention time : (III) — 7.8 min.

4. Conclusions

1. The PGE obtained by synthesis may be separated from the accompanying products (phenol, PHPC, DPP) by high-pressure liquid chromatography.

2. The analysis of the sample may be performed without any chemical modification by working with solvent gradient ; the necessary time is about 15 min.

3. The good separation of PGE makes its quantitative analysis possible.

Received, March 14, 1990

Polytechnic Institute, Jassy,
Department of Physical Chemistry

REFERENCES

1. * * * Asahi Chemical Industry Co., Japan Patent *60 119 216*, June 26, 1985; Chem. Abstr., **103**, 216 818 (1985).
2. * * * Toray Industries Inc., Japan Patent *57161 124*, Oct. 4, 1982; Chem. Abstr., **98**, 90947 (1983).
3. * * * Matsushita Reiki Co., Japan Patent, *59 157 170*, Sept. 6, 1984 ; Chem. Abstr., **102**, 27 406 (1985)
4. * * * Nishi Nippon Tsusansho, Japan Patent, *59 102 990*, June 14, 1984; Chem. Abstr., **101**, 154 705 (1984).
5. Dobinson B. Hofmann W., Stark B. P., *The Determination of Epoxide Groups. Monographs in Organic Functional Group Analysis.* Vol. **1**, Pergamon Press, Oxford, 1970.
6. Fischer E., Chem.-Zig., **97**, 635 (1973).
7. Чимутова Г. А., Файзлин Е. М., Кузина В. А., ЖФХ, **47**, 2139 (1973).
8. * * * *Organicum—Chimie organică practică.* Ed. Șt. și Enciclopedică, București, 1982, 706.

DETERMINAREA FENIL-GLICIDIL-ETERULUI PRIN CROMATOGRAFIE ÎN FAZA LICHIDĂ DE ÎNALTĂ PRESIUNE

(Rezumat)

S-a elaborat o metodă bazată pe cromatografia în fază lichidă de înaltă presiune, pentru amestecuri fenil-glicidil-eter, fenol, clorură de 3-fenoxi-2-hidroxipropil, 1, 3-difenoxi-2-propanol. Probele au fost cromatografiate pe o coloană în fază inversă, folosind drept bază mobilă un amestec metanol—apă acidulată și un detector în UV.

Pentru analiza unei probe sînt necesare 15 minute. Metoda este specifică, rapidă și suficient de sensibilă.

BULETINUL INSTITUTULUI POLITEHNIC DIN IAŞI
Tomul XXXVI (XL), Fasc. 3—4, 1990
Secţia II
CHIMIE ŞI INGINERIE CHIMICĂ

D. C. 547.746.6 ; 542.956

KINETICS OF THE REACTION OF MONOMETHYLADIPATE SYNTHESIS

BY

NATALIA HURDUC, LUCIA ODOCHIAN, C. LUCA, ELENA MIHAI, ŞT. UNGUREANU and ELENA IONESCU

1. Introduction

Recent investigations performed confer a significat importance to some esters of the adipic acid, employed as raw material in the synthesis of sebacic acid, for the production of synthetic fibres or platifiers in plastics industry.

The literature in the field discusses several methods to be applied in the synthesis of monomethyladipate [1]...[4], known as having the disadvantage of employing corrosive catalysts ; that is why, we proposed the utilization of the *p*-toluenesulfonic acid [5].

The aim of these paper is to establish kinetic factors such as : molar ratio of the reactants, temperature, catalyst concentration and duration of the reaction, corresponding to a maximum conversion degree as well as to estimate the fundamental kinetic parameters, by computer processing of the experimental data.

2. Experimental

Monomethyladipate synthesis was performed in melt, in a laboratory installation which permit to maintain the isothermal conditions and measurement of the reaction mixture temperature. It consists of a three neck bulb (balloon flask) equipped with ascending refrigerator/ cooler and a precision thermometer ($\pm$ 1°C).

Heating of the reaction mixture was made with a THS-100 type casing.

The development of the kinetic study required prelevation, at equal time intervals, of melt samples, that were treated with distilled water and chlorophorm known as extracting the non-reacted dimethyladipate, which was further dosed by chromatographic analyses. The dimethyladipate and the adipic acid employed are high purity reagents [6].

The following methods have been applied.

a) *Thermogravimetric analysis*, requiring a Paulik—Paulik—Erdey type derivatograph (MOM Budapest), recording simultaneously thermogravimetric (TG), derivated thermogravimetric (DTG) and differential thermal (DTA) curves, as well as the temperature curve (T). For the obtainment of comparable data, the same working conditions have been maintained namely heating rate

12°C/min, sample weight 20 mg, control material Al_2O_3 calcinated at 1 200°C, in atmospheric air.

b) *Chromatographic analysis* was performed on a Pye chromatograph (series 104, model 34), equipped with a detector of thermal conductivity, glass separation column lenght l=2 m and 3 mm in diameter, filled with chromosorb W 60/80 mesh, on which 15 % PEG 2 059 have been deposited. The temperature of the column and of the detector was of 200°C, while the bridge current of 50 mA. Argon at a flow of 40 ml/min has been used as carrier gas. The injected amount of the sample was of 5 μl.

3. Results and Discussion

The kinetic study has been performed by the thermogravimetric method, the dimethyladipate and the adipic acid being analyzed, in order to establish the temperature range within the reaction may occur.

Table 1 presents the thermogravimetric characteristics of dimethyladipate and of the adipic acid, namely : T_i — initial decomposition temperature ; T_M — temperature corresponding to the maximum decomposition rate ; T_t — melting temperature ; W_∞ — weight losses, [%].

Table 1

Thermogravimetric Characteristics of Dimethyladipate and of the Adipic Acid

Compound to analyze	T_i, [°C]	T_M, [°C]	ΔT	T_t,[°C]	W_∞,[%]
Dimethyladipate	90	210	90...270	—	100
Adipic acid	180	320	180...350	153	100

The thermogravimetric characteristics suggest selection of reaction temperatures close to the adipic acid's melting temperature (150°...160°C), on considering that the initial decomposition temperatures, under dynamic conditions, are lower than under statical ones.

To establish the molar ratio which correspond to a maximum conversion degree, the synthesis of monomethyladipate has been performed at various molar ratios of the reactants, keeping constant the temperature (160°C) and the catalyst's concentration (0.1 %). Kinetic curves, the conversion degree as a function of time for different diester : adipic acid molar ratios, evidence that an increase of this ratio in the reaction mixture induces a significant lowering of the conversion degree (Fig. 1), while its decrease would not lead to essential modifications (Fig. 2) ; the conclusion to be drawn is that the optimum molar ratio is of 1 : 1.

Development of the monomethyladipate synthesis if the catalyst's concentration is maintained constant (0.1 %), permit the study of the influence of temperature ; results are given in Fig. 3.

The conversion degree is seen as increasing with the increase of temperature, which is another evidence that the optimum temperature domain is 150°...160°C.

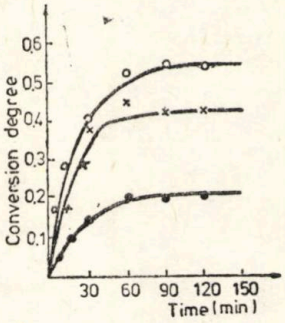

Fig. 1.— Influence of the diester : adipic acid molar ratio upon the conversion degree, at a temperature of 160°C : o — 1 : 1 ; x — 1.5 ; 1 ; ● — 2 : 1.

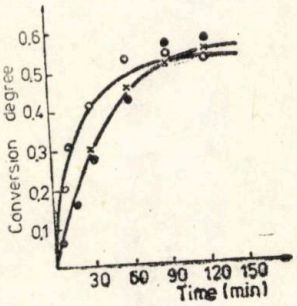

Fig. 2.— Influence of the diester : adipic acid molar ratio upon the conversion degree, at a temperature of 160°C : o — 1 : 1 ; x — 1 : 2 ; ● — 1 : 3.

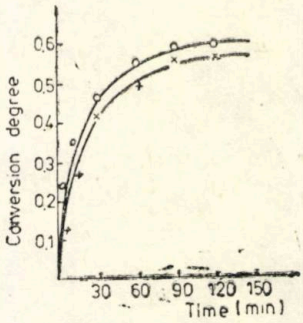

Fig. 3.— Influence of temperature upon the conversion degree, at a molar ratio of the reactants 1 : 1 ; x — 150°C ; o — 160°C.

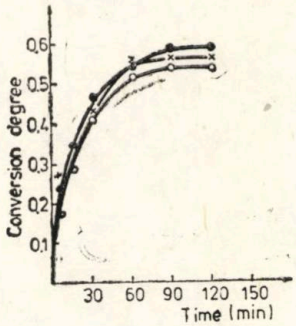

Fig. 4.— Influence of the catalyst's concentration upon the conversion degree, at a molar ratio of 1 : 1 : o — acid *p*-toluenesulfonic 2 % ; x — acid *p*-toluenesulfonic 1 % ; ● — acid *p*-toluenesulfonic 0.1 %.

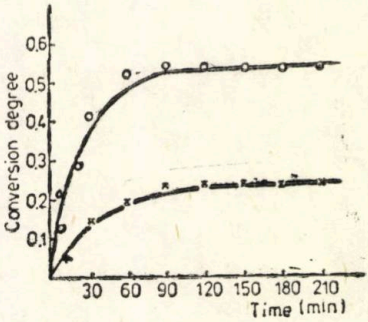

Fig. 5.— Influence of the working duration upon the conversion degree, for various diester : adipic acid ratios : o — 1 : 1 ; x — 2 : 1.

The influence of the catalyst's concentration upon the conversion degree is plotted in Fig. 4. One may observe that no essential modifications of the conversion degree do appear with increasing the catalyst's concentration, which suggests the autocatalytic character of the reaction, the optimal concentration of the catalyst (the *p*-toluenesulfonic acid) of 0.1 % being selected.

In order to establish the working duration which correspond to the maximum conversion degree, a constant temperature of 155°C has been selected, at a diester : adipic acid molar ratio of 1 : 1 and 2 : 1. The obtained results are plotted in Fig. 5.

The aspect of the kinetic curves illustrates that after 90 min., the curves become flat, which indicates the installation of the equilibrium at a maximum conversion degree of 0.54 and a molar ratio 1 : 1.

Starting from this study, the following optimum kinetic conditions, if a maximum conversion degree is considered, have been selected for the estimation of the fundamental kinetic parameters: molar ratio of the reactants 1 : 1, temperature range 150°...160°C, catalyst's concentration 0.1 %, duration of the reaction 90 min.

The obtained experimental data have been processed in a FORTRAN programme, by applying the differential method (the ORDIF programme), as well as the integral method (the ORIN programme). The obtained results are given in Table 2.

Table 2

Kinetic Parameters of the Monomethyladipate Synthesis

T, (°C)	ORDIF programme		ORIN programme			
	Reaction order	k_3 $mol^{-2}.l^2.min^{-1}$	Reaction order	k_3 $mol^{-2}.l^2.min^{-1}$	A $mol^{-2}.l^2.min^{-1}$	E kJ/mol
150	3	28.70	3	29.70	1.27×10^7	48.5
160	3	37.86	3	37.76	1.27×10^7	48.5

Analysis of the kinetic parameters presented in Table 2 indicates a good agreement between the two employed methods permitting to establish the following kinetic equation :

(1) $$k_3 = 1.27 \times 10^7 (\exp. -45\,800/8.314\ T),\ [mol^{-2}.l^2.min^{-1}].$$

According to literature data, transesterification in acid medium occurs through a complex mechanism, a succesion of reversible elementary reactions.

The value of the reaction order recorded at catalytic transesterification in melts, would suggest that the determining rate stage is trimolecular, being probably favourized [7] the formation under synthesis conditions of some complexes through hydrogen bonds between the reactants and the catalyst, which generates, through splitting, the protonated substrate participating in subsequent reactions.

4. Conclusions

The performed kinetic study permitted the elaboration of a synthesis method of the monomethyladipate, in melts, using the *p*-toluenesulfonic acid as catalyst. The method has the advantage of employing a catalyst with a low corrosion degree.

The above deduced, kinetic equation establishes that, in melts, the reaction is developed according to a three order kinetic law.

Received, June 11, 1990

Polytechnic Institute, Jassy,
Department of Physical Chemistry

REFERENCES

1. Puskas I., Fields E. K., Ind. Eng. Chem. Prod. Develop., **9**, *3*, 403 (1970).
2. * * * Japan Patent, *2 457 851* (1979).
3. * * * RFG Patent, *2 404 359* (1979).
4. * * * USA Patent, *4 237 317* (1980).
5. Hurduc N., Odochian L., Luca C., Mihai E., Ungureanu Șt., Ionescu E., Romanian Patent, *93 557* (1987).
6. * * * EGA Catalog Handbook, 1981/1982.
7. Murgulescu I. G., Segal E., Oncescu T., *Introducere în Chimia Fizică*. Vol. **2**, *Cinetică și cataliză*, Ed. Acad. București, 1981, 573.

CINETICA REACȚIEI DE SINTEZĂ A MONOMETILADIPATULUI

(Rezumat)

Se întreprinde studiul cinetic al reacției dintre dimetiladipat și acidul adipic, în topitură, în prezența acidului *p*-toluensulfonic drept catalizator.

S-au stabilit factorii cinetici optimi și s-a dedus ecuația cinetică a reacției de forma (1).

BULETINUL INSTITUTULUI POLITEHNIC DIN IAȘI
Tomul XXXVI (XL), Fasc. 3—4, 1990
Secția II
CHIMIE ȘI INGINERIE CHIMICĂ

D. C. 541.182.6 ; 661.97

MASS TRANSFER IN FLOW OF THIN FILMS OF SUSPENSIONS

I. ABSORPTION OF CARBON DIOXIDE IN WATER FILMS

BY

RADU Z. TUDOSE, ECATERINA MERICĂ and I. MĂMĂLIGĂ

1. Introduction

The present paper is a part of an ample study regarding the mass transfer in flow of thin films of suspensions [1].

To investigate the manner in which the presence of a solid phase influences the mass transfer process in liquid phase, particularly the absorption of carbon dioxide in a falling film, on a cylindric tube, a previous study with water and suspensions has been performed.

A large series of runs with water as absorbent and CO_2 as solute was required since, in the absence of literature informations concerning absorption in thin films of suspensions, a comparison system was necessary in discussing the experimental results.

The runs with water have also been used for checking the equipment, the working procedure and the reproducibillty of the obtained results. The experimental results have been compared with those reported in literature which provided a real scientific base for the subsequent approach of the study on suspensions.

2. Experimental

The equipment used and the working procedure have been described in a previous paper [1].

3. Results and Discussion

In the present paper the obtained results are compared with the main theoretical models and the experimental data reported in the field.

In 1970 Coeuret, Jamet and Ronco [2] analysed the main theoretical models for the mass transfer, with and without chemical reaction, for a falling liquid film on cylindric walls in the laminar and transition regime (Table 1).

As can be seen in Table 1 the mass transfer coefficient is considered to depend on the coefficient of diffusion of solute either at the power 1/2 or 5/8 according to the penetration theory (5/8) or that of eddy diffusivity (1/2).

Table 1

Theoretical Solutions

Regime	Laminar with waves			Turbulent	
Authors	Lewich [10]	Ruckenstein and Berbente [11]	Banerjee, Rhodes and Scott [12]	Lewich [13] Atkinson[14]	Banerjee, Scott and Rhodes [15]
without chemical reaction	$\bar{k}_L^0 = \psi(\bar{k}_L^0)_{\text{lam.}}$	$\bar{k}_L^0 = \psi(\bar{k}_L^0)_{\text{lam.}}$	$\bar{k}_L^0 = 0.7 \frac{D_A^{5/8}}{\bar{H}^{1/4}\bar{t}^{3/8}}$	$\bar{k}_L^0 = \frac{D_A}{2}\left(\frac{\rho v_0^3}{2\sigma\alpha D_A}\right)^{1/2}$	$\bar{k}_L^0 = \left(\frac{D_A}{\bar{\tau}}\right)^{1/2}$
with chemical reaction	$\psi = 1.15$	$\psi = 1.3$	$\bar{H} = \left(\frac{\sigma\nu}{\rho\bar{v}_w}\right)^{1/2}$ $\bar{t} = \lambda/(\bar{v}_w - \bar{v})$	$\alpha = 0.5$ [13] $\alpha = 1$ [14]	$\bar{\tau} = a^{-2}k^{-3}\bar{v}_W^{-1}$

The Pigford model, not included in Table 1, which predicts a linear dependence of the mass transfer coefficient vs. the coefficient of diffusion, on the basis of the two-film theory, can also be mentioned but a discrepancy of about 150...200 % between the predicted theoretical data and the experimental results is reported [3].

3.1. Levich Model

According to the Levich model:

$$k_L = (k_L)_{\text{lam}} = \bar{v}_s \frac{D_A^{0.5}}{h}, \tag{1}$$

where h is the height of the wetted column and $\bar{v}_s$ — the mean velocity of the liquid in the vicinity of the film surface. The latter is related to the liquid mean velocity by the relationship $\bar{v}_s = 1.5\ \bar{v}$, which is valid for a parabolic distribution of rates but is considered as acceptable over a wide range of $\mathcal{R}e$ variation in wave films.

The amount $\bar{v}_s$ can be calculated with the relationship:

$$\bar{v}_s = 1.5 \frac{D}{\text{section}} = 1.5 \frac{D}{d(d \mp \delta)}, \tag{2}$$

where δ is the thickness of the thin film (in the above cited paper this value is taken from a plot δ vs. $\mathcal{R}e$).

As can be seen in Table 2 a clear disagreement occur between the calculated and experimental data. This disagreement can be accounted for by the fact that in calculating the transfer coefficient the geometrical parameters (the column diameter and height) have a considerable weight.

Table 2

Values Calculated by Means of Levich Model and Our Experimental Data

$\mathcal{R}_e$	D cm²/s	v_s cm/s	k_L calcd. $\times 10^4$ cm/s	k_L exp. $\times 10^4$ cm/s
600	14.53	0.75	4.8	54.1
900	18.58	0.95	6.4	84.7
1 100	24.50	0.84	5.80	77.7

As a matter of fact C o e u r e t and co-workers used a wetted wall column of 0.4 cm diameter and 5 cm height while our experimental data have been obtained on a column of 5 cm diameter and 228.5 cm height (that is a diameter of 7.5 times larger and a height of 45·7 times larger) which results in much different hydrodynamic features.

3.2. Bannerjee — Rhodes — Scott Model

According to this model in the relationship for calculating the individual mass transfer coefficient, k_L, the coefficient of diffusion is used at the 5/8 power :

$$\frac{k_L}{D_A^{5/8}} = \frac{0.7}{\bar{H}^{1/4}\,\bar{t}^{3/8}}, \tag{3}$$

where :

$$\bar{H} = \left(\frac{\tau\nu}{\bar{v}_w^3}\right), \tag{4}$$

$$v_w = 2.95\mathcal{R}e^{0.5}, \text{ [cm/s]} \tag{5}$$

$$\bar{t} = \frac{\bar{\lambda}}{\bar{v}_w - \bar{v}_s}, \tag{6}$$

$$\bar{v}_s = 1.5\left(\frac{\nu g}{3}\right)^{1/3}\left(\frac{\mathcal{R}e}{4}\right)^{2/3}. \tag{7}$$

In the relationships (3)...(7) k_L denotes the mass transfer coefficient in liquid phase, [cm/s]; D_A — the coefficient of diffusion of solutes, [cm²/s]; $\bar{H}$ — the mean distance of eddy approach to the free surface, [cm]; $\bar{t}$ — the mean period between eddies, [sec.]; $\bar{v}_s$ — the mean rate at the film surface, [cm/s]; $\bar{v}_w$ — the mean velocity of wave, [cm/s]; ν — the kinematic viscosity of water, [cm²/s]; λ — the mean wavelength, [cm] — (admited $\lambda = 1$ cm); τ — the surface tension of water, [dyn/cm]; g — the gravitational acceleration, [cm/s²].

In Fig. 1 the theoretical curve, the above cited author's results and our experimental values are plotted.

As can be seen the experimental data lie much below the theoretical curve. The model is based on the action of large single eddies associated with wave motion and evidences the influence of hydrodynamic conditions on the transfer rate. In this model the geometric parameters are not considered. The agreement between our data and this model cannot be considered as satisfactory.

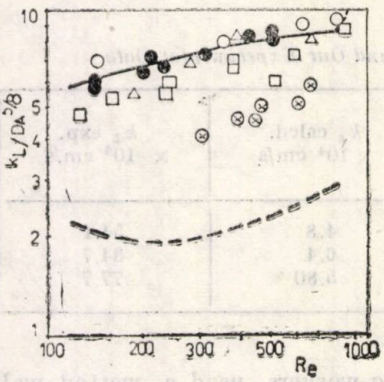

Fig. 1. — Check of data by means of Bannerjee—Rhodes—Scott model:— theoretical model; --- Pigford model; ⊗ obtained results.

3.3. Prasher-Fricke Model

According to this model of eddy-diffuzivity, for the turbulent regime, the equation for calculating the individual mass transfer coefficient, k_L, is of the form:

$$k_L = C^{1/2}\frac{2\rho^{1/2}}{\pi\sigma^{1/2}}\left(\frac{\delta^3\mathcal{E}^3}{g\nu}\right)^{1/2} D_A^{1/2}, \tag{8}$$

where:

$$\delta = (400)^{-1/5}\left(\frac{3\nu^2}{g}\right)^{1/3}\left(\frac{\mathcal{R}e}{4}\right)^{8/15} \tag{9}$$

is the thickness of the turbulent film (Brauer's equation); $\mathcal{E}$ — the rate of energy dissipation for a turbulent film ($\mathcal{E} = gv_m$), with

$$v_m = (400)^{1/5}\left(\frac{\nu g^4}{3}\right)^{1/3}\left(\frac{\mathcal{R}e}{4}\right)^{7/15}. \tag{10}$$

By introducing the relationship for v_m in the equation for the calculus of the rate of energy dissipation, $\mathcal{E}$, it result:

$$\mathcal{E} = (400)^{1/5}\left(\frac{g^4\nu}{3}\right)^{1/3}\left(\frac{\mathcal{R}e}{4}\right)^{7/15}. \tag{11}$$

In the above relationship g, ν, $\mathcal{R}e$ and ρ have the usual significance. By using a plot of the form

$$k_L = f\left(\frac{2}{\pi}\cdot\frac{\rho\delta^{3/2}\mathcal{E}^{3/2}}{g^{1/2}\nu^{1/2}}D_A^{1/2}\right), \tag{12}$$

the constant C in Eq. (8) can be determined.

The plot of our results, for a series of $\mathcal{R}e$ values (Fig. 2), indicate a very good correlation of data with the model.

The fact that our data lie at the lower part of the figure is due to the $\mathcal{R}e$ values (up to 3 500) at which the measurements have been taken while the abscissa is for $\mathcal{R}e$ values up to 11 000.

3.4. Lamourelle—Sandall Model

According to this model, the coefficient of mass transfer is proportional with the coefficient of diffusion of solute at the power 0.5 (Fig. 3) [6]. In Fig. 3 our experimental results are also depicted. As can be seen a satisfactory

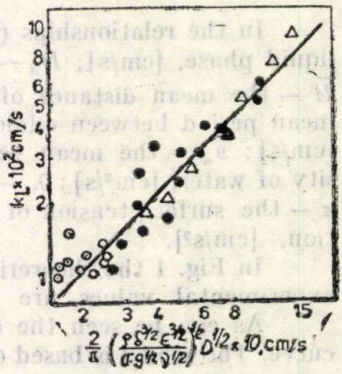

Fig. 2. —Check of data by means of Prasher—Fricke model: —theoretical model; ⊙—obtained results.

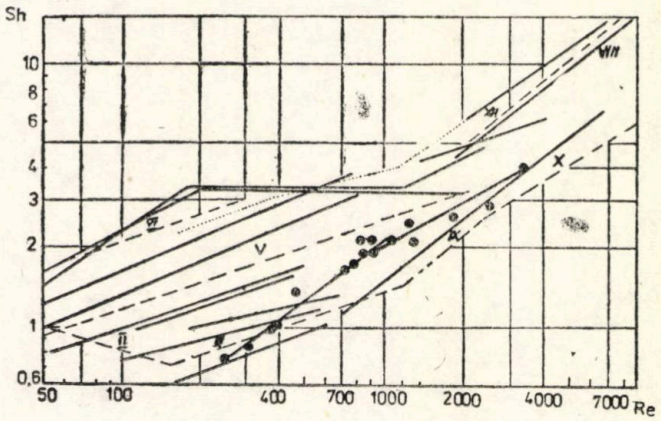

Fig. 4. — Place of the obtained data w.r.t. those determined by various investigators for the CO_2 absorption in thin falling films of water : . . . experimental data obtained by K o z i o l and co-workers [7] ; — — — theoretical or semiempirical solutions ; ——— experimental results ; • obtained results.

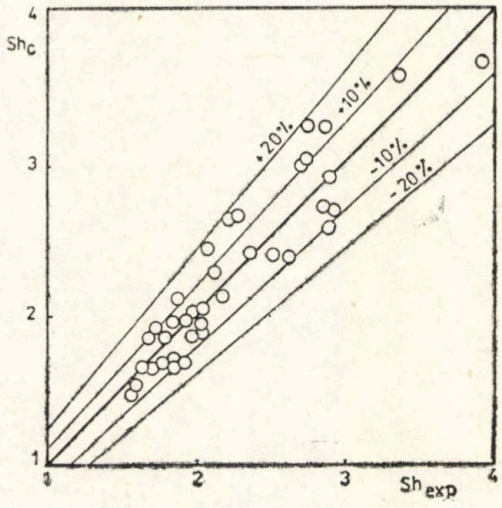

Fig. 5. — Comparison between Sh_{exp} values with those calculated by means of Eqs. (14) and (15).

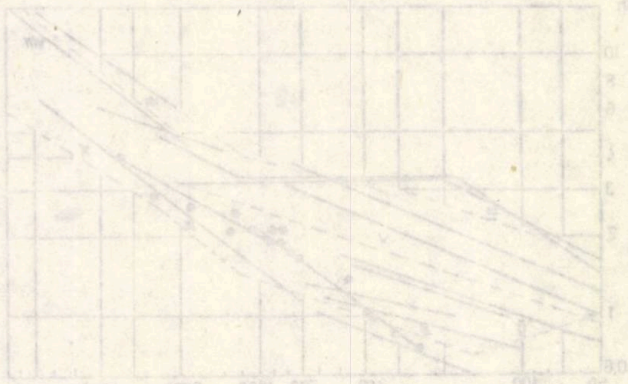

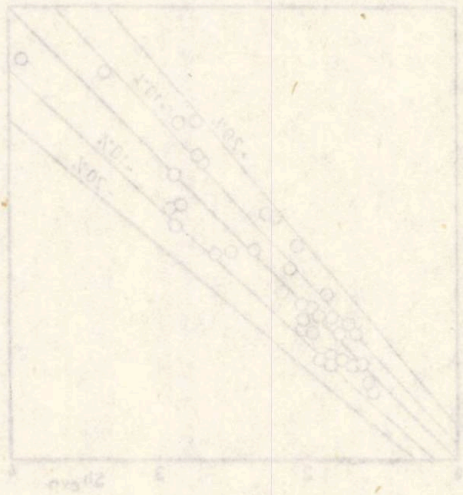

agreement is shown between the calculated k_L values and our experimental data. For calculating k_L the authors advanced the following relationship :

(13) $k_L = 0.339\,\mathcal{R}e^{0.839} D_A^{0.5}$, [ft/h].

In fig. 4 the experimental results reported in literature and the main theoretical relationships derived for the absorption of carbon dioxide in thin liquid films are plotted. For the sake of clearness the middle of the figure, where the most of the results lie (the boundary lines represent theoretical correlation) has been left almost empty. In this space our data have been depicted and our relationships plotted (full lines).

The fact can be noticed that our data are placed within the range of maximum density, that is where most of

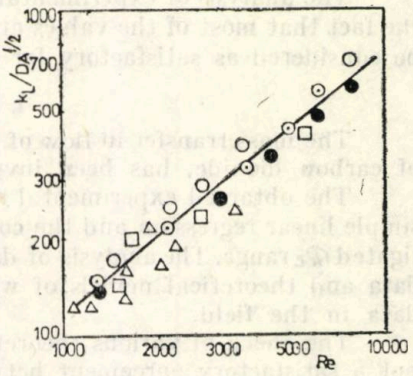

Fig. 3.—Check of data by means of L a m o u r e l l e—S a n d a l l model: —theoretical equation; ● —experimental data for CO_2 absorption in water obtained by L a m o u r e l l e and S a n d a l l [6]; ○, ⊙ data for other systems (absorption of O, H_2, He in water) obtained by the same authors); Δ — obtained results.

Table 3

Comparison between our Experimental Data and those Calculated with the Lamourelle—Sandall Model

$\mathcal{R}e$	k_L calculated m/h	k_L experimental m/h	Deviation %
1 096	0.325	0.316	−2.7
1 187	0.358	0.343	−4.2
1 187	0.358	0.329	−8.1
1 265	0.372	0.365	−2.0
1 265	0.372	0.350	−6.0
1 364	0.403	0.355	−12
1 671	0.462	0.436	−6.0
1 671	0.462	0.439	−5.0
1 743	0.495	0.407	−17.0
1 841	0.483	0.441	−8.6
1 841	0.483	0.475	−1.0

data are located. However, the data obtained for low $\mathcal{R}e$ lie near the boundary of the field. This can be accounted for by the possibility of incomplete wetting of the column at low flowrates [8].

By working the obtained data by simple regression — the least square method — the following relationships have obtained :

(14) $170 < \mathcal{R}e < 470$, $\mathcal{S}h = 5.335 \times 10^{-3} \mathcal{R}e^{0.893}$, $r = 98.3\,\%$,

(15) $470 < \mathcal{R}e < 3\,500$, $\mathcal{S}h = 0.0292 \mathcal{R}e^{0.593}$, $r = 97.17\,\%$.

The analysis of experimental and calculated $\mathcal{S}h$ values (Fig. 5) evidences the fact that most of the values are located within $\pm 15\,\%$ interval which can be considered as satisfactory for engineering purposes [8].

4. Conclusions

The mass transfer in flow of thin water films, particularly the absorption of carbon dioxide, has been investigated.

The obtained experimental results have been worked on a computer by simple linear regression and the correlation $\mathcal{S}h = f(\mathcal{R}e)$ derived, for the investigated $\mathcal{R}e$ range. The analysis of data and tneir comparison with tne literature data and theoretical models of wide recognition allowed the location of our data in the field.

The check of various theoretical models indicated the fact that there is not a satisfactory agreement between the experimental results and the calculated ones in case of models where in calculus of the mass transfer coefficient a large weight is awarded to the geometric parameters as well as in case of those where the latter are not considered.

With other theoretical models our results agree in a satisfactory manner within the range of $\pm$ 15 %.

In a sketch depicting the theoretically predicted $\mathcal{S}h$ values versus those found experimentally by various workers in the field, our data are well placed within the middle part, of maximum density of data, tending towards the field boundaries only for small $\mathcal{R}e$ values. This fact has been accounted for by the possibility of nonuniform wetting of the column at low flowrates, difficult to observe experimentally as well as by the higher temperature the runs have been carriet at.

Received, April 20, 1990

Polytechnic Institute, Jassy,
Department of Chemical Engineering

REFERENCES

1. Tudose R. Z., Mercă Ec., Ungureanu Șt., Bul. Inst. polit., Iași., **XXXI (XXXV)** Suppl. Fasc., s. II, 135 (1985).
2. Coeuret P., Jamet B., Ronco J. J., Chem. Eng. Sci., **25**, 17 (1970).
3. Emmert R. E. Pigford R. L., Chem. Eng. Progr. **50**, 87 (1954).
4. Bannerjee S., Rhodes E., Scott D. S., Chem. Eng. Sci., **22**, 43 (1967).
5. Prasher B. D., Fricke A. L., Ind. Eng. Chem. Process Des. Develop., **13**, *4*, 336 (1974).
6. Lamourelle A. P., Sandall O. C., Chem. Eng. Sci., **27**, 1 035 (1972).
7. Koziol K., Bronziarz L., Novicka T., Int. Chem. Eng., **20**, *1*, 137 (1980).
8. Boyadjiev Gh., Beskov V., *Mass Transfer in Liquid Film Flow*. Publ. House of the Bulgarian Acad. of Sci., Sofia, 1984.

TRANSFERUL DE MASĂ LA CURGEREA SUSPENSIILOR ÎN FILM SUBȚIRE (I)

(Rezumat)

Cercetarea întreprinsă se încadrează într-un studiu mai amplu privitor la transferul de masă la curgerea suspensiilor în filme subțiri. Datorită lipsei de informații în literatura de specialitate asupra absorbției CO_2 în filme subțiri de suspensii au fost efectuate un mare număr de experimente cu apă pentru constituirea unui sistem de referință.

Studiile cu apă au fost necesare pentru verificarea aparaturii, a metodei de lucru și a reproductibilității rezultatelor. Datele obținute au fost comparate cu rezultatele publicate pe plan mondial și verificate prin intermediul unor modele teoretice cunoscute.

S-a constatat că datele obținute se încadrează bine în domeniul datelor furnizate de literatură și prezintă o bună concordanță cu modele teoretice cunoscute, ceea ce se constituie într-o bază de abordare reală, științifică, a studiului ulterior asupra suspensiilor.

BULETINUL INSTITUTULUI POLITEHNIC DIN IAȘI
Tomul XXXVI (XL), Fasc. 3—4, 1990
Secția II
CHIMIE ȘI INGINERIE CHIMICĂ

D. C. 66.093.6 ; 678.746.22

STUDIES ON KINETICS OF STYRENE— DIVINYLBENZENE COPOLYMER DRYING

II. FLUIDIZED BED DRYING

BY

GH. CRISTIAN, RALUCA STAICU, GERASELA ȘFABU and DANIELA IONESCU

1. Introduction

Fluidization is a technique of contacting a granular solid phase with a fluid one, the fluidized bed showing properties similar to those of liquids. This method is based on the general principle of passing the hot gas through the material layer on the distributor or the fluidization grate. It is largely applied in different industrial fields due to the advantages offered by the fluidized bed technique, such as : a) intensification of the heat and mass transfer ; b) uniform and controllable temperature of the two phases ; c) low energy consumption per tone of dry product ; d) short drying time in comparison with the conventional dryers ; e) automation of the drying process and achievement of the optimum regime.

A particularly important feature of the fluidized bed is the achievement of high rates of the transfer processes.

The fluidized bed drying depends on the hydrodynamic regime, heat and mass transfer, technological conditions and on the optimum regime of the drying equipment.

The present paper presents the experimental results concerning hydrodynamics of the fluidized bed consisting of beads of styrene — divinylbenzene copolymer as well as the kinetic curves of the fluidized bed drying of the copolymer.

2. Experimental Results

2.1. Fluidized Bed Hydrodynamics

The fluidized bed represents an heterogeneous system with the solid particles in a continuous motion under the influence of the gas stream. The fluidization state is a two phase gas — solid system consisting of a solid phase, through which a gas stream flows, and a phase of gas bubbles with a small amount of suspended solid particles. Due to its structure and laws, the fluidized bed is an intermediary form between the fixed bed and the pneumatic entrainment of the solid.

The formation of the fluidized bed is based on the following principle : when a gas stream passes upward through a granular layer at a low rate the fixed bed flowing is achieved. When the gas rate becomes high enough so that the gas pressure exceeds the layer weight the fluidized bed flowing occurs. In this case, the gas rate is known as the minimum fluidization rate and it represents one of the most important parameters of the fluidized bed.

The behaviour of the gas and of the particles in the fluidized bed is entirely different from the fixed bed one. The fluidized bed density decreases with increasing gas rate due to increasing intervals between the solid particles so that the homogeneous fluidization appears. At higher gas rates the bubble fluidization appears. At a gas rate higher than the particle floating rate in the fluidization gas the solid particles are carried off pneumatically from the apparatus.

The minimum fluidization rate can be either determined experimentally by studying the variation of the pressure drop as a function of gas rate or calculated by means of the literature relationships [1]...[3].

The minimum fluidization rate was determined on a laboratory equipment (Fig. 1) consisting of a fluidization column (*8*) with an inner diameter of 50 mm and hight of 450 mm, supplied with a metallic sieve at the lower part for supporting the copolymer beads and for the uniform distribution of the fluidization agent. The cyclone (*9*) at the higher column part retains the entrained solid particles. The pressure drop was measured by the differential manometer (*10*). The laboratory installation also contains the pressure reducer (*1*), the rotameter (*2*), the air pre-heater (*3*), the autotransformer (*4*) and the thermometers (*5*) and (*6*).

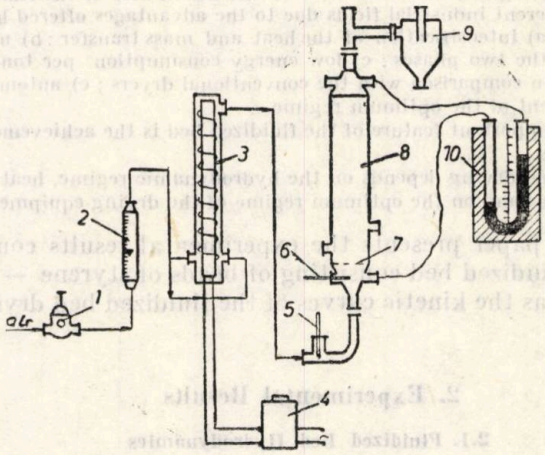

Fig. 1 — Equipment for the hydrodynamic study on the fluidized bed drying.

For fluidized bed drying, the air was heated in the tube (*3*) by means of electric resistances and then introduced at the lower part of the fluidization column.

The fluidized bed hydrodynamics were studied with the copolymer particles of 0.625 mm and 0.88 mm diameters. The fixed bed hight was of 30 ; 50 and 70 mm and the air temperature of 20°C.

The Fig. 2 presents the pressure drop in function of the gas rate for three cases : a) curve *1* — pressure drop through the distribution sieve and the empty column ; b) curve *2* — pressure drop through the distribution sieve and the fluidization column containing copolymer particles of

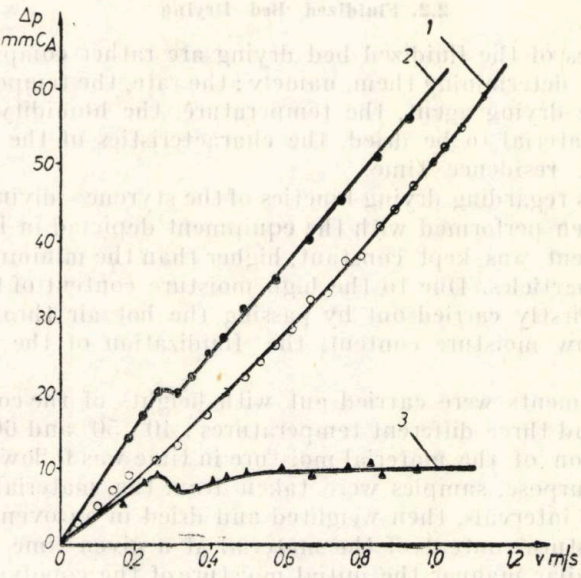

Fig. 2. — Pressure drop versus gas rate.

0.88 mm in a fixed layer of 30 mm height ; c) curve *3* — pressure drop through the styrene — divinylbenzene copolymer layer.

Experimental results regarding the pressure drop through the copolymer layers are depicted in Fig. 3.

The pressure drop is seen to increase linearly with increasing gase rate in case of flowing through the copolymer fixed bed. The increase in the pressure drop is much smaller in the fluidized bed than in the fixed one. For the layers of short hight it may be considered constant.

A comparison of the pressure drop for the two sizes of the solid particles, at the same gas rate and fixed layer height, shows a higher value in case of the particles of small size. This might be explained by the smaller porosity of the layers of small-sized particles. The fact deserves mention that the maximum pressure drop and, hence, the minimum fluidization rate, increase with increasing height of the fixed layer. That is probably due to the increased pressure exercised by the copolymer layer which must be exceeded to occur the layer swelling.

The experimental minimum fluidization rate was compared with that calculated by means of literature data [3], the best agreement being noticed with the equations ;

(1) $$v_m = 8.1 \times 10^{-4}(\rho_p - \rho_f) d_p^2 \eta_f^{-1} b, \qquad (2) \qquad \mathcal{R}e = C\mathcal{A}r^m,$$

where :

$$\mathcal{R}e = \frac{d_p v_m \rho_f}{\eta_f}; \; C = 1.069 \times 10^{-3}; \; m = 1;$$

$$\mathcal{A}r = \frac{d_p^3(\rho_p - \rho_f)\rho_f g}{\eta_f^2},$$

2.2. Fluidized Bed Drying

The kinetics of the fluidized bed drying are rather complex due to the numerous factors determining them, namely: the rate, the temperature and the properties of the drying agent, the temperature, the humidity and the properties of the material to be dried, the characteristics of the fluidized bed: height, porosity, residence time.

The studies regarding drying kinetics of the styrene—divinyl-benzene copolymer have been performed with the equipment depicted in Fig. 1. The rate of the drying agent was kept constant, higher than the minimum fluidization rate of the dry particles. Due to the high moisture content of the copolymer, the drying was firstly carried out by passing the hot air through the fixed bed. Then, at low moisture content, the fluidization of the solid particles was achieved.

The experiments were carried out with heights of the copolymer fixed bed of 50 mm and three different temperatures; 40°, 50° and 60°C.

The variation of the material moisture in time was followed experimentally. In this purpose, samples were taken from the material under drying at different time intervals, then weighted and dried in an oven till constant weight. The moisture content of the material at a given time was then calculated. In a similar manner the initial moisture of the copolymer was determined. The experimental results are shown in Fig. 4.

Fig. 4 shows the copolymer moisture to decrease linearly at the beginning and then as described by a curve of higher degree.

Since the copolymer is porous the moisture is retained both between the grains and inside them. The greater porosity the higher content of the retained moisture is.

The experimental results indicate the drying process to proceed in two stages, namely: a) the drying at a constant rate; b) the drying at a decreasing rate in time.

During the first period only the moisture at the particle surface is considered to evaporate and the heat transfer is the process controlling step in comparison with the mass transfer. To increase the heat transfer the thermal resistance of the boundary layer at the particle surface must be lowered and the convection through the gas mass increased. By the circulation and the internal mixing of the phases as well as by the increase in the gas—solid particle relative rate hydrodynamic conditions for the optimum process development are created.

During the drying at a decreasing rate the drying rate depends on the rate of heat and mass transfer within the solid particle. The mass transfer inside particle becomes process - controlling step. Since the drying rate is a function of the temperature in the layer it must be kept at the maximum admissible value.

The average drying rate found experimentally, expressed as the moisture percentage evaporated in the time unity, was compared with the theoretical value calculated by means of the empirical equations advanced by Guinzburg and Rezčikov [2]:

$$U=[0.46(t-60)^{0.7}+k_0(w_i-25)+8]\left(\frac{M_i}{A_0}\right)^{-0.6}\sqrt{\rho_v} \tag{3}$$

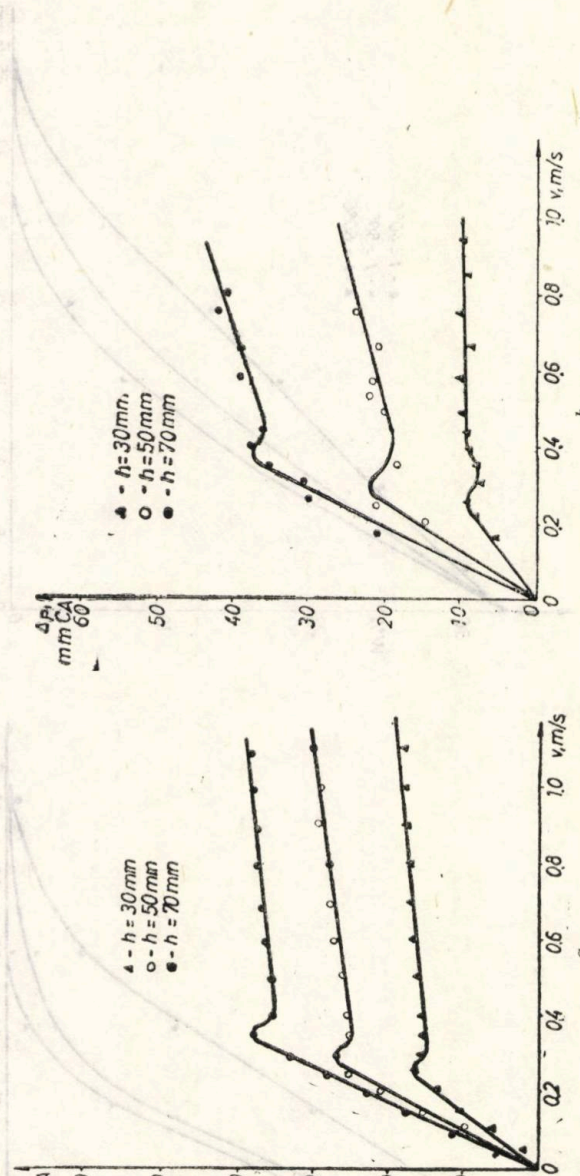

Fig. 3. — Pressure drop versus gas rate : a — d_p=0.625 mm, b — d_p = 0.88 mm.

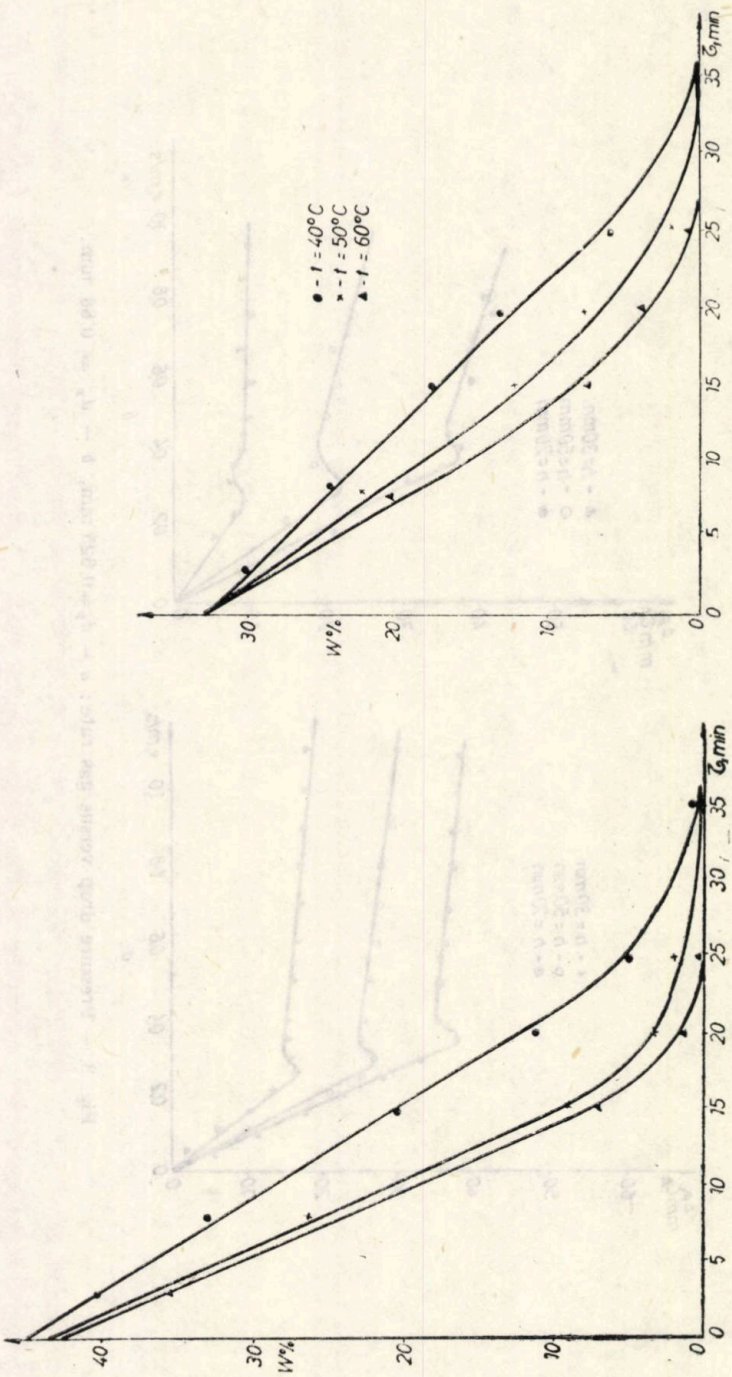

Fig. 4. — Variation of the copolymer moisture drying ; $a - d_p = 0{,}625$ mm; $b - d_p = 0.88$ mm

and a fairly good agreement found. The order of magnitude of the experimental drying rate is in agreement with the values obtained by other investigators with different porous materials [2].

The thermal calculation of the fluidized bed dryers is based on the determination of the time of heating the particle till the maximum admissible temperature. The variation of the material temperature during drying and the duration of the solid particle mixing are essential for the quality of the dry product.

3. Conclusions

The experimental results on the fluidized bed drying of the styrene — divinilbenzene copolymer allowed the plotting of the material moisture variation versus time. These plots are indicative of the process development in two stages : the constant drying rate stage, when the moisture between the copolymer particles evaporates, and the decreasing drying rate stage, when the moisture within the solid pores evaporates. The process duration decreases with increasing temperature of the fluidization agent.

Notations

d_p — particle diameter, [m] ;
g — acceleration due to gravity, [m/s^2] ;
h — fixed bed height, [m] ;
k_0 — coefficient,
t — fluid temperature, [°C] ;
U — drying rate, [% moisture/h] ;
v — gas rate, [m/s] ;
v_m — minimum fluidization rate, [m/s] ;
w_i — initial moisture of the material, [%] ;
M_i/A_g — initial loading of the material on the distribution plate, [Kg/m^2] ;
ρ_f — gas density, [Kg/m^3] ;
ρv — particle density, [Kg/m^3] ;
η_f — gas viscosity, [Pa. s] ;
τ — time, [h].

Received, January 12, 1990

Polytechnic Institute, Jassy,
Department of Chemical Engineering

REFERENCES

1. Strumitto C., *Bazele teoriei și tehnicii uscării* (transl. from Polish). Ed. Tehn. București, 1984.
2. Mihăilă C., Caluianu V., Marinescu M., Dănescu Al., *Procese și instalații industriale de uscare*. Ed. Tehn., București, 1982.
3. Jinescu Gh., Vasilescu P., Revista de chimie, **23**, *4* (1977).

STUDII DE CINETICA USCĂRII COPOLIMERULUI STIREN—DIVINILBENZEN

II. Uscarea în strat fluidizat

(Rezumat)

Sînt prezentate rezultatele experimentale obținute în cazul uscării în strat fluidizat a perlelor de copolimer stiren — divinilbenzen la diferite temperaturi. De asemenea este prezentat un studiu hidrodinamic la curgerea agentului de uscare prin stratul de copolimer.

BULETINUL INSTITUTULUI POLITEHNIC DIN IAŞI
Tomul XXXVI (XL), Fasc. 3—4, 1990
Secţia II
CHIMIE ŞI INGINERIE CHIMICĂ

C. D. 547.85 ; 661.8..341

PYRIDAZINIUM-YLURES.

ACTION DU BROMURE DE *p.* MÉTHOXY-PHÉNACYLE SUR LA PYRIDAZINE ET QUELQUES 3-ARYLE-PYRIDAZINES

PAR

MARIA CAPROŞU, I. DRUŢĂ, I. FULGER, MAGDA PETROVANU et DANA DOROHOI

1. Introduction

Dans une Note antérieure [1] on a étudié l'action du bromure de *p.* méthoxy-phénacyle sur la 3-phényle pyridazine. Dans le but d'approfondir les études concernant les relations structures —propriétés dans la classe des pyridazinium-ylures [2], nous avons envisagé d'obtenir de nouveaux sels de cycloimmonium et ylures par l'action du bromure de p.méthoxy-phénacyle sur la pyridazine (1), la 3-*p*-tolyle-pyridazine (2, R=CH_3) et la 3-*p*-chlor phényle-pyridazine (2, R=Cl).

En gardant le groupement carbanionique non modifié dans une série de pyridazinium-ylures on peut établir l'influence des modifications du groupement cationique sur la stabilité et la réactivité des ylures respectifs.

2. Résultats et discussions

Dans la première étape des recherches on a synthétisé une série de sels de cycloimmonium du type (3) et (4) selon le schéma réactionnel *a*.

Les structures des sels de pyridazinium (3) et 3-aryle-pyridazinium (4, R=CH_3, —Cl) sont confirmées par les analyses chimiques et spectrales (IR, RMN).

En éliminant l'acide bromhydrique à partir des sels de pyridazinium (3) et (4), en milieu alcalin acqueux, on obtient les pyridazinium ylures (5) respectivement les 3-aryle-pyridazinium ylures (6) et (7) selon le schéma réactionnel *b*.

Le pyridazinium-(*p*.méthoxyphénacylure) (5) est coloré en jaune, les 3(*p*. tolyle) - pyridazinium - (*p*. méthoxy-phénycylures) sont colorés en orange respectivement en orange foncé.

Dans des recherches antérieures [3], l'un de nous avec d'autres collaborateurs, a étudié les spectres électroniques en visible de quelques pyridazinium-ylures et a attribué les bandes électroniques en visible de ces ylures à des transitions *I—II*, accompagnées par un transfert intramoléculaire de charge (schema *c*).

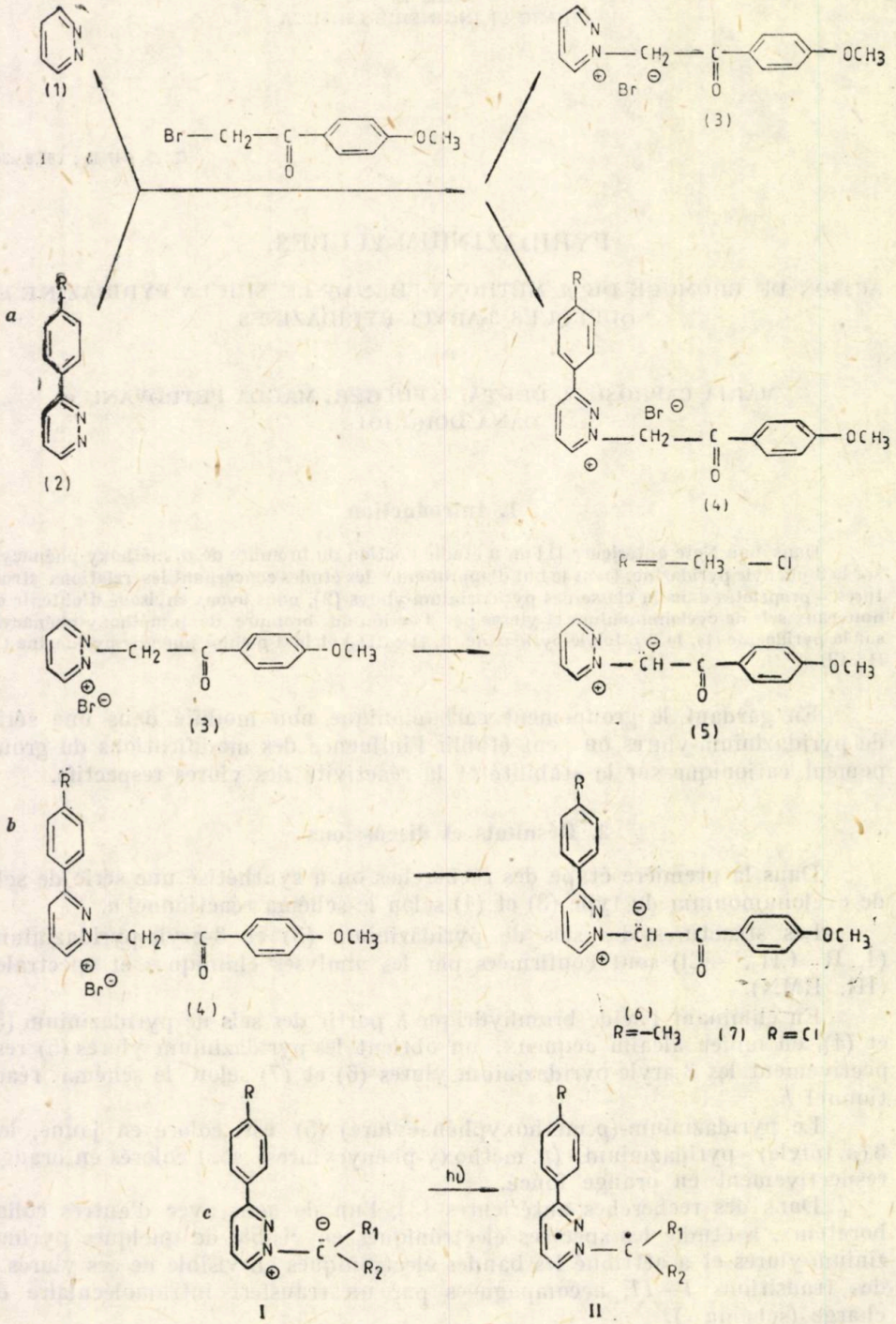
(1)
Br — CH2 — C(=O) — OCH3
(3)
a
(2)
(4)
R = — CH3 — Cl
(3)
(5)
b
(4)
(6) R=—CH3 (7) R=Cl
c
hν
I
II

L'étude des spectres électroniques des trois pyridazinium ylures (5), (6) et (7) présentés dans ce travail confirme les constatations antérieures compte tenu que la fréquence de l'absorbtion augmente paralèllement à la décroissance de la densité électronique dans le hétérocycle (*p*-chlorphényle<*p*-tolylepyridazine<pyridazine non-substituée). Autrement dit, les transitions électroniques s'effectuent d'autant plus facilement que la densité électronique dans les cycles pyridaziniques est plus faible par suite des effets accepteurs d'électrons exercés par les groupements aryliques en position 3 des cycles pyridaziniques.

Les données expérimentales sont présentées dans le Tableau 1.

Tableau 1

Nr.	Hétérocycle	Solvant	Absorbtion	Fréquence Nombres $\nu=1/\lambda$ d'onde
1	Pyridazine	Benzène	478	20 920
2	*p*-tolyle-pyridazine	Benzène	475	21 240
3	*p*-chlor-phényle-pyridazine	Benzène	465	21 500

Les structures des sels de cycloimmonium ainsi que celles des ylures correspondants ont été établies par voies chimiques et spectrales.

Les spectres IR et RMN des ylures (5), (6), et (7) ont été analysés aussi en comparaison avec ceux de quelques 3-aryle-pyridazinium-p.nitrophénacylures (8) obtenus par deux d'entre nous antérieurement [4].

En ce qui concerne les spectres IR l'observation générale que l'on doit faire est basée sur le fait que l'absorbtion dûe au carbonyle lié au carbanion ylurique est déplacée vers des fréquences plus basses en comparaison avec l'absorbtion dûe au même groupements dans les sels de cycloimmonium correspondants. Cette observation est confirmée particulièrement dans les cas ou il n'existe pas de substituants dans le groupement phénacylique ou les substituants sont accepteurs d'électrons. Ainsi, dans le cas du 3-aryle-pyridazinium-*p*.nitrophénacylure (8) on observe des déplacements des bandes d'absorbtion correspondants aux carbonyles à partir des valeurs d'environ $\nu_{C=O}=1\,700$ cm^{-1} jusqu'à des valeurs d'environ. $\nu_{C=O}=1\,550$ cm^{-1}, en fonction de la nature du substituant en position 3 du noyau pyridazinique. Par exemple, dans les cas du [3-(*p*-cumyle-pyridazinium)-*p*.nitrophénacylure (8) R=$-CH\begin{matrix}CH_3\\CH_3\end{matrix}$ on constate un déplacement de l'absorbtion du carbonyle à partir de 1 680 cm^{-1} à 1 540 cm^{-1} ($\Delta\nu=140$ cm^{-1}).

Par contre, si en position *para* du reste phénacylique il se trouve un groupement méthoxy, comme dans les composés (6) et (7), le déplacement de l'absorbtion du carbonyle est beaucoup plus faible c'est-à-dire de 1 674 cm^{-1} à 1 663 cm^{-1} pour le produit (6) et de 1 677 à 1 660 cm^{-1} pour le produit (7) ($\Delta\nu=11...17$ cm^{-1}).

Les différences assez importantes qui apparaissent entre les spectres des produits (5), (6) et (7) d'une part et (8) d'autre part, pourraient être expliquées par une participation plus importante des structures du type 6(...*c*, *d*) et 7(... *c*, *d*) dans les cas des produits qui contiennent un méthoxyle en position *para* du noyau phénacylique, qui par son effet $+M$ provoque des déplacements électroniques.

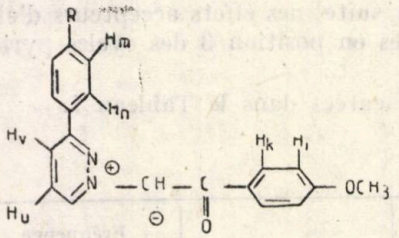

6.7 (a)

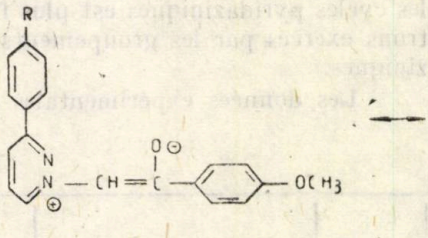

6.7 (b)

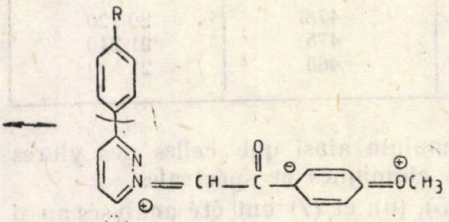

6.7 (d)

Les spectres RMN confirment les structures proposées. Ainsi, dans le composé (8) le signal du proton *Hz* est déplacé à un champ très bas ($\delta = 11{,}47$ ppm) à cause de la liaison d'hydrogène possible entre ce hydrogène et l'oxygène phénacylique. Le sigual de ce même proton a un déplacement chimique plus faible que 8,2 ppm dans les produits (6) et (7), faisant ainsi partie du multiplet correspondant aux protons hétéroaromatiques parce que, dans ce cas, la liaison d'hydrogène est moins probable à cause de l'apparition de coefficients de charges négatives sur l'atome de carbone en position 6 du noyau pyridazinique (les structures (6, 7 *d*)). La même observation est valable pour les signaux fournis par les protons (H_v et H_u) du noyau pyridazinique qui sont déplacés de 8,83 ppm dans le composé (4, R = $-CH_3$) à $\delta < 8{,}2$ ppm. Les intégrales des signaux dans les spectres des ylures montrent la présence de 11 protons dans le multipet aromatique.

3. Partie expérimentale

Les spectres IR sont obtenus à partie de pastilles de KBr avec un appareil Specord 71. Les spectres de RMN sont déterminés avec un appareil JEOL 60 MHz. Les déplacements chimiques sont exprimés en δ par rapport au tétraméthylsilane utilisé comme référence interne. Les constantes de couplage sont exprimées en Hz. Les microanalyses élémentaires ont donné des résultats en accord avec les pourcentages théoriques.

3.1. Bromure de N-(*p*.méthoxy-phénacyle)-pyridazinium

On dissout 0,8 g (0,1 mol) de pyridazine dans 15 ml alcool méthylique anhydre et on ajoute une solution de 2,29 g (0,1 mol) de bromure de N-*p*. méthoxy-phénacyle dans 30 ml d'alcool mé-

thylique anhydre. On mélange les deux solutions et on abandonne le mélange réactionnel à la température ambiante pendant 24 h. On filtre le produit blanc séparé. On recristallise dans de l'alcool éthylique. Cristaux blancs à p.f. 219°C.

Analyse : $C_{13}H_{13}O_2N_2Br$ (M=309)

	N %
Calculé :	9,06
Trouvé :	9,38

Spectre IR (KBr), [cm^{-1}] : $\nu_{C=O}$=1 673, $\nu_{C=C,\ C=N}$ =1 598, 1 569, 1 507, ν_{C-O-C}=1 228, 1 165.

3.2. Bromure de N-(*p*.méthoxy-phénacyle)-pyridazinium (4, R=$-CH_3$)

On dissout 1,7 g (0,01 mol) de *p*.tolyle-pyridazine dans 20 ml alcool méthylique anhydre et on ajoute une solution de 2,29 g (0,1 mol) de bromure de *p*.méthoxy-phénacyle dans 35 ml d'alcoole méthylique anhydre. On mélange les deux solutions et on abandonne le mélange reactionnel à la température ambiante pendant 24 h. On obtient un produit blanc à p. f. 134°C.

Analyse : $C_{20}H_{19}O_2N_2Br$ (M=399)

	C %	H %	N %
Calculé :	60,15	4,76	7,01
Trouvé :	61,07	4,46	7,16

Spectre IR (KBr), [cm^{-1}] : $\nu_{C=O}$=1 674, $\nu_{C=C,\ C=N}$=1 596, 1 567, 1 503, 1 442, ν_{C-O-C}= = 1 163, 1 232.

Spectre de RMN ($CDCl_3$, TMS, δ [ppm]) : 2,36 (singulet (3 H, CH_3)) ; 3,77 (singulet (3H, OCH_3)) ; 6,82 (doublet, 2H, H_i) ; J=7,5 Hz ; (singulet) 6,86 (2 H, CH_2) ; 7,17 doublet (2 H, H_m), J = 7,5 Hz ; 7,85 doublet (2 H, H_n), J = 7,5 Hz ; 7,96 doublet (2 H, H_k), J = 7,5 Hz ; 8,76 multiplet (1 H, H_u), J = 9 Hz ; J = 5 Hz ; 8,83 multiplet (1 H, H_v), J = 9 Hz, J = 1,8 Hz ; 10,2 multiplet (1 H, H_z), J=5 Hz, J=1,8 Hz.

3.3. Bromure de N-(*p*-méthoxy-phénacyle)-3-(*p*.chlorphényle)-pyridazinium (4, R=Cl)

On dissout 1,9 g (0,01 mol) (*p*.chlor-phényle)-pyridazine dans 20 ml d'alcool méthylique anhydre et 2,23 g (0,01 mol) bromure de N-*p*-méthoxy-phénacyle dans 30 ml d'alcool méthylique anhydre. On mélange les deux solutions et on abandonne le mélange réactionnel à la température ambiante pendant 24 h. On filtre le produit séparé. Cristaux blancs à p. f. 109°C.

Analyse : $C_{19}H_{16}O_2N_2ClBr$ (M=419)

	N %
Calculé :	6,68
Trouvé :	7,02

Spectre IR(KBr), [cm^{-1}]:$\nu_{C=O}$=1 677, $\nu_{C=C,\ C=N}$=1 555, 1 568, 1 504, 1 443 ; ν_{C-O-C}= =1 160 ; 1 233 ; ν_{C-Cl}=737.

Spectre de RMN ($CDCl_3$, TMS, δ, [ppm]) : 3,83 singulet (3 H, OCH_3) ; 6,76 doublet (2H, H_i), J=7,5 Hz ; 6,85 singulet (2 H, CH_2) ; 7,35 doublet (2 H, H_m), J=7,5 Hz ; 7,90 doublet (4 H, $2H_k+2H_n$), J=7,5 Hz ; 8,9...9,2 multiplet (2 H, H_u+H_v) ; 10,2...10,45 multiplet (1H, H_z).

3.4. Pyridazinium-(*p*.méthoxy)-phénacylure (5, R=H)

On suspend 3,09 g (0,01 mol) de sel (3) dans 40 ml eau froide et on ajoute, en petites portions, une solution de 1,4 g K_2CO_3 dans 20ml eau froide en agittant continuellement. On observe la précipitation de l'ylure coloré en jaune intense. P. f. 145°C.

Analyse : $C_{13}H_{12}O_2N_2$ (M=228)

	N %
Calculé :	12,28
Trouvé :	13,02

Spectre IR (KBr), [cm^{-1}] : $\nu_{C=O}$= 1 665 ; $\nu_{C=C,\ C=N}$ = 1 596, 1 567, 1 503, 1 441 ; ν_{C-O-C}=1 160, 1 232.

3.5. 3-(*p*-tolyl)-pyridazinium-(*p*-méthoxy)-phénacylure (6, R=CH_3)

On dissout 4 g (0,01 mol) de sel ((4), R=CH_3) dans 40 ml eau froide et on ajoute, goutte à goutte, une solution de 1,4 g (0,01 mol) K_2CO_3 dans 20 ml d'eau. Il se sépare un produit orange. On filtre, on lave à l'eau jusqu'à pH neutre. Produit orange à p. f. 124°C.

Analyse : $C_{20}H_{18}O_2N_2$ (M=318)

	N %
Calculé :	8,80
Trouvé :	7,88

Spectre IR(KBr, [cm^{-1}]) : $\nu_{C=O}$ = 1 663 ; $\nu_{C=C,\ C=N}$ = 1 594, 1 566, 1 502, 1 442 ν_{C-O-C}=1 161, 1 231.

Spectre de RMN ($CDCl_3$, TMS, δ, [ppm] : 2,31 singulet (3 H, CH_3) ; 3,8 singulet (3H OCH_3) ; 6,7...8,2 multiplet (11 H aromatiques $+\overset{(-)}{\underset{\cdot\cdot}{C}}H$).

3.6. 3-(*p*.chlor-phényle)-pyridazinium-(*p*.méthoxy-phénacylure) (6, R = $-Cl_8$)

On suspend 4,19 g (0,01 mol) de sel (4, R = —Cl) dans 40 ml d'eau et on ajoute, goutte goutte, une solution de 1,4 g (0,01 m) K_2CO_3 dans 20 ml d'eau en agittant continuellement. On observe la précipitation de l'ylure coloré en orange foncé. On filtre, on lave à l'eau. Produit orange foncé à p. f. 134°C.

Analyse : $C_{19}H_{15}N_2O_2Cl$ (M=338)

	N %
Calculé :	8,28
Trouvé :	7,92

Spectre IR (KBr, [cm^{-1}]) : $\nu_{C=O}$ = 1 660 ; $\nu_{C=C}$, $\nu_{C=N}$ = 1 596, 1 568, 1 503, 1 445 ν_{C-O-C}=1 165, 1 236 ; ν_{C-Cl}=738.

Reçue le 8 mars 1990

Institut Polytechnique, Jassy,
Chaire de Chimie et Technologie
Organique et Macromoleculaire

BIBLIOGRAPHIE

1. Caproşu M. Ungureanu M., Petrovanu M., Bul. Inst. polit., Iaşi, **XXX (XXXIV)**, *1—4*, s. II, 73 (1984).
2. Zugrăvescu I., Petrovanu M., *Chimia N-ilidelor*. Ed. Acad. Bucureşti, 1974, 232.
3. Petrovanu M., Dorohoi D., Mai Van Tri, An. Şt. Univ. „Al.I. Cuza", Iaşi, Fizică, **XXII**, 41 (1979).
4. Mai Van Tri, *Compuşi dipolari din clasa difenilpiridazinei, arilpiridazinei, arilpiridazinelor şi alcoxipiridazinelor*. Thèse de doctorat, Inst. polit., Iaşi, 1975.

ACŢIUNEA BROMURII DE *p*-METOXI-FENACIL ASUPRA PIRIDAZINEI ŞI A UNOR 3-ARIL-PIRIDAZINE

(Rezumat)

În scopul aprofundării studiului privind relaţia structură—proprietăţi în clasa piridaziniu-ilidelor ne-am propus să obţinem noi săruri de cicloimoniu (3) (4, *a*, *b*) şi ilide (5), (6), (7) prin acţiunea bromurii de *p*.metoxi-fenacil asupra piridazinei, a 3-*p*.tolil-piridazinei şi 3-*p*.clorfenil-piridazinei. Păstrînd componenţa carbonionică nemodificată în seria piridaziniu-ilidelor respectiv se poate urmări influenţa modificărilor componentei cationice asupra stabilităţii şi reactivităţii ilidelor corespunzătoare.

BULETINUL INSTITUTULUI POLITEHNIC DIN IAŞI
Tomul XXXVI (XL), Fasc. 3—4, 1990
Secţia II
CHIMIE ŞI INGINERIE CHIMICĂ

D. C. 66.095.6 ; 615.45

SYNTHESIS OF ANTICANCEROUS SUBSTANCES

BY

VALERIU ŞUNEL and AL. CECAL

1. Introduction

Among the substances inhibiting the maligne tumours some alkylating compounds, such as N-mustards, deserve mention. The alkylating compounds are desadvantageous due to their toxicity affecting some normal tissues such as the intestinal epithelium and the haematopoetic organs.

The actual researches are aimed to improve the biologic characteristics of the alkylating agents by increasing their therapeutic indices and decreasing the toxicity. Thus, by binding the di-(β-chloroethyl)-amine residue on different biologically active substances [1]...[15] as well as by blocking the nitrogen unshared electrons by involving them in an amidic conjugated system [16]... [23], N-mustards with more selective action, lower toxicity and without side effects have bun prepared.

2. Results and Discussion

In order to study the correlation between the chemical structure and the biological action, in the present paper a N-mustard was synthetised with its active group graffed on a tripeptide consisting in the ester residue of to the di-[β-(bis-ethyl)-amino]-ethyl N-glycyl-N′-(*p*-aminobenzoyl)-L-aspartate.

In this aim, the di-[β-bis-ethyl)-amino]-ethylic ester of the N-(*p*-aminobenzoyl)-L-asparagic acid, (I) [24] was acylated by monochloroacetyl chloride in anhydrous benzene and in the presence of pyridine and the monochloroacetyl-N-(*p*-aminobenzoyl)-L-aspartate of di-[β-(bis-ethyl)-amino]-ethyl (II) obtained.

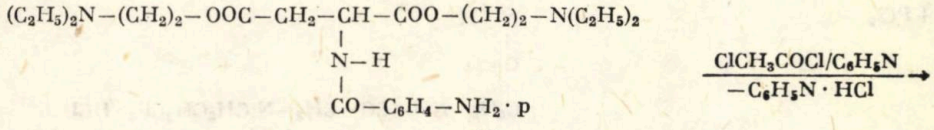

(I)

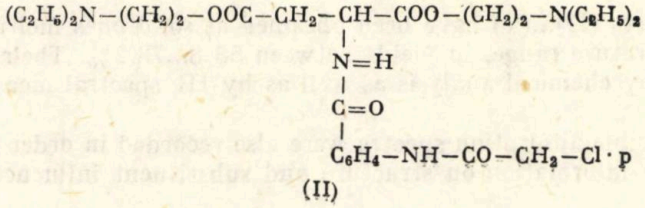

(II)

By the condensation of the product (II) with diethanolamine in acetone medium and in the presence of sodium acetate and kalium iodide the N-[di-(β-hidroxyethyl)-glycyl]-N'-(*p*-aminobenzoyl)-L-aspartate of di-[β-(bis-ethyl)-amino]-ethyl (III) was obtained :

$$(II) + \frac{HN(CH_2CH_2OH)_2/CH_3COONa/KI}{-NaCl\,;\ -CH_3COOH} \rightarrow$$

$$(C_2H_5)_2N-(CH_2)_2-OOC-CH_2-\underset{\displaystyle N-H}{\underset{|}{CH}}-COO-(CH_2)_2-N(C_2H_5)_2$$

$$\underset{\displaystyle C=O}{\underset{|}{}}$$

$$C_6H_4-NH-CO-CH_2-N(CH_2CH_2OH/2\cdot p$$

(III)

By the action of the cold gaseous hydrogen chloride on the ethanol solution of the compound (III), the di-[β-(bis-ethyl)-amino]-ethyl N-[di-(β-hydroxiethyl)-glycyl]-N'-(*p*-aminobenzoyl)-L-aspartate nydrochloride (IV) was obtained in a high yield :

$$(C_2H_5)_2N-(CH_2)_2-OOC-CH_2-\underset{\displaystyle N-H}{\underset{|}{CH}}-COO-(CH_2)_2-N(C_2H_5)_2$$

$$(III) + HCl/0...2°C \rightarrow \qquad \underset{\displaystyle C=O}{\underset{|}{}}$$

$$C_6H_4-NH-CO-CH_2$$

$$\overline{N(CH_2)CH_2OH)_2}\cdot HCl$$

(IV)

According to literature methods [8], [9], [14], [20], [25], by substituting chlorine for the hydroxy groups in the di-(β-hydroxyethyl)-glycylamino-compound the corresponding di-(β-chloroethyl)-glycyl-amino derivative resulted.

Thus, the treating of the hydrochloride (IV) with phosphorus pentachloride at a temperature between −5° and −8°C, in a chlorophorm medium resulted in obtaining the di-[β-(bis-ethyl)-amino]-N-[di-(β-chlotoethyl)-glycyl]-N'-(*p*-aminobenzoyl)-L-aspartate hydrochloride (V) :

$$(C_2H_5)_2N-(CH_2)_2-OOC-CH_2-\underset{\displaystyle N-H}{\underset{|}{CH}}-COO-(CH_2)_2-N(C_2H_5)_2$$

$$(IV) + PCl_5 \rightarrow \qquad \underset{\displaystyle C=O}{\underset{|}{}}$$

$$C_6H_4-NH-CO-CH_2-N(CH_2CH_2Cl)_2\cdot HCl$$

(V)

The products (II)...(V) have been obtained as solid ones melting within a narrow temperature range, in yields between 58.8...78.2%. Their structure was confirmed by chemical analysis as well as by IR spectral measurements [26].

The UV-visible absorption spectra were also recorded in order to obtain a more complete information on structure and substituent influence.

As known [27], the grafting of substituents on the benzene ring results in shifting the $\pi-\pi^*$ absorption bands toward longer wavelengths. The shifting of the absorption maximum depends on the substituent character and position. The largest shifting of the absorption maximum appears with the *para*-substituents [27], [28].

The electronic absorption spectra of the compounds (I) ...(V) were recorded in dimethylformamide solution by a Spekord UV—VIS spectrophotometer.

The cell thickness was of 0.2 cm in all measurements.

The obtained results are given in Table 1. The UV absorption bands were identified by taking the di-[β-bis-ethyl)-amino]-ethylic ester of the N-(*p*-aminobenzoyl)-L-asparagic acid (I) as a standard; the compounds under study shaw a single UV absorption band between 280.3...365 nm. The ε_{max} values of the 10^4 order of magnitude of the five products are indicative of a $\pi-\pi^*$ type transition. The shifting of the absorption maximum toward longer wavelengths is probably due to the substituent influence on the nitrogen unshared electrons while are implied in a conjugation with the aromatic system.

In the compounds (II)...(V) the substituents at the amino group exert a stronger batochromic effect on the molecule in the following decreasing order of the charge density on the nitrogen atom :

$$-COCH_2Cl < -COCH_2N(CH_2CH_2OH)_2 < -COCH_2N(CH_2CH_2OH)_2 \cdot HCl <$$

$$< -COCH_2N(CH_2CH_2Cl)_2 \cdot HCl$$

Table 1

Absorption Maxima and Extinction Coefficients of Compounds (I)... (V)

Compound	Concentration mol · l^{-1}	λ_{max} nm	ε_{max}
(I)	2×10^{-4}	280.3	1.93×10^4
(II)	2×10^{-4}	284.0	2.01×10^4
(III)	2×10^{-4}	308.2	2.15×10^4
(IV)	2×10^{-4}	344.0	2.74×10^4
(V)	2×10^{-4}	365.0	3.75×10^4

3. Experimental

3.1. Di-[β-(bis-ethyl)-amino]-ethylic Ester of N-(*p*-aminobenzoyl)-L-asparagic Acid (I)

It was obtained by the reduction of the di-[β*(bis-ethyl)-amino]-ethylic ester of the N-(*p*-nitrobenzoyl)-L-asparagic acid by Ni-Raney in anhidrous ethylic alcohol [24].

3.2. Di-[β-(bis-ethyl)-amino]-ethylic Ester of Monochloroacetyl-N-(*p*-aminobenzoyl)-L-asparagic Acid (II)

In a 250 ml flask, provided with reflux condenser a suspension of 0.0125 moles ester (I) in 150 ml anhidrous benzene is prepared and 0.015 moles monochloroacetyl chloride and 5 ml pyridine added. The mixture is refluxed for 3 hours on a water bath. The benzene excess is then removed by distillation under vacuum and resulting pyridine hydrochloride by repeated washings

with distilled water. The oil product thus obtained is converted into yellow crystalls by washing with anhydrous ethylic ether. It is purified by dissolution in ethylic alcohol followed by the precipitation in a small amount of water. After filtration the product is dryied under vacuum at 45...50°C for 6 hours.

Product melting at 110°...112°C. Reaction yield 78.2%.

Analyses ($C_{25}H_{39}ClN_4O_6$)	C%	H%	Cl%	N%
Calculated :	63.76	8.28	7.54	11.90
Found :	63.65	8.61	7.90	12.31
	63.97	8.70	7.97	12.38

The IR spectrum (KBr : 3 100 cm^{-1} ν_{N-H} ; 1 735 cm^{-1} $\nu_{C=0\ ester}$; 1 640 cm^{-1} 1 645 cm^{-1} $\nu_{C=0}$;1 180 cm^{-1} ν_{C-H} ; 785 cm^{-1} ν_{C-C}[1] ; 795 cm^{-1}, 805 cm^{-1} $\nu_{C-H\ aromatic}$.

3.3. Di-[β-(bis-ethyl)-amino]-ethyl N-[di-(β-hydroxyethyl)-glycyl]-N′-(*p*-aminobenzoyl)-L-aspatate (III)

In a 100 ml flask provided with reflux condenser, 0.010 moles of compound (II) are solved in 30 ml anhydrous acetone and 0 015 moles anhydrous sodium acetate, 0.015 moles diethanolamine and 0.0015 moles Kalium iodide added. The reaction mixture is refluxed on a water bath for 10 hours. The insoluble salts are filtred aff and the acetone distilled. The residue is purified by acetone dissolution followed by distilled water addition till precipitation. After filtration and drying under vacuum at 60°...65°C, the pure product is obtained as a colorless powder melting at 152°...155°C.

Yield 70.7%.

Analyses ($C_{29}H_{49}N_5O_8$)	C%	H%	N%
Calculated :	58.48	8.23	11.76
Found :	58.65	8.24	11.95
	58.81	8.47	12.00

The IR spectrum (KBr) : 3 210 cm^{-1}, 3 400 cm^{-1} ν_{N-H} ; 1 735 cm^{-1} $\nu_{C=0\ ester}$; 1 640 cm^{-1}, 1 645 cm^{-1} $\nu_{C=0amidic}$; 1 170 cm^{-1}, 1 195 cm^{-1} ν_{C-O} ;1 070 cm^{-1} ν_{C-OH}; 1 300 cm^{-1} ν_{C-N}; 820 cm^{-1}; 840 cm^{-1} $\nu_{C-H\ aromatic}$.

3.4. Di-[β-(bis-ethyl)-amino]-ethyl N-[di-(β-hydroxyethyl)-glycyl]-N′-(*p*-amihobenzoyl) L-aspartate Hydrochloride (IV)

In a 100 ml two-neck flask provided with stirring and hydrogen chloride bubbler 0.005 moles of the compound (III) are solved in 25 ml ethylic alcohol.

The reaction mixture is cooled to 0°C, and a stream of anhydrous gaseous hydrogen chloride admitted till saturation. Ethylic ether previously saturated by hydrogen chloride is then added stepwise till a colorless crystalline product precipitates. After filtration and drying in an oven under low pressure at 80°...100°C the pure product melting at 240°...243°C is obtained in 72.3% yield.

Analyses ($C_{29}H_{50}ClN_5O_8$)	C%	H%	Cl%	N%
Calculated :	55.10	7.91	5.62	11.08
Found :	55.47	8.09	6.03	11.46
	55.53	8.19	6.10	11.52

The IR spectrum (KBr) : 3 258 cm^{-1}, 3 450 cm^{-1} ν_{N-H} ; 1 740 cm^{-1} $\nu_{C=0\ ester}$; 1 642 cm^{-1},1 645 cm^{-1} $\nu_{C=0\ amidic}$; 1 175 cm^{-1}, 1 200 cm^{-1} ν_{C-H} ; 1 075 cm^{-1} ; 1 310 cm^{-1} ν_{C-N}; 830 cm^{-1}, 845 cm^{-1} $\nu_{C-H\ aromatic}$.

3.5. Di-[β-(bis-ethyl)-amino]-ethyl N-[di-(β-chloroethyl)-glycyl]-N′-(*p*-aminobenzoyl)-L aspartate Hydrochloride (V)

In a 250 ml three-neck flask provided with condenser with calcium chloride tube, stirring and cooling system, a suspension of 0.01 moles of product (IV) in 150 ml anhydrous chloroform

is prepared 0.005 moles of phosphorous pentachloride is then added stepwise under good stirring between −5° and −6°C, during 40...50 min. The reaction mixture is then maintained under stirring for another 90 min. at the same temperature. The chloroform is then evaporated under low pressure at 30°...35°C, till a volume of 30...40 ml. By adding anhidrous ethylic ether and petroleum ether (3 : 1) a colorless crystalline product separated. It is filtred, dried under vacuum at 40°C for 6 hours. The pure product melting 128°... 130°C is thus obtained in 58.8% yield.

Analyses ($C_{29}H_{48}Cl_3N_5O_6$)	C%	H%	Cl%	N%
Calculated :	52.05	7.18	15.93	10.47
Found :	52.41	7.42	16.27	10.57
	52.53	7.48	16.23	10.59

The IR spectrum (KBr): 3 370 cm^{-1}, 3 455 cm^{-1} ν_{N-H} ; 1 745 cm^{-1} $\nu_{C=O\ ester}$; 1 655 cm^{-1}, 1 660 cm^{-1} $\nu_{C=O\ amidic}$; 1 150 cm^{-1}, 1 170 cm^{-1} ν_{C-H} ; 1 300 cm^{-1} ν_{C-N} ; 745 cm^{-1}, 770 cm^{-1} ν_{C-Cl}.

4. Conclusions

Four new derivatives (II)...(V) of the di-[β-(bis-ethyl)-amino]-ethylic ester of the N-(*p*-aminobenzoyl)L-asparagic acid (I) have been synthesized.

A new N-mustard (V) was obtained as hydrochloride by substituting chlorine for hydroxy group in the di-(β-hydroxyethyl)-glycyl-amino-derivative (IV) hy means phosphorous pentachloride.

The di-(β-chloroethyl)-amino group grafted on a tripeptide might confer a lower toxicity and higher selectivity as well as properties of an alkylating agent to the product (V).

The structures of the compounds (II) ...(V) were elucidated by means of elementar analysis data as well as by IR and UV spectral measurements. The UV spectra made evident some electronic influen es of some atom groups in the structure of the compounds under study.

Received, March 12, 1990

Polytechnic Institute, Jassy,
Department of Macromolecular and
Organic Chemistry

REFERENCES

1. Bergel F., Stock J., J. Chem. Soc., 4 568 (1957).
2. Берлин А. Е., Брановицкая В. П., ЖОХ, **30**, 324 (1960),
3. Кнунянц И. Л., Килдышева О.В., Голубова Н.Е., Изв. АН СССР, ОХН, 133 (1969).
4. Budeanu C. H., Şunel V., An. şt. Univ. „Al. I. Cuza", Iaşi, S. Ic, **18**, 169 (1972).
5. Budeanu C. H., Şunel V., Iancu I., Dăneţ R., Rev. Medico-Chirurgicală, Iaşi, **77**, 817 (1973).
6. Budeanu C. H., Şunel V., An. şt. Univ. „Al. I. Cuza", Iaşi, s. Ic, **20**, 207 (1974).
7. Budeanu C. H., Şunel V., Bul. Inst. polit., Iaşi, **21** (**25**), *1—2*, s. II, 71 (1975).
8. Şunel V., Budeanu C. H., Mazilu I., Apostolescu M., Bul. Inst. polit. Iaşi **25** (**29**), *1—2*, s. II, 85 (1989).
9. Budeanu C. H., Şunel V., Iorga T., Cecal A., Rev. Farmacia, Bucureşti, **28**, 1 (1980).
10. Şunel V., Apostolescu M., Budeanu C.H., Dăneţ D., Rev. de chimie, **33**, *12*, 1 099 (1982).
11. Şunel V., Budeanu C. H., Herdan J., Sîrghie I., Bul. Inst. polit., Iaşi, **28** (**33**), *1—4*, s. II, 77 (1982).
12. Cecal A., Şunel V., J. Radioanal. Chem., **78**, *2*, 247 (1983).

13. Năstasă V., Șunel V., Dăneț D., Dăneț R., Rev. Medico-Chirurgicală, Iași, **87** 619 (1983).
14. Șunel V., Cecal A., Rev. de chimie, **34**, 5, 394 (1983).
15. Șunel V., Ciugureanu C., Budeanu C. H., Antohe N., Rev. de chimie, **36**, *5*, 397 (1985).
16. Arnold H., Bourseaux F., Angew. Chem, **70**, 539 (1958).
17. Budeanu C. H., Șunel V., An. șt. Univ. „Al. I. Cuza", Iași, **17**, s. Ic, 207 (1971).
18. Budeanu C. H., Șunel V., An. șt. Univ. „Al. I. Cuza", Iași, s. Ic, **20**, 199 (1974).
19. Budeanu C. H., Șunel V., Bul. Inst. polit., Iași, **24** (**28**), *1—2*, s. II, 95 (1978).
20. Budeanu C. H., Ivas E., Șunel V., Bul. Inst. polit., Iași, **27** (**31**), *3—4*, s. II, 71 (1981).
21. Șunel V., Ivas E., Budeanu C.H., Bul. Inst. polit., Iași, **33** (**37**), *1—4*, s. II, 57 (1987).
22. Șunel V., Ciugureanu C., Budeanu C.H., Antohe N., Popa M., Rev de chimie, **39**, 7, 577 (1988).
23. Șunel V., Ciugureanu C., Bul. Inst. polit., Iași, **35** (**39**), *3—4*, s. II, 51 (1989).
24. Șunel V., Ciugureanu C., Budeanu C. H., Rev. de chimie, **37**, *10*, 855 (1986).
25. Fletchor L. T., Wetzel H. W., J. Org. Chem., **25**, 1 348 (1960).
26. Avram M., Mateescu C. D., *Spectroscopia în infraroșu. Aplicații în chimia organică*. Ed. Tehn., București, 1966.
27. Pogany I., Banciu M., *Metode fizice în chimia organică*. Ed. Științifică, București, 1972.
28. Jaffe H., Orchim M., *Theory and Application of Ultraviolet Spectroscopy*, John Willey a. Sons, New-York, 1962.

SINTEZE DE SUBSTANȚE ANTICANCEROASE

(Rezumat)

În scopul încercărilor asupra acțiunii citostatice a unor combinații chimice față de tumori experimentale s-a sintetizat un nou achilant cu gruparea di-(β-cloretil)-aminică grefată pe un tripeptid, format din restul esterului N-glicil-N(*p*-amino-benzoil)-L-aspartatului de di-[β-(bis-etil)-amino]-etilic.

BULETINUL INSTITUTULUI POLITEHNIC DIN IAȘI
Tomul XXXVI (XL), Fasc. 3—4, 1990
Secția II
CHIMIE ȘI INGINERIE CHIMICA

D. C. 542.973.8 ; 547.533

DEPENDENCE BETWEEN THE ACTIVITY AND SELECTIVITY OF NaLaY AND NaCeY CATALYSTS IN THE CATALYTIC DISPROPORTIONATION OF TOLUENE

BY

A. AZZOUZ, D. BOUTARFA, D. NIBOU, B. ABBAD, EMIL DUMITRIU and V. HULEA

1. Introduction

Although high silica/alumina zeolites with improved shape selectivity are intensive used in *p*-dialkylbenzenes production [1]...[7] the faujasites still present scientific interest [8]...[12]. They remain the most flexible is all hydrocarbon conversions due to of their large pore structure. According to the cation introduced and working conditions, especially the conversion degree, the faujasites selectivity could be orientated.

The activity is the main criterion to estimate a catalyst performances but the selectivity is also a determinant factor of the efficiency. Although there is an inverse pseudoproportionality between the activity and selectivity of a catalyst in the toluene disproportionation. The number of involved reactions in the global process is a direct function of the reaction temperature. In a limited temperature range the selectivity may be a linear function of the activity. The notion of selectivity can be applied only if the conversion are appreciable (for example, more than 10 ...15 % mol). Otherwise, for conversions higher than 50 % it is difficult to deal with selectivity because of the preponderance of side reactions. Moreover the deposited coke modifies somewhat the catalysts specifications and reduces considerably their lifetimes. So the resulting compromise the limits of the activity—selectivity correlation to a field of moderated working conditions which permit to obtain conversions in the range 15...45 % mole at molar ratios B/T and $B/(X+2TMB)$ not exceeding a value of 1.5. In this context the present work was achieved.

The study deals with the dependence between activity and selectivity of some rare earths exchanged faujasites in toluene disproportionation.

2. Experimental

In order to obtain reproductible and comparable results, the conversion process of toluene was carried out in the same conditions for all the catalysts tested (a glass tubular reactor with a fixed bed of catalyst, WHSV=0.7 h^{-1}, Nitrogen/Toluene=0.134 mole/mole, $P=1$ atm, $t=90$ min, at different temperatures). The catalysts were Y-faujasites ion-exchanged with lanthanum or cerium and calcined at 500°C under nitrogen during 3 hours. The catalyst granulometry (1...2 mm) permit to avoid or at least to minimize extremly the diffusion phenomenon under such working conditions. The catalysts were compared to those modified with strontium and cobalt [13]...[15].

The chronological sampling of the reactional mixture was followed by gas chromatography analysis using a 4 mm ×4.7 m column filled with bentone and dynonylphthalate/chromosorb WAWS.

3. Results and Discussions

The selectivity in relation to the main process is correlated by the molar ratios B/T or $B/(X+2\,TMB)$, whereas the activity is represented by the molar conversion of toluene. The better the selectivity (to methyl transposition processes), the closer to unity will be these ratio values. The limit value corresponds to the stoechiometric reactions of toluene disproportionation (with or without xylenes isomerization, and which produces as much benzene as xylenes) or to the extented process to xylenes disproportionation :

(I) $2T \rightarrow B + p\text{-}X$, (II) $2T \rightarrow B + o\text{-}X$, (III) $o\text{-}X \rightarrow m\text{-}X$,
(IV) $p\text{-}X \rightarrow m\text{-}X$, (V) $2X \rightarrow B + TMB$.

The increase of the conversion degree enhances B/X molar ratio for both types of catalysts (Figs. 1 and 2). The shape of curves show that the fraction of converted toluene is not equal to the sum of benzene and xylenes fractions produced, even at low conversion degrees. This means that a part of toluene is cracked or polycondensed.

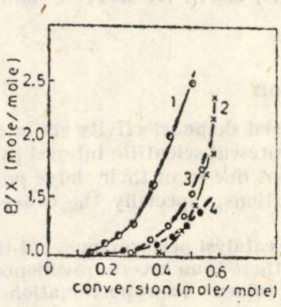

Fig. 1. — Variation of B/X ratio vs. conversion degree for NaLaY catalyst with various degrees of Na substitution : *1* — 74% ; *2* — 73% ; *3* — 71% ; *4* — 54%.

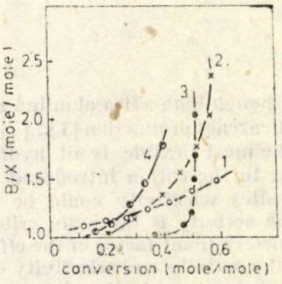

Fig. 2. —Variation of B/X ratio vs. conversion degree for NaCeY catalyst with various degrees of Na^+ substitution : *1* — 75% ; *2* — 73% ; *3* — 70% ; *4* — 56% .

This observation is valid for both type of catalysts and the curves molar ratio B/X versus conversion degree are very similar. For high values of B/X ratio, the conversion degree tends to 60 % mol, which corresponds to the thermodynamic equilibrium [13]. The selectivity to the main products is maximal when B/X value is equal to unity. It was found that the $B\ X$ ratio is a linear function of conversion over some catalysts [5]. In the present case, this ratio depends not only on conversion but also on the number and the cation nature introduced and the curves present a certain concavity.

Another limit consists in a perpendicular line, i.e. $B/X=1$, for low conversion degrees. The resulting area could be considered as the functionality field of a catalyst.

On the other hand, the shape of the curves show certain differences regarding the behaviour of different catalysts. These behaviour are specifical rather by the nature and the number of the active sites than by the reactional

mechanisms. In this context a special interest must be devoted to catalysts such $NaCeY_3$ and $NaLaY_2$.

All the alkylbenzenes undergo a cracking process and the required acidity strenghth decreases with their increasing molecular weights. The increase of conversion degree improves unavoidably TMB formation. $B/(X+2TMB)$ molar ratio will represent, by extension, the catalyst selectivity with respect to the global process devoided of dissociation and condensation reactions, i.e. only to methyl rearrangement processes. Anyway, the coke formation occurs even at low conversion degrees (Fig. 3) but its amount may be limited by the number of Lewis sites. The coke amount seems to present a certain dependance on these two ratios.

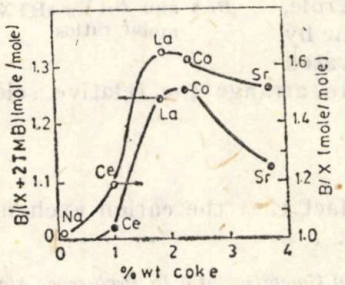

Fig. 3.—Dependence of the selectivity on coke yielding.

Trimethylbenzenes seem to be not implied in the dissociation processes even for a non-negligible amount of coke (1%). This proves that coke is formed overall from toluene and xylene for B/X value smaller than 1.1. Above this value (coke amount of 1...2%), the TMB contribution (increase of $B/(X+2\,TMB)$) is more evident. For an excessive coke deposit (2.0... 2.25%), B/X and $B/(X+2\,TMB)$ ratios reach maximal values (1.32 and 1.25 respectively). The contributions of xylenes and trimethylbenzenes become appreciable.

For more important coke deposits, the values of the two ratios decrease again as result of the slightly improving of selectivity. This decrease results by the implication of higher molecular weight substances, therefore being necessary to take into consideration other types of ratios. Theoretically, the coke amount is proportionnal to the molecular weight of the contributing substances. However, this figure allows to situate accurately the selectivity for each catalyst.

The Bronsted acid sites catalyze as toluene disproportionation as isomerization and disproportionation of xylenes according to acidity strenghth. The zeolite dehydration by the temperature increase improves dissociation processes [14]...[16]. Excessive poisoning of the surface enhances the selectivity. Anyway, the dealkylation facility is proportional to the number of around it.

The effect of B/X value upon trimethylbenzenes formation (Fig. 4) shows that the fraction of the latters is smaller than that of converted xylenes. Thus the toluene cracking and the disproportionation of xylene occur simultaneously.

The Fig. 4 confirms the previous conclusions. Thus, the unit value of ratio $B/(X+2TMB)$ seems be a limit corresponding to the beginning of the xylenes consumption in trimethylbenzenes and coke formation. Therefore, the chronological succesion could be as follows : 1° disproportionation and pyrolysis of toluene ; 2° isomerization and pyrolysis of xylenes ; 3° xylene disproportionation and trimethylbenzenes isomerization ; 4° trimethyl-

benzenes pyrolysis; 5° polyalkylation — condensation; 6° pyrolysis of heavy products.

4. Conclusion

The above presented data allow us to affirm that the thermodynamic equilibrium existing between these different processes can be disturbed by the catalysts specifications. On the other hand, the stability to the pyrolysis depends of the molecule weight and the catalysts specifications. If the shape selectivity is not very important, the nature of the surface selectivity plays the main role. Anyway, this process is attenuated in the time by the progressive poisoning of the most activated centers by coke. All tested catalysts permit to arrange the relative selectivities of these in the following order :

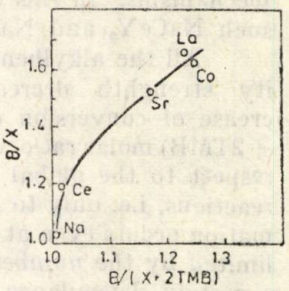

Fig. 4.— Relation between B/X and $B/(X+\text{sBTX})$ molar ratios.

$$CeY > LaY > CoY,$$

and the experimental results converge to the fact that the cation exchange by cerium ions seem to be most advantageous.

Received, March 21, 1990

Haut Commisariat à la Recherche, Algier
Organic Synthesis Division
and
Polytechnic Institute, Jassy,
Department of Organic Chemical Technology

REFERENCES

1. Corma A., Cortes A. A., Rev. Acad. Cien. Exactas, Fis. Mat., Madrid, **79**, *3*, 449 (1985),
2. Ciambelli P., Bagnasco G., Nastro A., Aiello R., Crea F., Chem. Express. **1**, *2*, 741 (1986).
3. Neshram N. R., Hedge S. G., Kulkarni S. B., Zeolites, **6**, *6*, 434 (1986).
4. Kuerscher U., Parlitz B., Schreiner E., Appl. Catal., **30**, *4*, 159 (1987).
5. Nayak V. S., Riekert L., Appl. Catal., **23**, *2*, 403 (1986).
6. Meshram N. R., J. Chem. Tech. Biotch., **37**, *2*, 111 (1987).
7. Benzouharova C., Dimitrov C., Nenova V., Spassov B., Lechert H., Appl. Catal., **21**, *1*, 149 (1986).
8. Mai T. Dimitrov Kh., Van D., Khim Fak., **73**, 124 (1981), (publ. 1985).
9. Barooah M. K., Chand S., Rao B. K. B., 7th. Adv. Catal. Proc. Symp. Catal., 1985, 365.
10. Barakat Y., Mikhail S., Ayoub S. M., Zeolites, **7**, *3*, 235 (1987).
11 Дадашев Б. А., Сариджанов А. А., Кадинова А. А., ДАН АзССР. **40**, *1*, 59 (1984).
12. Bein T., Tielen M., Jacobs P. A., Ber. Bensen-Ges. Phy. Chem., **90**, *4*, 395 1981)
13. Oprea S., Azzouz A., Dumitriu E., Constantinescu M., Bull. Soc. Chim. Belg., **92**, *3*, 289 (1983).
14. Azzouz A., Fourar M., Berrak A., Bull. Soc. Chim. Belg., **95**, *12*, 1 059 (1986).
15. Oprea S., Azzouz A., Dumitriu E., Bîlbă N., Rev. Roum. Chim., **29**, *11—12*, 887 (1984).
16. Chu Y. F., Chester A. W., Zeolites, **6**, *3*, 195 (1986).
17. Mikhail S., Ayoub S. M., Barakat Y., Zeolites, **7**, 231 (1987).

DEPENDENŢA DINTRE ACTIVITATEA ŞI SELECTIVITATEA CATALIZATORILOR NaLaY şi NaCeY ÎN DISPROPORŢIONAREA CATALITICĂ A TOLUENULUI

(Rezumat)

S-a studiat reacţia de disproporţionare a toluenului pe faujasit Y schimbat ionic cu lantanide. S-a urmărit relaţia activitate — selectivitate în diverse condiţii de operare, precum şi influenţa cocsului depus pe suprafaţă asupra proprietăţilor catalizatorilor testaţi.

Pe baza rezultatelor obţinute s-a făcut o ordonare a catalizatorilor în funcţie de activitatea lor :

$$CeY > LaY > CoY.$$

BULETINUL INSTITUTULUI POLITEHNIC DIN IAȘI
Tomul XXXVI (XL), Fasc. 3—4, 1990
Secția II
CHIMIE ȘI INGINERIE CHIMICĂ

D. C. 615.414

MODELING OF PROCESS OF ATROPINE EXTRACTION FROM *RADIX ATROPA BELLADONNA*

BY

CORNELIU ONISCU, EUGEN HOROBA, IONEL MARCEL POPA, CAMELIA ȘOLDEA and OLGA NĂSTASĂ

1. Introduction

The atropine is an alkaloid with characteristic drug properties, being used in ophthalmology for its mydriatic action as well as in treatments of digestive tube, of gastric hyperacidity, etc. [1]. It may be obtained either by extraction from different plants of the *Solanaceae* species or by synthesis from tropic acid and tropanol and has formula :

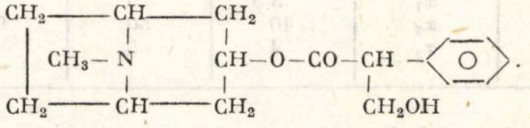

Atropa Belladonna, *Datura Stramonium* and *Hyoscyamus* are the principal natural sources of atropine which is contained in roots, leavs and seeds. Since the greatest amount of atropine is contained in roots we studied the extraction process from dried roots [2], [3].

2. Experimental

The roots of *Atropa Belladonna* were finely ground and the obtained powder treated with a 10% sodium carbonate solution to release the atropine from its salts. The aqueous phase was then separated and the plant submitted to extraction in ethylic alcohol.

The extraction process has been accomplished in a glass vessel having a 2 L volume. An impeller with the diameter of the active element of $0.5D$ (D — the inner diameter of the extractor) has been used. The temperature has been kept constant by means of a thermostat.

The quantitative analysis of atropine in the obtained extracte was carried out by high performance liquid chromatography using a VARIAN, model 5020, chromatograph. The optimum wave length for atropine detection is of 256, nm, under the following conditions : a) a column of the MicroPak®CN-10 type of 250 ×4.5 mm; b) mobile phase : acetonitrile (Merck, for HPLC)/ water (brought to pH=2.5 by perchloric acid), 80/20 V/V at a flow rate of 0.5 mL/min. ; c) a detector of variable wavelength, of the VARICHROM type ; the detection was performed at the wavelength of 256 nm and sensitivity of

0.2 AUFS; d) the volume of the automatically injected sample of 10 μL ; e) the paper recording rate : 1 cm/min.

The quantitative dosing of atropine in the samples was made automatically, by the external standard method using a CDS-111 L integrator type

3. Results and Discussion

The studies on the modelling of the atropine extraction process from *Radix Atropa Belladonna* were aimed to settle a correlation between the extraction performances and the variables influencing the process : solvent / plant massic ratio, temperature and duration.

In this purpose, real values of the process variables were arbitrary chosen as well as their variation limits and coding (Table 1).

Table 1

Level of Independent Variables

Variable	Notation	Coded levels			Step
		−1	0	+1	
Ethanol/plant mass ratio	x_1	3.5	5	6.5	1.5
Temperature, [°C]	x_2	40	50	60	10
Duration, [h]	x_3	4	5	6	1

The model advanced for settling the correlation between the quantity of extracted atropine and the variables influencing the process is of the following form :

(1) $$Y=b_0+b_1x_1+b_2x_2+b_3x_3+b_{12}x_1x_2+b_{13}x_1x_2+b_{23}x_2x_3+b_{123}x_1x_2x_3,$$

where : Y denotes the amount to be modeled and describes the performance of the extraction process measured by the atropine quantity in the extract, [g atropine/100 g plant]; b_{jk} — coefficients of regression equation and x_i — independent variable (coded values).

The used experimental matrix, of the 2^3 type, is given in Table 2, with Y_i — the answer.

According to the programme eight independent runs were made as well as four runs to settle the precision of the experimental method [4].

The results in the programme center were checked by using the test Q [5]; the amplitude of the series is :

(2) $$M=Y_{max}-Y_{min}=0.7514-0.1142=0.6372$$

and :

(3) $$Q_c=\frac{0.6228-0.1142}{0.6372}=0.8138.$$

Since Q_c exceeds the tabulated value of Q :

(4) $$Q_t(P=95\%,\ n=4)=0.77,$$

Table 2

Experimental Matrix

Experiment No.	Independent variables			Y g atropine /100 g plant	Y_c
	x_1	x_2	x_3		
1	−1	−1	−1	0.1657	0.1657
2	−1	−1	+1	0.5024	0.5025
3	−1	+1	−1	0.2171	0.2171
4	−1	+1	+1	0.4314	0.4315
5	+1	+1	+1	0.4776	0.4775
6	+1	+1	−1	0.2624	0.2623
7	+1	−1	−1	0.1657	0.1657
8	+1	−1	+1	0.4257	0.4257
....	.....	.....	.....	.....	.....
9	0	0	0	0.6228	
10	0	0	0	0.7514	
11	0	0	0	0.1142	$\overline{Y}$=0.7086
12	0	0	0	0.7515	

the run *11* in Table 2 is eliminated.

The coefficients of the regression equation were calculated by means of the relationships :

$$b_0 = Y, \quad b_j = \frac{1}{\sum_{i=1}^{8} x_{ji}^2} \sum_{i=1}^{9} x_{ji} Y_i, \tag{5}$$

$$b_{jk} = \frac{1}{\sum_{i=1}^{8} x_{ji}^2 x_{ki}^2} \sum_{i=1}^{8} x_{ji} x_{ki} Y_i \tag{6}$$

and the dispersion of the experimental error was settled based on the result of the repeated experiments (runs *9. 10, 12*) in the center of the experimental programme by the relation :

$$s_r^2 = \frac{1}{n-1} \sum_{i=1}^{n} (\overline{Y}_i - \overline{Y})^2, \tag{7}$$

where $s_r^2 = 0.00367$.

The values of the regression coefficients are given in Table 3.

Table 3

Values of Progression Coefficients

b_0	b_1	b_2	b_3	b_{12}	b_{13}	b_{23}	b_{132}
0.3310	0.0018	0.0161	0,1283	0.0210	−0.0095	−0.0209	0.0097

The numerical values from Table 3 show the process performance within the domain under study to be strongly influenced by the process duration (b_3=0.1283). The influence of temperature is about eight times lower (b_2 = =0.0161) and that of the ethanol/plant mass ratio of about seventy times lower (b_1=0.0018).

The equation describing the performance of the atropine extraction process is :

$$Y_c = 0.3310 + 0.0018x_1 + 0.0161x_2 + 0.1283x_3 + 0.0210x_1x_2 - \\ -0.0095x_1x_3 - 0.0209x_2x_3 + 0.0097x_1x_2x_3. \tag{8}$$

The limits between which the Y_c values calculated with help of Eq. (8) oscillate about the experimental values can be determined using the Student test by means of the relation [5] :

$$Y_c \pm t_\alpha \sqrt{s^2_{Yx_1x_2x_3}}. \tag{9}$$

For a confidence level α=0.05 and ν=7 degrees of freedom, t_α =2.365 and :

$$s^2_{Yx_1x_2x_3} = \frac{\sum_{i=1}^{8} (Y_i - Y_{ic})^2}{n-(k+1)} = 5.7 \times 10^{-9}. \tag{10}$$

Under these conditions, the variation limits of the Y_c values toward the real values are :

$$Y_c \pm 1.35 \times 10^{-8}.$$

In order to appreciate the overall influence of the factors under consideration on Y_i, the coefficient of multiple correlation was calculated:

$$R = \sqrt{1 - \frac{s^2_{Yx_1x_2x_3}}{s^2_Y}} = 0.9999, \tag{11}$$

where s^2_Y is the dispersion of the individual values Y_i around the mean value $\bar{Y}$:

$$s^2_Y = \frac{1}{n-(k+1)} \sum_{i=1}^{n} (Y_i - \bar{Y})^2. \tag{12}$$

We have found that R=0.9999, so we can conclude that the variation of the quantity of extracted atropine is 99.99% caused by the variation of the studied parameters.

4. Conclusions

a) An equation describing the dependence between the amount of atropine extracted from *Radix Atropa Belladonna* and the variables under study (temperature, extraction time and ethanol/plant mass ratio) was derived.

b) The quantitative extraction of atropine was found to depend strongly on the process duration. The influence of the temperature is about eight times lower and that of the ethanol/plant mass ratio of about seventy times lower.

c) In about 95 % of the runs the limits of variation of values can be determined by an accuracy of $\pm 1.35 \times 10^{-8}$.

d) The amount of extracted atropine is influenced by the variables under consideration in an extent of 99.99 %.

Received, April 20, 1990

Polytechnic Institute, Jassy,
Department of Organic Industries

REFERENCES

1. Lebeau P., *Traité de Pharmacie Chimique.* T. **II**, Ed. Masson, Paris, 1966.
2. Popescu H., *Medicamente de biosinteză şi extracţie.* Ed. Dacia, Cluj-Napoca, 1985.
3. Monske R. H., *The Alkaloids Chemistry and Physiology.* Vol. **XI**, Acad. Press, New York, 1968, 294.
4. Glück A., *Metode matematice în industria chimică.* Ed. Tehn., Bucureşti, 1971.
5. Mihail R., *Introducere în strategia experimentării, cu aplicaţii în tehnologia chimică,* Ed. Şt. şi Encicl., Bucureşti, 1976.

MODELAREA PROCESULUI DE EXTRACŢIE A ATROPINEI DIN *RADIX ATROPA BELLADONNA*

(Rezumat)

Se prezintă rezultatele unui studiu privind extracţia atropinei din rădăcini de *Atropa Belladonna*. Dozarea cantitativă a atropinei s-a efectuat prin cromatografie lichidă de înaltă presiune. Studiile privind modelarea procesului de extracţie au urmărit stabilirea corelaţiei dintre performanţa procesului de extracţie şi factorii ce influenţează procesul : raport masic etanol/plantă, temperatura şi durata procesului de extracţie. S-a elaborat o ecuaţie de regresie care descrie dependenţa dintre cantitatea de atropină extrasă şi variabilele considerate.

BULETINUL INSTITUTULUI POLITEHNIC DIN IAȘI
Tomul XXXVI (XL), Fasc. 3—4, 1990
Secția II
CHIMIE ȘI INGINERIE CHIMICĂ

D. C. 678.675.426 ; 547.298

STUDY ABOUT THE BEHAVIOUR OF THE POLYAMID-6 TECHNICAL YARN IN CONDITIONS OF LOW TEMPERATURES PROCESSING

BY

CLEOPATRA VASILIU-OPREA, N. HURDUC and IULIANA VLAD

1. Introduction

The knowing of morpho-structural modifications which induces changes of the technological and exploitation polymer properties is a first importance thing for theory and practice.

The polymers used as made objects or manufacturing materials by their purpose in processing, suffer a strain force in association with environmental factors (temperature, light, humidity, air—oxygene action, and so on).

The technical objects made by polymers, even in the low intensity but in long time exposure, suffer inevitabil mechanical and chemical modifications which had been observated in all structural levels.

The mechanical-chemical reactions develop and take place in molecular structures, in a particular elastic energy concentration mechanism on structural distorsions.

Because the fault zone extends on certain dimensions, the molecular fractures do not occur on single molecular chain, but on a number of chain parts which occurs the activated defect under the force action.

The mechanical-chemical degradation effects and fractures of the polymers are favorised by the low values of temperature. The lower is the temperature in which the polymer is processed, the more its chains stiffens by diminution of the flexibility, and the mechanical-chemical and fracture effects became more evident [1].

Both the mechanical-chemical phenomena which occurs on atom-molecular levels and the fracture phenomena which affects all structural-organisation levels of the processed object, take place in chained mechanism by free radicals.

V. P. K a r g u i n showed for the first time the mechanical-chemical modifications which take place in the exposed on low temperatures polymers structures in order to explain the theory of the generating mechanisms [2]...[5].

Some data refers on Polyamid behaviour in low temperature strain traction work, the results being brought up by the drawing of effort-temperature curves.

Such studies have been developed on Polyamides.

In the present work, we proposed to develop a study about the behaviour of the Polyamid technical yarn in low temperature processing. The work conditions had been selected in order to simulate, as closer as possible, the processing ones.

We mark the fact that the results described in the literature refers to the research of the polymer solutions first frozen then defreezed, in a various number of cryolithic cycles, in which case the degradations phenomena are favourised and the obtained effects are more evident.

2. Experimental

In what follows a study on Nylon-6 technical yarn was made having the following characteristics : $\bar{M}$ =29.000 ; crystalinity index=55.0 % ; melting temperature T_m = 225°...226°C ; tensile strength = 28,4 Kgf ; tenacity = 6,96 gf/dtex ; elongation fracture = 19.44 % ; title = 4 080 dtex.

The technical yarn had been alternatively imersed in low temperature phases (the „frozen" one took place at −40°C, 60 min.) and high temperature (the „defreezing" took place at +50°C, 60 min.).

Also, a constant mechanical processing study of the yarn took place using the elongation strain in creep conditions. The dynamic strain of the yarn took place in supersounding conditions.

The freezing—defreezing cycles had been processed in V_2A stainless steel phials filled up with methanol. The cooling agent was a mixture of technical acetone and liquid nitrogen.

The tensile processing was carried out by suspending a 6 Kg weigh from a 6 m yarn sample. The processing took place between 100 and 1 750 hours.

The humidity and temperature processing took place by suspending the yarn sample in an essicator in the presence of a Mn acetate saturated solution which assures a 60 % humidity.

The yarn had been characterized by the following techniques : a) the determination of the molecular mass was made by viscosimetry using an Ubbelhode nr. 2 viscosimeter having $k = 0.09018$; b) the determination of the cristallinity degree was made by X-ray diffraction technique using a TUR—M60 equipment ; c) the strenght fracture, elongation and tenacity processing was made by using a Zwick Universal 1 441 dynamometer.

3. Results and Discussions

3.1. The Freezing—Defreezing Cycling Processing of the Yarn

The data written in Table 1 concerning the dependence of the molecular mass according to the freezing —defreezing cryolithic cycles, shows up a light

Table 1

Processing in Cryolithic Cycles

Sample	Number of cryolitic cycles	M_v	Crystallinity index %	Fracture strength Kgf	Tenacity gf/dtex	Elongation fracture %	Title dtex
1	0	29,000	55.0	28.4	6.96	19.44	4 080
2	5	33,834	60.9	27.5	6.42	30.08	4 279
3	10	31,730	65.0	28.0	6.37	31.40	4 421
4	15	33,130	67.3	28.5	6.48	31.20	4 401
5	25	26,245	70.0	27.4	6.27	32.60	4 365
6	30	25,237	76.4	27.3	6.21	36.00	4 393
7	40	22,000	75.8	27.0	6.24	31.50	4 337
8	50	22,000	72.8	27.1	6.21	30.50	4 352
9	75	22,000	73.0	26.5	5.93	33.50	4 464
10	100	21,900	71.9	26.8	6.14	32.60	4 360

growth of it in 10...15 cryolithic cycles, after that the molecular mass goes down slowly until the value of 22,000 is reached from 40 cycles more.

The initial growth of the molecular mass in the first processing rang (5...15 cycles) must be putted on direct line with the behaviour of the macromolecules and their filiform formations of overmolecular organization, in conditions of changing the thermal rate [6].

The primary changes which take place under the thermal shock are the modification of the chain conformation and dimensions on the molecular level and the vanishing of the physical interactions number, both in hydrogen link type and in van der Waals one too. Such changes take place on both sides of the cryolithic cycle even in freezing phase and in defreezing one. In the freezing phase, by getting the temperature to the value of −50°C, a marked effect of macromolecules, over molecular beams and morphological formations theirselves contraction takes place which makes first the vanishing of a number of interchains physical interactions. The released molecules, at least one part, from such interactions, became rigid as consequence of the temperature. They extend themselves in the direction of the inside tensions appeared when the temperature decreases, and in the same time the contraction takes place. The macromolecules are growing their package density between them a quite great number of physical interactions are rebuilt, an overeffect of orientation in the initial amorph zones shows up, fact which explaines the crystallinity growing from the initial value of I_a=55.0 % to those of 67.3 % on 15 cryolithic cycles.

The supposition of the macromolecules elongation is also in the line with the growing of the elongation fracture factor, from 19.44 % in the unprocessed sample to 31.2 %.

In the defreezing phase, macromolecules grows in mobility. Due to the shock state produced by the important change of temperature, those with larger dimensions than the medium value, fracture themselves into shorter fragments. The macromolecules fractures are statistic so distributed that it is possible to appear fragments shorter than the little ones being in the initial polydispers system. By proceeding the freezing phase once again, the shorter but more mobile fragments get to the line themselves easier in conditions of contraction and becoming rigid mode and explaines the continuous growing of crystallinity which reaches the top value of 76.4 % in 30 cryolithic cycles.

We must underline that the rebuilding of physical interaction in each defreezing phase does not consist in a rigorous rebuilding of the initial structural order. In the overprocess of lineing and crystallization shown by the crystallinity index growth, the defects growing from the structure accentuates especially because of polydispersity changing. These modifications produced in experimentaly mode reflects accumulation of the destructive phenomena unreversible induced by the thermal and mechanical shock, conclusion which is supported by the smaller values of the molecular mass (22,000).

3.2. Processing of the Technical Yarn in Constant Mechanical Mode by Using Elongation in Creep Conditions

Polymers, especially fibres, processed in elongation mode for long time, suffers catenas distortions and valence angles also lineing of macromolecules in the force direction.

In the time the polymer is under force action, the physical interactions vanish, macromolecules translate, move one against the other, i.e. „flows". The „flowing" is known as creep.

The technical yarn samples had been processed in creep conditions for 100...1 750 hours (Table 2). The results show the fact that the molecular structure is directly affected ; so, in 100 hours, the value faile from 29,000 to 21,992, this process continues in low speed until 1 750 hours are reached, the final value being 19,153.

Table 2

Tensile Processing in Steady State

Sample	Time of processing hours	M_v	Fracture strength Kgf	Tenacity gf/dtex	Elongation fracture %	Title dtex
1	0	29,000	28.4	6.96	19.44	4 080
2	100	21,920	26.0	6.09	17.0	3 886
3	200	20,886	28.0	7.08	17.4	3 954
4	300	20,452	26.7	6.95	17.9	3 839
5	400	20,128	27.2	6.80	17.4	4 002
6	500	20,782	25.7	6.10	16.0	4 183
7	800	22,740	26.0	6.22	17.6	4 180
8	1 000	20,510	26.5	6.32	18.4	4 190
9	1 750	10,153	26.5	6.33	16.7	4 137

The other measurements values are quite constant, the tensile strength being an exception because its value leightly fails from 28.4 to 26.0 Kgf.

3.3. The Yarn Processing in Cryolisis and Creep Conditions

By processing the Polyamid-6 yarn in cryolisis and than in creep conditions, a more accentuated failure of the molecular mass is observed comparing with isolate processing in cryolisis or creep (Table 3).

This fact reflects a mechanical-chemical degradation more advanced than in isolate procedures, behaviour which concordes with creep and cryolitic studies.

The catenas flexibility modification reflects the elongation fracture variation, some values, between 30...33% in cryolisis and 17% in creep conditions, being obtained. This fact reflects the rebuilding of a certain interchains connections number by creep processing, by paralleling macromolecule in fact, connections which are destroyed in cryolisis.

Intermediary values between cryolisis and creep processing are also observed in fineness of the yarn, fact that shows a less elongation of the macromolecules than in simple creep processing.

The fracture strength also takes values in short limits in comparison with the whitness sample one.

Table 3

Yarn Processing in Cryolisis and Creep Conditions

Sample	Cryolisis cycles number	Hours creep number	M_v	Elong-ation fracture %	Fracture strength Kgf	Tenacity gf/dtex	Title dtex
1	25	—	26,245	32.6	27.4	6.27	4 365
2	—	100	21,992	17.0	26.0	6.69	3 886
3	25	100	20,635	24,3	24.8	5.84	4 246
4	50	—	22,000	30.5	27.1	6.21	4 352
5	—	100	21,992	17.0	26.0	6.69	4 246
6	50	150	19,000	26.8	27.4	6.32	4 337
7	—	300	20,452	17.4	26.7	6.95	3 839
8	50	200	15,000	23.4	27.8	6.44	4 315
9	75	—	22,000	33.5	26.5	5.93	4 464
10	—	100	21,992	17.0	26.0	6.69	4 246
11	75	150	22,751	25.6	26.1	6.32	4 128
12	—	300	20,452	17.4	26.7	6.95	3 839
13	75	300	23,244	23.3	27.0	6.49	4 160
14	100	—	22,000	32.6	26.8	6.14	4 360
15	—	100	21,992	17.0	26.0	6.69	4 246
16	100	100	23,244	21.9	26.7	6.83	4 284

3.4. The Technical Yarn Temperature Processing in Humidity

The temperature processing in humidity conditions was made at 42°C, 25°C and 4°C using samples mentained at 96,122 and 300 hours in a workshop with constant humidity of 65%. The obtained results are concentrated in Table 4.

Table 4

Yarn Processing in Constant Humidity (60%) versus Temperature

Sample	Time of processing hours	M_v	Temper-ature °C	Fracture strength Kgf	Tenacity gf/dtex	Elongation fracture %	Title dtex
1	0	29,000	—	28.4	6.96	19.44	4 080
2	96	24,659	42	28.5	6.81	23.0	4 179
3	96	24,411	25	28.4	6.67	21.2	4 254
4	96	22,423	4	27.9	6.89	20.4	4 058
5	192	20,635	42	26.5	6.26	24.0	4 231
6	192	25,908	25	27.0	6.41	21.9	4 211
7	192	26,076	4	28.4	6.83	21.6	4 155
8	300	25,830	42	28.6	6.38	23.9	4 481
9	300	27,513	25	29.2	6.99	25.5	4 175
10	300	16,676	4	27.7	6.74	21.7	4 112

The way the physical properties and physical-mechanical indexes are moving concordes with the conclusions obtained by cryolitic freezing — defreezing procedure. In the processed samples, a failure of the medium molec-

ular mass from 29,000 till 16,676 is observed, in conditions of 300 hours processing at 4°C.

The humidity influence must be interpretated by the activation of some hydrolitic destruction effectuated of the —CO—NH— groupes. They must wait that in the present study conditions, this phenomena produces only in the superficial layers of the yarn, because this polymer has large crystallinity and compact structure.

The elongation fracture growth on thermal procedure in humidity must be shown up also by the development of some interchain physical connections fracture phenomena. The catenas fracturing by hydrolisis does small discontinuites in the affected local formations inside structure ; so, localy develops strengths which grows by temperature failure, fact that produces the vanishing of some physical interactions and rebuilding of the new ones, but in other positions than the initials. This effect grows the capacity of distortion of the macromolecules and the overorganisation system in which these are part, this thing being the explanation for the yarn fineness light growing.

The fracture strength does not essentialy change from a sample to an other, the sample processed 300 h at 4°C being an exception, so lower temperature processing being necessary.

4. Conclusions

By correlating the obtained results in different conditions processing, we conclude that in the used force and temperature range, evident changes are observed in atom-molecular level, characterised by the short range modification of the physical-mechanical indexes in the way they have been interpretated.

It is marked the fact the present study refers to the most simple case, the one in which the yarn is a part in a manufactured object.

On the other side, the types of processing had been separately studied, so a concentrated all factors study being necessary.

From the effectuated study the following conclusions may be drawn:

1. By processing the Polyamid-6 technical yarn in steady state, mechanical-chemical degradation reactions are developed, reflected in molecular mass failure.

2. The modifications present at molecular level induce changes on overmolecular-morphological level which can be measured by crystallinity, fracture elongation and title changing.

3. Purposing results a study of the manufactured texture is necessary, not only the yarn separately.

4. It is also necessary to research processing in both different thermal and environmental conditions, facts which would stimulate the fatigue and ageing phenomena responsable for the destruction of the polyamidic objects in processing conditions.

Received, May 17, 1990

Polytechnic Institute, Jassy,
Department of Macromolecules

REFERENCES

1. Casale A., Poster R. S., *Polymer Stress Reactions.* Vol. I and II, Academic Press, New York, 1978.
2. Каргин В. А., Высокомол., соедин. **1**, 2 330 (1959).
3. Каргин В. А., Высокомол., соедин. **3**, 7, 1094 (1964).
4. Бронников С. В., Веттегрен В. И., Корфавин Л. Н., Френкел С. И., Механика композ. матер., **5**, 920 (1983).
5. Vasiliu-Oprea C., Negulianu C., Popa M., Simionescu C., Plaste u. Kautschuk, **9**, 604 (1977).
6. Vasiliu-Oprea C., Negulianu C., Simionescu C., Popa M., Plaste u. Kautschuk, **10**, 689 (1977).

COMPORTAREA FIRULUI DE POLIAMIDĂ-6 LA TEMPERATURI SCĂZUTE

(Rezumat)

Se prezintă rezultatele unui studiu al comportării firului de poliamidă-6, tip cord, în diverse condiţii de solicitare. Firul a fost solicitat în condiţii de îngheţ—dezgheţ, la tracţiune, în condiţii statice, la umiditate şi temperatură, influenţa acestor factori fiind studiată separat şi împreună. În urma acestui studiu a rezultat că firul de poliamidă-6 nu suferă modificări esenţiale ale indicilor fizico-mecanici, în condiţiile experimentale folosite.

BULETINUL INSTITUTULUI POLITEHNIC DIN IAȘI
Tomul XXXVI (XL), Fasc. 3—4, 1990
Secția II
CHIMIE ȘI INGINERIE CHIMICĂ

D. C. 542 ; 518.5

EXPERIMENTAL DATA PROCESSING

3. POLYNOMIAL CORRELATION AND REGRESSION

BY

SIMION PETROVAN

1. Introduction

In many cases of data processing, a regression function of the following form :

$$y = a_0 + a_1 x + a_2 x^2 + a_3 x^3 + \ldots \tag{1}$$

must be determined.

In this paper, a method and the FORTRAN program are given for the obtaining of the correlation coefficients of the dependent variable y with every power of the independent variable x, up to the maximum possible one or to the power given in the program, and also, for the determination of the regression equation (1). The program belongs to a set of programs for data processing [1], [2].

2. The Proposed Method

Let an experimental data set as that given in Table 1, where x is an independent variable and y a dependent one. In order to determine the regression coefficients from Eq. (1) let rewrite this in function of the deviations from the mean of the independent variable :

$$y - \bar{y} = a_1(x - \bar{x}) + a_2(x^2 - \bar{x}^2) + \ldots, \tag{2}$$

or in a normalized form :

$$\frac{y - \bar{y}}{S_y} = \frac{x - \bar{x}}{S_x} b_1 + \frac{x^2 - \bar{x}^2}{S_{x^2}} b_2 + \ldots \tag{3}$$

where S_y, S_x, S_{x^2}, ..., are standard deviations and $b_1, b_2, \ldots$, are weight coefficients defined by :

$$b_i = \frac{S_x i}{S_y} a_i. \tag{4}$$

Table 1

The Experimental Data Set

No. exp.	x	y_e
1	x_1	y_1
2	x_2	y_2
3	x_3	y_3
.	.	.
.	.	.
.	.	.
N	x_N	y_N

Let us apply to the Eq. (3) the least squares method, that is :

$$(5)\quad E=e^t\cdot e=\left(\frac{y_e-\bar{y}_e}{S_{y_e}}-\frac{y-\bar{y}}{S_y}\right)^2=\left(\frac{y_e-\bar{y}_e}{S_{y_e}}-b_1\frac{x-\bar{x}}{S_x}-b_2\frac{x^2-\bar{x}^2}{S_{x^2}}-\cdots\right)^2 ! \text{ minim.}$$

By partial derivation of the equation (5) with respect to b_1, b_2, ..., one can obtain :

$$\begin{gathered}
b_1\frac{\sum(x-\bar{x})^2}{S_x^2}+b_2\frac{\sum(x-\bar{x})(x^2-\bar{x}^2)}{S_xS_{x^2}}+\ldots+b_k\frac{\sum(x-\bar{x})(x^k-\bar{x}^k)}{S_xS_{x^k}}=\\
=\frac{\sum(x-\bar{x})(y_e-\bar{y}_e)}{S_xS_{y_e}},\\
b_1\frac{\sum(x^2-\bar{x}^2)(x-\bar{x})}{S_{x^2}S_x}+b_2\frac{\sum(x^2-\bar{x}^2)^2}{S_{x^2}^2}+\ldots+b_k\frac{\sum(x^2-\bar{x}^2)(x^k-\bar{x}^k)}{S_{x^2}S_{x^k}}=\\
(6)\qquad =\frac{\sum(x^2-\bar{x}^2)(y_e-\bar{y}_e)}{S_{x^2}S_{y_e}},\\
\cdots\cdots\cdots\cdots\cdots\cdots\cdots\cdots\cdots\cdots\\
b_1\frac{\sum(x^k-\bar{x}^k)(x-\bar{x})}{S_{x^k}S_x}+b_2\frac{\sum(x^k-\bar{x}^k)(x^2-\bar{x}^2)}{S_{x^k}S_{x^2}}+\ldots+b_k\frac{\sum(x^k-\bar{x}^k)^2}{S_{x^k}^2}=\\
=\frac{\sum(x^k-\bar{x}^k)(y_e-\bar{y}_e)}{S_{x^k}S_{y_e}},
\end{gathered}$$

where y_e and x^k are vectors of the dimension N, the number of the experiments. Eqs. (6) can be written in matrix form as :

$$(7)\qquad br_{xx}=r_{xy},$$

because the sums from these equations are correlation coefficients, between the powers of the independent variable in the left part and between the powers of x and the dependent variable y, in the right part, as given by the following relations :

$$(8)\quad r_{ij}=\frac{\sum(x^i-\bar{x}^i)(x^j-\bar{x}^j)}{S_{x^i}S_{x^j}},\qquad (9)\quad r_{iy}=\frac{\sum(x^i-\bar{x}^i)(y_e-\bar{y}_e)}{S_{x^i}S_{y_e}}.$$

The system of equations (7) is the so called system of normal equations. The regression coefficients and the intercept of equation (1) can be determined as following :

$$a_i=b_i\frac{S_{y_e}}{S_{x^i}},\qquad a_0=\bar{y}_e-a^t\bar{x},$$

where :

$$b=r_{xx}^{-1}r_{xy}.$$

Based on the method presented above, the algorithm of the program can be summarized as following :

1. Read the parameters of the program and the experimental data.
2. Compute and print the correlation coefficients.
3. Invert the correlation matrix.
4. Compute intercept, regression coefficients, standard errors of the regression coeficients, computed t values, determination coefficent and the elements of the variance analysis by the following formula [3]...[5]:

a) Determination coefficient :

$$R^2 = b^t r_{xy}. \tag{10}$$

b) Sum of squares due to regression :

$$\text{SUMAR} = R^2 D_{yy}, \tag{11}$$

where D_{yy} is the sum of squares of deviations to the mean for the dependent variable ($D_{yy} = S^2_{y_e}(N-1)$).

c) Sum of squares for the deviation from the regression :

$$\text{SUMDR} = D_{yy} - \text{SUMAR}. \tag{12}$$

d) Standard errors of the regression coefficients :

$$S_a i = \frac{\text{SUMDR}}{N-k-1} \sqrt{r_{ii}^{-1} / S^2_{x^i}(N-1)}. \tag{13}$$

e) Computed t_c values :

$$t_c = \frac{a_i}{S_{a^i}}. \tag{14}$$

f) Computed F values :

$$F = \frac{\text{SUMAR}(N-k-1)}{\text{SUMDR} \cdot k}. \tag{15}$$

5. Compute the values of the dependent variable, using equation (1), without elimination of the unsignificant regression coefficients according to t-test (y_c) and after the elimination of the unsignificant coefficients (y_t). Also, the following differences are computed :

$$\text{DY} = y_e - y_c, \tag{16}$$

$$\text{DYT} = y_e - y_t. \tag{17}$$

The elimination of the unsignificant coefficients is performed if the following condition is fulfilled :

$$t_e < t_t(N-k-1\,;\,\alpha), \tag{18}$$

where $t_t(N-k-1\,;\,\alpha)$ is the tabulated t test for $N-k-1$ degrees of freedom and α—the significance level.

The computations are repeated for every degree of the polynomial equation (1), up to the maximum possible one ($k_{\max} = N-2$), to the given one by the program or in function of the determination coefficient R^2.

3. The Program and Data Input

Matrix inversion is performed by using MINV subroutine [6]. Data are introduced in the following order :

1. Tabulated t values for 1 to 30 degrees of freedom with 8F10.5 format.

2. Number of the experiments, maximum degree of the polynomial equation and ε (EPS) value, in function of which regression termination is tested (ε=1 for the maximum polynomial degree) with 215, F5.3 formats.

3. Experimental data by using 8F10.5 format.

The program is given in the Table 2.

4. Application

Diphyl is a thermal agent which is wide used for heating the systems in chemical industry. The properties of this mixture are given in Tables [7] on a temperature domain between 20° and 400°C. In Table 3 the regression equations obtained by using the above program are given, for some of the diphyl properties in function of temperature.

Table 3

The Properties of the Liquid Diphyl in Function of Temperature (°C) *in the Domain* 20°...400°C

Property	Determination coefficient, R^2	Equation
Density, [KG/m^3]	0.9999	$1\,076.763-0.7751725\,t-0.3035772\times10^{-3}\,t^2$
Latent heat of condensation, [KJ/KG]	0.9997	$378.1614-0.3813561\,t+0.6049988\times10^{-3}\,t^2-0.1837453\times10^{-5}\,t^3$
Specific heat, [KJ/KG.K]	0.9993	$1.45878+0.5598176\times10^{-2}\,t-0.1820739\times10^{-4}\,t^2+0.2816901\times10^{-7}\,t^3$
Dynamic viscosity, [Pa.s$\times10^4$]		$54.24187-0.8668297\,t+0.5552322\times10^{-2}\,t^2-0.1543024\times10^{-4}\,t^3+0.1541141\times10^{-7}\,t^4$
Thermal conductivity, [W/mK]	0.9994	$0.1413867-0.1446997\times10^{-3}\,t-0.4964622\times10^{-8}\,t^2$

As can be seen from the determination coefficients, R^2, the accuracy of the equations is very high.

Received, March 21, 1990

Polytechnic Institute, Jassy,
Department of Macromolecules

REFERENCES

1. Petrovan S., Mase plastice, **22**, 236 (1985).
2. Petrovan S., Mase plastice, **23**, 48 (1986).
3. Văduva I., *Analiza dispersională*. Ed. Tehn., Buc., 1970.
4. Mihail R., *Introducere în strategia experienţelor, cu aplicaţii din tehnologia chimică*. ESE, Buc., 1976.
5. Cochran W. G., Cox G. M., *Experimental Designs*. J. Wiley, NY, 1968.

Table 2

The Proposed Program

```
      * DEFINE FILE *1=1, *2=3
        DIMENSION X(40), Y(40), XR(60), RX(100), XM(10), EMX(60),
        EMY (10), S(10), RY(10), BETA(10), A(11), AT(11), ES(10), T(10)
        YC(40), LM(10), LN(10), DY(10), DYT(10), TT(40), YT(40)
      1 FORMAT (2I5, F5.3)
      2 FORMAT (8F10.5)
      3 FORMAT (8(2X, E13.7))
      4 FORMAT (10X, 'COEFFICIENT OF DETERMINATION', 5X, F9.7)
      5 FORMAT (// 10X, 'POLYNOMIAL REGRESSION OF DEGREE', I4)
      6 FORMAT (10X, 'REGRESSION COEFFICIENTS')
      7 FORMAT (10X, 'STANDARD  ERRORS')
      8 FORMAT (10X, 'COMPUTED T-VALUES')
      9 FORMAT (/35X, 'ANALYSIS OF VARIANCE'/)
     10 FORMAT (15X, 'SOURCE', 5X, 'DEGREE OF', 5X, 'SUM OF', 9X,
        'MEAN', 11X, 'F', 8X, 'IMPROVEMENT' /27X, 'FREEDOM', 7X,
        'SQUARES', 7X, 'SQUARES', 8X, 'VALUE'/)
     11 FORMAT (13X, 'REGRESSION', 4X, I4, 4X, 4(2X, E12.6))
     12 FORMAT (13X, 'DEVIATION', 5X, I4, 4X, 2(2X, E12.6))
     13 FORMAT (15X, 'TOTAL', 7X, I4, 6X, E12.6)
     14 FORMAT (// 30X, 'TABLE OF RESIDUALS'/16X, 'X', 11X, 'Y',
        11 X, 'YC', 10X, 'DY', 10X, 'YT', 10X, 'DYT'/)
     15 FORMAT (8X, 6(2X, F10.5)).
     16 FORMAT (10 X, 'REGRESSION COEFFICIENTS AFTER T TEST')
     17 FORMAT (/10X, 'PROBLEM NO., I5)
     18 FORMAT (10X, 'WSMA=', E13.7)
        READ (1, 2) (TT(I), I=1,40).
        NP=0
     24 READ (1, 1) N, MMAX, EPS
        IF (N.EQ.0) GO TO 140
        NP=NP+1
        WRITE (3, 17) NP
        READ (1, 2) (X(I), I=1, N), (Y(I), I=1, N)
        WRITE (3, 3) (X(I), I=1, N)
        WRITE (3, 3) (Y(I), I=1, N)
        SUMAR=0.
        YM=0.
        DO 25 I=1, N
     25 YM=YM+Y(I)
        YM=YM/FLOAT (N)
        EMYY=0.
        DO 26 I=1, N
     26 EMYY=EMYY+(Y(I)-YM)*(Y(I)-YM)
        SY=SQRT (EMYY/FLOAT(N-1))
        M=0
     30 M=M+1
        MP=M+1
        IF (M.EQ.(N-1)) GO TO 24
        SUMARZ=.SUMAR
        XM (M)=0.
        DO 40 I=1,N
     40 XM(M)=XM(M)+X(I)**M
        XM (M)=XM(M)/FLOAT(N)
        L=M*(M-1)/2
        DO 50 I=1, M
        L=L+1
        EMX(L)=0.
        DO 42 J=1, N
     42 EMX(L)=EMX(L)+(X(J)**I-XM(I))*(X(J)**M-XM(M))
```

```
      IF(I.LT.M) GO TO 50
      EMY(M)=0.
      DO 45 J=1,N
   45 EMY(M)=EMY(M)+(X(J)*M-XM(M))*(Y(J)-YM)
      S(M)=SQRT(EMX(L)/FLOAT(N-1))
      RY(M)=EMY(M)/SQRT(EMYY*EMX(L))
   50 CONTINUE
      L=M*(M-1)/2
      L1=M*(M+1)/2
      DO 60 I=1, M
      L2=I*(I+1)/2
      L=L+1
      IF (I-M) 58, 55, 58
   55 XR (L)=1.
      GO TO 60
   58 XR(L)=EMX (L)/SQRT(EMX(L1)*EMX(L2))
   60 CONTINUE
      L1=0
      DO 70 I=1, M
      DO 70 J=1, I
      L1=L1+1
      IF (J.EQ.I)  GO TO 65
      L2=(J-1)*M+I
      RX(L2)=XR(L1)
      L2=(L-1)*M+J
      RX(L2)=XR(L1)
      GO TO 70
   65 L2=(I-1)*M+I
      RX(L2)=XR(L1)
   70 CONTINUE
      K=M*M
      WRITE (3, 3) (RX(I), I=1, K)
      WRITE (3, 3) (RY(I), I=1, M)
      CALL MINV(M, DET, RX, LM, LN)
      WRITE (3, 3) (RX(I). I=1, K)
      DO 90 I=1, M
      BETA (I)=0.
      DO 80 J=1, M
      L=I+M*(J-1)
   80 BETA(I)=BETA(I)+RX(L)*RY(J)
      A(I+1)=BETA(I)*SY/S(I)
   90 AT(I+1)=A(I+1)
      A(1)=YM
      DO 95 I=1, M
   95 A(1)=A(1)-A(I+1)*XM(I)
      AT(1)=A(1)
      IGL=N-1
      IGLR=M
      IGLA=N-M-1
      SUMAR=0
      DO  100 I=1, M
  100 SUMAR=SUMAR+BETA(I)*RY(I)
      CD=SUMAR
      SUMAR=SUMAR*EMYY
      SUMDR=EMYY-SUMAR
      SMR=SUMAR/FLOAT(IGLR)
      SMA=SUMDR/FLOAT(IGLA)
```

```
116         F=SMR/SMA
117         DSUM=SUMAR-SUMARZ
118         DO 110 I=1, M
119         L=M*(I-1)+I
120         L1=I*(I+1)/2
121         WSMA=RX(L)*SMA/EMX(L1)
122         IF(WSMA) 105, 105, 108
123     105 WRITE (3, 18) WSMA
124         GO TO 24
125     108 ES(I)=SQRT (WSMA)
126         T(I) =A(I+1)/ES(I)
127         IF(ABS(T(I)). LT. TT(IGLA)) AT (I+1)=0
128     110 CONTINUE
129         WRITE (3, 5) M
130         WRITE (3, 6)
131         WRITE (3, 3) (A(I), I=1, MP)
132         WRITE (3, 7)
133         WRITE (3, 3) (ES(I), I=1, M)
134         WRITE (3, 8)
135         WRITE (3, 3) (T(I), I=1, M)
136         WRITE (3, 16)
137         WRITE (3, 3) (AT (I), I=1, MP)
138         WRITE (3, 4) CD
139         WRITE (3, 9)
140         WRITE (3, 10)
141         WRITE (3, 11) IGLR, SUMAR, SMR, F, DSUM
142         WRITE (3, 12) IGLA, SUMDR, SMA
143         WRITE (3, 13) IGL, EMYY
144         WRITE (3, 14)
145         DO 130 I=1, N
146         YC(I)=A(1)
147         YT(I)=A(1)
148         DO 120 J=1, M
149         YC(I)=YC(I)+A(J+1)*X(I)**J
150         YT(I)=YT(I)+AT(J+1)*X(I)*J
151         DYT(I)=YT(I)-Y(I)
152     120 DY (I)=YC(I)-Y(I)
153     130 WRITE (3, 15) X(I), Y(I), YC(I), DY(I), YT(I), DYT(I)
154         IF (M.EQ.MMAX) GO TO 140
155         IF (CD. LT. EPS) GO TO 30
156         GO TO 24
157     140 STOP
158         END
```

6. * * IBM System 360 (360 A-CM-03X), Scientific Subroutine. Packager Programmer's Manual, Version III, H20-0205-3, 1968.
7. Raznjevic K., *Tabele și diagrame termodinamice*. Ed. Tehn., Buc., 1978.

PRELUCRAREA DATELOR EXPERIMENTALE

3. Corelație și regresie polinomială

(Rezumat)

Se prezintă un program pentru prelucrarea datelor experimentale în vederea obținerii unei ecuații de regresie polinomială. Se calculează coeficienții de regresie, erorile lor standard testul *t*, coeficientul corelației multiple, valoarea testului *F* și se întocmesc analiza dispersională și tabelul reziduurilor.

Final se dă o aplicație în care se corelează unele proprietăți ale agentului de transfer de căldură difil cu temperatura.

BULETINUL INSTITUTULUI POLITEHNIC DIN IAȘI
Tomul XXXVI (XL), Fasc. 3—4, 1990
Secția II
CHIMIE ȘI INGINERIE CHIMICĂ

D. C. 547.473.2 ; 678.4

POLYMER BLENDS OF POLICAPROLACTAM WITH ELASTOMERS

BY

VICTOR BULACOVSCHI, AURELIA IOANID, N. HURDUC and P. ONU

1. Introduction

The nylons have found a steadily increasing application as plastics materials for speciality purposes where their toughness, rigidity, abrasion resistance, good hydrocarbon resistance and resonable heat resistance are important. The largest applications of the homopolymers have been in mechanical engineering [1].

Whilst the aliphatic nylons are generally classified as being impact resistant, they are affected by stress concentrators like sharp corners which may lead to britle failures. As a way to overcome this drowback, the incorporation of rubbers is usually recomanded. As a consequence, blends of nylons with rubbers or various other components are intensively studied and they are increasingly now replacing homopolymers [4]...[8].

This paper deals with the preparation and characterization of some nylon 6 blends with powdered rubber from the used tyres and with Romanian rubber CAROM (butadiene (70)-α-methylstyrene (30) copolymer). As synthetic routes the activated anionic polymerization of caprolactam in solution and in molten state were employed.

2. Experimental

Caprolactam (from Săvinești plant) of commercial grade and additives were carefully dried before use. Toluene, used as solvent in polymerization, was dried over sodium wire and used as such. The bulk polymerization was carried out in test tubes under nitrogen. Thus, a mixture of 25 g caprolactam and 2 g of powdered rubber was charged in the tube which was then heated in a silicone oil bath at 90°...95°C. At this moment 0.02 g of Na were added in order to obtain Na-caprolactam. After 15...20 min. the temperature was rised to 150°C and 0.2 mL of activator, *m*-toluilenediizocianate (TDI), were introduced. In 15...20 min. reaction was completed and the vial was cooled slowly down. In order to prevent the sedimentation of the powdered rubber, bubling of the nitrogen was maintained until the high viscosity was reached. There were used various caprolactam / powdered rubber ratios.

The solution polymerization was carried out in a 250 mL reactor fitted with mechanical stirring, reflux condenser, nitrogen inlet tube and thermometer.

Tipically, 30 g of caprolactam are dissolved in 100 mL of rubber solution (5%) in toluene at 90°...95°C. Then 0.03 g of Na are added. After 15 min. the

temperature is rised to reflux and 0.2 mL of TDI are introduced. Reaction is continued for 4 h and the content is then poured in acidified (HCl) methanol. The precipitate is filtered off, washed with methanol and dried.

Characterization of polyblends was done by IR (KBr pellets on a Perkin-Elmer instrument), thermal analysis on a Paulik—Paulik—Erdey MOM Budapest apparatus, X-ray diffraction on a Kristalloflex-4-Siemens diffractometer with 2°/min. registration speed and transmission electronic microscopy on a TESLA 513 A apparatus. The cross sections were coloured with OsO_4, reactive for C=C double bonds.

Bars from blended polycaprolactam were machined to prepare test specimens for impact testing and the obtained values are an average of at least ten samples.

3. Results and Discussion

The powdered rubber obtained from reconditioning of used tyres consists in a mixture of particles of various dimensions. When such material is dispersed in the molten caprolactam, the bulky particles tend to deposit, resulting a compound with ununiform distribution of the additive. Therefore, the powder was firstly sifted and fractions of different particles size were isolated (Table 1).

Table 1

Granulometric Distribution in the Powdered Rubber

Fraction	*I*	*II*	*III*	*IV*	*V*	*VI*
Particle size, μ	1 000	630	400	315	90	<90
%	35.86	10.79	13.75	14.40	24.60	0.60

Most of the composites were prepared by using fraction (V) which could be almost uniform dispersed in the polymer and the obtained samples proved to have better mechanical properties compared to controle sample (polycaproamide obtained in the same conditions). Thus, the measured impact strength (I_s=10· 7 ×10^{-3} J/mm²) was three times higher and the tensile strength (T_s= =31 MPa) increased with 10...15% compared to control sample (I_s=3.45 × ×10^{-3} J/mm²; T_s=27.2 MPa). When particles of higher or lower size were used a decrease of the two indices was observed. There appears to be an optimum particle size of rubber for such systems.

Based on generally accepted theory that the toughening effect is associated with the crazing behaviour, the rubber particles should be not too small so that they are completely embeded in a craze. When a propagating craze reaches a particle it often divides so that if there is a large number of particles per unit volume and of proper size, there is a high dissipation of energy.

It is generally accepted that the more the rubber present, the greater the reinforcing effect. So, we intended to obtain a structure in which the rubber to exist not simply as particle embeded in the polyamide matrix, but in the

Fig. 1. — Electron micrograph of the nylon 6 blend with poly(butadiene-co-α-methyl styrene) (×8,400).

form of the interpenetrated structure. With that end in view, the activated anionic polymerization of caprolactam was carried out in the rubber solution prepared in toluene (Table 2).

Table 2

Solution Polymerization of Caprolactam

No.	Rubber concentration, [%]	Polymer yield, [%]		Softenin grange,[°C]
		per total	related to lactam	
1	—	55.6	55.6	205...215
2	1	21.07	21.77	195...205
3	2	15.16	12.2	182...195
4	5	55.91	65.17	179...192
5	10	38.7	51.6	185...195

Reaction conditions: Caprolactam 30 g; volume of solution 100 mL; Na=0.03 g; TDI=0.2 mL; Temperature=reflux; Time=4 h.

The electronomicroscopic picture shows that the rubber exists as droplets embeded in the glassy polymer (Fig. 1).

The X-ray diffraction patterns of the obtained products reveal some morphological modifications outlined by diminution of the 20.5° maximum (Fig. 2). This may originate in the interpenetration to some extent of the two macromolecular networks. However, one may assume for still a high degree of crystallinity of the polyblends.

Benzene extraction of the composites have revealed that the two components are chemically bondless. Gravimetrically it was established that the rubber can be completely extracted by the solvent. The lack of the chemical bonds between the two components is asserted also by IR spectrum of the extracted polyamid (Fig. 3). There are not absorbtions specific to the rubber.

Thermal properties of polycaproamide and corresponding blend were examined by thermogravimetric analysis (TG), differential thermal analysis (DTA) and derivative thermogravimetry (DTG) which were performed simultaneously by heating the polymers at a constant rate of 6°C $min.^{-1}$ in nitrogen atmosphere.

The initial decomposition temperature (IDT) (taking the sharp drop in the curves as the onset of the decomposition reaction) and the temperature of the maximum decomposition (T_{max}), are listed in Table 3. As an illustration, the complete thermograms of the polycaproamide and polyblend are shown in Fig. 4.

The results show that the IDT of these materials varies between 125° and 380°C. A further increase in temperature causes rapid decomposition of polymers (Fig. 4).

Unlike the polycaproamide the DTG curve of the polyblend show T_{max} twice. This indicates that the decomposition of this compound occurs in two steps. The first peak should be attributed to the decomposition of the rubber

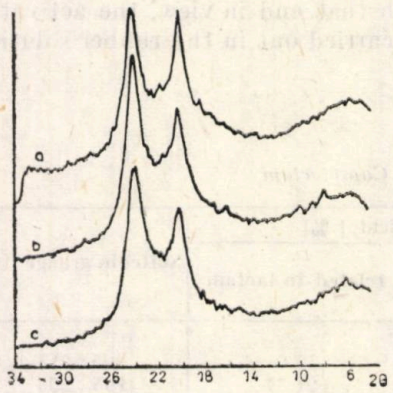

Fig. 2. — X-ray diffraction patterns for : *a* — polycaproamide, *b* — polycaproamide blend 3 (s. Table 2) and *c* — polycaproamide blend 4 (s. Table 2).

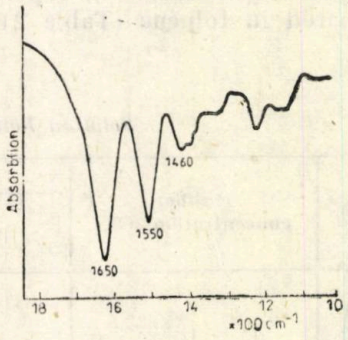

Fig. 3. — IR spectrum of the extracted nylon polyblend.

Table 3

Thermal Characteristics of the Polycaproamide and Nylonblend, obtained in Solution (concentration of rubber 5 %)

Polymer	Temperature at various percentage decompositions, [°C]				T_{max} °C	IDT °C	ΔE Kcal/mol	n
	1%	14%	60%	80%				
Polycaproamide	110	375	435	510	435	380	60	0.6
Polyblend	115	260	437	510	*I* 260	125	13.73	0.9
					II 437	325	48.2	1.1

ΔE — activation energy of the thermal decomposition reaction ;
n — order of the decomposition reaction ;
I and *II* refear to the first and second process, respectively.

structure, whereas the second, at higher temperatures, is due to decomposition of amide linkages.

It can be seen also that polycaproamide holds the highest IDT value and that the introduction of rubber reduces IDT by 55°C (second process). It is most likely that the polyamide component in polyblend is of lower molecular weight. But, it is worth mentioning that both polymers show practically the same T_{max} corresponding to polyamide decomposition (435°C and 437°C respectively).

The thermal decomposition kinetic parameters (Table 3) (energy of activation, E and order of thermal decomposition, n) were calculated by the method of Freeman—Carroll [9] and only the first half of the decomposition was examined in this purpose. Again one may observe that the second process in polyblend degradation show a lower activation energy, which may have the same ground as depression of IDT.

The test of mechanical properties have been done on samples prepared by moulding the powdered blend at high pressure and temperature (not more than 150°C). The obtained results were not conclusive so that further work is in progress on this aspect.

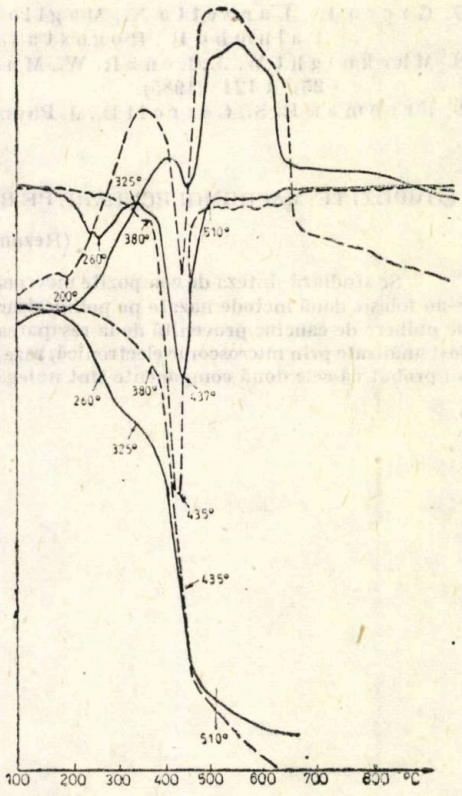

Fig. 4. — Thermograms of polycaproamide (-------) and polyblend (———).

4. Conclusions

Two methods were used to prepare nylon 6-blends with rubber. The experimental data show that in both cases two phase systems are obtained since the rubbery component is not compatible with polycaproamide and it exists in a droplets embeded in the glassy polymer or dispersed in its matrix. Nevertheless, the obtained composites with powdered rubber reveal improved mechanical properties.

Received, July 13, 1990

Polytechnic Institute, Jassy
Department of Macromolecules

REFERENCES

1. Brysdon J. A., *Plastics Materials.* 5 th Ed., Butterworths, London, Sydney, Toronto, 1989
2. Alfonso G. C., Bonta G., Russo S., Traverso A., Makromol. Chem., *182*, 929 (1981).
3. Alfonso G. C., Cirillo G., Russo S., Turturro A., Eur. Polym. J., **19**, 949 (1983).
4. Kazumasa C., Plast. Age, **31**, 124 (1985).
5. Cimmino S., D'Orazio L., Greco R., Maglio G., Malinconico M., Mancarella C., Martuscelli E., Musto P., Polumbo R., Ragosta G., Polym. Eng. and Sci., **25**, 193 (1985).
6. D'Orazio L., Mancarella C., Martuscelli E., Casale A., Filippi A., Speroni F., J. Mater. Sci., **22**, 429 (1987).

7. Greco R., Lanzetta N., Maglio G., Malinconico M., Martuscelli E., Palumbo R., Rogosta G., Scarinzi G., Polymer, **27**, 299 (1986).
8. Macknight W. J., Lenz R. W., Musto P. V., Somani R. J., Polym. Eng. a. Sci., **25**, 1124 (1985).
9. Freeman E. S., Carroll B., J. Phys. Chem., **62**, 394 (1958).

COMPOZITE MACROMOLECULARE PE BAZĂ DE CAUCIUC ȘI POLICAPROLACTAMĂ

(Rezumat)

Se studiază sinteza de compozite macromoleculare pe bază de cauciuc și policaprolactamă S-au folosit două metode bazate pe polimerizarea anionică activată a caprolactamei în prezentă de pulbere de cauciuc provenită de la reșaparea anvelopelor și cauciuc CAROM. Compozitelele au fost analizate prin microscopie electronică, raze X și termogravimetrie. Rezultatele experimentale au probat că cele două componente sînt nelegate chimic.

BULETINUL INSTITUTULUI POLITEHNIC DIN IAȘI
Tomul XXXVI (XL), Fasc. 3—4, 1990
Secția II
CHIMIE ȘI INGINERIE CHIMICĂ

D. C. 678.744 ; 547.26

SEMI - INTERPENETRATING NETWORKS BASED ON POLYVINYL CHLORIDE AND METACRYLIC ESTERS

II. MORPHOLOGY AND PROPERTIES

BY

CORNELIA VASILE, GH. ADAMESCU, LUCREȚIA CHICU, AURELIA IOANID, MIHAELA MIHĂIEȘ, COSMIN DURNESCU and AUREL STOLERIU

1. Introduction

Semi-Interprenetrating Networks (semi-IPN) are obtained of a linear or branched polymer and a very reactive polyfunctional monomer, while the latter is polymerized in the presence of the former.

Networks including polyvinyl chloride (PVC) are of an outstanding practical interest, because the polymerization of the crosslinkable monomer can take place either during processing (extrusion, injection, molding, a.s.o.) due to high operating temperatures in the presence of an initiator, or in semi-finished products through irradiation [1].

A result of reticulation is an increased resistance to the environment (temperature, ozone, water, oil, a.s.o.).

The crosslinkable monomers which are often applied are : dimetacrylic oligoesters, adipates, oligourethanes, oligodimethylsiloxanes, a.s.o. [2].

Semi-IPN structure, morphology and properties depend on a great number of factors, such as: nature of the polyfunctional monomer, polymerization and processing conditions a.s.o., these influence both the crosslinked polymer characteristics and its compatibility with polyvinyl hcloride.

The present paper investigates the dependence on the synthesis conditions of the morphology and properties of semi-IPN based on PVC and dimetacrylic esters.

2. Experimental

Semi-IPN have been synthetized from suspension PVC with $K_w = 70$ or 67 and three ethylene glycol dimetacrylic esters (EA) with the structure :

$$CH_2 = \underset{\displaystyle CH_3}{\overset{|}{C}}-COO-(CH_2-CH_2-O)_n CO-\underset{\displaystyle CH_2}{\overset{|}{C}}= CH_2$$

where $n=1$ (MED), $n=2$ (DED) ; $n=3$ (TED).

The ratio between PVC/EA components ranges between 95/5 and 60/40. The concentration of the initiator, used in polymerization, the benzyol peroxide (Bz_2O_2), ranged between 0.5 and 2% (s. Table 1).

Polymerization temperature was 110°...120°C.

Mixing of components was performed on roll or in 10% solution in tetrahydrofuran followed by solvent evaporation at room temperature.

Characterization of semi-IPN obtained was done by means of the following methods : optical microscopy (polarized light, 600 × magnification), electronic microscopy (4 200 × or 11 300 × magnification), determination of physico-mechanical indices (Schöpper dynamometer), behaviour on Brabender plastograph (160°C, 60 rpm, 34 g mass of sample) thermogravimetry (MOM — Budapest derivatograph, heating rate 12°C/min., 50 mg mass of sample as film), thermooptics to determine glass transition temperatures [3], IR spectroscopy (Perkin—Elmer spectrophotometer, KBr tablets) and elementary analysis.

3. Results and Discussion

In a previous paper, the kinetics of polymerization reaction of ethylene glycol dimetacrylic esters in the presence of PVC was studied [4].

The reaction has been followed both in solid state and in solution, and it was established that diffusion becomes the determining rate step, when there is an increase in temperature and molecular mass of the polyfunctional monomer.

The change of polymerization conditions leads to a change of the reaction rate, as a variable number of gelifying points appear, out of which the three dimensional network develops, and thus the morphology of the samples is particular for each system.

For small concentrations of ester polymer the samples are homogeneous and no morphological differences can be seen.

In concentrations higher than 15...20 % the systems become differentiated.

In case of semi-IPN with mono- and diethylene glycol dimetacrylates, with a high degree of polymerization, distinct areas appear in the ester polymer, to be seen both on the level of optical microscopy (Fig. 1) and through electronic microscopy (Fig. 2).

Phase distribution in the network obtained with TED is more uniform (Fig. 3 *a*) ; interpenetration of the two components is clearly distinguished by means of electronic microscopy at a higher magnification scale (11 300 × — Fig. 3 *b*).

Accordingly, the incompatibility of PVC with crosslinkable dimetacrylic esters appears to be better marked in higher percents of ester polymer.

Morphological changes are also accompanied by structural changes by building up intermolecular bonds between the two components of the system. These have been emphasized by analysing the insoluble fraction in the 3/2 cyclohexanone/acetone mixture. The elementary composition of this fraction is : 55 % C ; 6.7...7 % H ; 11...11.5 % Cl and 26...27 % O.

The rather high chlorine and oxygen content is noticed, which associated with the rather high content in this fraction (~ 50 %) shows a chemical structure which is particular for the semi-IPN built up.

The proof of this change is brought by the IR spectra (Fig. 4). The IR spectra of the semi-IPN made up of 60 % PVC /40 % TED and of the insoluble fraction of this network are similar in most wavelength ranges. Broadening and flatening of spectral bands in case of the insoluble fraction indicates the existence of a high crosslinking degree, so that in the end, the structure semi-IPN is going to come nearer to that of a real IPN.

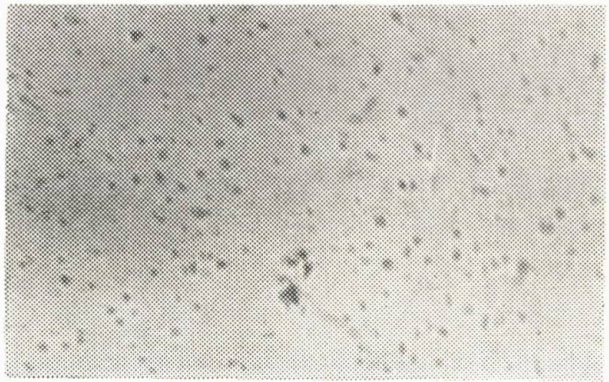

Fig. 1. — Microscopic aspect of semi-IPN film : 60 % PVC /40 % MED, mixing in solution ; 1 % Bz_2O_2 ; polymerization temperature 110°C ; magnification 600 x.

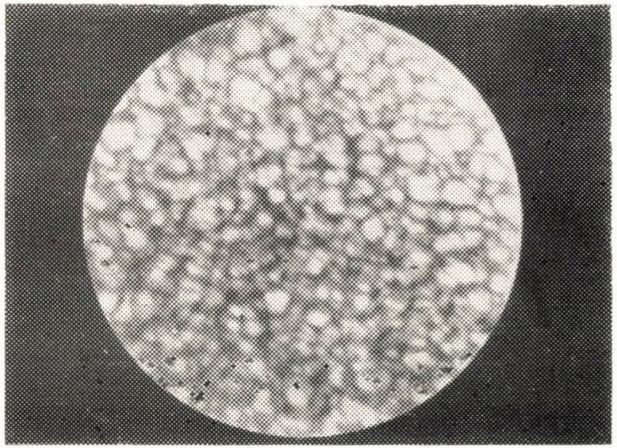

Fig. 2. — Electromicroscopic aspect of semi-IPN film : 60 % PVC/40 % DED, mixing in solution ; 1 % Bz_2O_2;polymerization temperature 110°C ; magnification 4 200 ×.

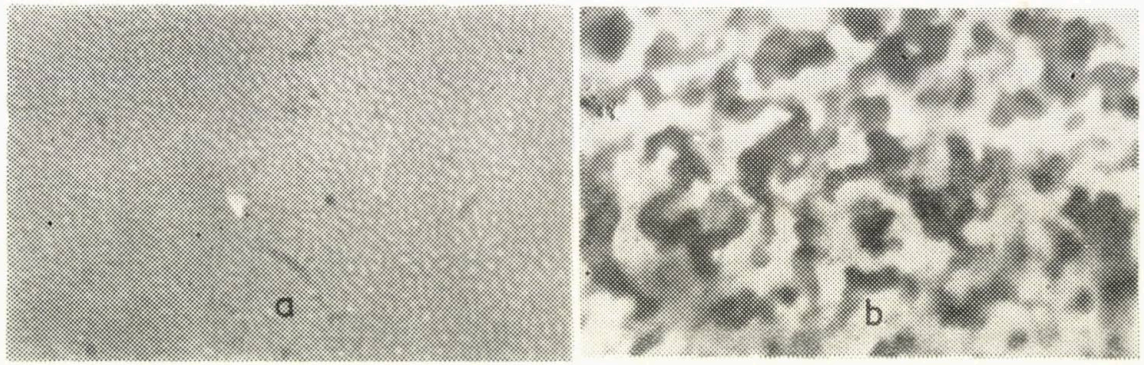

Fig. 3.—Microscopic aspect (*a*) (magnification 600×) and electronomicroscopic aspect (*b*) (magnitude 11 300×) of the semi-IPN film of 60 % PVC/40 % TED, mixing in solution; 1%Bz_2O_2; polymerization temperature 110°C

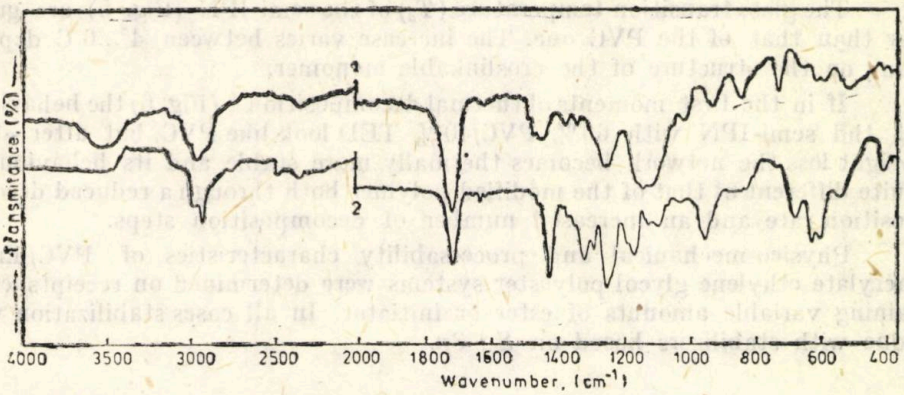

Fig. 4. — IR spectra for the system 60 % PVC/40 % TED polymerized at 110°C, 1 %, Bz_2O_2 (*2*) and of the insoluble fraction (*1*) in 3/2 cyclohexanone/acetone mixture.

The already mentioned structural morphological changes will, of course, reflect themselves in the variation of all properties as it comes out from Figs. 5 and 6 and Table 1.

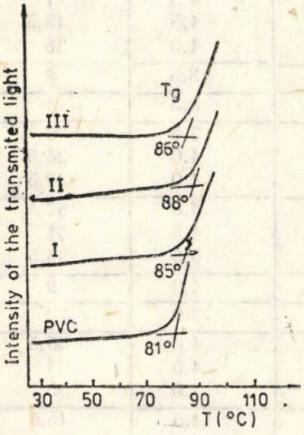

Fig. 5.— Glass transitions temperatures for the following semi-IPN ; *I*—60 % PVC/40 % DED; *II*—60%PVC/40 %TED and *III*—60 % PVC/40 %MED.

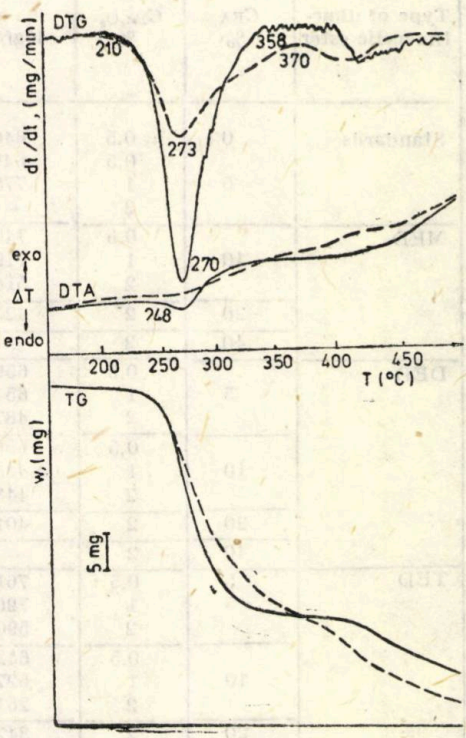

Fig. 6. — Derivatograms of PVC (——) and of semi-IPN 60 % PVC/40 % TED (---).

The glass transition temperature (T_g) of the semi-IPN (Fig. 5) are greater than that of the PVC one. The increase varies between 4°...6°C depending on the structure of the croslinkable monomer.

If in the first moments of thermal decomposition (Fig. 6) the behaviour of thd semi-IPN with 60% PVC/40% TED look like PVC, but after ~7% weight loss the network becomes thermally more stable and its behaviour is quite different of that of the modified polymer both through a reduced decomposition rate and an increased number of decomposition steps.

Physico-mechanical and processability characteristics of PVC/dimetacrylate ethylene glycol polyester systems were determined on receipts containing variable amounts of ester or initiator. In all cases stabilization was done with stabilizers based on S_n, 3p.

Table 1

Physico-mechanical and Processability Characteristics of the Systems Semi-IPN : PVC—Dimetacrylic Polyesters

Type of dimethacrylic ester	C_{EA} %	$C_{Bz_2O_2}$ %	σ Kgf/cm²	Charpy impact strength Kgf/cm²	Gelifying time min.	Thermodynamic stability min.
Standards	0	0.5	640,8	2,41	7,5	30
		0,5	646	2,24	3.5	35.5
	5	1	778,3	2,32	4.0	30
		2	—	—	4,0	29
MED		0.5	740,52	2.52	4.5	77
	10	1	719.2	2,91	4.5	45,5
		2	514.4	2.22	4.0	36
	20	2	423.4	2,33	3,5	8
	40	2	—	1.17	3,5	4
DED		0.5	659.7	2,34	3,5	36
	5	1	654.7	1.93	4.0	26,5
		2	487.4	2,02	4.0	29,5
		0.5	650	2,5	4.0	67
	10	1	418	2,13	4.5	61
		2	448.5	2,5	5.5	35,5
	20	2	401.2	2,58	4,0	9
	40	2	—	1,04	3.0	12
TED	5	0.5	761.4	2.01	4.0	36.5
	5	1	796.5	2,04	4,5	34
		2	590.5	2,12	7.0	30
		0.5	642.7	1.61	4.5	45.5
	10	1	627.0	1,96	3.5	59
		2	261.2	1,72	4.0	46
	20	2	347.2	1.80	3.5	7.5
	40	2	—	1,01	3.0	5

4. Conclusions

From the results shown in Table 1, the followings conclusion can be noticed :

a) Networks with 5...10% ester ethylene glycol dimetacrylate have a tensile strength and a thermodynamic stability greater than of the PVC (etalon sample). Better results are obtained when ester component polymerization is done in the presence of small initiator amounts.

b) Impact strength is maintained constant or is slightly increased for systems with 5...10% ester polymer.

c) Gelifying time is markedly decreasing showing a good processability of semi-IPN studied.

d) Further increase in ester component content leads to a worsening of all physico-mechanical indices due to the phase separation of the system.

Received, February 20, 1990

The „P. Poni" Institute of Macromolecular Chemistry, Jassy
and
The Research Institute of Rubber and Plastics Processing Bucharest, The Research Laboratory, Jassy

REFERENCES

1. Penczek P., *Synthesis of Interpenetrating Polymer Networks and their Possible Uses.* In *Polymer Blends. Processing, Morphology and Properties*, Eds. E. Martuscelli, R. Polumbo, M. Kryszewski, Plenum Press, 1979, 333.
2. Berlin A. A. et al., Plaste u. Kautschuk, **18**, *8*, 563 (1971); Ibid., **20**, *10*, 728 (1973); Пластические масы, **4**, 47 (1975); Высокомол. Соед., **20**, 420, 483, 1369 (1978).
3. Vasile C., Stoleriu, A. Eşanu M., Adamescu Gh., Materiale Plastice, **27**, *3*, 117 (1990).
4. Vasile C., Adamescu Gh., Odochian L., Poinescu Ign., Chicu L., Badea M., Bul. Inst. polit., Iaşi, **XXVI (XL)**, *1—2*, s. II (1990).

REŢELE SEMI-INTERPĂTRUNSE CONSTITUITE DIN POLICLORURĂ DE VINIL ŞI ESTERI METACRILICI

II. Morfologie şi proprietăţi

(Rezumat)

S-a studiat corelaţia condiţii de obţinere—morfologie — proprietăţi pentru reţelele semi-interpătrunse constituite din policlorură de vinil şi diferiţi esteri dimetacrilici.

În acest scop s-au folosit următoarele metode: microscopia optică şi electronică, spectroscopia IR, determinarea indicilor fizico-mecanici, termogravimetria şi analiza termică diferenţială.

BULETINUL INSTITUTULUI POLITEHNIC DIN IAȘI
Tomul XXXVI (XL), Fasc. 3—4, 1990
Secția II
CHIMIE ȘI INGINERIE CHIMICĂ

RECENZII

BOOK REVIEWS РЕЦЕНЗИЙ

REED J. S., *Introduction to the Principles of Ceramic Processing.* John Wiley & Sons, New York, 1988, XVII+486 pp., ISBN 0-471-84-5545-x.

Recent successes in developing, producing, and applying advanced ceramics in high-tech application have heightened the interest in ceramic processing. This book is primarily concerned with the scientific principles and technology involved in processing particulate ceramic materials into fabricated products.

The material in this book is divided into eight parts and twenty six chapters. The text begins with a preface of the author and ends with four appendices and an index. Each chapter has a summary, a list of supplementary literature suggested, and several problems proposed.

Part I, *Introduction*, has two chapters. Chapter 1 describes applications and compositions of both modern and traditional ceramic products, gives a brief history of ceramic technology and presents a perspective of the increasing rol of science in ceramic processing. Chapter 2 reviews several general principles of physical chemistry which are especially important for understanding the processing behaviour of particle systems.

Part II, *Ceramic Raw Materials*, is also divided into two chapters. In Chapter 3, the more common ceramic materials are considered. These include crude materials from natural deposits, refined industrial minerals, and high-tonnage industrial inorganic chemicals with high chemical purity and improved physical characteristics. The powders and the colloidal materials with special or very precisely controlled characteristics, some that have been developed for research studies and for the industrial production of some advanced ceramics, are discussed in Chapter 4.

Part III, *Material Characterization*, has four chapters. Chapter 5 considers the general characteristics of particle system and specifications provided for ceramic raw materials. The following three chapters present in some detail the most important characteristics namely: chemical and phase composition (Chapter 6), particle size and shape (Chapter 7), density, pore structure, and specific surface area (Chapter 8).

Part IV, *Processing Additives*, considers the structure and functions of the additives which must be incorporated in the batch to produce the flow behaviour and properties requisite for forming. These processing additives are: liquids and wetting agents (Chapter 9), deflocculants and coagulants (Chapter 10), flocculants, binders and bonds (Chapter 11), plasticizers, foaming and antifoaming agents, lubricants, and preservatives (Chapter 12).

Part V, *Particle Mechanics and Rheology*, presents the particle packing characteristics (Chapter 13), examines the flow and deformation behaviour of cohesive powders and plastic ceramic materials (Chapter 14), and discusses the principles of rheology and the flow behaviour of slurries and pastes (Chapter 15).

Part VI, *Beneficiation Process*, considers processes for modifying the characteristics of batch components and the rheology for forming, to improve the microstructure in the final product. These processes include size reduction or comminution (Chapter 16), batching dispersion, and mixing processes for dry and wet systems (Chapter 17), particle separation, concentration and washing processes (Chapter 18), direct and indirect granulation (Chapter 19).

Part VII, *Forming Processes,* presents the principles of transformation of the feed material into a consolidated body of a particular geometry and microstructure. The four chapters of this part consider the important forming methods: dry-pressing of powders (Chapter 20), extrusion, plastic transfer pressing, jiggering, and injection molding of the plastic ceramic materials (Chapter 21), casting processes (Chapter 22), molecular polymerization forming by sol—gel process and chemical vapour deposition (Chapter 23). Causes and the prevention of defects in formed products are explained for each method.

Part VIII, *Drying, Surface Processing, and Firing,* has three chapters in which the final, postforming processes, are discussed: drying (Chapter 24), shaping, surface finishing, film printing, and glazing processes (Chapter 25), firing processes (Chapter 26). These last include presintering processes, sintering, and cooling.

The author, James S. Reed, professor at the New York State College of Ceramics, Alfred University, is well known to the specialists in ceramics of all over the world by his previous publications in the field, numerous papers appeared especially in the journals of American Ceramics Society, the volume *Ceramic Fabrication Processes* published by Academic Press, and so on. By this *Introduction to the Principles of Ceramic Processing,* James S. Reed becomes a founder of a new branch of chemical engineering: *Ceramic Engineering.*

Ilie Siminiceanu

SANDLER S. I., *Chemical and Engineering Thermodynamics.* John Wiley & Sons, New York, 1989, XXIII+622 pp., ISBN 0-471-83050-x.

This book is written to be used as a two-semester thermodynamics course for undergraduate students in chemical engineering. The subject is presented in an orderly, coherent fashion. Derivations are complete, rigorous, and easily followed. The book is divided into nine chapters.

Chapter 1, *Introduction,* is a qualitative presentation of the central problems and fundamental concepts of thermodynamics. The most important experimental observations upon which the science of thermodynamics has been developed, are also listed here.

Chapter 2, *Conservation of Mass and Energy,* is concerned with the development of the equations of mass and energy conservation to be used in the thermodynamics of systems of pure substances. These equations are derived for a general black-box system. Though, the illustrations and the problems in this chapter make it clear that these two equations alone are not always sufficient to solve all thermodynamic energy flow problems. We need a balance equation for an additional state variable. It is also necessary to incorporate into the thermodynamic description the unidirectional character of natural processes.

Chapter 3, *Entropy: An Additional Balance Equation,* shows that both objectives above can be accomplished by introducing a single new thermodynamic function: the *entropy.* This chapter also deals with the properties and the utility of this new variable and its balance equation.

Chapter 4, *The Thermodynamic Properties of Real Substances,* deals with the use of the three balance equations to solve thermodynamic problems for real substances given heat capacity data, and data on the relationship between pressure, volume, and temperature. In other words, the method for the evaluation of changes in the thermodynamic properties of real substances accompanying a change of state (ΔH, ΔS, ΔU), using volumetric equations of state and heat capacity data, is presented. The principle of corresponding states and generalized equations of state are also considered in this chapter. Chapter 4 ends with the Appendix A 4.1 describing a BASIC language program for pure fluid thermodynamic properties calculations using the Peng—Robinson equation of state.

In the Chapter 5, *Equilibrium and Stability in One-Component Systems,* the conditions for the existence of a stable equilibrium state in a single-component system, with particular reference to the problem of phase equilibrium, are examined. The practical problem of the fugacity and vapour pressure of a pure fluid calculation from an equation of state is followed by many illustrations and problems. The equilibrium of a single-component multiphase system, the Gibbs phase rule, and the phase transition classification are also presented.

In the Chapter 6, *The Thermodynamics of Multicomponent Mixtures*, the study of thermodynamics, which was restricted to pure fluids in the first five chapters, is extended to mixtures. The first section of this chapter deals with the thermodynamic description of mixtures or the correlation of the thermodynamic properties of a mixture (enthalpy, entropy, free energies) to its temperature, pressure, and composition. Then, the equations of change for a multicomponent mixture are derived with more emphasis on the *heat of reaction* in reacting mixtures. Using the equations of change and the positive nature of the entropy generation term, the general equilibrium criteria for mixtures are considered and shown to be formally identical to the pure fluid equilibrium criteria. These criteria are then used to establish the conditions of phase, chemical, and combined chemical and phase equilibria in mixtures.

Chapter 7, *The Estimation of the Gibbs Free Energy and Fugacity of a Component in a Mixture*, presents the methods for estimating the partial molar Gibbs free energy and its equivalent, the fugacity of species in gaseous, liquid, and solid mixtures. The main methods discussed in this chapter are those based on the equations of state, those based on the principle of corresponding states, and the activity coefficient models (or excess Gibbs free energy) including those based on the Henry's law standard state. In the special case of electrolyte solutions, the activity coefficients can be predicted by semitheoretical modifications of the Debye—Hückel limiting law, or by the more recent model of Pitzer. In addition to the numerous illustrations and problems, the author gives two BASIC programs. The Appendix A 7.2 describes a BASIC language program for species fugacity and vapour—liquid equilibrium calculations using the Peng—Robinson equation of state. The Appendix A 7.4 describes a BASIC language program for the prediction of activity coefficients using the fourth revision of the UNIFAC method.

In the Chapter 8, *Phase Equilibrium in Mixtures*, many different types of phase equilibria are considered : vapour—liquid equilibria, the solubility of gas in a liquid, the solubility of a liquid in a liquid, liquid—liquid—vapour equilibria, the solubility of a solid in a liquid, the distribution of a solute among two liquid phases, osmotic equilibrium and osmotic pressure. The different types of equilibria are predicted using activity coefficient models and/or equations of state. The conclusion is that for mixtures containing only hydrocarbons and some inorganic gases, the equation of state description is prefered. For all other mixtures, activity coefficient models are used.

Chapter 9, *Chemical Equilibrium and the Balance Equations for Chemically Reacting Systems*, deals with the prediction of the equilibrium state in both simple and complex chemical reaction systems. The simple case of a single-phase single-reaction system is generalized, in steps, to the combined chemical and phase equilibrium. The Appendix A 9.1 describes a BASIC language program for the calculation of chemical equilibrium constants and standard state heats and free energies as a function of temperature.

To demonstrate that thermodynamics can be useful in reactor design, too, the author derives the mass and energy balance equations for a CSTR as well as for a tubular reactor. As an application, the computing of the *adiabatic reaction temperature* is presented.

This book may be considered as a model for a modern course in thermodynamics for the students in chemical engineering. It is not only an academic treatise, remarkable for its high scientific level and its pedagogical style, but also a handbook for practicing engineers. An important feature of the book is the great number of illustrations followed by solutions, and problems proposed to be solved. There are 87 illustrations and 274 problems. The author has also included four BASIC language computer programs on an accompanying diskette. These programs permit students to concentrate their efforts on the data interpretation rather than on numerical analysis and computer programming. Last but not least we have to notice an educational aspect. At the end of the Preface, refering to the impact of the students to the development of this course, the author says : „In fact, I am not longer sure whether the form of this book is more a result of my vision or their guidance". Therefore, we warmly recommand this book not only for our students but also for our professors in chemical engineering.

Ilie Siminiceanu

COMYNS A. E., *Fluoride Glasses*. John Wiley & Sons, New York, 1989, 219 pp., ISBN 0-471-92352-4.

This is the first book to be written on those glasses composed entirely of fluoride anions with metal cations. The emphasis is on the heavy metal fluoride glasses (HMFGs), discovered in 1974 by the P o u l a i n brothers in the laboratory of J a c q u e s L u c a s, at the University of Rennes, France. The most widely studied HMFGs are those based on the glass former zirconium tetrafluoride (ZrF_4) and network modifier barium fluoride (BaF_2), with a variety of minor component fluorides acting as stabilizers and modifiers of physical properties such as viscosity and refractive index. Much of current glass development is centred on the ZBLAN system, typically 53 ZrF_4—20 BaF_2—4 LaF_3—3 AlF_3—20 NaF. The basic ZBLAN composition is frequently modified by the substitution of ZrF_4 by hafnium tetrafluoride (HfF_4) or thorium tetrafluoride (ThF_4) which shift the infrared absorption edge from 6...7 to 7...8 and 8...9 μm, respectively. For control of glass stability, aluminium fluoride (AlF_3) may be substituted by gallium trifluoride (GaF_3) or indium trifluoride (InF_3). Lithium fluoride (LiF) provides an alternative to sodium fluoride (NaF). Viscosity and refractive index may be modified by the addition of small quantities of zinc fluoride (ZnF_2), cadmium fluoride (CdF_2) and lead fluoride (PbF_2). Many of the fluorides used for modification of ZBLAN glass may themselves become major components of alternative glass-forming systems. These include CLAP mixture (CdF_2—LiF—AlF_3—PbF_2) and the new Rennes University BIZYT composition (BaF_2—InF_3—ZnF_2—YF_3—ThF_4). There are thousands of fluoride glasses compositions already reported.

One of the major stimuli for the development of HMFGs has been the prospect of long-distance telecommunication systems based on ultra-law-loss fluoride fibres operating in the near infrared region of the spectrum. Today, fluoride glasses and fibres are used in many ways in industry, medicine, research and defense. Many applications of fluoride glass fibres, in the field of telecommunications and sensors, are within sight and will be developed when the appropiate components become available.

The nine chapters of this book have been written by different renowned specialists in the field. Chapter 1, *Introduction*, belongs to the editor of the book, A l a n E. C o m y n s (England). This is a short review of the fluoride glasses subject. Scope, history, nomenclature, technical problems, status and outlook of HMFGs are presented. Chapter 2, *Glass Systems and Structures*, has been written by M a r c e l P o u l a i n (France), one of the discoveres of the first ZrF_4-based fluoride glasses. The fundamental aspects of glass formation in fluoride systems, structures, synthesis, and composition are deeply analysed in this text. In Chapter 3, *Nucleation and Crystallization*, the authors (D. R. M a c F a r l a n e and L. J. M o o r e (Australia)) review nucleation and crystallization studies of fluoride glasses, as well as elements of the background theory of the processes involved. Chapter 4, *Raw Materials*, by B. E. K i n s m a n (England), deals with the general methods of fluoride preparation, the methods of precursors and melt purification, as well as with the metal fluorides and other reagents used as raw materials. Chapter 6, *Optical Properties and Applications*, belongs to a group of researchers from British Telecom Research Laboratories (England), P. W. F r a n c e, S. F. C a r t e r, C. R. D a y and M. W. M o o r e. In the first section, dealing with bulk glasses, the transparency, the refractive index and dispersion, and the fluorescence are considered. The second part of the chapter deals with optical properties of fibres: extrinsic absorption, extrinsic scattering, target losses. Finally, the present and future applications of fibres are reviewed: sensors, fibre lasers, medical applications. In the Chapter 6, *General Physical Properties*, J. M. P a r k e r (England) presents a complete characterization of fluoride glasses by the following physical properties: thermal properties (thermical expansion coefficient, thermal conductivity, specific heat), viscosity, elastic properties, strength, electrical conductivity and diffusion, magnetic properties. Chapter 7, *Chemical Properties*, written by A n g e l a B. S e d d o n (England), reviews the main types of reactions of fluoride glasses with water and aqueous solutions, and with gases, as well as the chemical reactions taking place during glass melting. In Chapter 8, *Fibre Drawing*, H. V. S c h n e i d e r (Siemens AG, Germany) presents the state of the art of fibre preparation steps: melting,

preform casting, fibre pulling and coating. Chapter 9, *Applications and Prospects*, belonging to G. Mazé (France), is confined to the applications of the HMFGs. The chemical and optical applications are reviewed. The subject of optical fibres is also treated in some detail. In the future, besides the telecom fibres, the active fibres could be useful for multispectral laser sources and for all the optical amplification components to be used in data transmission systems and sensing devices.

This book is very useful for students, researchers and practicing engineers in the field of material science and technology.

Ilie Siminiceanu

* * * *Evaluation sensorielle. Manuel méthodologique.* Technique & Documentation, Lavoisier, APRIA, Paris, 328 pp., ISBN 2-85206-588-6.

L'évaluation sensorielle c'est l'étude des réponses humaines aux propriétés physico-chimiques des aliments et boissons.

Élaboré par un collectif de dix auteurs sous la coordination de la Société Scientifique d'Hygiène Alimentaire et l'Institut Scientifique d'Hygiène Alimentaire „Florence Sztrygler" l'ouvrage est destiné aux utilisateurs de l'évaluation sensorielle, que ce soit dans le cadre du contrôle de la qualité de la production alimentaire au dans le domaine du développement des produits nouveaux, mais aussi aux étudiants des facultés des industries agro-alimentaires.

Dans ce livre les connaissances et méthodes concernant les deux aspects de l'évaluation sensorielle des aliments que constituent d'une part l'analyse descriptive des propriétés sensorielles et d'autre part l'étude des préférences et les aversions des consommateurs, sont judicieusement distinguées.

L'auvrage est organisé en quatre parties. Dans la première partie on présente les caractéristiques d'une réponse sensorielle et les notions concernant la métrologie sensorielle. Ensuite, dans la deuxième partie, *Les épreuves discriminatives et descriptives*, on présente l'organisation pratique de la mesure sensorielle et les domaines d'application des épreuves avec évaluation de l'intensité d'une grandeur sensorielle simple et d'une grandeur sensorielle complexe. Dans la troisième partie on présente les épreuves hédoniques (choix de l'épreuve, épreuve par paire, épreuve de classement, évaluation hédonique, épreuve de lassitude, épreuve d'aversion, épreuve monadique, épreuve de consommation). La quatrième partie, traite nombre de questions d'analyse statistique concernant l'interprétation des résultats.

Ce livre offre une vue d'ensemble des méthodes utilisées en évaluation sensorielle, base d'une stratégie vraiment souple de développement d'un produit, avec ses avantages et ses inconvénients qui forment un puissant outil d'optimisation d'un produit. Un lexique des termes spécifiques figure également au fin d'ouvrage.

Chaque chapitre contient les figures, les exemples, les tables et les relations de calcul. Les références bibliographiques contiennent 140 titres, des ouvrages publiés ces dernières années. L'ouvrage, par son style, par le contenu et la manière d'organisation est facile à lire et accessible à tous les niveaux.

D. Cozma

Tiparul executat sub cd. nr. 54
la S.C. „Dosoftei" S.A. Iași
Str. Sf. Lazăr, nr. 49

1992 APR 2

40822